

# Application of Plasma Phenomena

---



**Po-Yu Chang**

**Institute of Space and Plasma Sciences, National Cheng Kung University**

**Lecture 4**

**2024 spring semester**

**Tuesday 9:10-12:00**

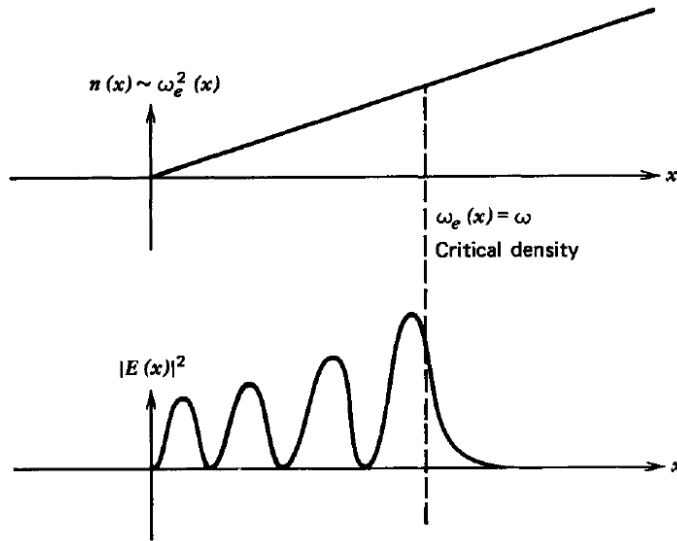
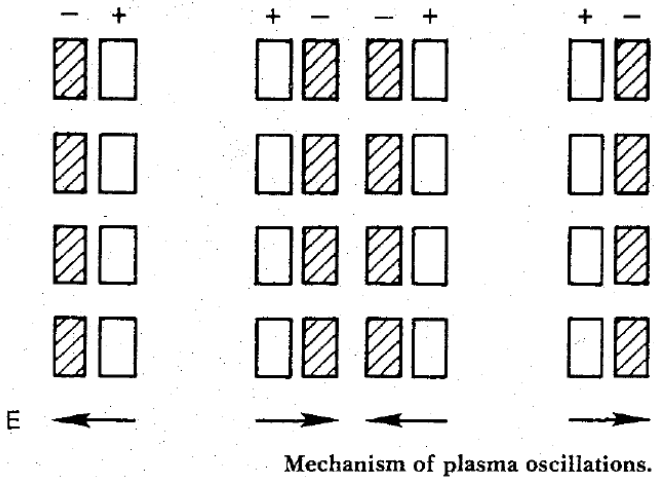
**Materials:**

**<https://capst.ncku.edu.tw/PGS/index.php/teaching/>**

**Online courses:**

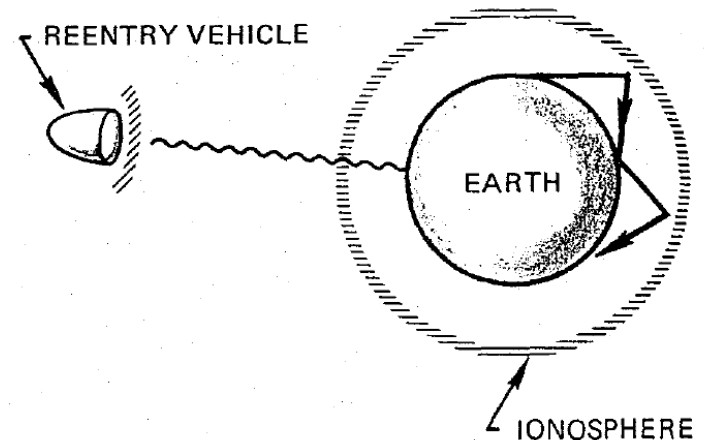
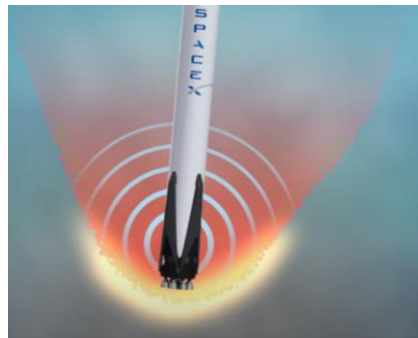
**<https://nckucc.webex.com/nckucc/j.php?MTID=m4082f23c59af0571015416f6e58dd803>**

# Electron plasma frequency is the characteristic frequency such that electrons oscillate around their equilibrium positions



$$\omega_{pe} \equiv \left( \frac{4\pi n_e e^2}{m_e} \right)^{1/2}$$

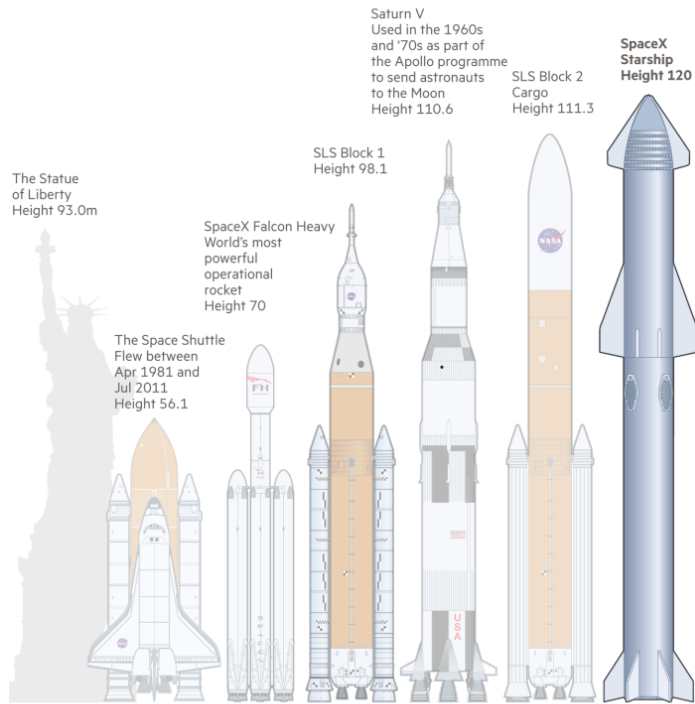
$$n_{cr} \equiv \frac{m_e}{4\pi e^2} \omega^2$$



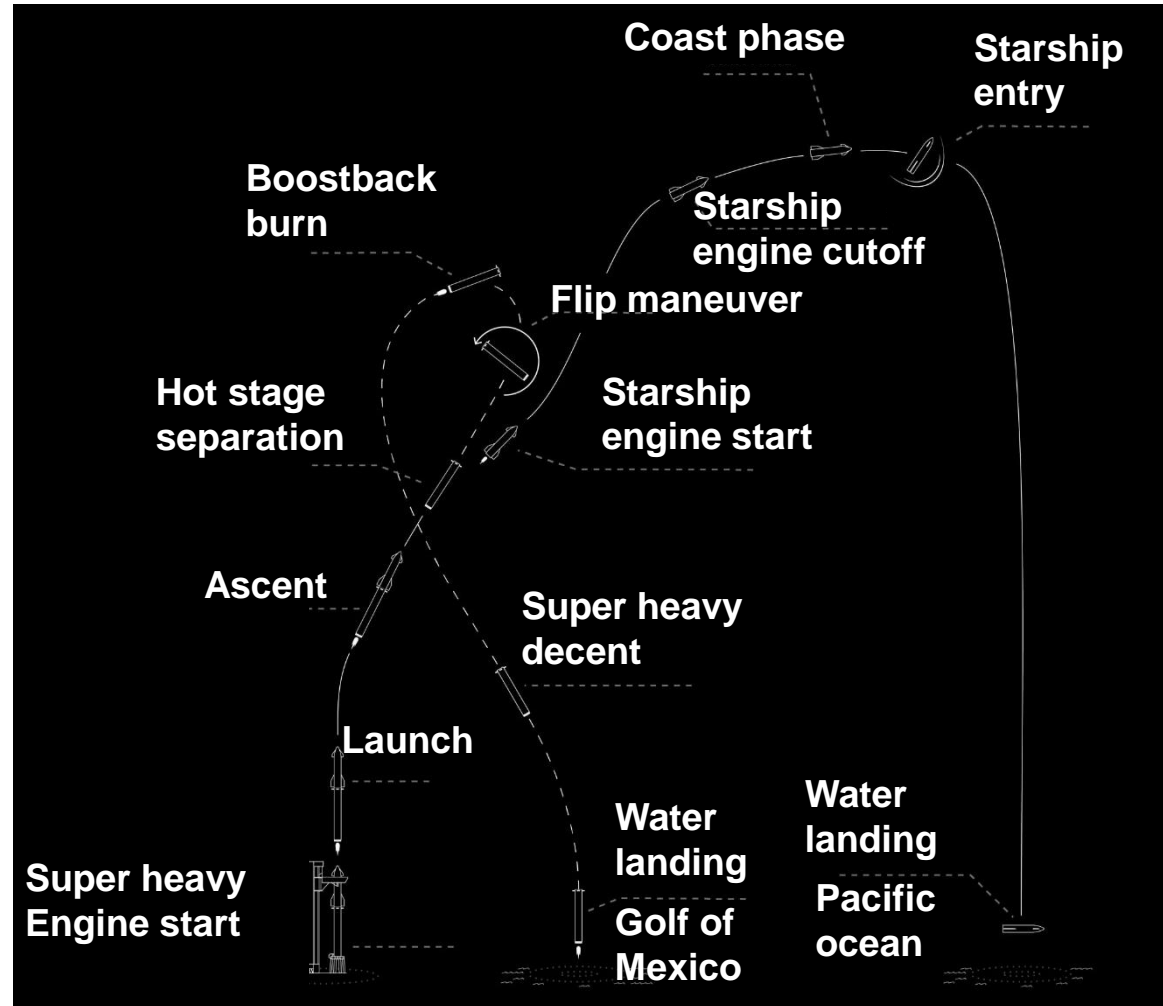
# SpaceX starship is the biggest rocket to date



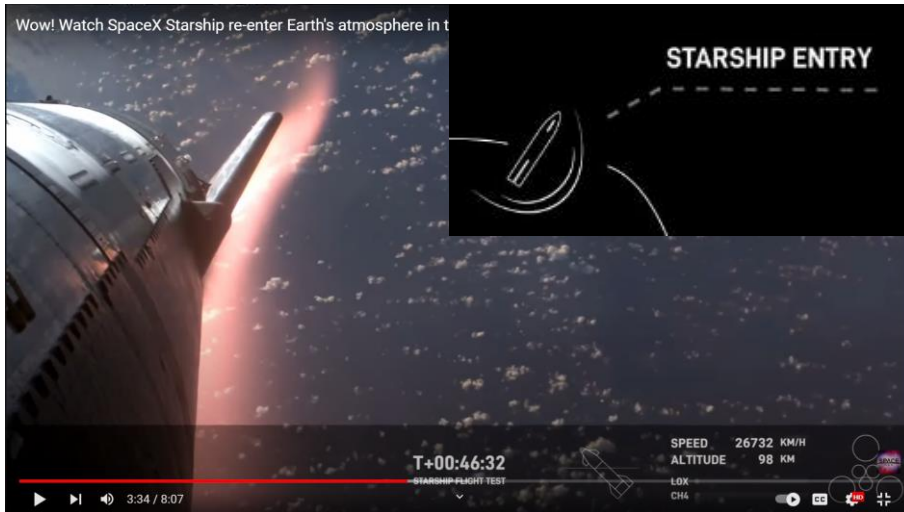
How the Starship compares  
Height (metres)



Sources: Nasa; SpaceX Graphic by Bob Haslett © FT

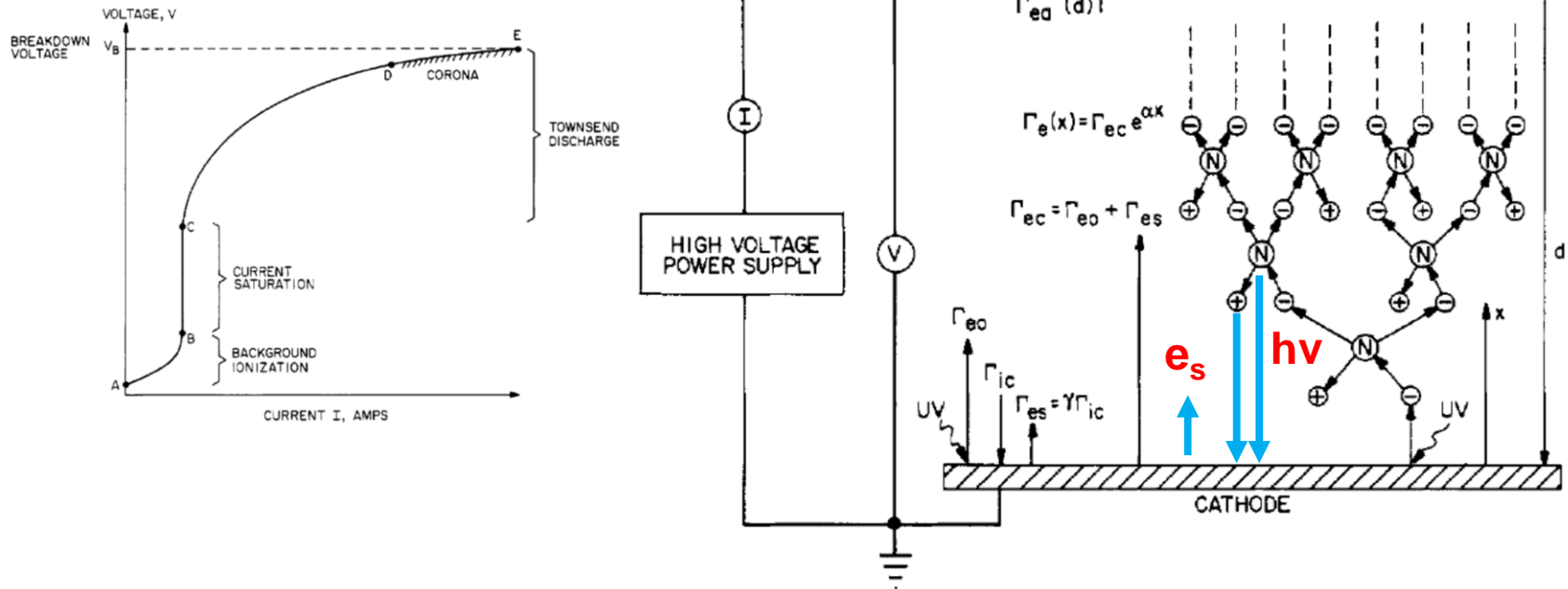


# Plasma was generated during the starship re-entry





# Electrical breakdown occurs when applied voltage is greater than the breakdown voltage



- **Primary electrons:** electrons from the cathode due to photoemission, background radiation, or other processes.
- **Secondary electrons:** electrons emitted from the cathode per incident ion or photon created from ionization in gas.

# Derivation of electrical breakdown



- Secondary electron emission coefficient:

$$\gamma \equiv \frac{\text{\# of electrons emitted}}{\text{\# of incident ions or photons}}$$

$$\Gamma_{es} = \gamma \Gamma_{ic}$$

$$\Gamma_{ec} = \Gamma_{e0} + \Gamma_{es}$$

$$I_{ea} = I_{ec} + I_{ic} \Rightarrow \Gamma_{ea} = \Gamma_{ec} + \Gamma_{ic}$$

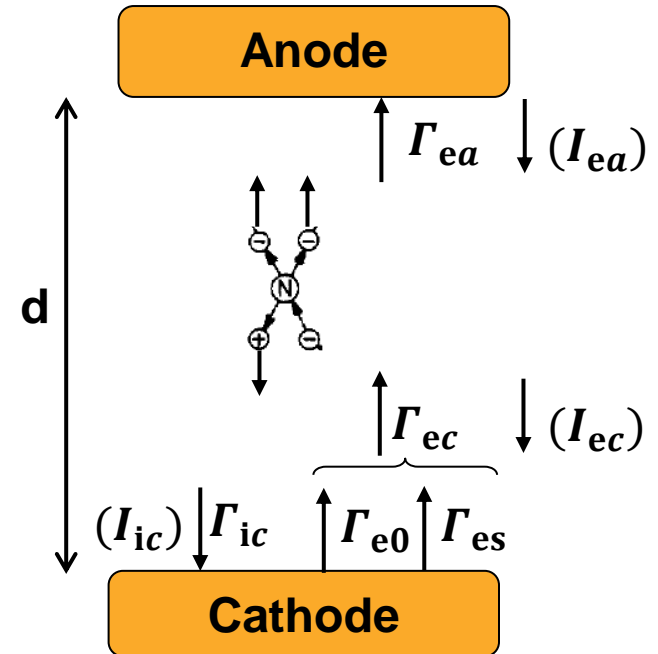
$$\Gamma_{ea} - \Gamma_{ec} = \Gamma_{ic} = \frac{\Gamma_{es}}{\gamma} \quad (\Gamma_{ea} = \Gamma_{ec} e^{\alpha d})$$

$$\Gamma_{es} = \gamma(\Gamma_{ea} - \Gamma_{ec}) = \gamma \Gamma_{ec}(e^{\alpha d} - 1)$$

$$\Gamma_{ec} = \Gamma_{es} + \Gamma_{e0} = \gamma \Gamma_{ec}(e^{\alpha d} - 1) + \Gamma_{e0}$$

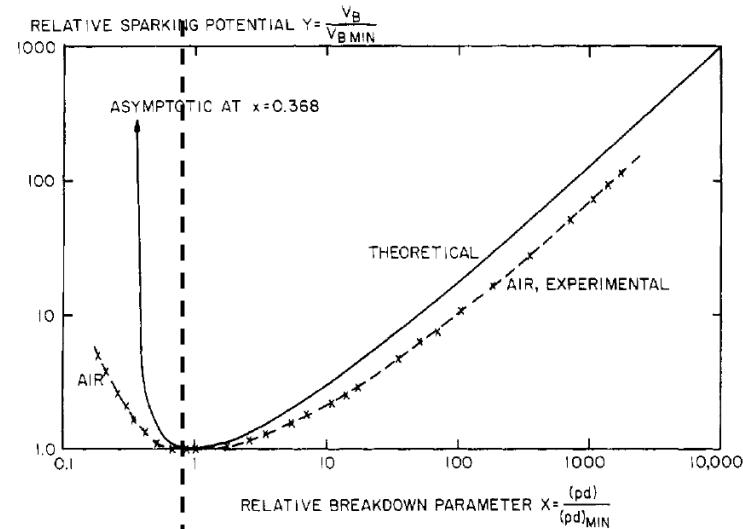
$$\Gamma_{ec} = \frac{\Gamma_{e0}}{1 - \gamma(e^{\alpha d} - 1)}$$

$$\Gamma_{ea} = \Gamma_{e0} \frac{e^{\alpha d}}{1 - \gamma(e^{\alpha d} - 1)} \quad (\text{electrons}/m^2 - s)$$



$$J = J_0 \frac{e^{\alpha d}}{1 - \gamma(e^{\alpha d} - 1)} \quad (A/m^2)$$

# Collision frequency and electron energy gained from electric field are both important to electrical breakdown

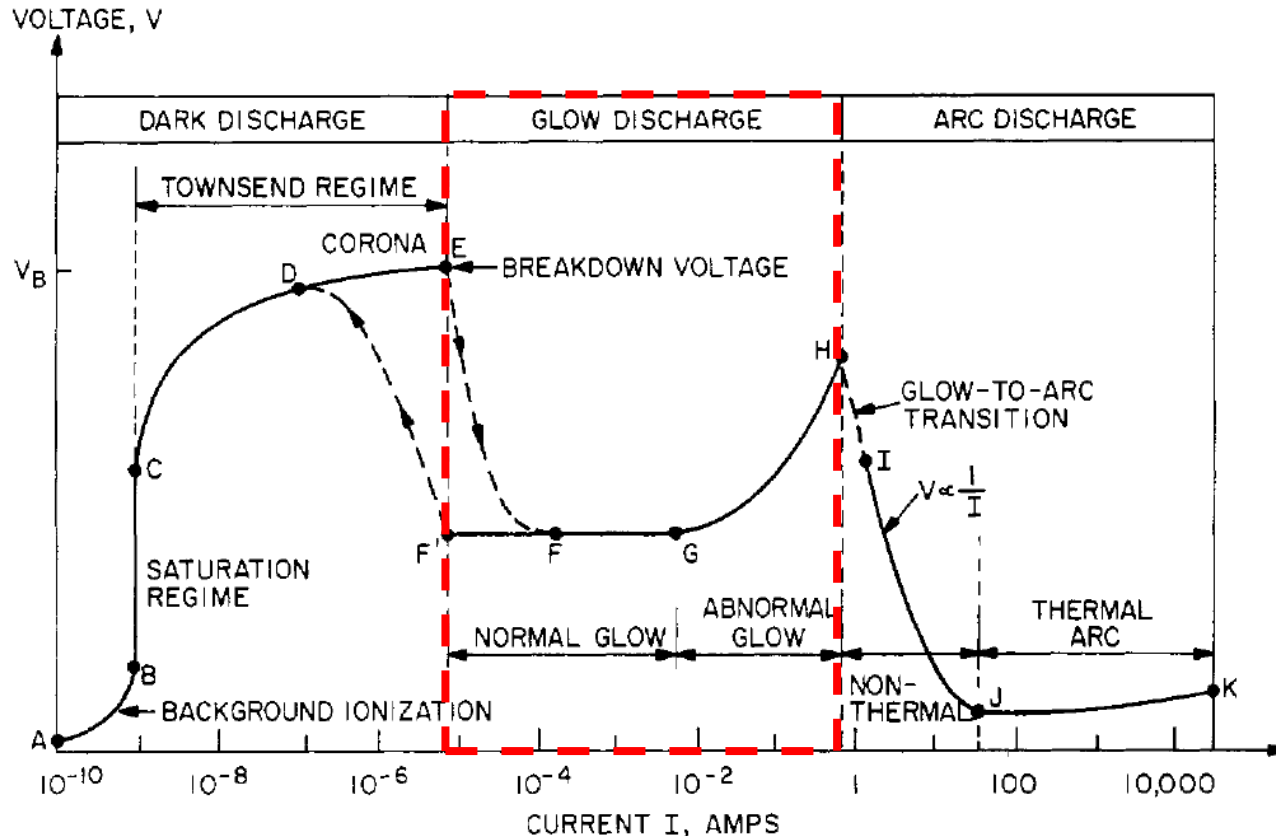


- Collision is not frequent enough even the electrons gain large energy between each collision.
- Electrons do not gain enough energy between each collision even collisions happen frequently.
- The minimum of the Paschen's curve corresponds to the Stoletow point, the pressure at which the volumetric ionization rate is a maximum.

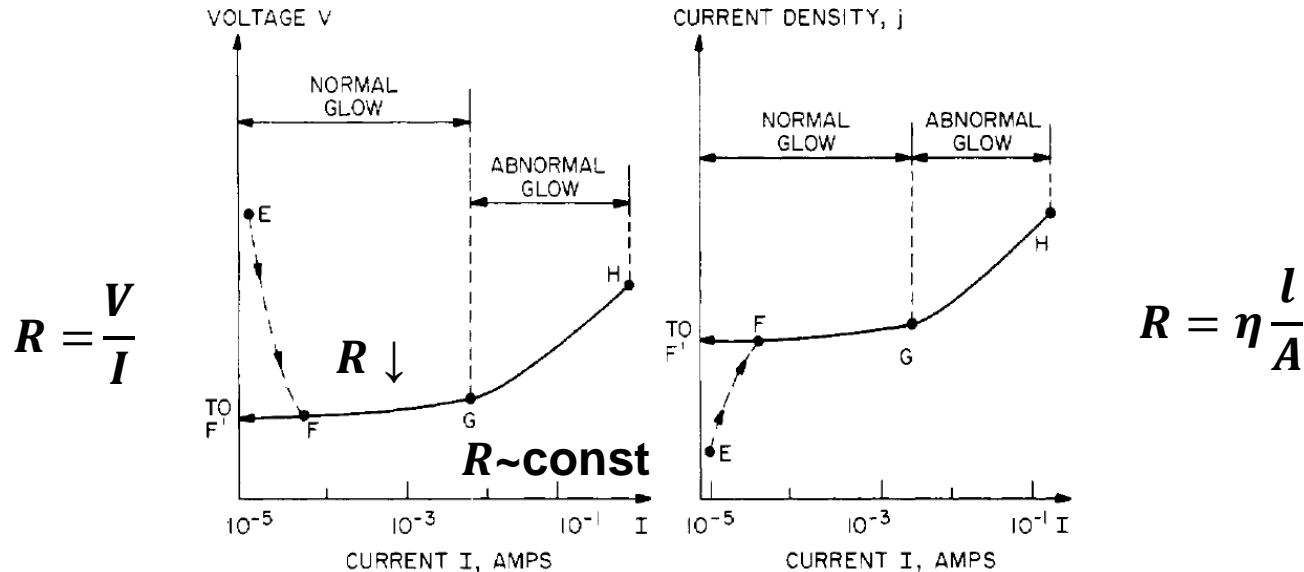
# DC electrical glow discharges in gases



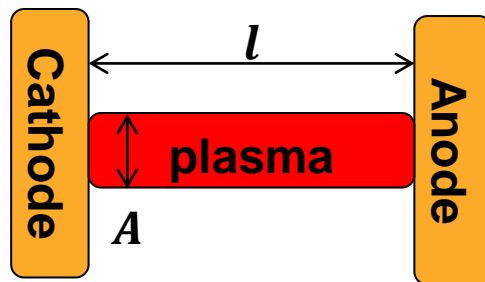
- The internal resistance of the power supply is relatively low, then the gas will break down at the voltage  $V_B$ , and the discharge tube will move from the dark discharge regime into the low pressure normal glow discharge regime.



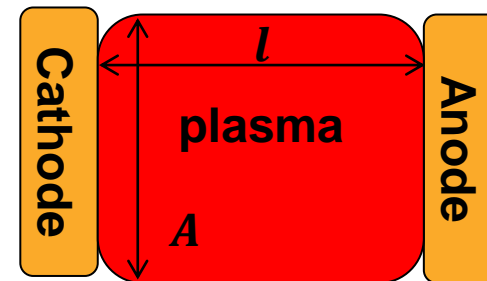
# Abnormal glow discharge occurs when the cross section of the plasma covers the entire surface of the cathode



- Normal glow discharge:

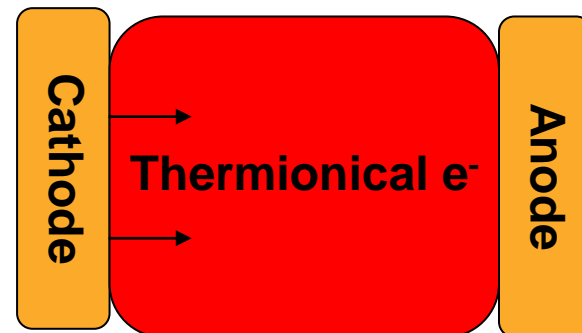
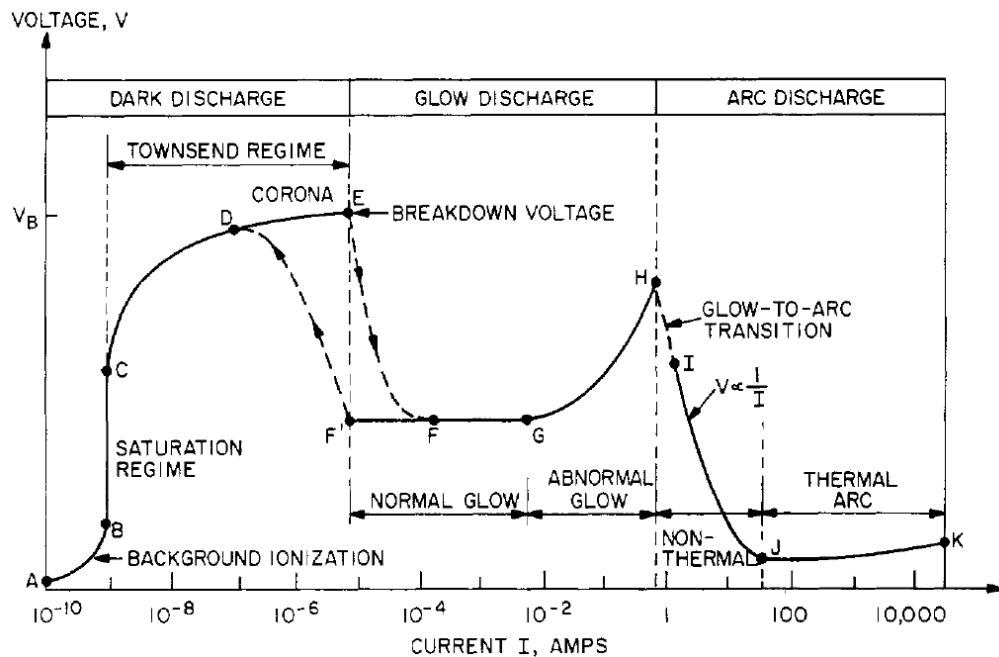


- Abnormal glow discharge:



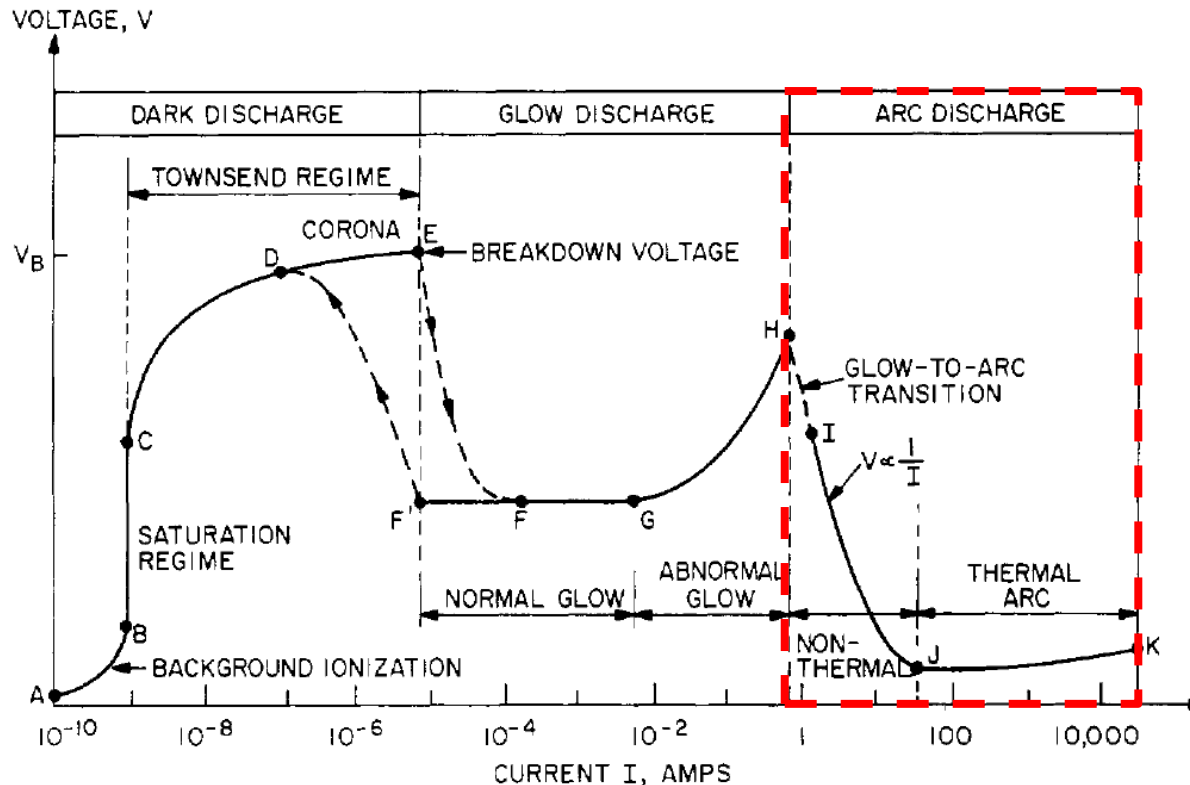
- Surface cleaning using plasma needs to work in the abnormal glow discharge region.

## Discharge may enter glow-to-arc transition region if the cathode gets hot enough to emit electrons thermionically



- If the cathode gets hot enough to emit electrons thermionically and the internal impedance of the power supply is sufficiently low, the discharge will make a transition into the arc regime.

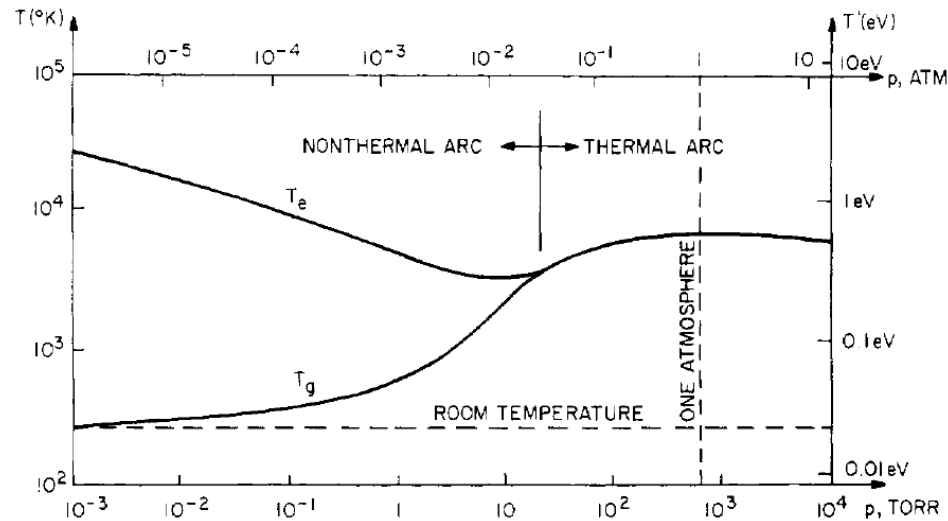
# DC electrical arc discharges in gases



- An arc is highly luminous and is characterized by high currents ( $> 1 \text{ A}$ ) and current densities ( $\text{A}=\text{cm}^2 \text{ t kA/cm}^2$ ).
- Cathode voltage fall is small ( $\approx 10 \text{ V}$ ) in the region of high spatial gradients within a few mm of the cathode.



# An arc can be non-thermal or thermionic

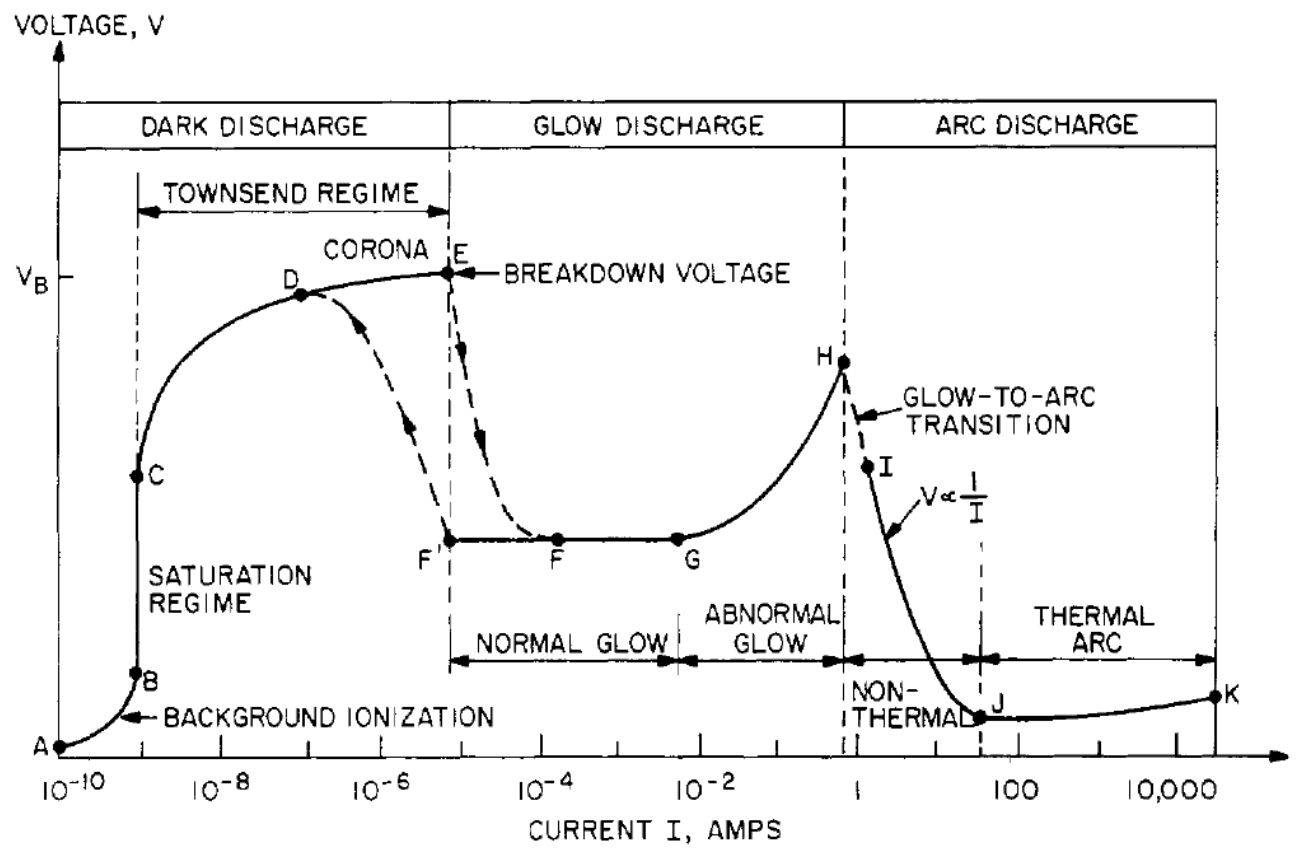


Plasma parameter	Non-thermal arc	Thermal arc
Equilibrium state	Kinetic	LTE
Electron density, $n_e$ (electrons/m <sup>3</sup> )	$10^{20} < n_e < 10^{21}$	$10^{22} < n_e < 10^{25}$
Gas pressure, $p$ (Pa)	$0.1 < p < 10^5$	$10^4 < p < 10^7$
Electron temperature, $T'_e$ (eV)	$0.2 < T'_e < 2.0$	$1.0 < T'_e < 10$
Gas temperature, $T'_g$ (eV)	$0.025 < T'_g < 0.5$	$T'_g = T'_e$
Arc current, $I$ (A)	$1 < I < 50$	$50 < I < 10^4$
$E/p$ (V/m-Torr)	High	Low
$IE$ (kW/cm)	$IE < 1.0$	$IE > 1.0$
Typical cathode emission	Thermionic	Field
Luminous intensity	Bright	Dazzling
Transparency	Transparent	Opaque
Ionization fraction	Indeterminate	Saha equation
Radiation output	Indeterminate	LTE

# DC electrical glow discharges in gases



- The internal resistance of the power supply is relatively low, then the gas will break down at the voltage  $V_B$ , and the discharge tube will move from the dark discharge regime into the low pressure normal glow discharge regime or in to the arc discharge regime.



# Methods of plasma production

---



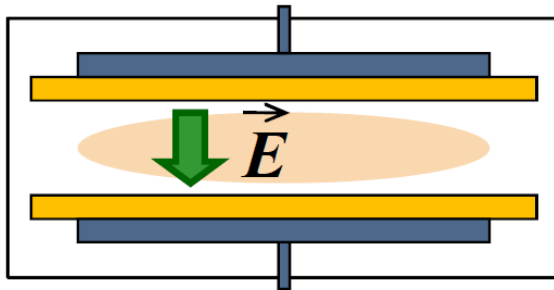
- **DC electrical discharges**
  - Dark electrical discharges in gases
  - DC electrical glow discharges in gases
  - DC electrical arc discharges in gases
- **AC electrical discharges**
  - **RF electrical discharges in gases**
  - Microwave electrical discharges in gases
  - Dielectric-barrier discharges (DBDs)
- **Other mechanism**
  - Laser produced plasma
  - Pulsed-power generated plasma

# RF can interact with plasma inductively or capacitively

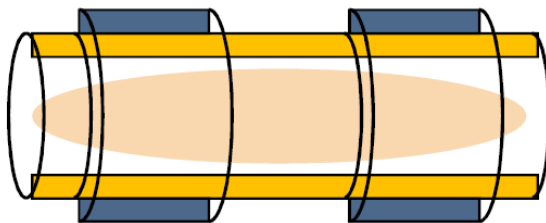


## Capacitively coupled

planar

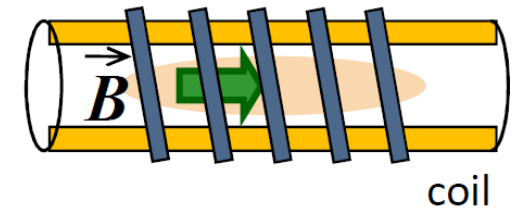


coaxial



## Inductively coupled

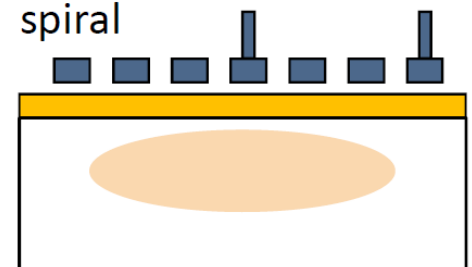
coaxial



coil

spiral

planar



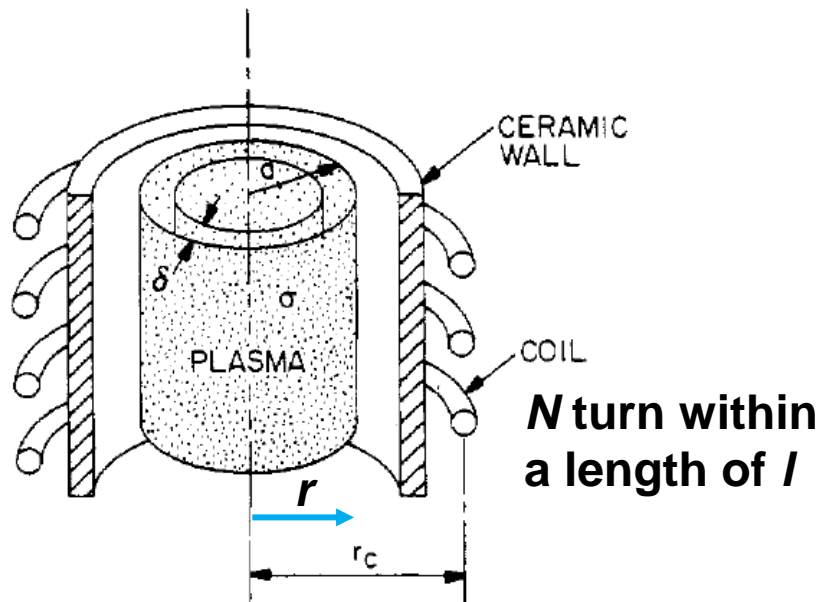
# AC electrical discharges deliver energy to the plasma without contact between electrodes and the plasma

---



- **DC electrical discharge** – a true current in the form of a flow of ions or electrons to the electrodes.
- **AC electrical discharge** – the power supply interacts with the plasma by displacement current.
  - **Inductive radio frequency (RF) electrical discharges**
  - Capacitive RF electrical discharges
  - Microwave electrical discharges
  - Dielectric-barrier discharges (DBDs)
- Other mechanism
  - Laser produced plasma
  - Pulsed-power generated plasma

# The plasma is generated by the induced electric field from the oscillating magnetic field



$$\nabla \times \vec{E} = -\frac{\partial \vec{B}}{\partial t}$$

$$\int (\nabla \times \vec{E}) \cdot d\vec{A} = \int \left( -\frac{\partial \vec{B}}{\partial t} \right) \cdot d\vec{A}$$

$$2\pi r E = -\pi r^2 \frac{\partial B}{\partial t}$$

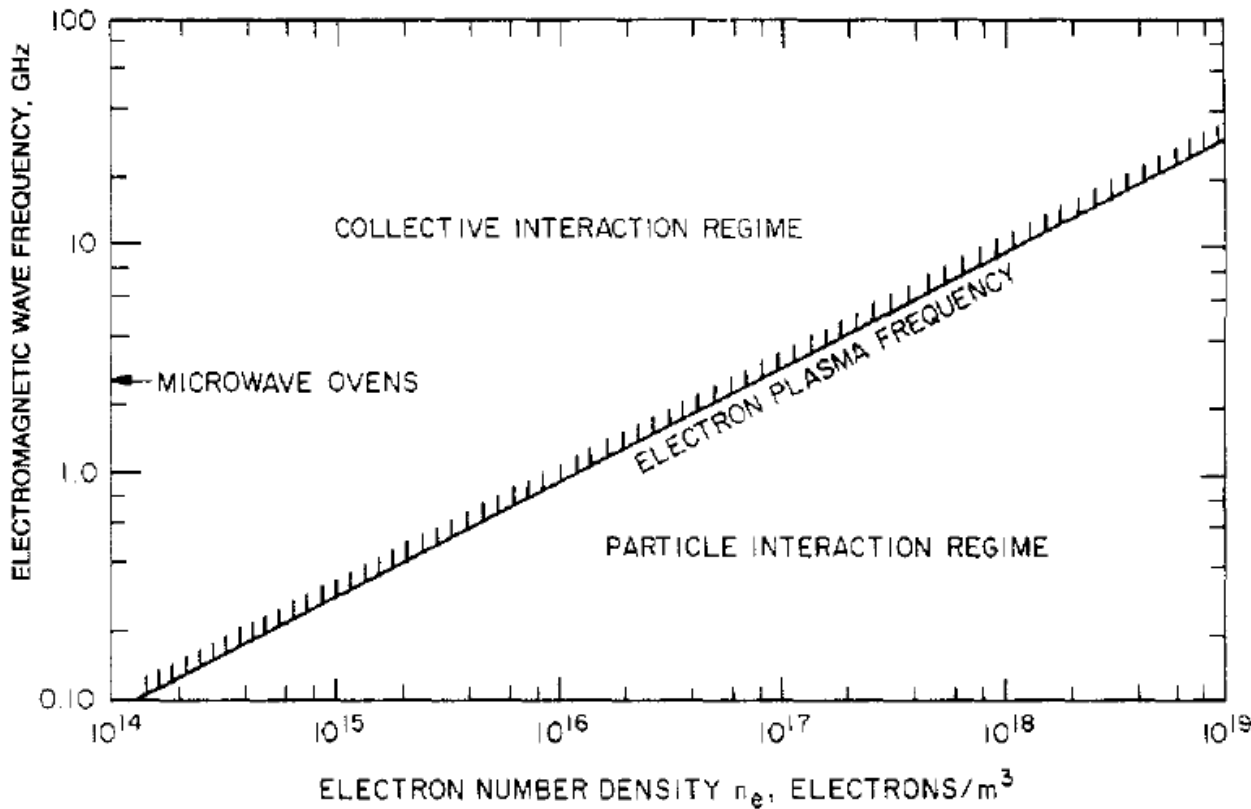
$$E = -\frac{r}{2} \frac{\partial B}{\partial t}$$

$$B \times l = \mu_0 N I$$

$$E = -\frac{r}{2} \mu_0 \frac{N}{l} \frac{\partial I}{\partial t}$$

$$|E| = \frac{r}{2} \mu_0 \frac{N}{l} \omega I$$

# How an electromagnetic wave interacts with a plasma depends on its frequency



$$\omega_{pe} = \sqrt{\frac{n_e e^2}{\epsilon_0 m_e}} \text{ (rad/s)}$$

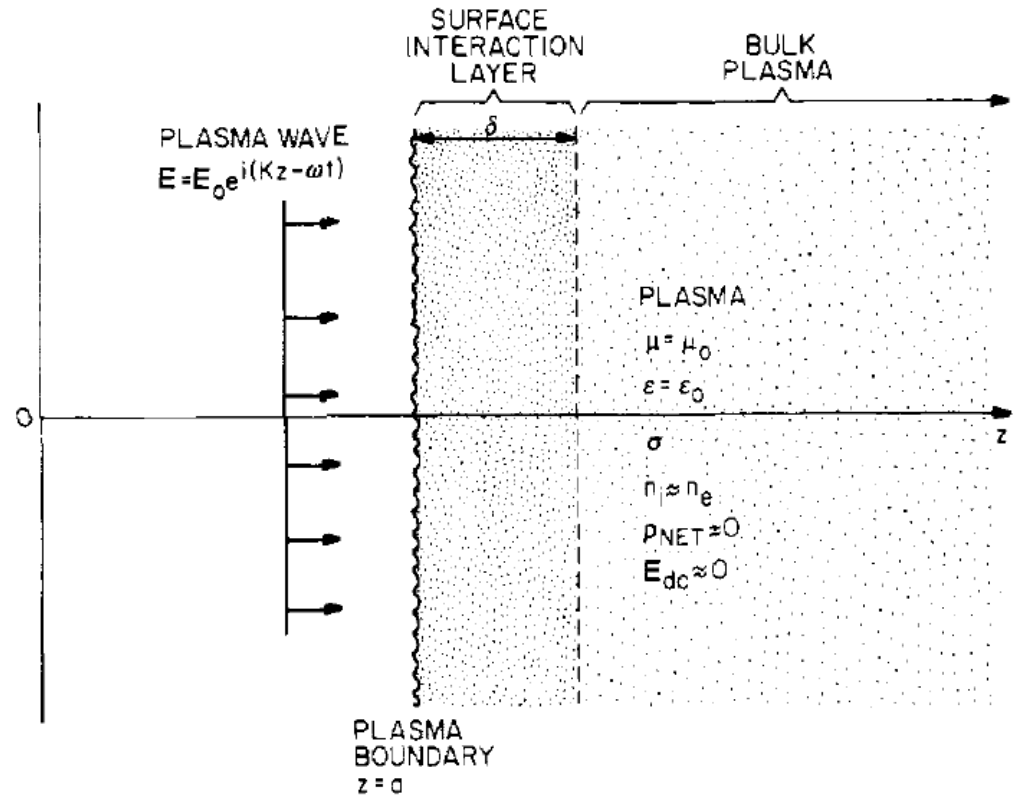
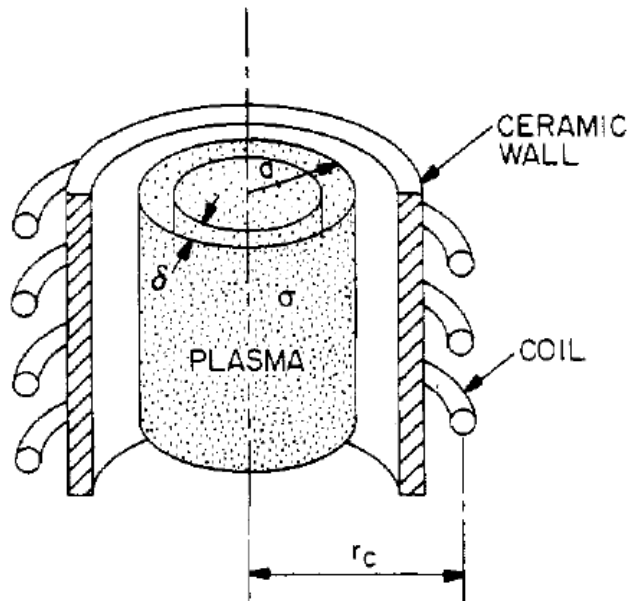
$$n_{cri} = \frac{\epsilon_0 m_e}{e^2} \omega_{pe}^2 \text{ (m}^{-3}\text{)}$$

$$n_{760 \text{ Torr} / 300\text{K}} = 2.45 \times 10^{25} \text{ m}^{-3}$$

$$n_{0.1 \text{ Torr}, 1\% \text{ ionization}} = 3.2 \times 10^{19} \text{ m}^{-3}$$



# RF energy is strongly absorbed within the skin depth if the frequency is below the electron plasma frequency



# Skin depth is calculated using Maxwell's equations



$$\nabla \cdot \vec{E} \approx 0 \text{ (quasi-neutral)} \quad \nabla \cdot \vec{B} = 0$$

$$\nabla \times \vec{E} = -\frac{\partial \vec{B}}{\partial t}$$

$$\nabla \times \vec{B} = \mu_0 \vec{J} + \mu_0 \epsilon_0 \frac{\partial \vec{E}}{\partial t}$$

$$\vec{J} = \sigma \vec{E} \text{ (Ohm's law)}$$

$$-\frac{\partial}{\partial t} (\nabla \times \vec{B}) = \nabla \times (\nabla \times \vec{E}) = \nabla(\nabla \cdot \vec{E}) - \nabla^2 \vec{E} \sim -\nabla^2 \vec{E}$$

$$\frac{\partial^2 \vec{E}}{\partial z^2} - \mu_0 \sigma \frac{\partial \vec{E}}{\partial t} - \mu_0 \epsilon_0 \frac{\partial^2 \vec{E}}{\partial t^2} = 0$$

$$\vec{E} = \vec{E}_0 \exp[-i(kz - \omega t)] \quad k \equiv \alpha + \frac{i}{\delta}$$

$$(-k^2 + i\omega\mu_0\sigma + \mu_0\epsilon_0\omega^2) \vec{E} = 0$$

$$\alpha = \sqrt{\frac{\sigma\mu_0\omega}{2}} \left[ \frac{\omega\epsilon_0}{\sigma} + \sqrt{1 + \left(\frac{\omega\epsilon_0}{\sigma}\right)^2} \right]^{1/2}$$

$$\frac{1}{\delta} = \sqrt{\frac{\sigma\mu_0\omega}{2}} \left[ \sqrt{1 + \left(\frac{\omega\epsilon_0}{\sigma}\right)^2} - \frac{\omega\epsilon_0}{\sigma} \right]^{1/2}$$

# Skin depth is calculated using Maxwell's equations



$$\alpha = \sqrt{\frac{\sigma\mu_0\omega}{2}} \left[ \frac{\omega\epsilon_0}{\sigma} + \sqrt{1 + \left(\frac{\omega\epsilon_0}{\sigma}\right)^2} \right]^{1/2} \quad \frac{1}{\delta} = \sqrt{\frac{\sigma\mu_0\omega}{2}} \left[ \sqrt{1 + \left(\frac{\omega\epsilon_0}{\sigma}\right)^2} - \frac{\omega\epsilon_0}{\sigma} \right]^{1/2}$$

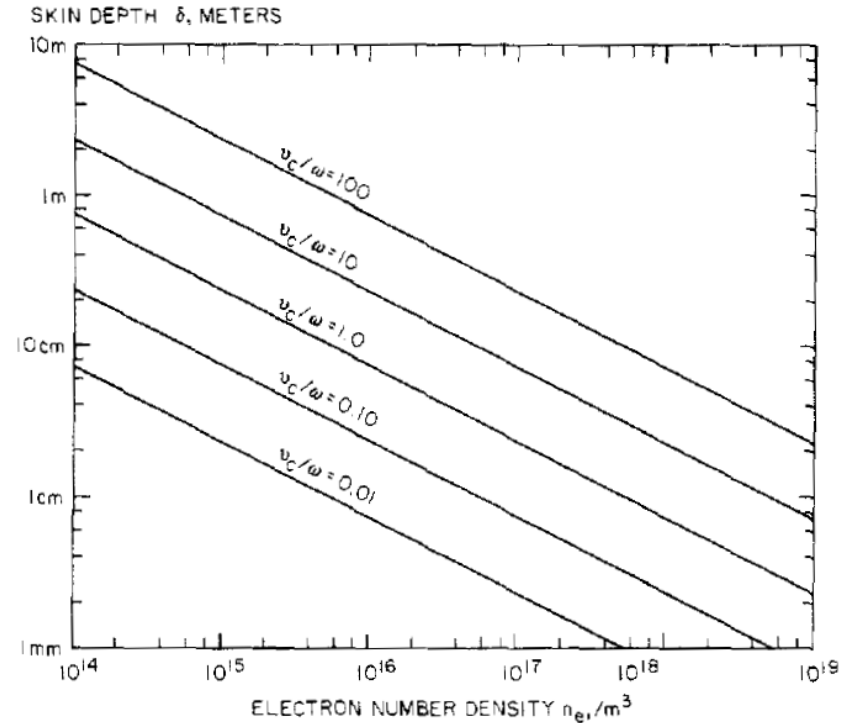
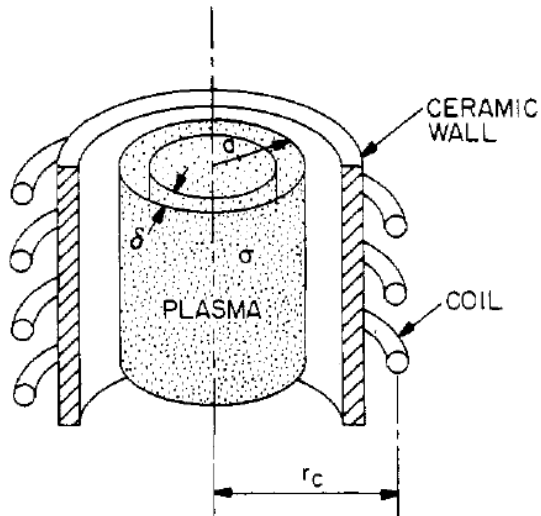
- In most industrial plasma,  $\frac{\omega\epsilon_0}{\sigma} \ll 1$ . Note that  $\sigma = \frac{e^2 n_e}{m_e \nu_c} = \frac{\epsilon_0 \omega_{pe}^2}{\nu_c}$  so  $\nu_c \omega \ll \omega_{pe}^2$  is required.

$$\alpha \approx \sqrt{\frac{\sigma\mu_0\omega}{2}} \quad (m^{-1})$$

skin depth: 
$$\delta \approx \sqrt{\frac{2}{\sigma\mu_0\omega}} = \frac{\sqrt{2}c}{\omega_{pe}} \sqrt{\frac{\nu_c}{\omega}} = \frac{c}{e} \sqrt{\frac{2m_e\epsilon_0}{n_e}} \sqrt{\frac{\nu_c}{\omega}} = \frac{c}{2\pi\nu_{pe}} \sqrt{\frac{\nu_c}{\pi f}} \quad (m)$$

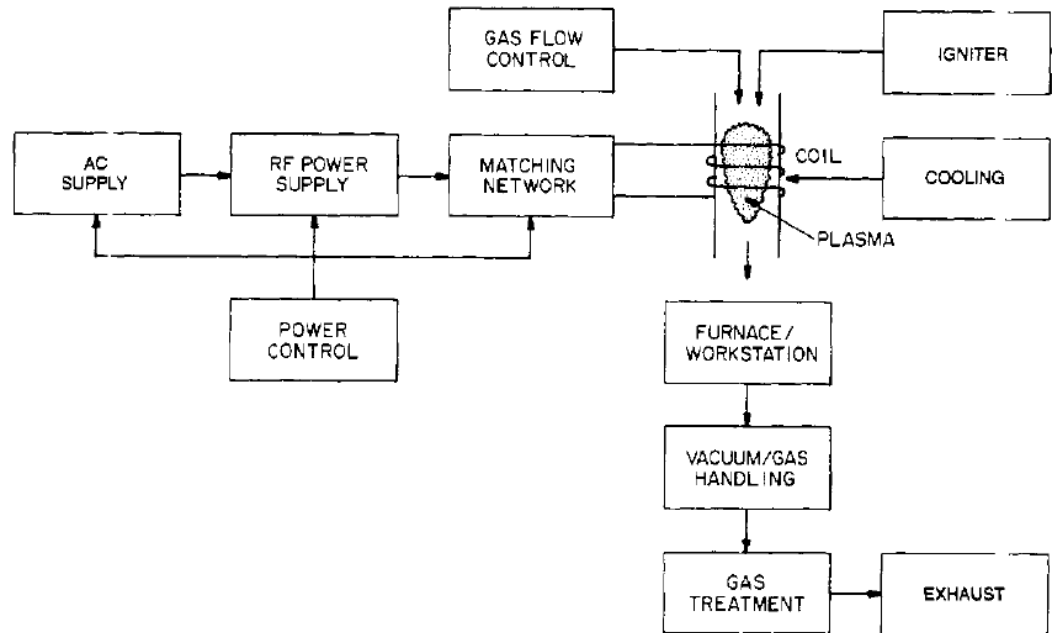
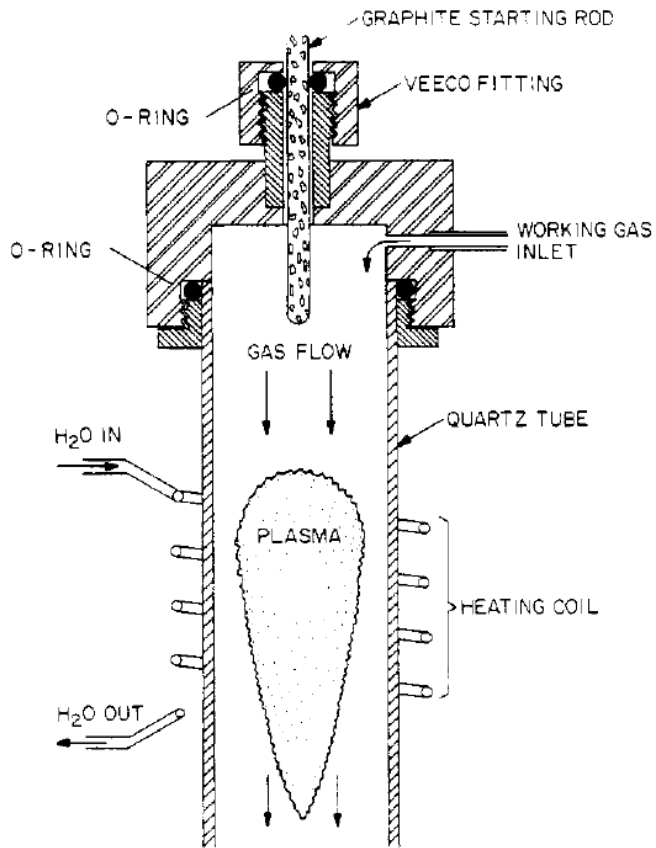
- The skin depth  $\delta$  ~ the distance that an electromagnetic wave propagates into a medium during one period of the electron plasma frequency.

# Skin depth needs to be carefully considered in the design of inductive industrial plasma reactors

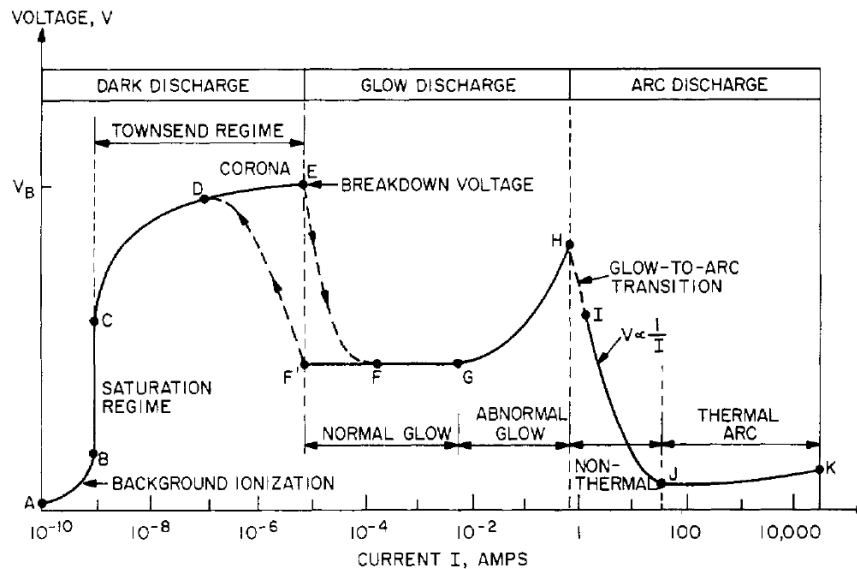
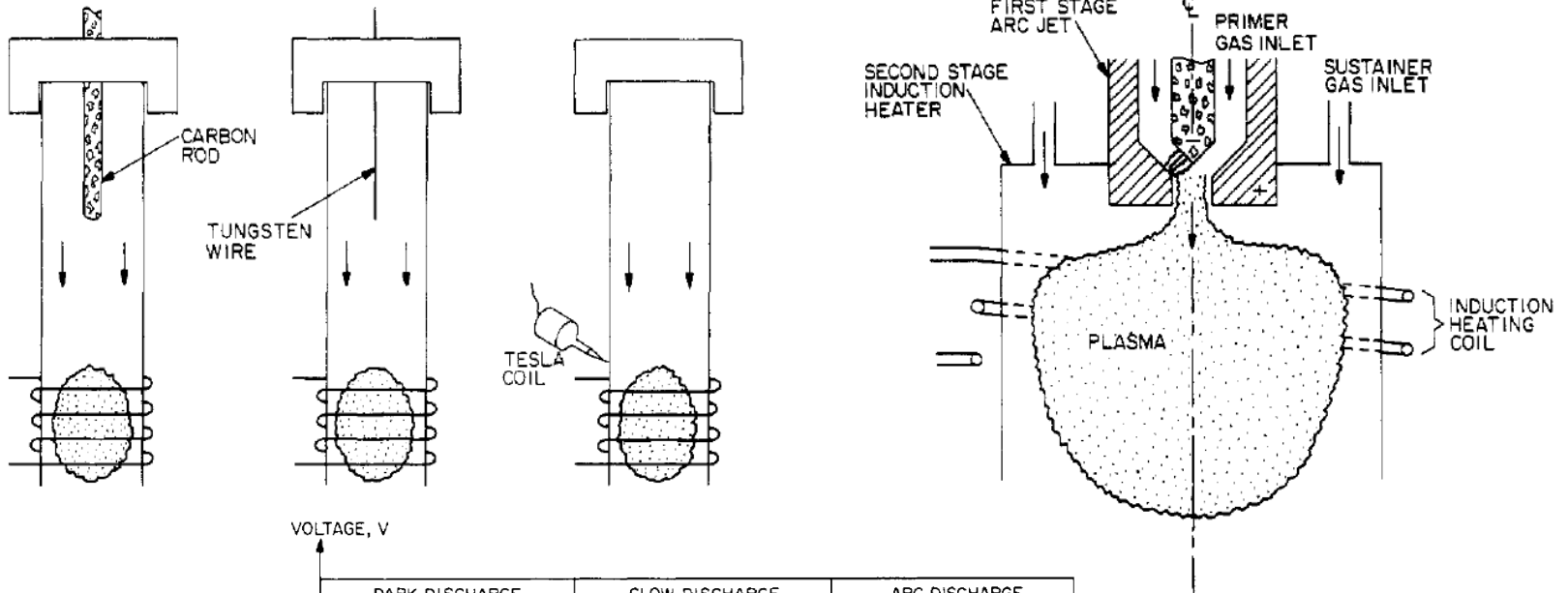


- **Boulos et al showed that the energy coupling parameter is maximum when  $1.5\delta \leq a \leq 3\delta$ . However, it doesn't mean the plasma will be uniformly heated.**

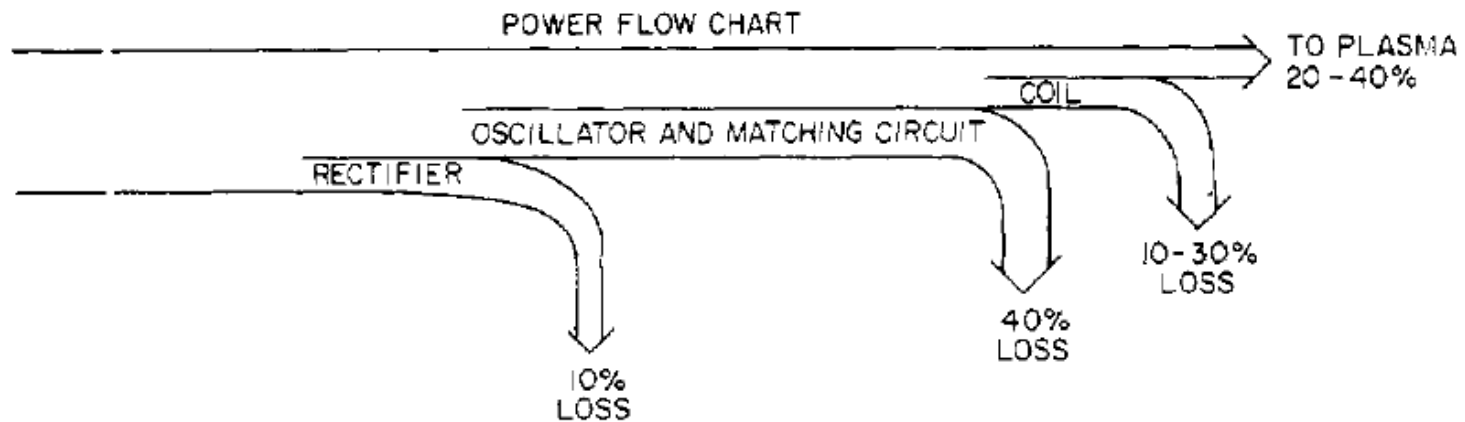
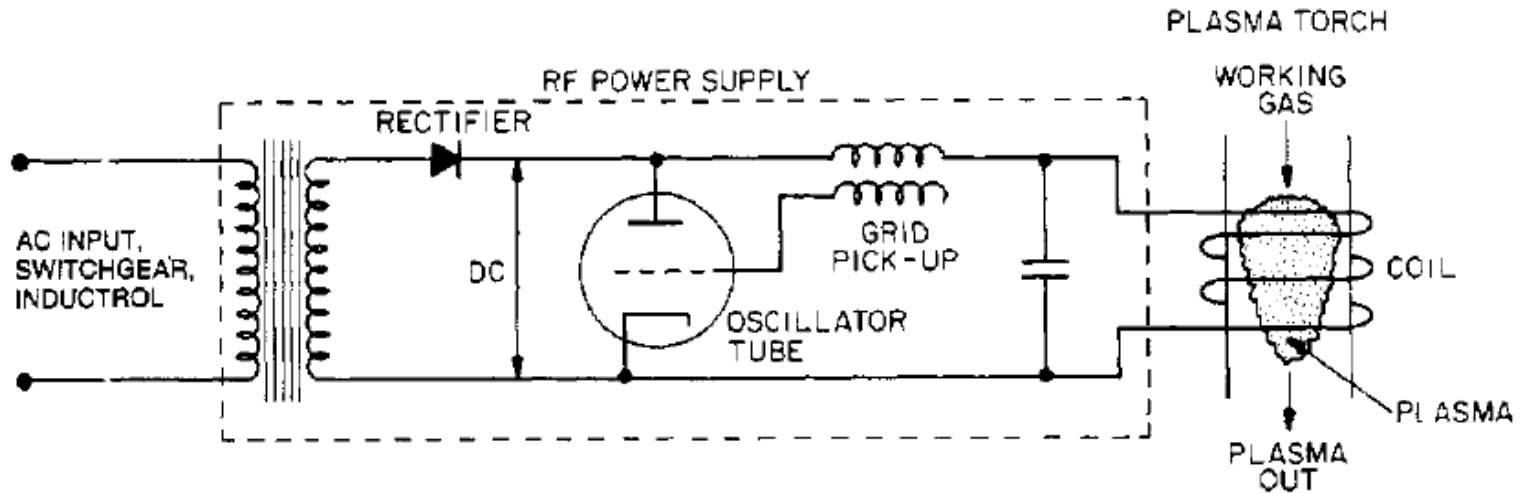
# A kilowatt-level inductively coupled plasma torch is shown



# High voltage initiation is usually required for inductive RF plasma torches



# The power supplies are relatively inefficient





# Operating regimes of inductively coupled plasma torches

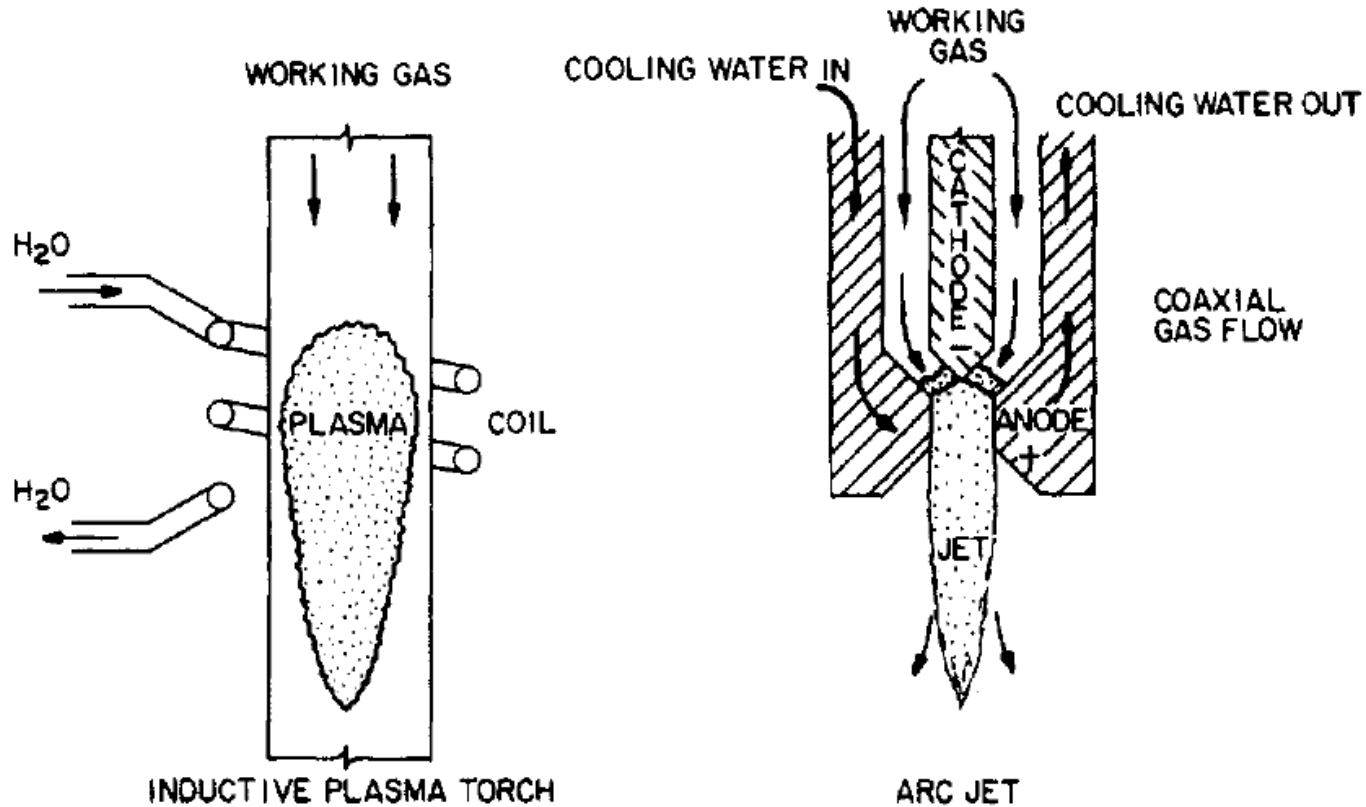


---

Parameter	Low	Characteristic	High
Frequency	10 kHz	13.56 MHz	100 MHz
Power	1 kW	30 kW	1MW
Efficiency	20%	35%	50%
Pressure	10 Torr	1 atm	10 atm
Gas temperature	1000 K	$10^4$ K	$2 \times 10^4$ K

---

# Inductive RF coupling provides a plasma with less contamination from the electrode

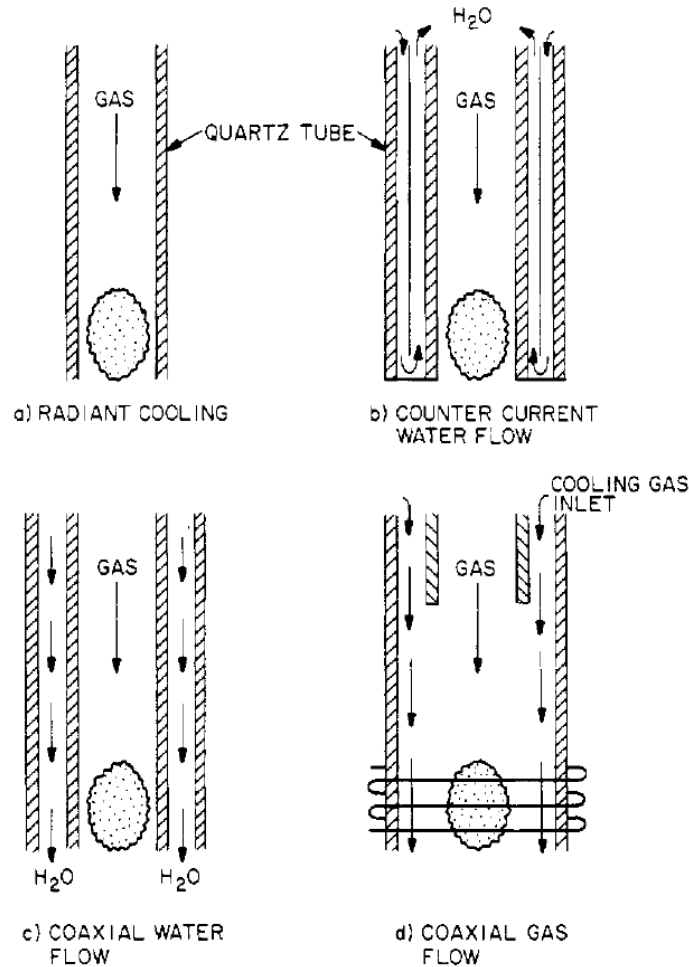


**INDUCTIVE PLASMA TORCH**  
 10 - 200 m/sec  
 4 - 40 mm  
 VARIABLE

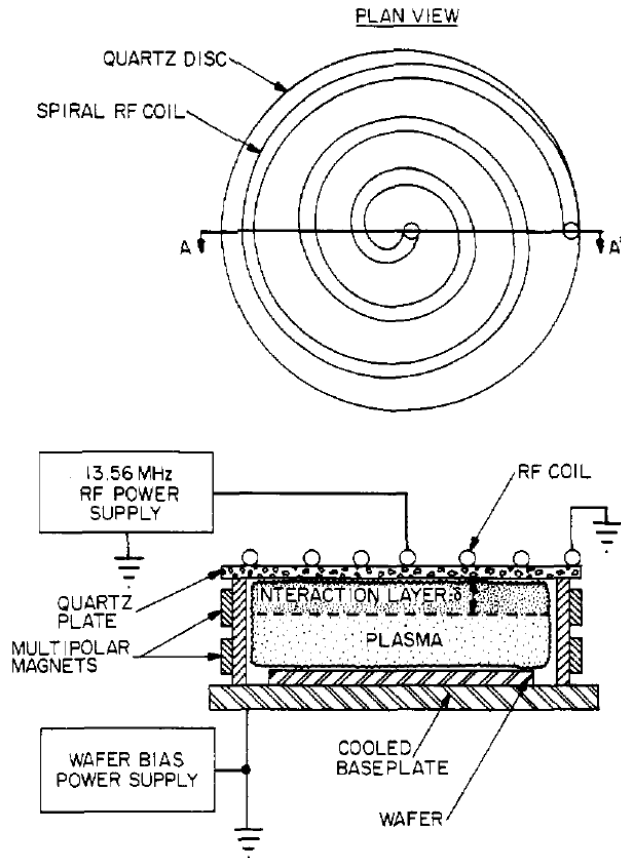
**JET VELOCITY**  
**JET DIAMETER**  
**JET SHAPE**

**ARC JET**  
 500 - 150 m/sec  
 6 - 10 mm  
 CYLINDRICAL

# Several cooling configurations are shown

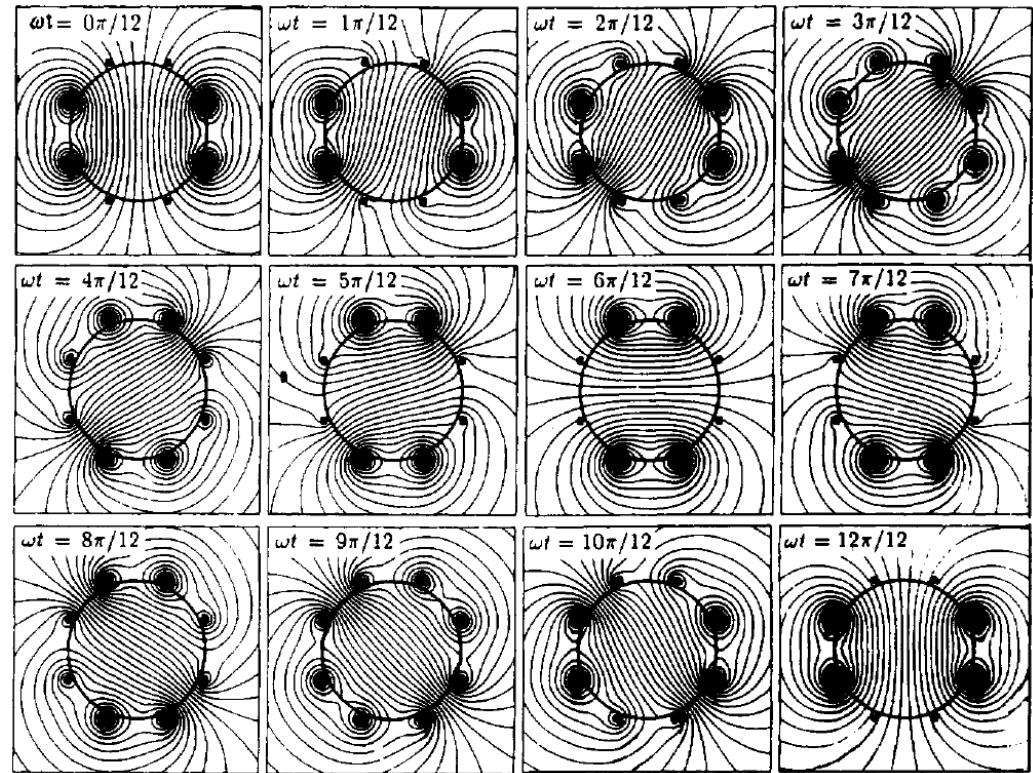
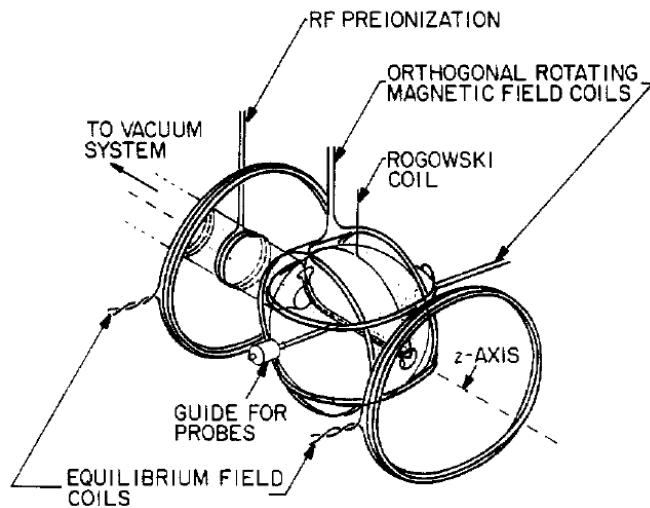


# Inductive parallel plate reactor



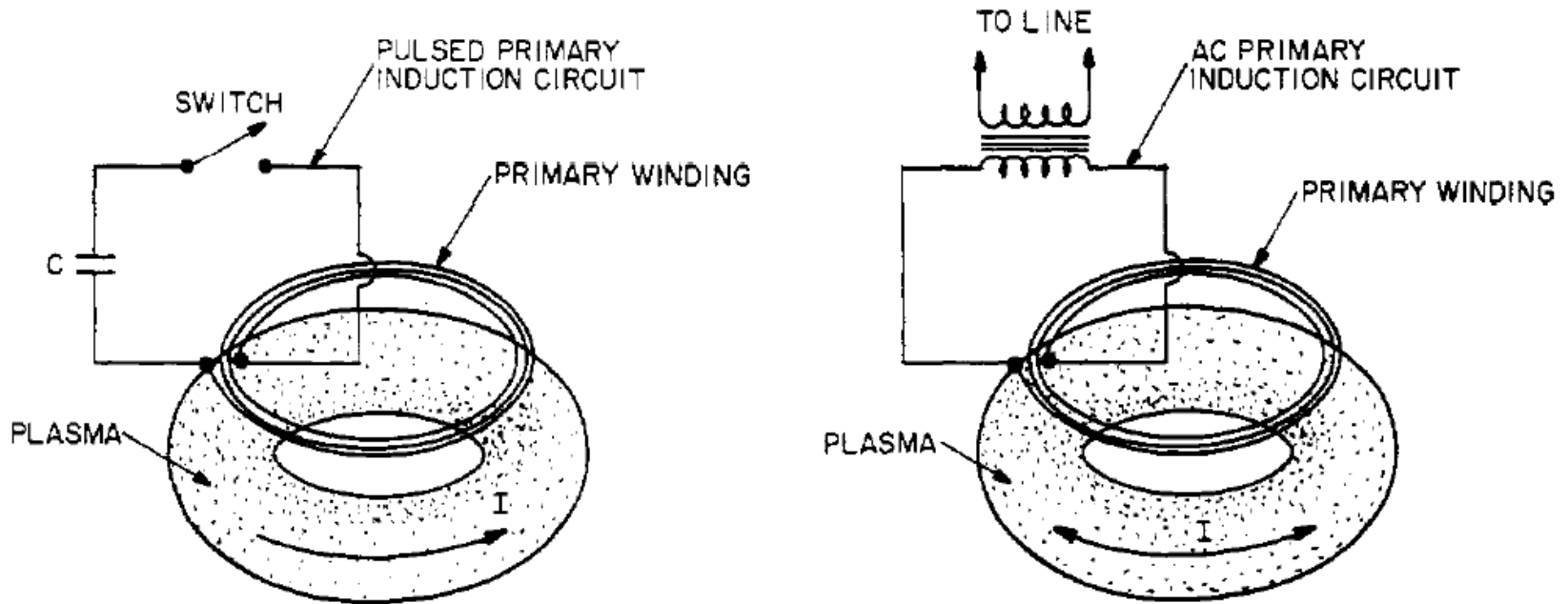
- **Uniform plasma source**
- **Higher power (2 kW) leading to higher plasma density (up to  $10^{18}$  electrons/m<sup>3</sup>)**
- **Lower gas pressure, i. e., longer mean free paths and little scattering of ions and is desired in deposition and etching applications.**

# Rotamak



- The rapidly rotating magnetic field generates large plasma currents, thus heating the plasma to densities and temperatures of interest in many industrial applications

# Inductively heated toroidal plasmas



- Large currents are induced in the plasma by transformer action from a ramped current in a pulsed primary induction circuit.

# Applications of inductive plasma torches

---



- **High purity materials production**
  - **Silica and other refractories**
  - **Ultrafine powder**
  - **Spherical fine powder**
  - **Refining/purification**
- **High temperature thermal treatment**
  - **Heat treatment**
  - **Plasma sintering**
- **Surface treatment**
  - **Oxidation**
  - **Nitriding**



# Applications of inductive plasma torches

---



- **Surface coating**
  - Plasma flame spraying
  - Surface coating of powder
- **Chemical vapor deposition (CVD)**
  - At atmospheric pressure
  - At reduced pressure
- **Chemical synthesis and processing**
- **Experimental applications**
  - Laboratory furnace
  - High intensity light source
  - Spectroscopic analysis
  - Isotope separation
  - Ion source
  - High power density plasma source

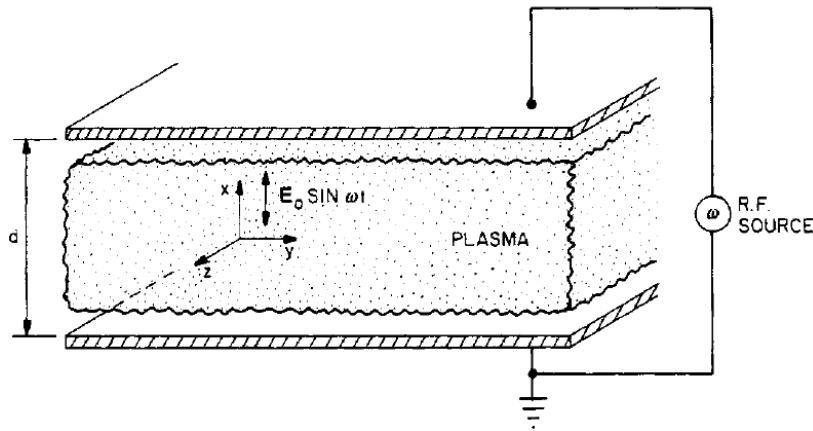
# AC electrical discharges deliver energy to the plasma without contact between electrodes and the plasma

---



- DC electrical discharge – a true current in the form of a flow of ions or electrons to the electrodes.
- AC electrical discharge – the power supply interacts with the plasma by displacement current.
  - Inductive radio frequency (RF) electrical discharges
  - **Capacitive RF electrical discharges**
  - Microwave electrical discharges
  - Dielectric-barrier discharges (DBDs)
- Other mechanism
  - Laser produced plasma
  - Pulsed-power generated plasma

# Capacitive RF coupling plasma without magnetic fields



$$\vec{F} = m \vec{a} = -\nu_c m \vec{v} - e \vec{E}$$

$$m \frac{dv_y}{dt} + m\nu_c v_y = 0$$

$$v_y(t) = v_{y0} \exp(-\nu_c t)$$

$$m \frac{d^2 x}{dt^2} + m\nu_c \frac{dx}{dt} = eE_0 \sin(\omega t)$$

$$x = C_1 \sin(\omega t) + C_2 \cos(\omega t)$$

$$C_1 = -\frac{eE_0}{m} \frac{1}{\omega^2 + \nu_c^2}$$

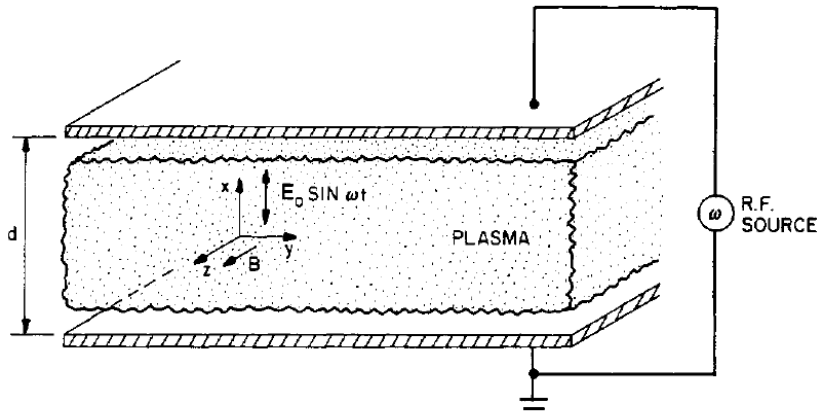
$$C_2 = -\frac{\nu_c eE_0}{\omega m} \frac{1}{\omega^2 + \nu_c^2}$$

$$v_x(t) = -\frac{eE_0 \omega}{m(\omega^2 + \nu_c^2)} \left[ \cos(\omega t) - \frac{\nu_c}{\omega} \sin(\omega t) \right]$$

$$P = \frac{dW}{dt} = eE_0 \sin(\omega t) v_x$$

$$\bar{P}_{\text{tot}} = n_e \bar{P} = \frac{1}{4} \epsilon_0 E_0^2 \frac{2n_e e^2}{m \epsilon_0} \frac{\nu_c}{\omega^2 + \nu_c^2}$$

# Capacitive RF coupling plasma with magnetic fields



$$\frac{d^2x}{dt^2} + \nu_c \frac{dx}{dt} + \omega_c \frac{dy}{dt} = -\frac{eE_0}{m} \sin(\omega t)$$

$$\frac{d^2y}{dt^2} + \nu_c \frac{dy}{dt} - \omega_c \frac{dx}{dt} = 0 \quad \omega_c = \frac{eB}{m}$$

$$\vec{F} = m \vec{a} = -\nu_c m \vec{v} - e(\vec{v} \times \vec{B}) - e\vec{E}$$

$$x = C_1 \sin(\omega t) + C_2 \cos(\omega t)$$

$$m \frac{d^2x}{dt^2} + m\nu_c \frac{dx}{dt} + eB \frac{dy}{dt} = -eE_0 \sin(\omega t)$$

$$y = C_3 \sin(\omega t) + C_4 \cos(\omega t)$$

$$m \frac{dv_y}{dt} + m\nu_c v_y - eB \frac{dx}{dt} = 0$$

$$C_1 = -\frac{eE_0}{2m} \left[ \frac{\omega + \omega_c}{(\omega + \omega_c)^2 + \nu_c^2} + \frac{\omega - \omega_c}{(\omega - \omega_c)^2 + \nu_c^2} \right]$$

$$m \frac{dv_z}{dt} + m\nu_c v_z = 0$$

$$C_2 = -\frac{\nu_c eE_0}{2\omega m} \left[ \frac{1}{(\omega + \omega_c)^2 + \nu_c^2} + \frac{1}{(\omega - \omega_c)^2 + \nu_c^2} \right]$$

$$v_z(t) = v_{z0} \exp(-\nu_c t)$$

$$C_3 = \frac{\omega_c (C_1 \nu_c + C_2 \omega)}{\omega^2 + \nu_c^2} \quad C_4 = -\frac{\omega_c (C_1 \omega - C_2 \nu_c)}{\omega^2 + \nu_c^2}$$

# The coupling efficient for capacitive RF with magnetic fields is less than DC electrical discharge



$$P = \frac{dW}{dt} = eE_0 \sin(\omega t) v_x$$

$$\begin{aligned} \bar{P}_{\text{tot}} = n_e \bar{P} &= \frac{1}{4} \epsilon_0 E_0^2 \frac{n_e e^2}{m \epsilon_0} v_c \left[ \frac{1}{(\omega + \omega_c)^2 + \nu_c^2} + \frac{1}{(\omega - \omega_c)^2 + \nu_c^2} \right] \\ &= \frac{1}{4} \epsilon_0 E_0^2 \times \omega_{pe}^2 v_c \left[ \frac{1}{(\omega + \omega_c)^2 + \nu_c^2} + \frac{1}{(\omega - \omega_c)^2 + \nu_c^2} \right] \end{aligned}$$

- DC, unmagnetized discharge ( $\omega = \omega_c = 0$ ):  $v_{*0} = \frac{2\omega_{pe}^2}{\nu_c}$
- Low collisionality ( $\omega_c \gg \nu_c$ ):  

$$v_* \approx v_{*0} \nu_c^2 \left[ \frac{\omega^2 + \omega_c^2}{(\omega^2 - \omega_c^2)^2} \right] \rightarrow v_{*0} \frac{\nu_c^2}{\omega_c^2} \ll v_{*0} \quad (\omega, \nu_c \ll \omega_c)$$
- High collisionality ( $\omega_c \ll \nu_c$ ):  

$$v_* \approx v_{*0} \frac{\nu_c^2}{\omega^2 + \nu_c^2} \approx v_{*0} (\omega, \omega_c \ll \nu_c)$$
- Resonant ( $\omega = \omega_c$ ):

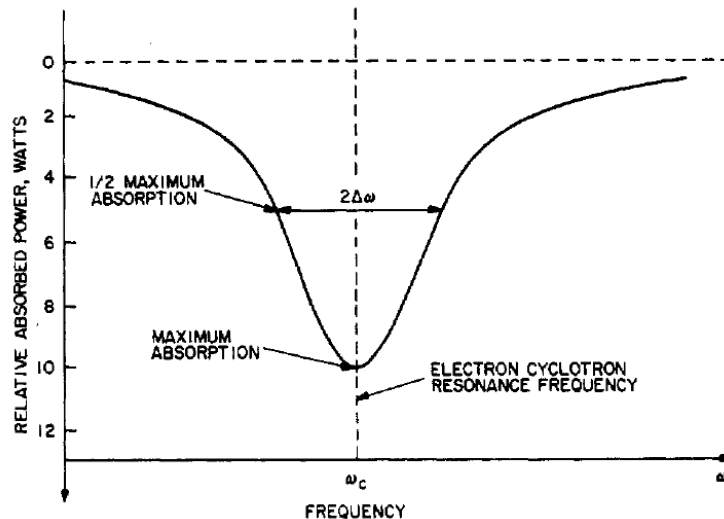
$$v_* = v_{*0} \frac{2\omega_c^2 + \nu_c^2}{4\omega_c^2 + \nu_c^2} \rightarrow \frac{1}{2} v_{*0} (\omega = \omega_c \gg \nu_c)$$

# Collision frequency can be measured using capacitive RF electrical discharges



$$\bar{P}(\omega_c) = \frac{1}{4} \epsilon_0 E_0^2 \times v_{*0} \frac{2 + (v_c/\omega_c)^2}{4 + (v_c/\omega_c)^2} = \frac{1}{4} \epsilon_0 E_0^2 \times v_{*0} \frac{2 + \epsilon^2}{4 + \epsilon^2}$$

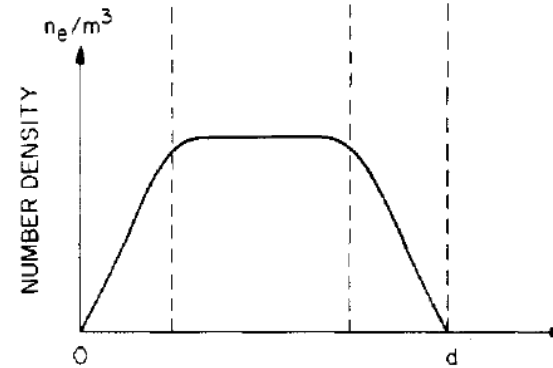
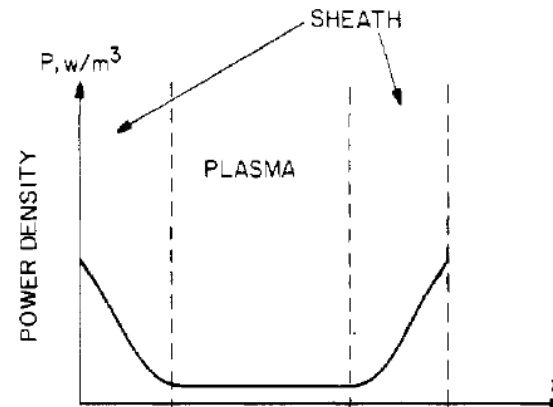
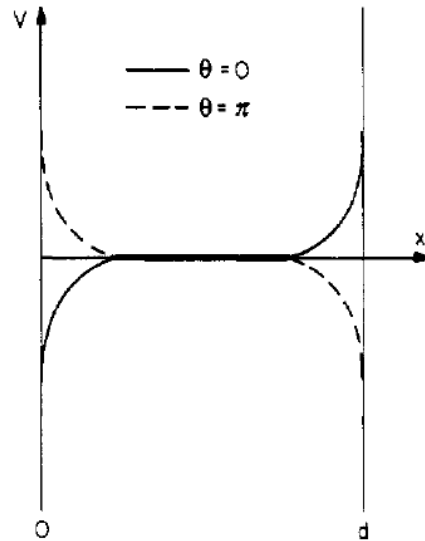
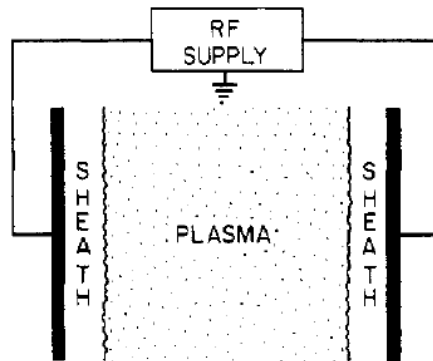
$$\begin{aligned} \bar{P}(\omega_c \pm \Delta\omega) &= \frac{1}{4} \epsilon_0 E_0^2 \times \frac{v_{*0}}{2} \left( \frac{v_c}{\omega_c} \right)^2 \left[ \frac{1}{(2 \pm \Delta\omega/\omega_c)^2 + (v_c/\omega_c)^2} + \frac{1}{(\Delta\omega/\omega_c)^2 + (v_c/\omega_c)^2} \right] \\ &= \frac{1}{4} \epsilon_0 E_0^2 \times \frac{v_{*0}}{2} \epsilon^2 \left[ \frac{1}{(2 \pm \delta)^2 + \epsilon^2} + \frac{1}{\delta^2 + \epsilon^2} \right] \quad \text{where } \delta \equiv \frac{\Delta\omega}{\omega_c}, \epsilon \equiv \frac{v_c}{\omega_c} \end{aligned}$$



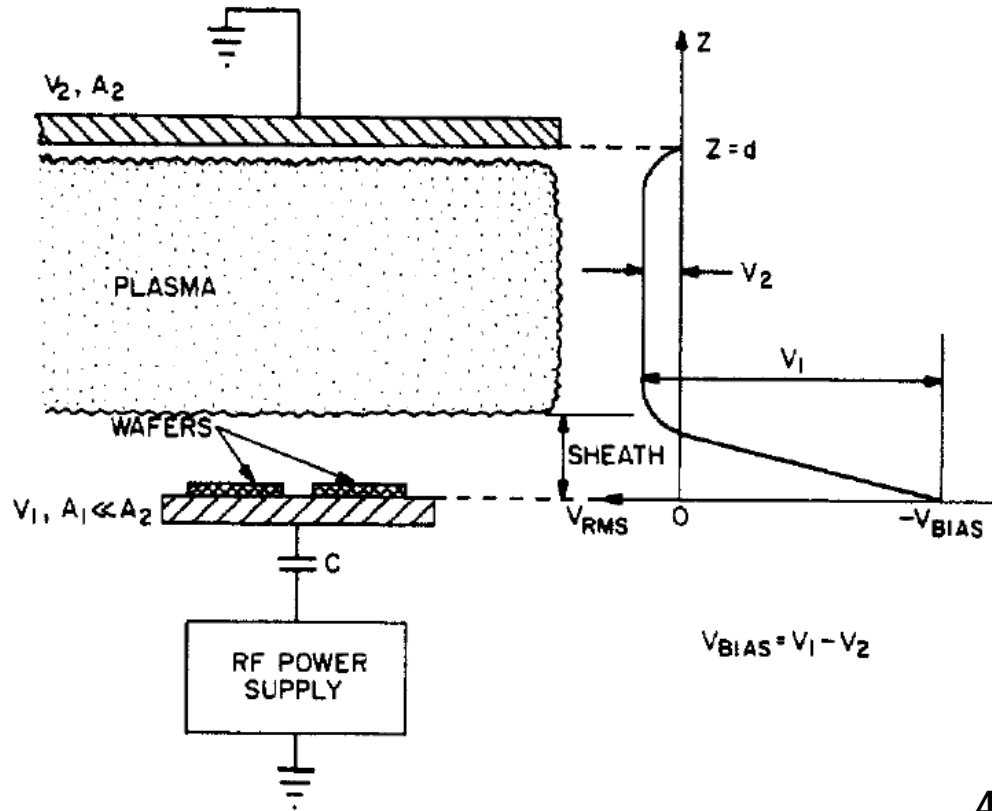
For  $\delta \approx \epsilon \ll 1$ ,

$$\bar{P}(\omega_c \pm v_c) = \frac{1}{2} \bar{P}(\omega_c)$$

# Symmetrical capacitive RF discharge model



# Empirical scaling of electrode voltage drop



$$I_1 = A_1 J_1 = A_1 e n_{i1} \bar{v}_{i1}$$

$$I_2 = A_2 J_2 = A_2 e n_{i2} \bar{v}_{i2}$$

$$\bar{v}_{i1} = \sqrt{\left(\frac{2eV_1}{m_i}\right)}$$

$$\bar{v}_{i2} = \sqrt{\left(\frac{2eV_2}{m_i}\right)}$$

Assuming:  $I_1 = I_2$      $n_{i1} = n_{i2}$

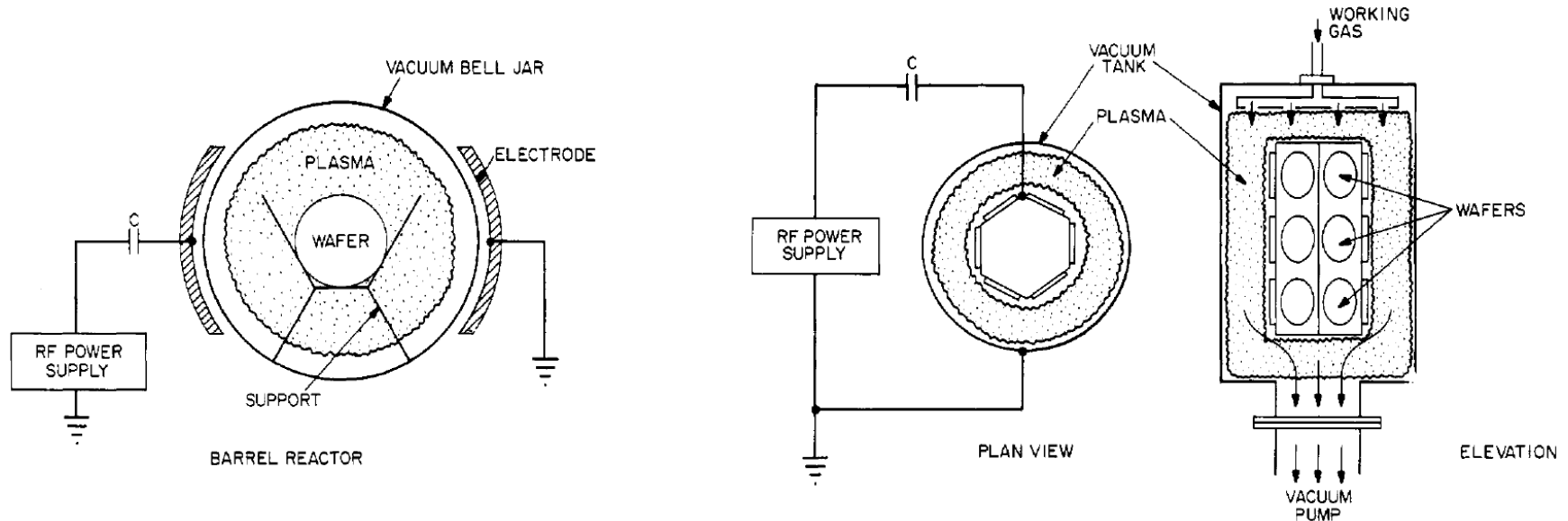
$$A_1 e n_{i1} \sqrt{\left(\frac{2eV_1}{m_i}\right)} = A_2 e n_{i2} \sqrt{\left(\frac{2eV_2}{m_i}\right)}$$

$$\frac{V_1}{V_2} = \left(\frac{A_2}{A_1}\right)^2$$

$$\frac{V_1}{V_2} = \left(\frac{A_2}{A_1}\right)^q \text{ where } 1.0 \leq q \leq 2.5$$



# Example of capacitively coupled RF plasma source 1



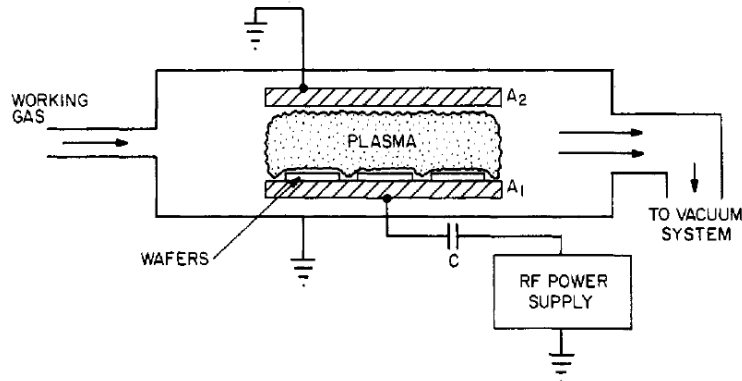
- **Barrier reactor – the wafers float electrically and have low ion bombardment energies**

- **Hexagonal reactor – the wafers develop a DC bias which leads to a relatively anisotropic, vertical etch.**

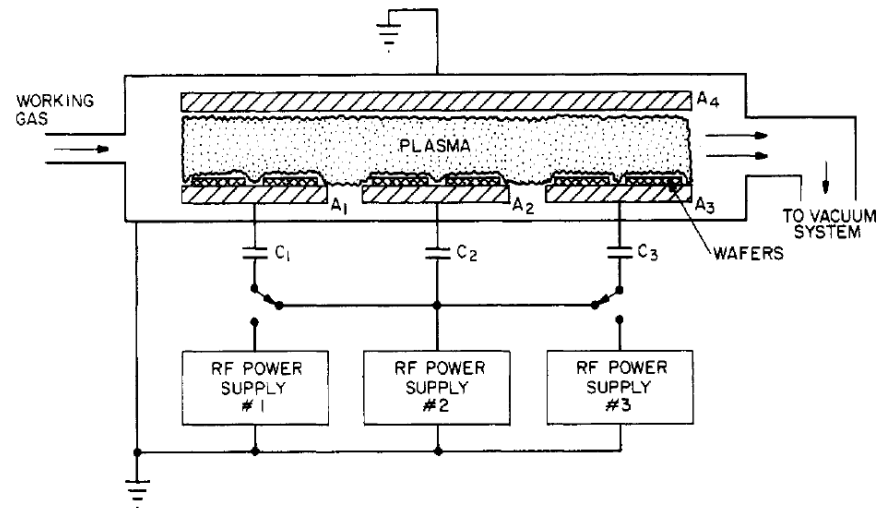
# Example of capacitively coupled RF plasma source 2



- Plane parallel reactor



- Multiple electrode system



# Operating regimes of capacitively coupled plasma reactors used for plasma processing



Parameter	Low value	Typical value	High value
Frequency	1 kHz	13.56 MHz	100 MHz
Gas pressure	3 mTorr	300 mTorr	5 Torr
Power level	50 W	$\approx 200$ W	500 W
rms electrode voltage	100 V	$\approx 300$ V	1000 V
Current density	0.1 mA/cm <sup>2</sup>	$\approx 3$ mA/cm <sup>2</sup>	10 mA/cm <sup>2</sup>
Electron temperature, $T_e$	3 eV	$\approx 5$ eV	8 eV
Electron density, $n_e$	10 <sup>15</sup> /m <sup>3</sup>	$\approx 5 \times 10^{15}$ /m <sup>3</sup>	3 $\times 10^{17}$ /m <sup>3</sup>
Ion energy, $\mathcal{E}_i$	5 eV	50 eV	500 eV
Electrode separation, $d$	0.5 cm	4 cm	30 cm

# AC electrical discharges deliver energy to the plasma without contact between electrodes and the plasma

---



- DC electrical discharge – a true current in the form of a flow of ions or electrons to the electrodes.
- AC electrical discharge – the power supply interacts with the plasma by displacement current.
  - Inductive radio frequency (RF) electrical discharges
  - Capacitive RF electrical discharges
  - **Microwave electrical discharges**
  - Dielectric-barrier discharges (DBDs)
- Other mechanism
  - Laser produced plasma
  - Pulsed-power generated plasma

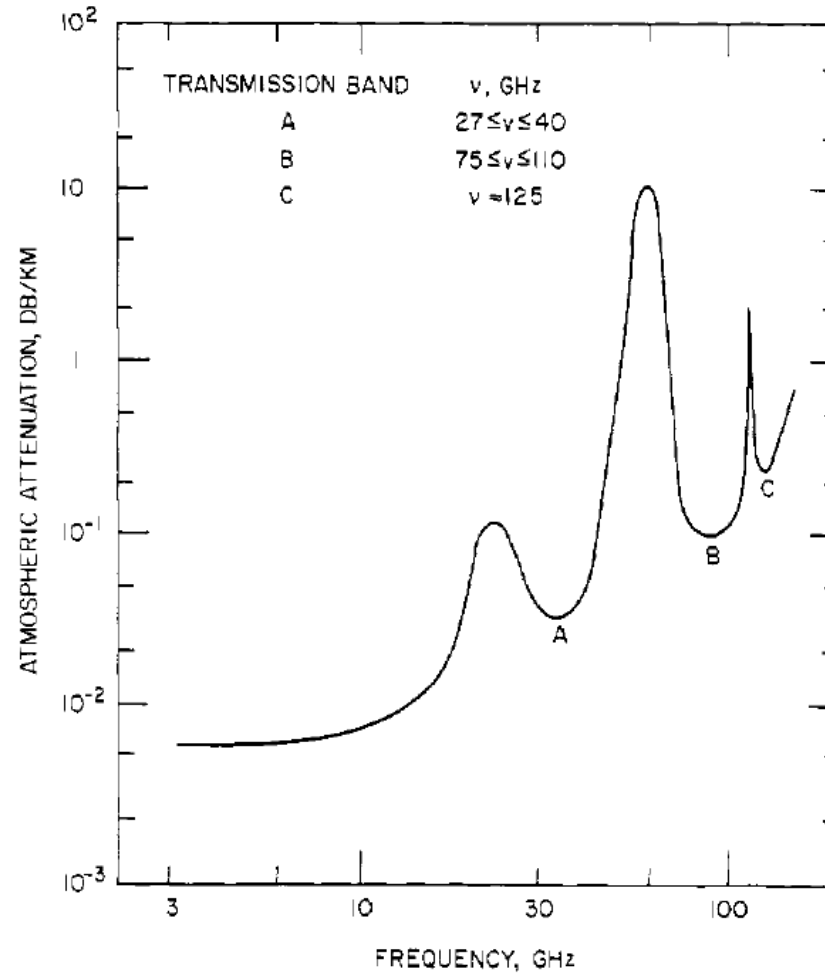
# Advantage of using microwave electrical discharges

---

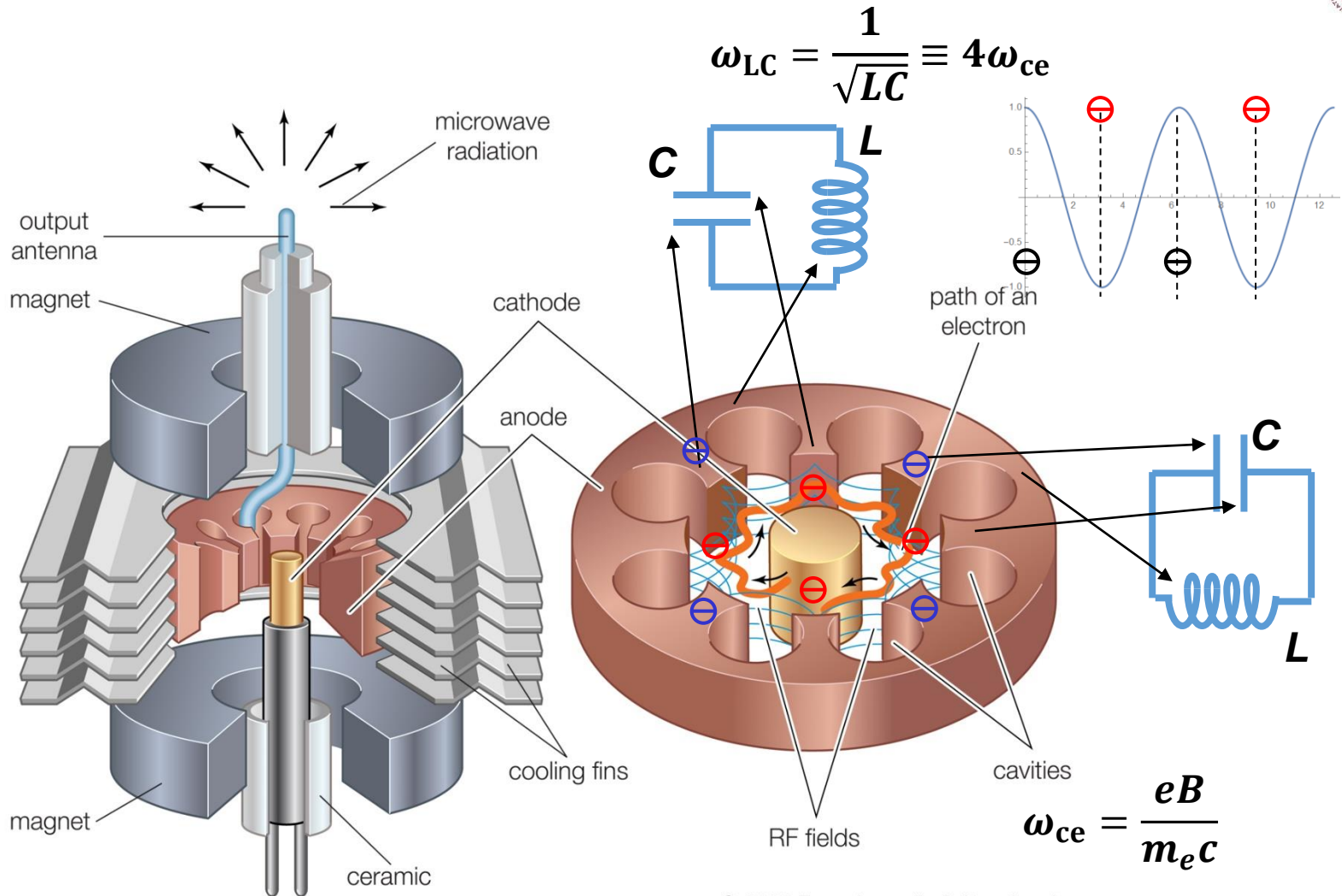


- The wavelength of the microwave is in centimeters range. In contrast, the wavelength is 22 m for RF frequency  $f = 13.6$  MHz.
- The electron number density can approach the critical number density. ( $7 \times 10^{16} \text{ m}^{-3}$ ) at a frequency of 2.45 GHz.
- The plasma in microwave discharges is quasi-optical to microwave.
- Microwave-generated plasmas have a higher electron kinetic temperature (5 ~ 15 eV) than DC or low frequency RF-generated plasmas (1 or 2 eV).
- Capable of providing a higher fraction of ionization.
- Do not have a high voltage sheath.
- No internal electrodes.

# Microwave frequency is determined for those used in communications and radar purposes

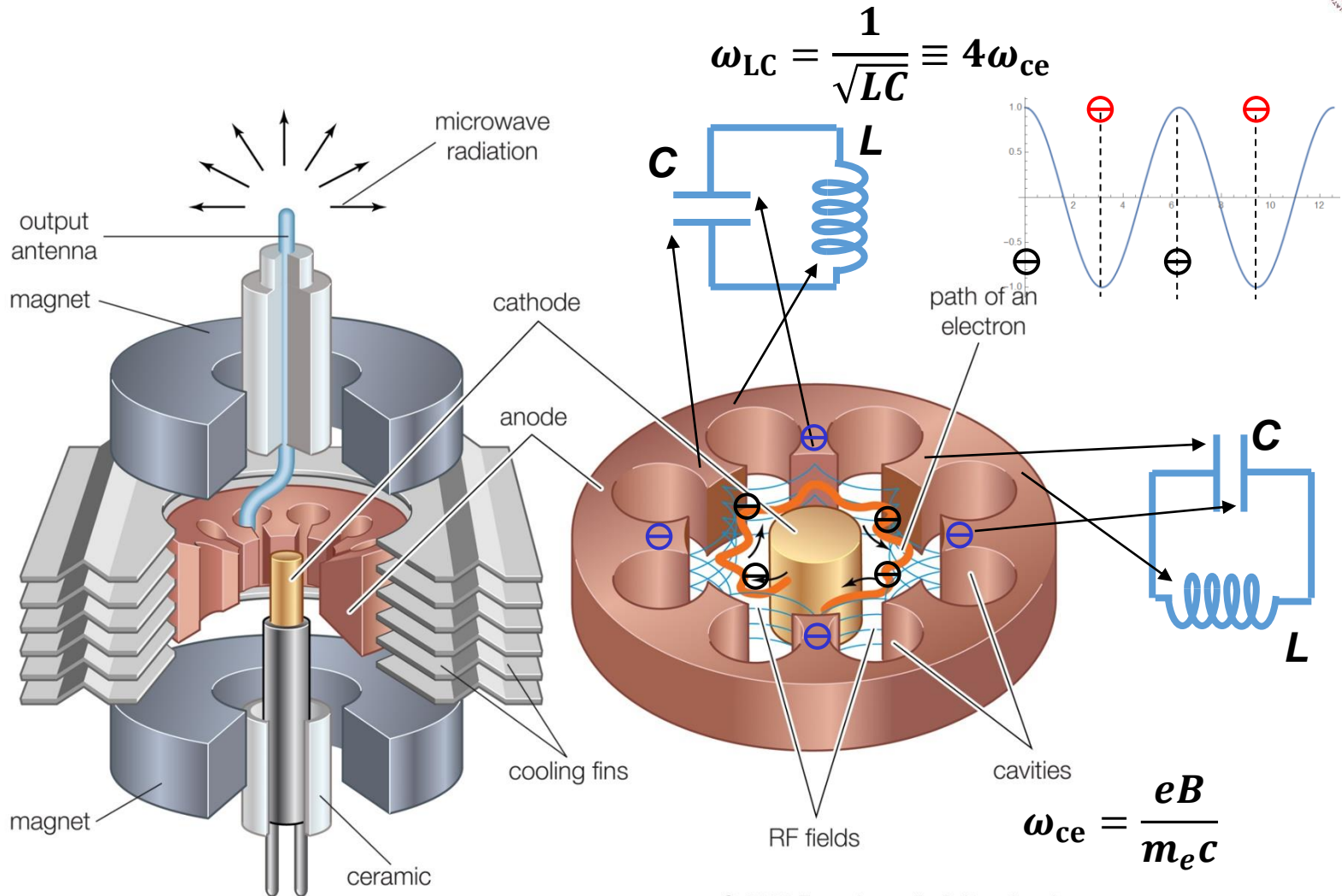


# Internal of a magnetron



© 2010 Encyclopædia Britannica, Inc.

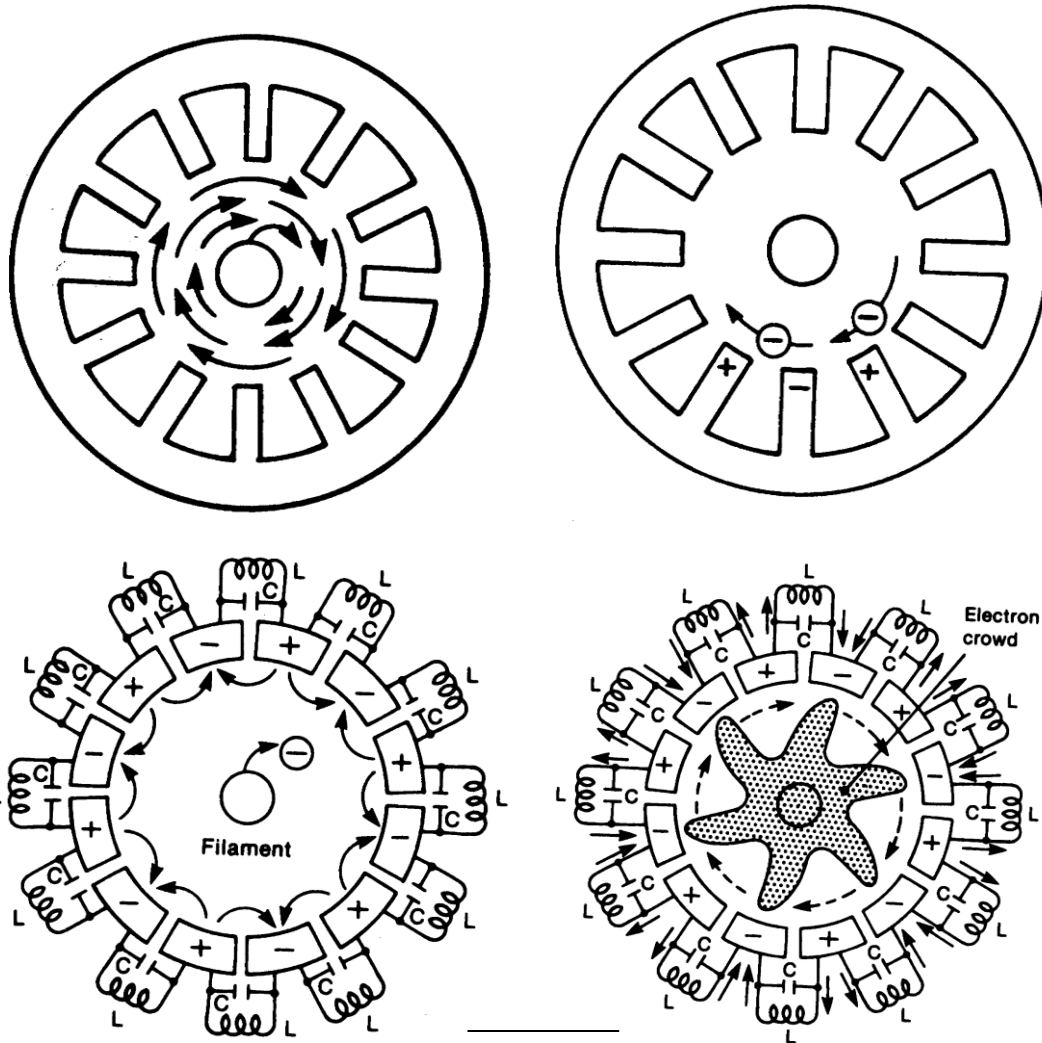
# Internal of a magnetron



© 2010 Encyclopædia Britannica, Inc.

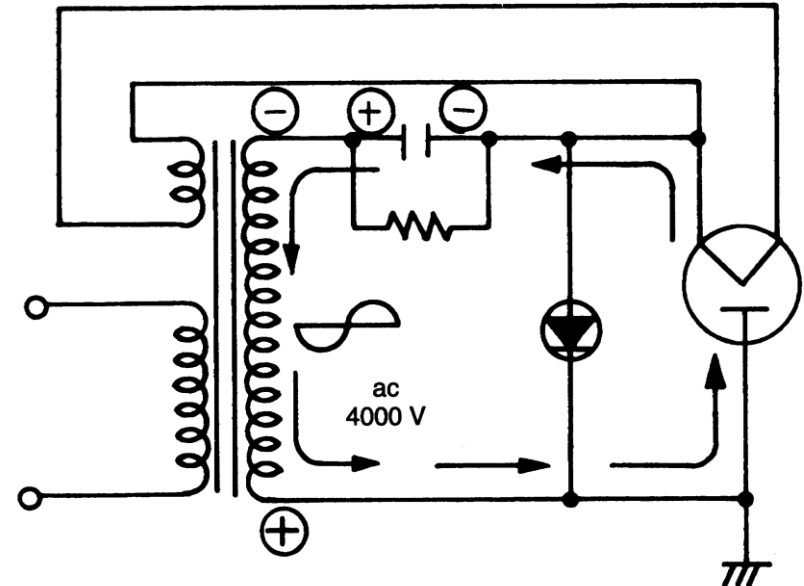
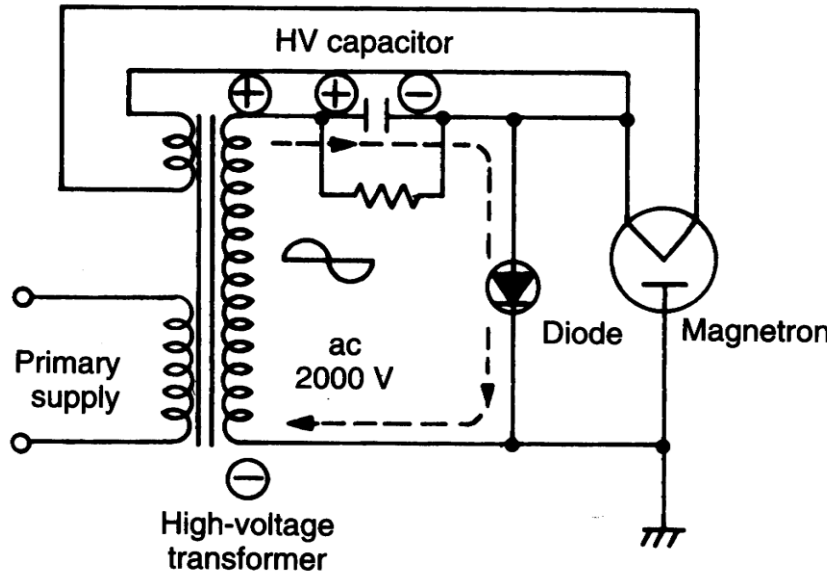


# Resonance in a magnetron



[http://cdn.preterhuman.net/texts/government\\_information/intelligence\\_and\\_espionage/homebrew.military.and.espionage.electronics/servv89pn0aj.sn.sourcedns.com/\\_gbpprorg/mil/herf1/index.html](http://cdn.preterhuman.net/texts/government_information/intelligence_and_espionage/homebrew.military.and.espionage.electronics/servv89pn0aj.sn.sourcedns.com/_gbpprorg/mil/herf1/index.html)

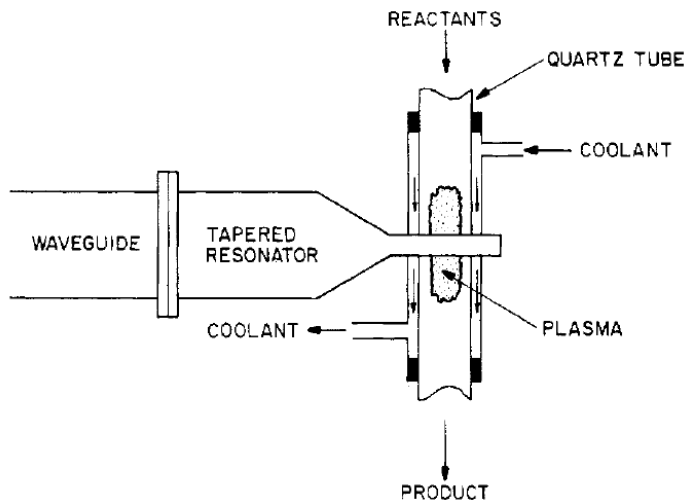
# Magnetron schematic diagram



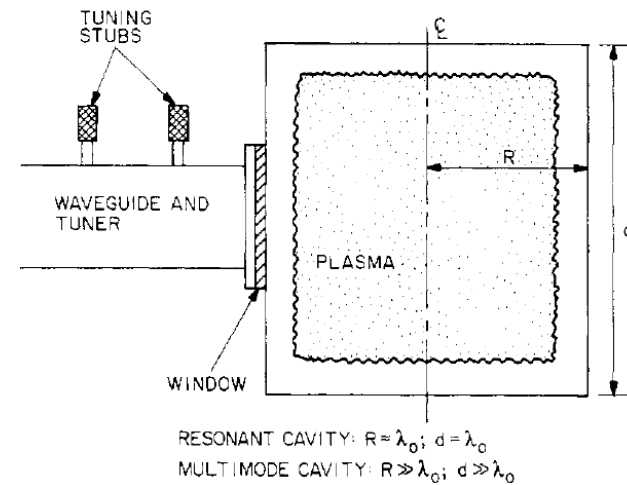
# Microwave plasma reactor configurations



- Waveguide coupled reactor



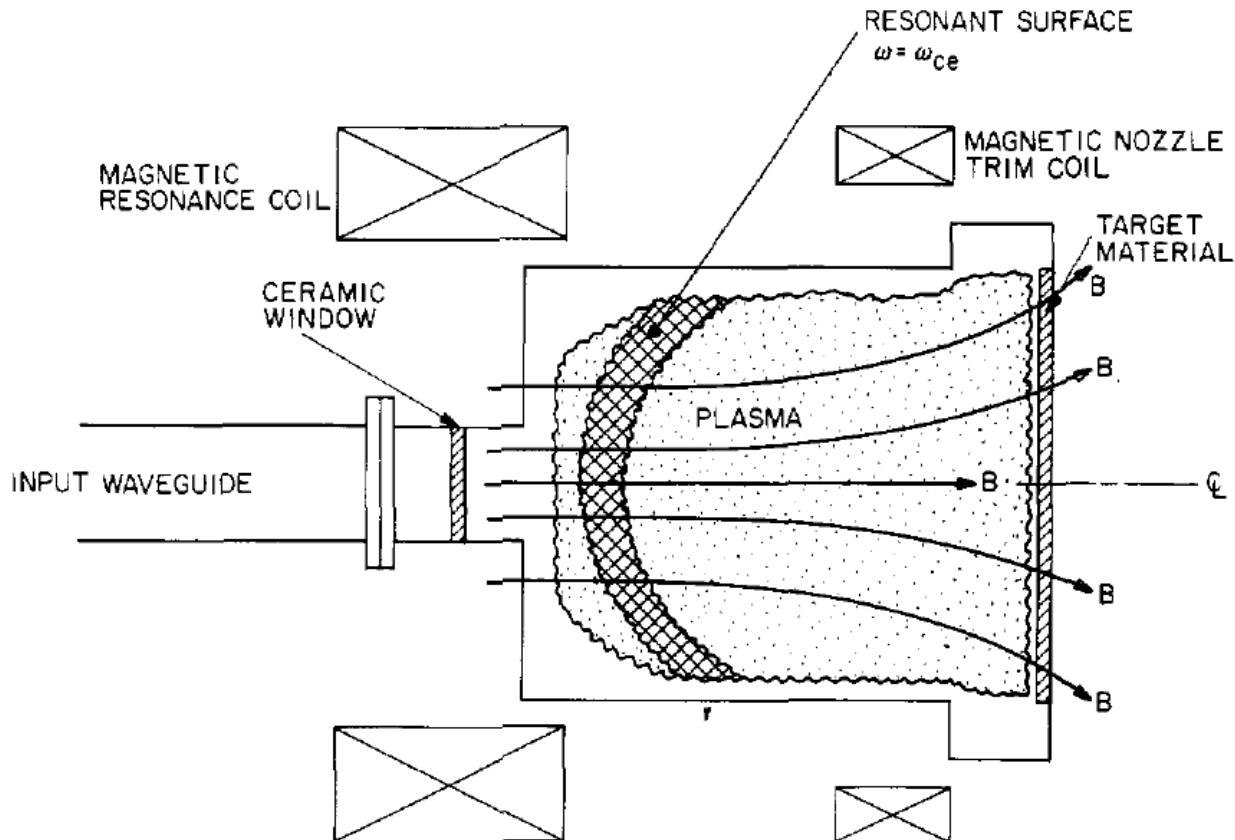
- Resonant or multimode cavity – if the impedance matching is good, more energy can be fed into the cavity.



# Strong absorption occurs when the frequency matches the electron cyclotron frequency



- Electron cyclotron resonance (ECR) plasma reactor



# Electron cyclotron frequency depends on magnetic field only



$$m_e \frac{d\vec{v}}{dt} = -\frac{e}{c} \vec{v} \times \vec{B}$$

- Assuming  $\vec{B} = B\hat{z}$  and the electron oscillates in x-y plane

$$m_e \dot{v}_x = -\frac{e}{c} B v_y \quad m_e \dot{v}_z = 0$$

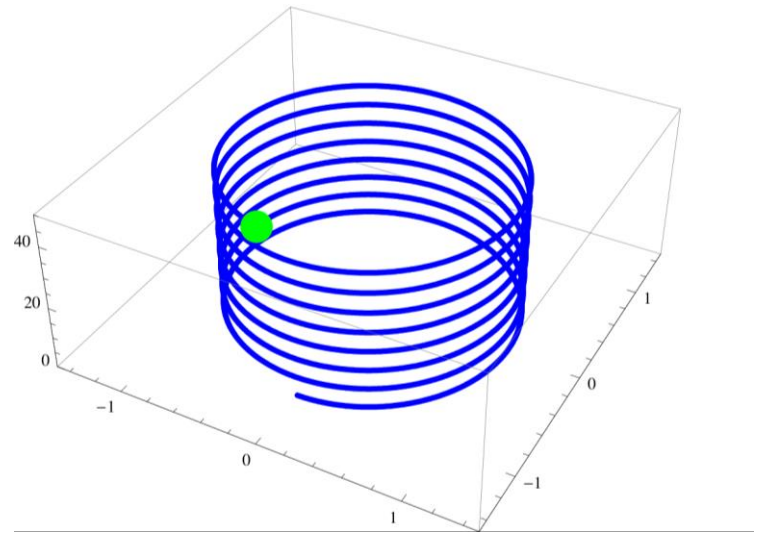
$$m_e \dot{v}_y = \frac{e}{c} B v_x$$

$$\ddot{v}_x = -\frac{eB}{m_e c} \dot{v}_y = -\left(\frac{eB}{m_e c}\right)^2 v_x$$

$$\ddot{v}_y = -\frac{eB}{m_e c} \dot{v}_x = -\left(\frac{eB}{m_e c}\right)^2 v_y$$

- Therefore

$$\omega_{ce} = \frac{eB}{m_e c}$$



# Electrons keep getting accelerated when a electric field rotates in electron's gyrofrequency



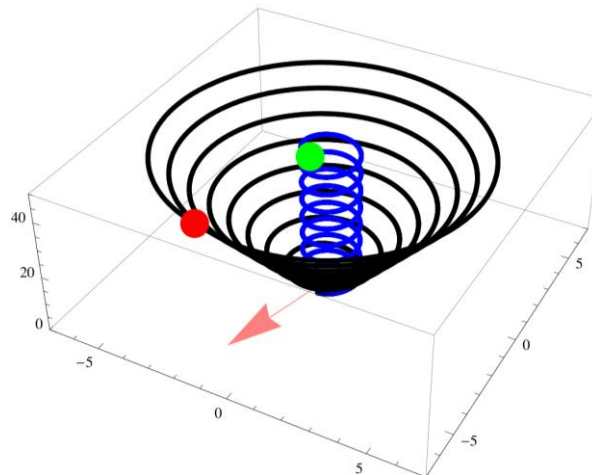
$$m_e \frac{d\vec{v}}{dt} = -\frac{e}{c} \vec{v} \times \vec{B} - e \vec{E} \quad \vec{B} = B_0 \hat{z} \quad \vec{E} = E_0 [\hat{x} \cos(\omega t) + \hat{y} \sin(\omega t)]$$

$$m_e \dot{v}_x = -\frac{e}{c} B v_y + E_0 \cos(\omega t) \quad m_e \dot{v}_y = \frac{e}{c} B v_x + E_0 \sin(\omega t) \quad m_e \dot{v}_z = 0$$

$$\ddot{v}_x = -\frac{eB}{m_e c} \dot{v}_y - \frac{E_0}{m_e} \omega \cos(\omega t) = -\omega_{ce}^2 v_x - \frac{E_0}{m_e} (\omega_{ce} + \omega) \cos(\omega t)$$

$$\ddot{v}_y = -\frac{eB}{m_e c} \dot{v}_x + \frac{E_0}{m_e} \omega \sin(\omega t) = -\omega_{ce}^2 v_y + \frac{E_0}{m_e} (\omega_{ce} + \omega) \sin(\omega t)$$

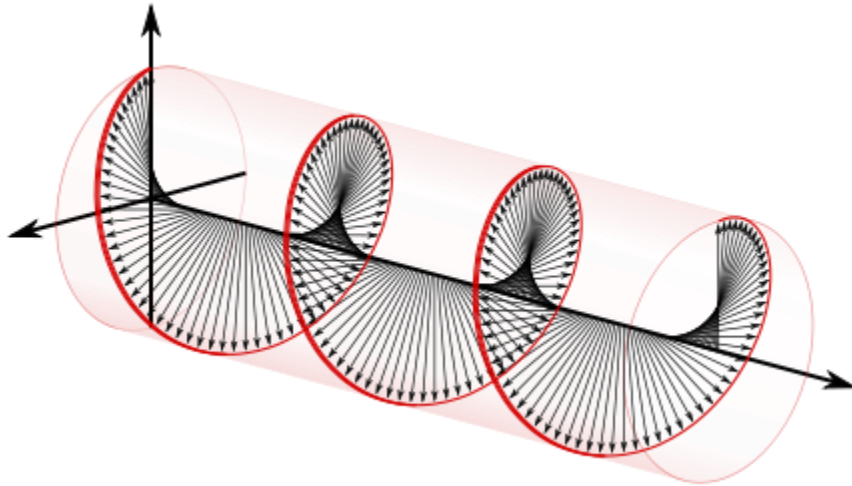
$$\omega_{ce} = \frac{eB}{m_e c}$$



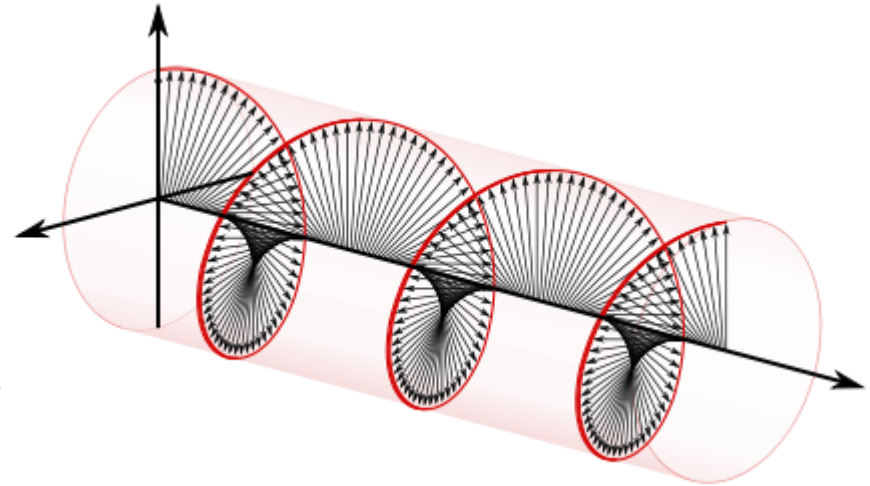
# Electric field in a circular polarized electromagnetic wave keeps rotating as the wave propagates



- Right-handed polarization



- Left-handed polarization



# Only right-handed polarization can resonance with electron's gyromotion

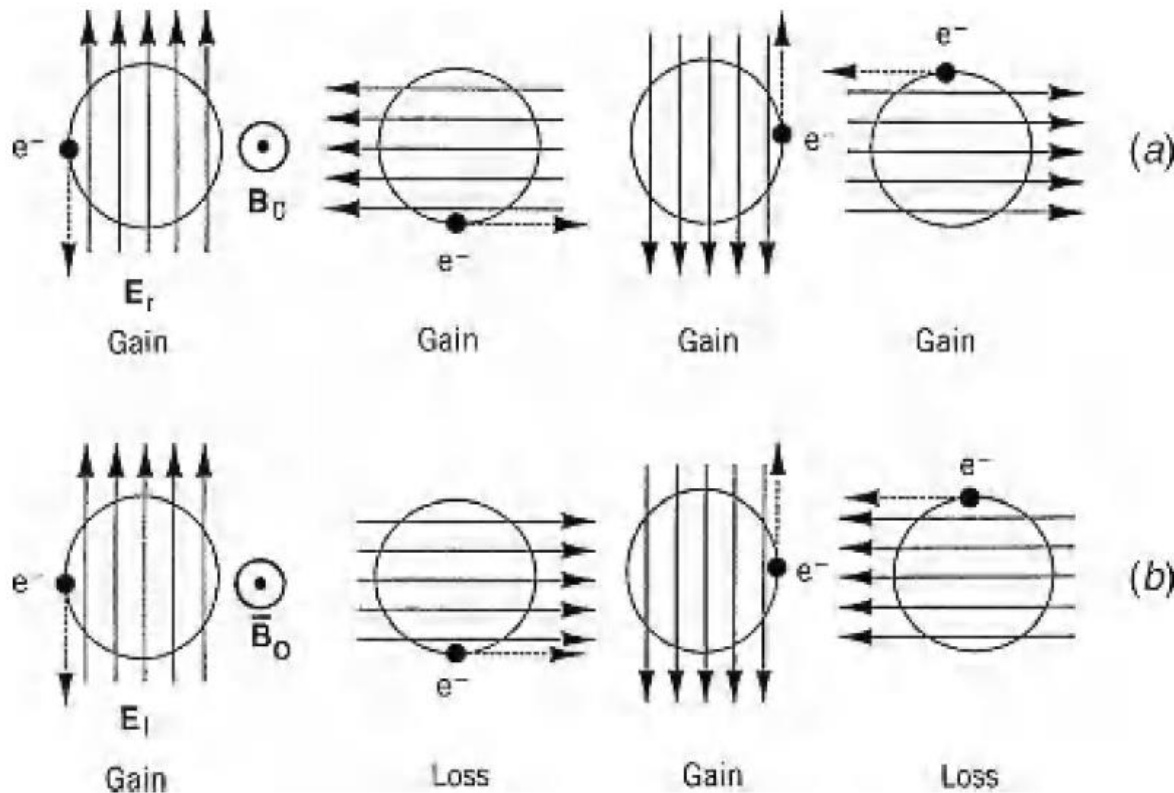


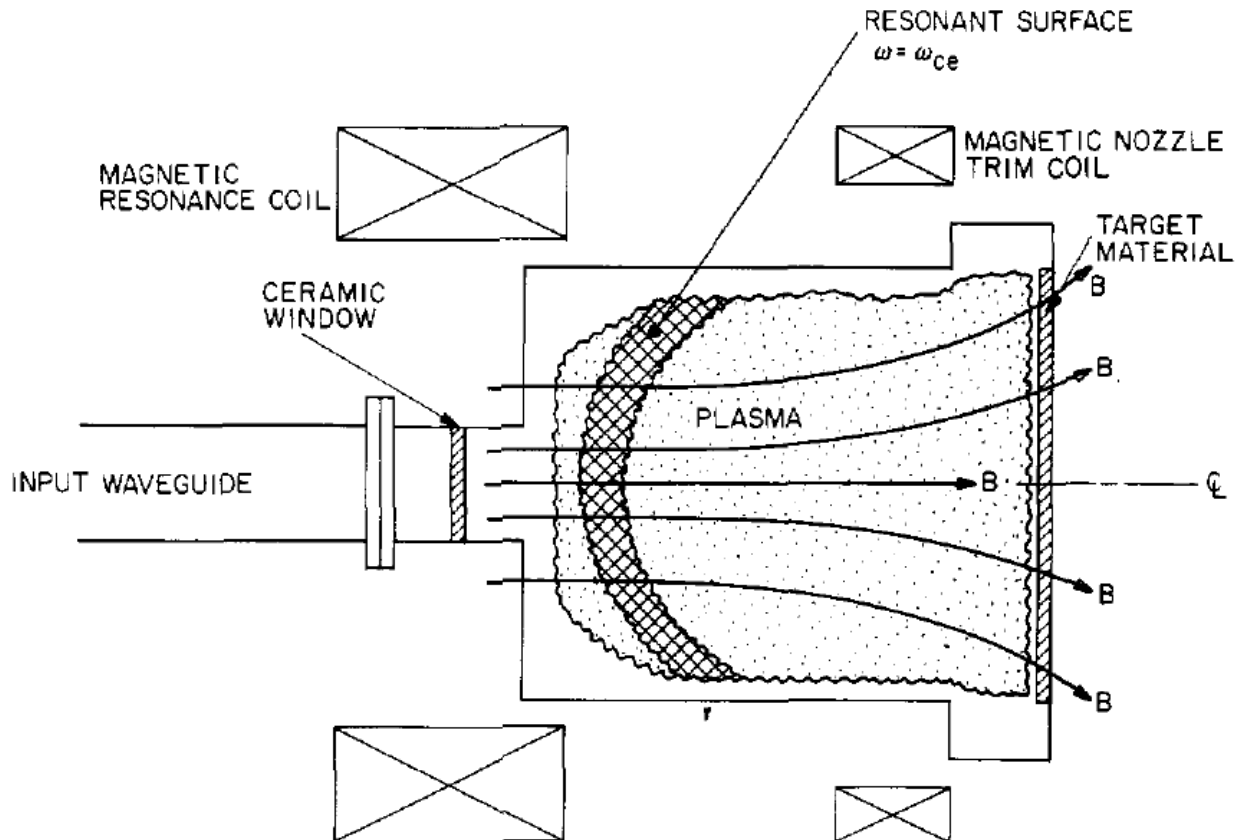
**FIGURE 13.5.** Basic principle of ECR heating: (a) continuous energy gain for right-hand polarization; (b) oscillating energy for left-hand polarization (after Lieberman and Gottscho, 1994).



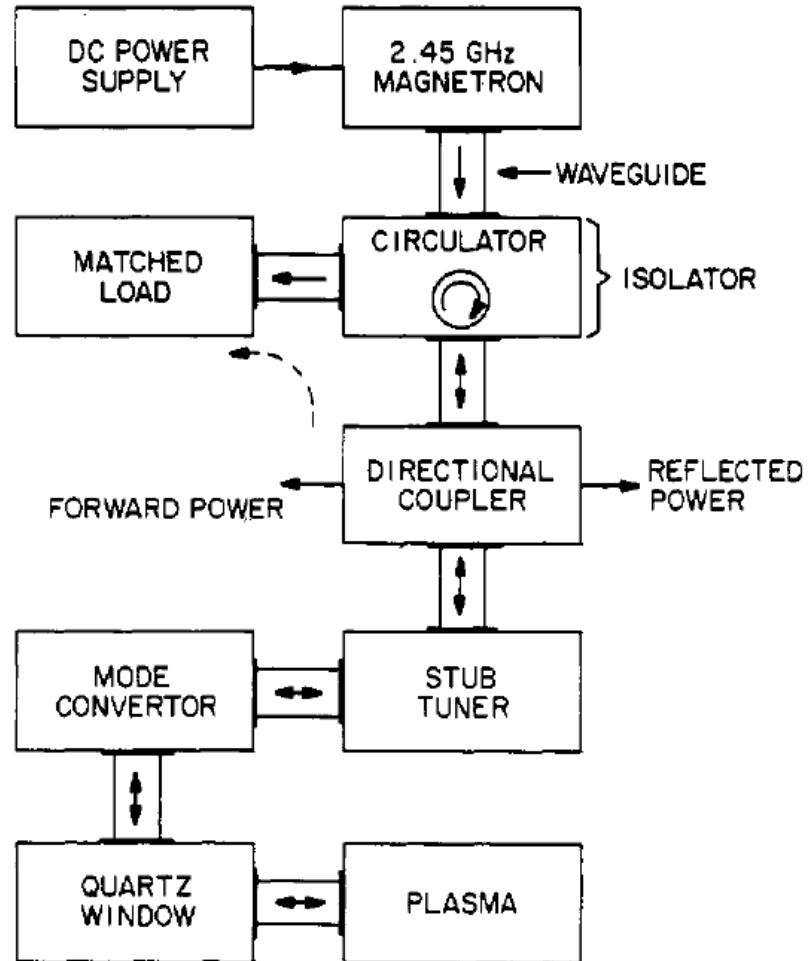
# Strong absorption occurs when the frequency matches the electron cyclotron frequency



- Electron cyclotron resonance (ECR) plasma reactor



# Electron cyclotron resonance (ECR) microwave systems

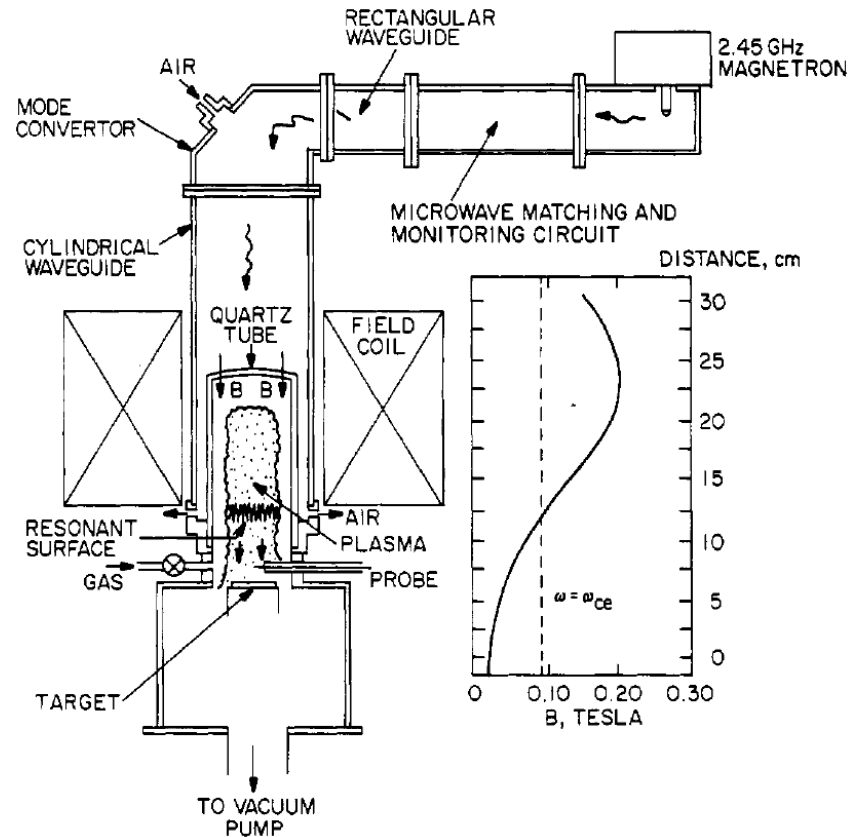


microwave systems

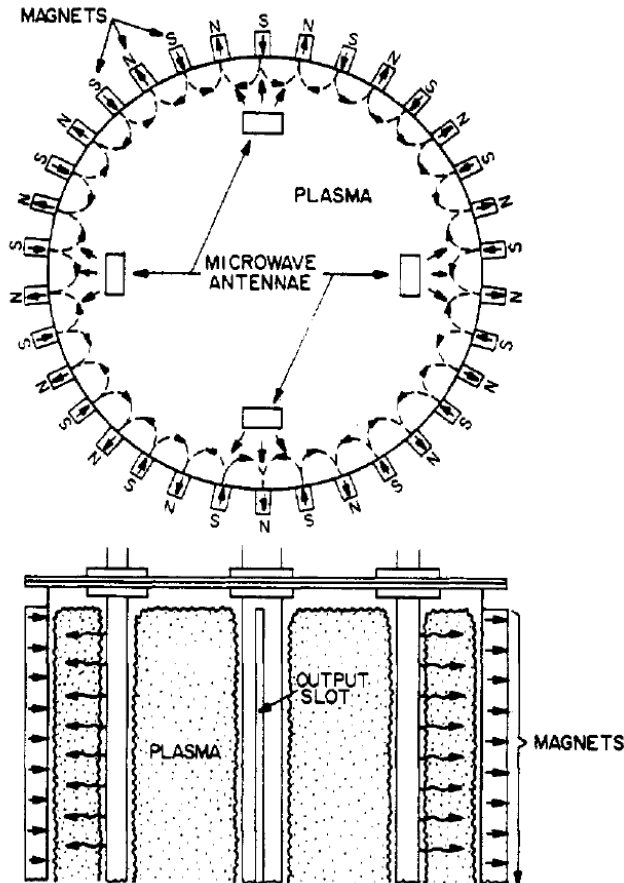
# Immersed ECR plasma source



- High particle fluxes on targets for diamond or other thin film deposition
- The ions in the plasma flux can be used for etching.

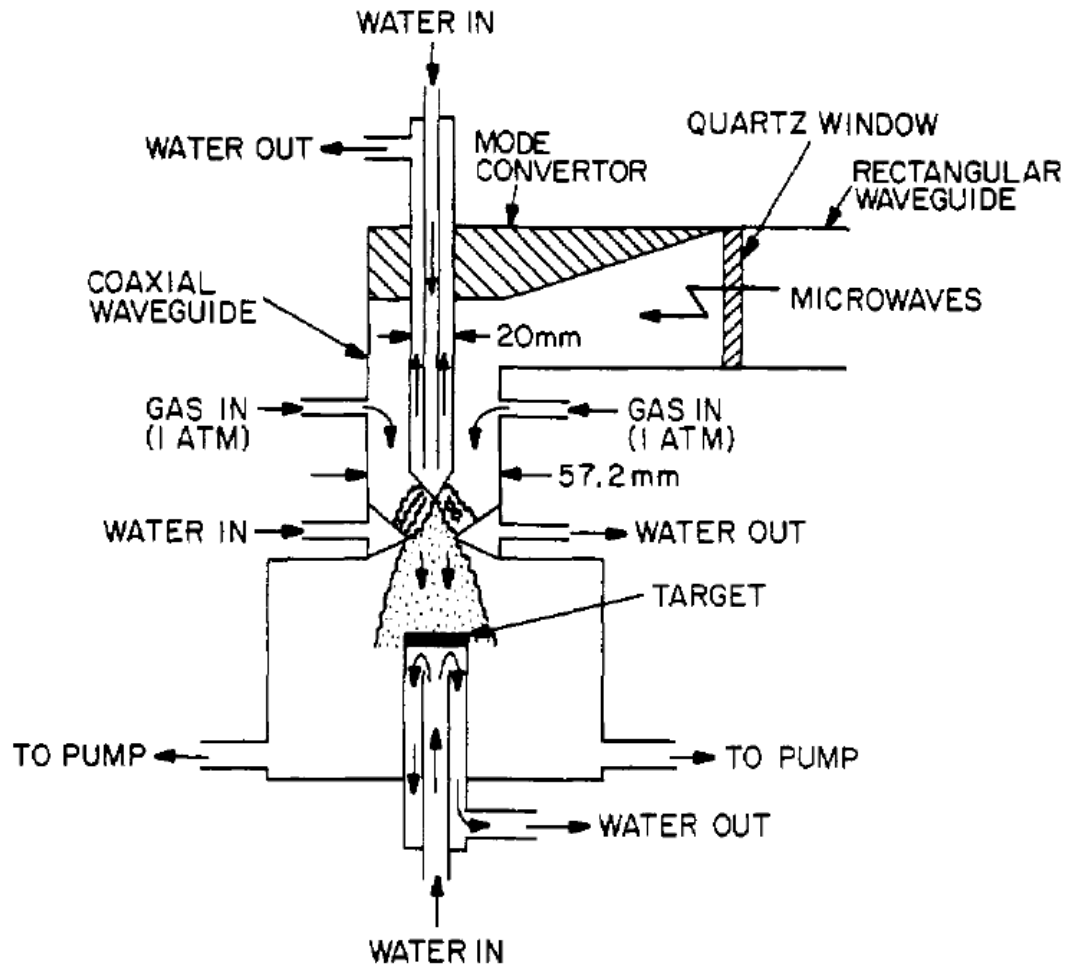


# Distributed ECR system



- **Function of the multipolar magnetic field at the tank boundary:**
  - Provide a resonant surface for ECR absorption
  - Improve the confinement of the plasma

# Microwave plasma torch deposit a much faster rate than other types of plasma source for diamond film deposition



# Microwave-generated plasmas have the capability of filling very large volumes with moderately high density

---



- **Advantages**

- Lower neutral gas pressure, i.e., longer ion and neutral mean free paths.
- Higher fraction ionize.
- Higher electron density.

- **Disadvantages**

- Lower ion bombardment energies.
- Less control of the bombarding ion energy.
- Difficult in tuning up and achieving efficient coupling.
- Much more difficult and expensive to make uniform over a large area.
- More expensive.

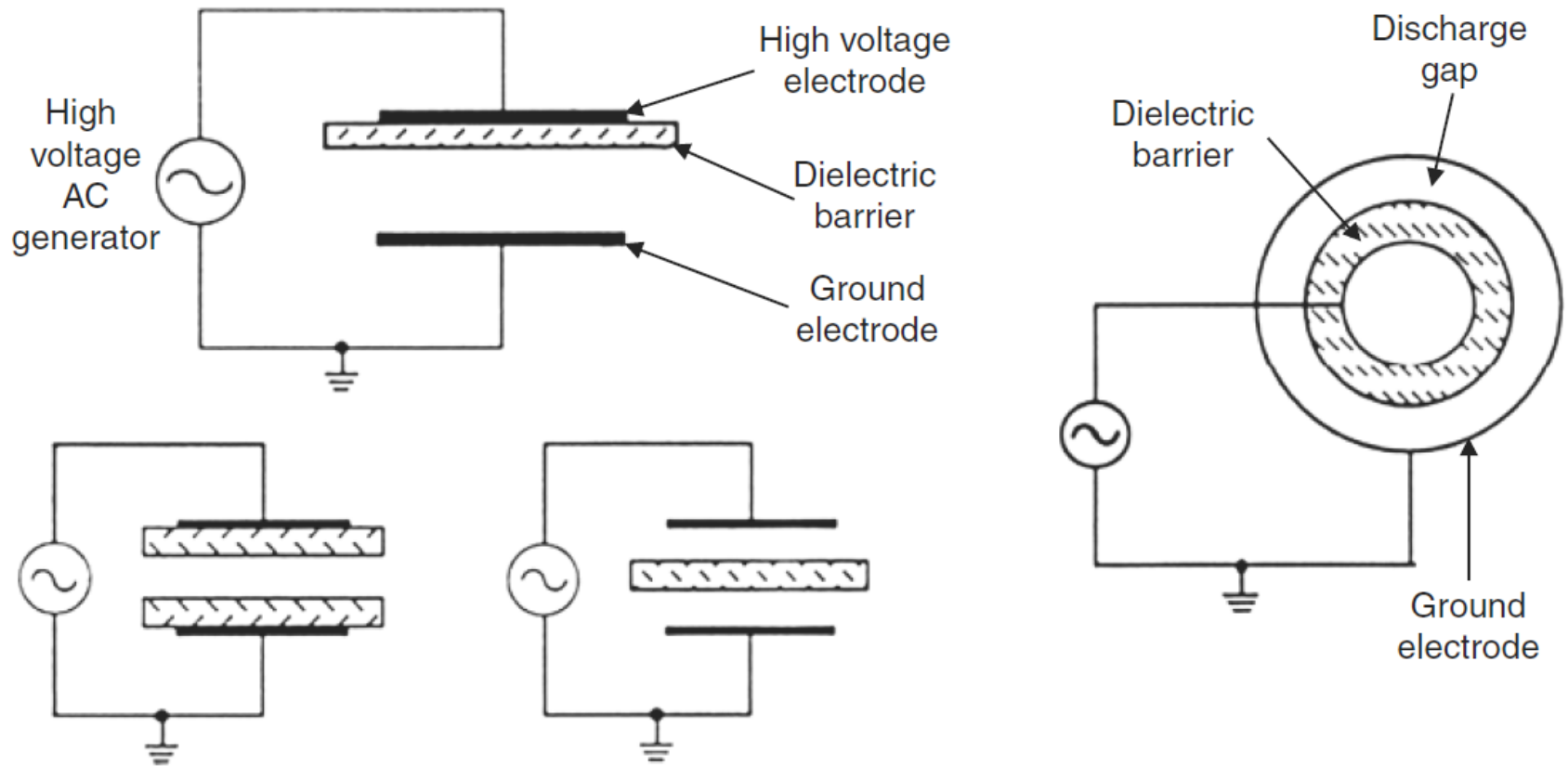
# AC electrical discharges deliver energy to the plasma without contact between electrodes and the plasma

---



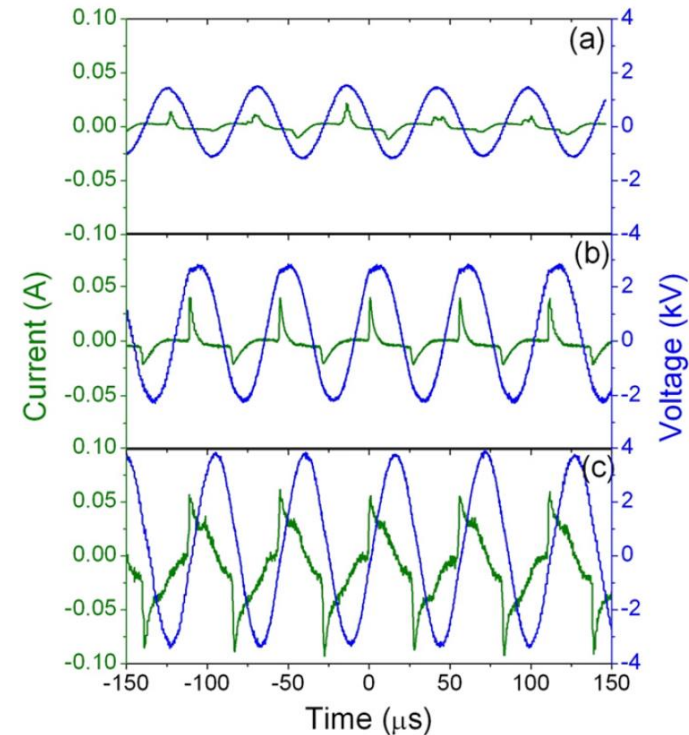
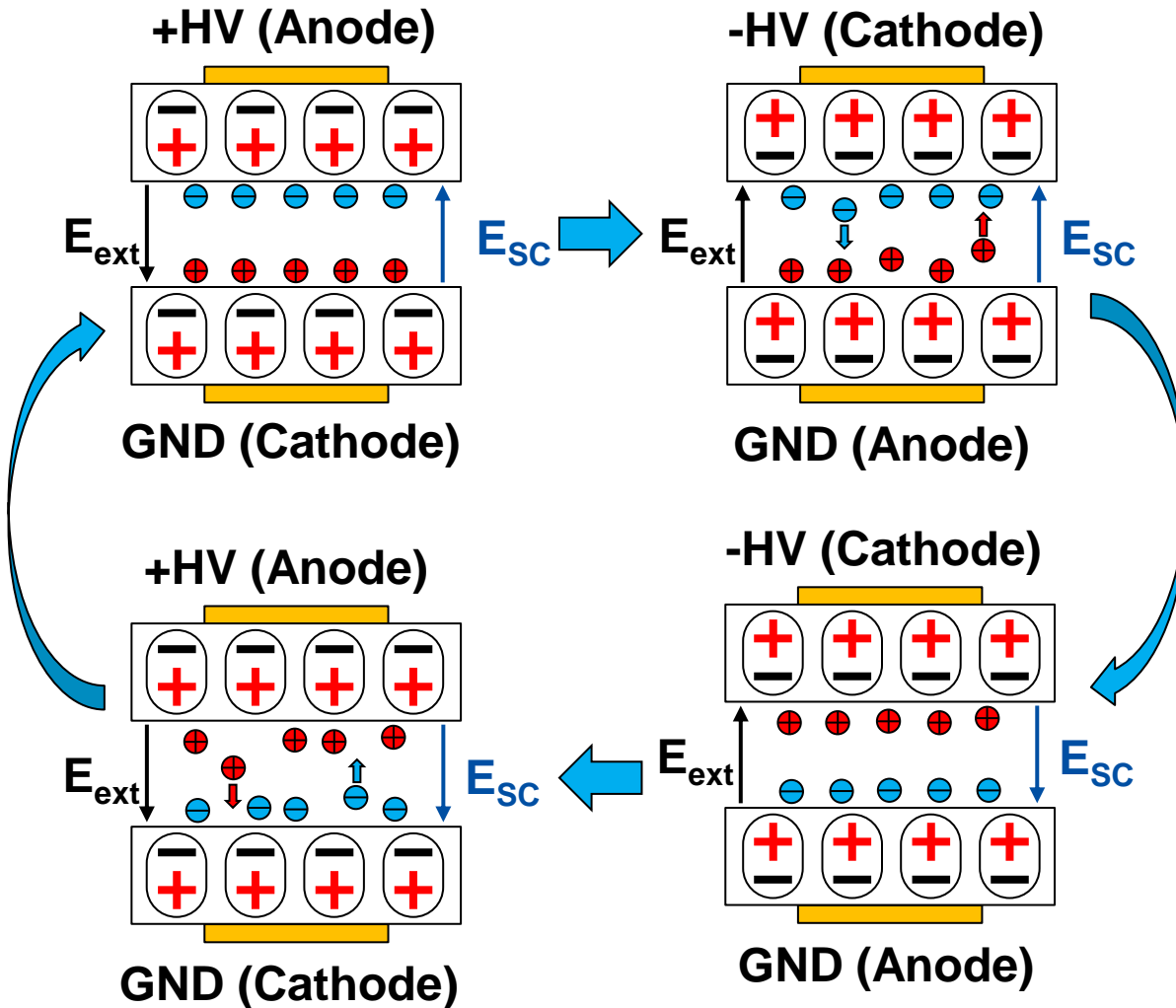
- DC electrical discharge – a true current in the form of a flow of ions or electrons to the electrodes.
- AC electrical discharge – the power supply interacts with the plasma by displacement current.
  - Inductive radio frequency (RF) electrical discharges
  - Capacitive RF electrical discharges
  - Microwave electrical discharges
  - **Dielectric-barrier discharges (DBDs)**
- Other mechanism
  - Laser produced plasma
  - Pulsed-power generated plasma

# Dielectric-barrier discharges (DBDs)

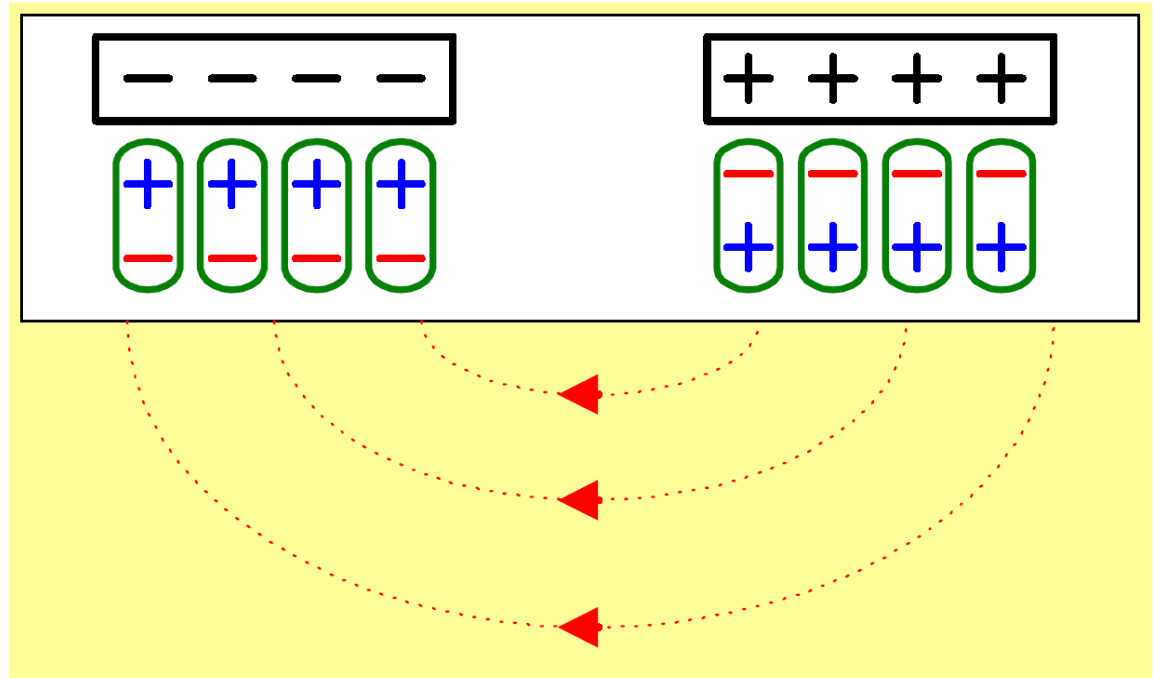
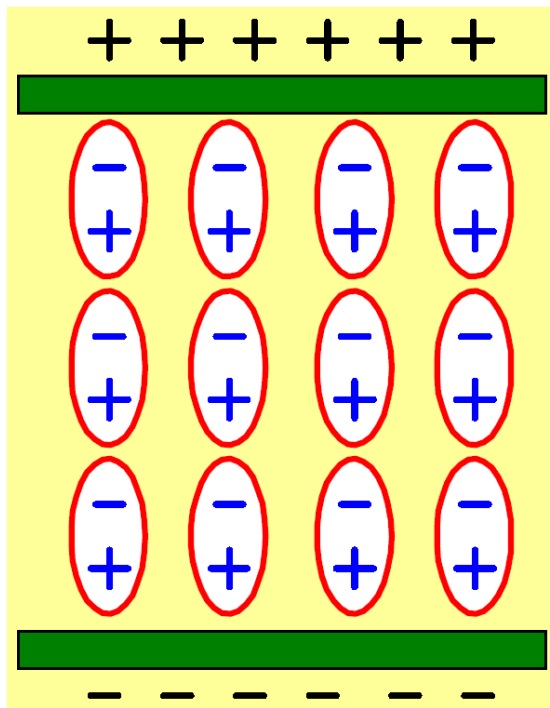




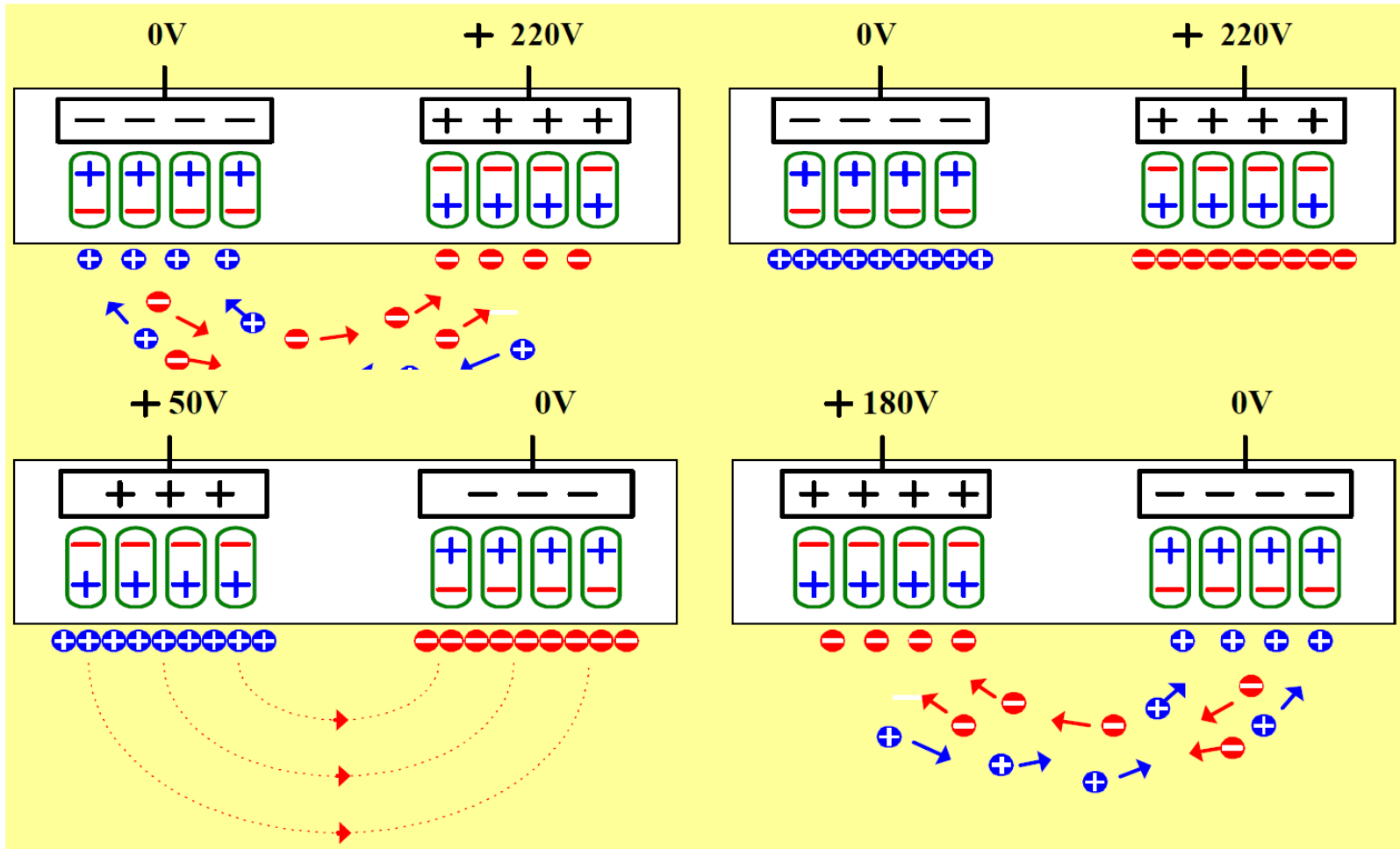
# Space charge effect enhance the electric field



# The foundation of AC discharge in plasma display panel

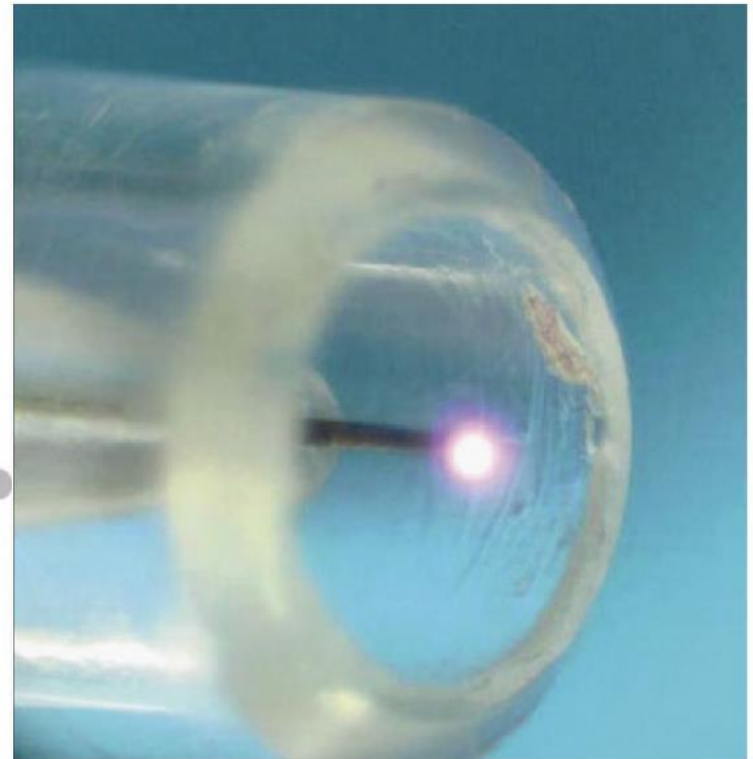
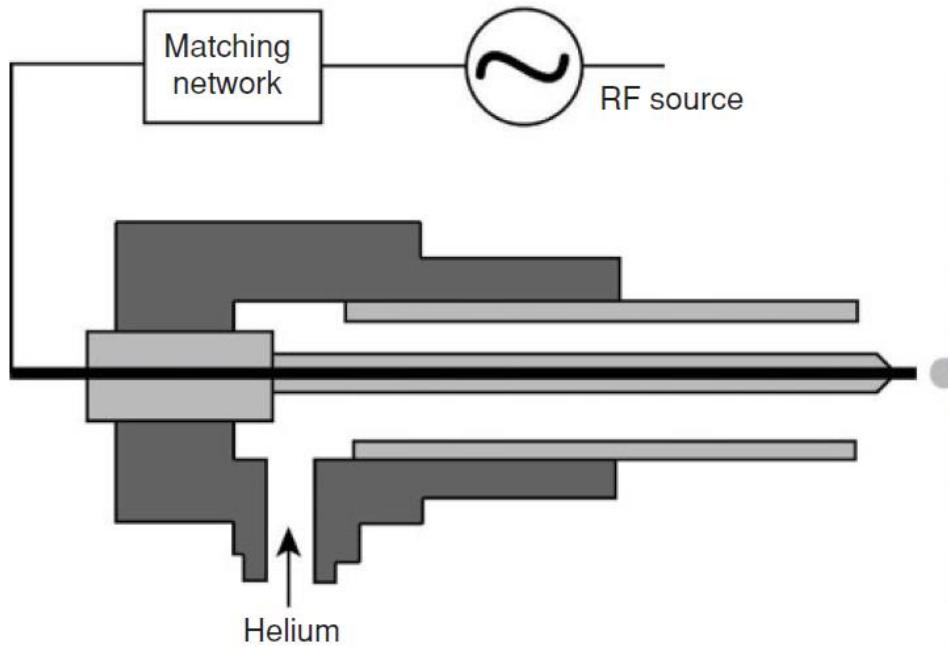


# The plasma can be sustained using ac discharged in plasma display panel

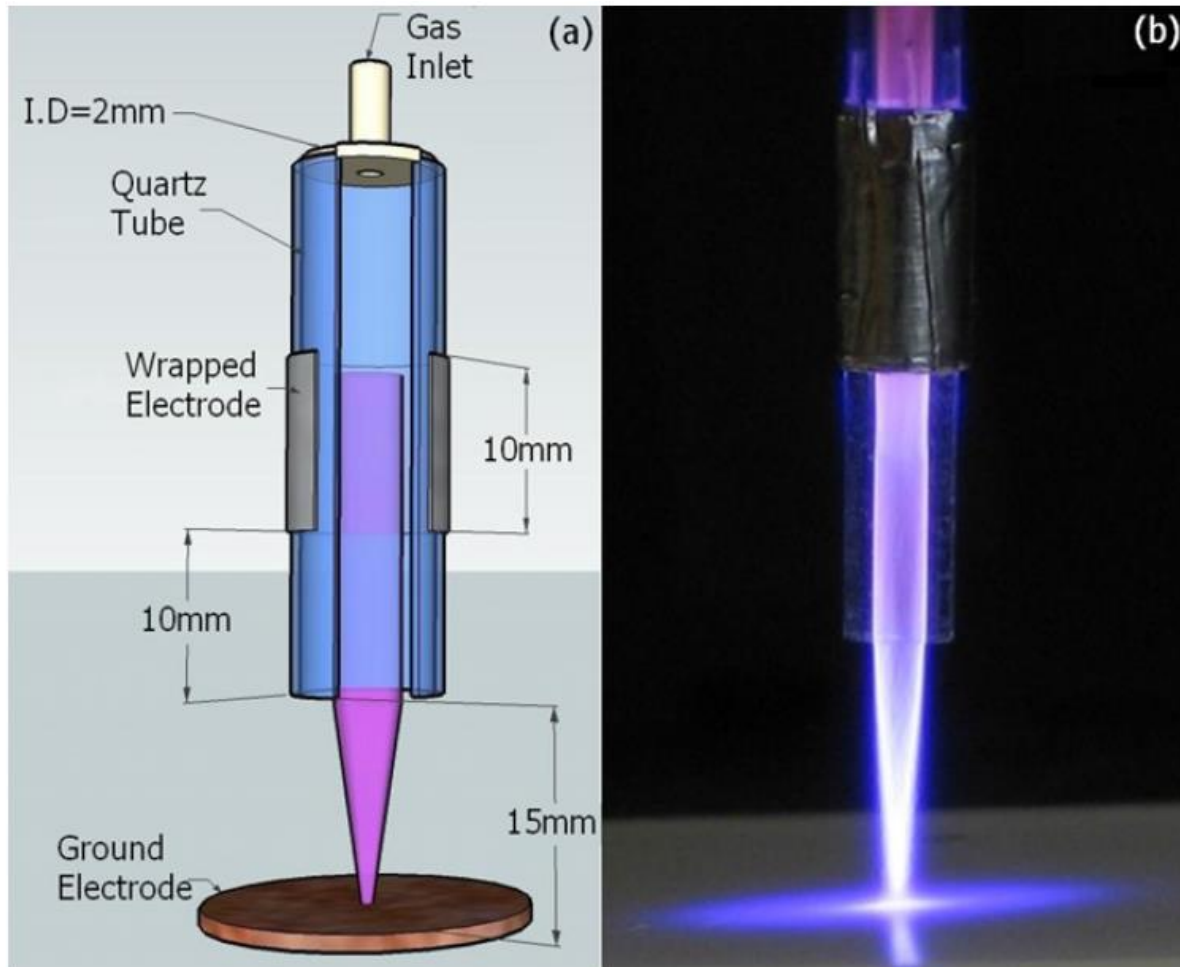


- **Wall discharge reduced the required discharge voltage**

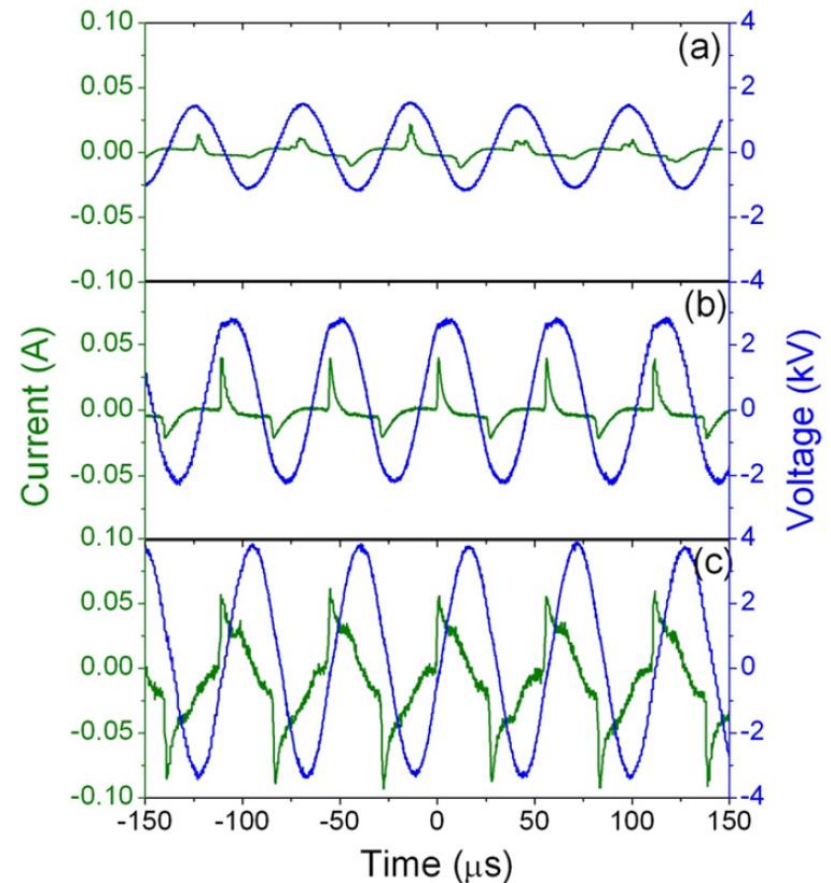
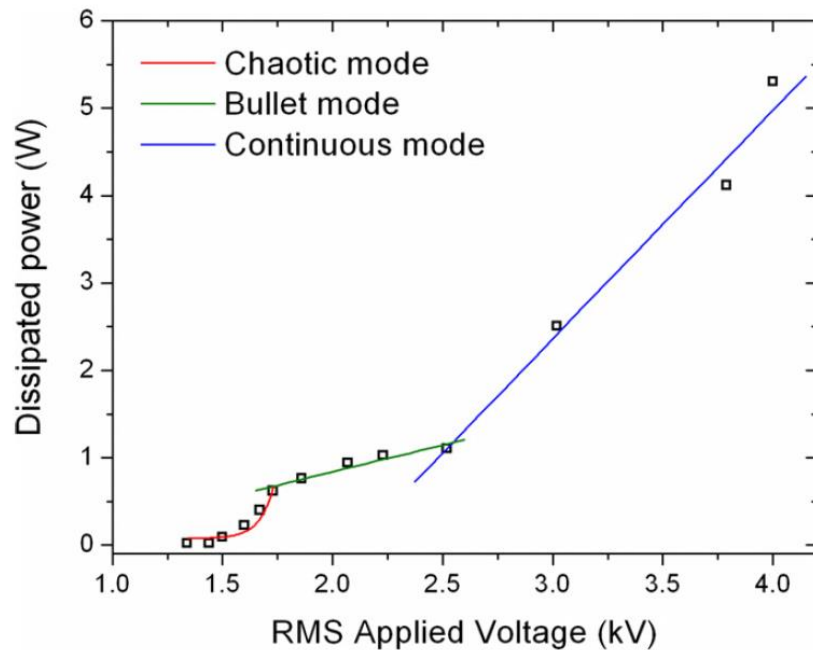
# Plasma-needle discharge



# Atmospheric-pressure cold helium microplasma jets



# There are three different modes: chaotic, bullet, and continuous mode



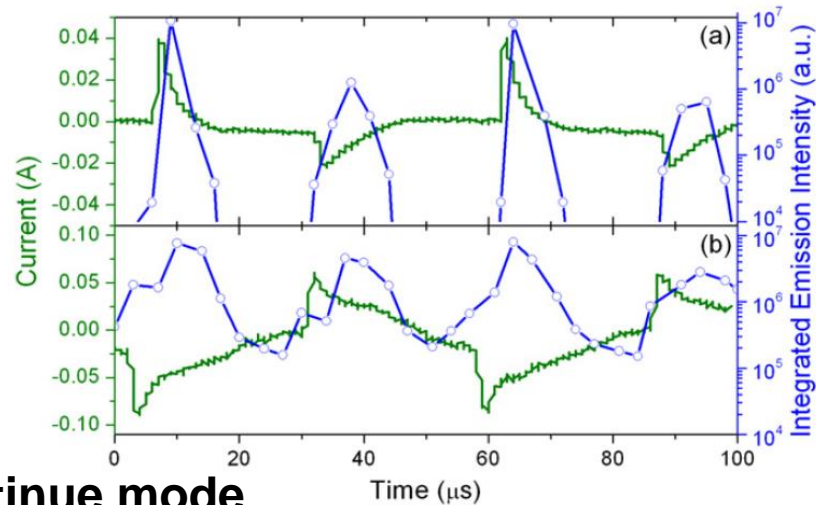
# In bullet mode, the plasma jet comes out as a pulse



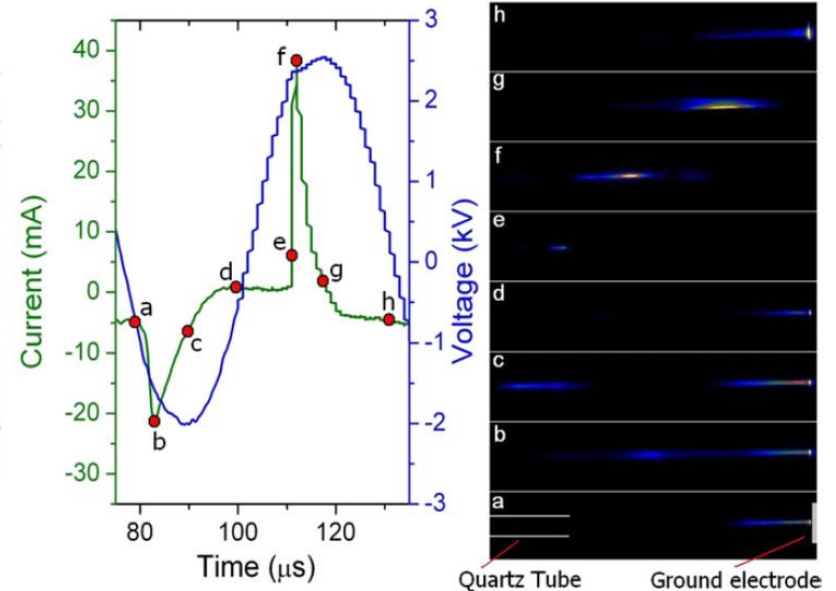
- wavelength-integrated optical emission signal (350–800 nm)

- Images of bullet mode

## Bullet mode



## Continue mode



# AC electrical discharges deliver energy to the plasma without contact between electrodes and the plasma

---



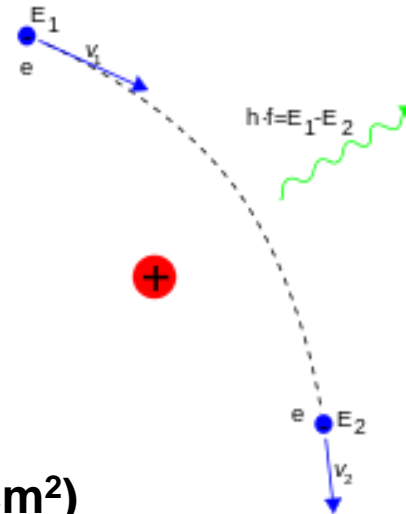
- DC electrical discharge – a true current in the form of a flow of ions or electrons to the electrodes.
- AC electrical discharge – the power supply interacts with the plasma by displacement current.
  - Inductive radio frequency (RF) electrical discharges
  - Capacitive RF electrical discharges
  - Microwave electrical discharges
  - Dielectric-barrier discharges (DBDs)
- Other mechanism
  - **Laser produced plasma**
  - Pulsed-power generated plasma



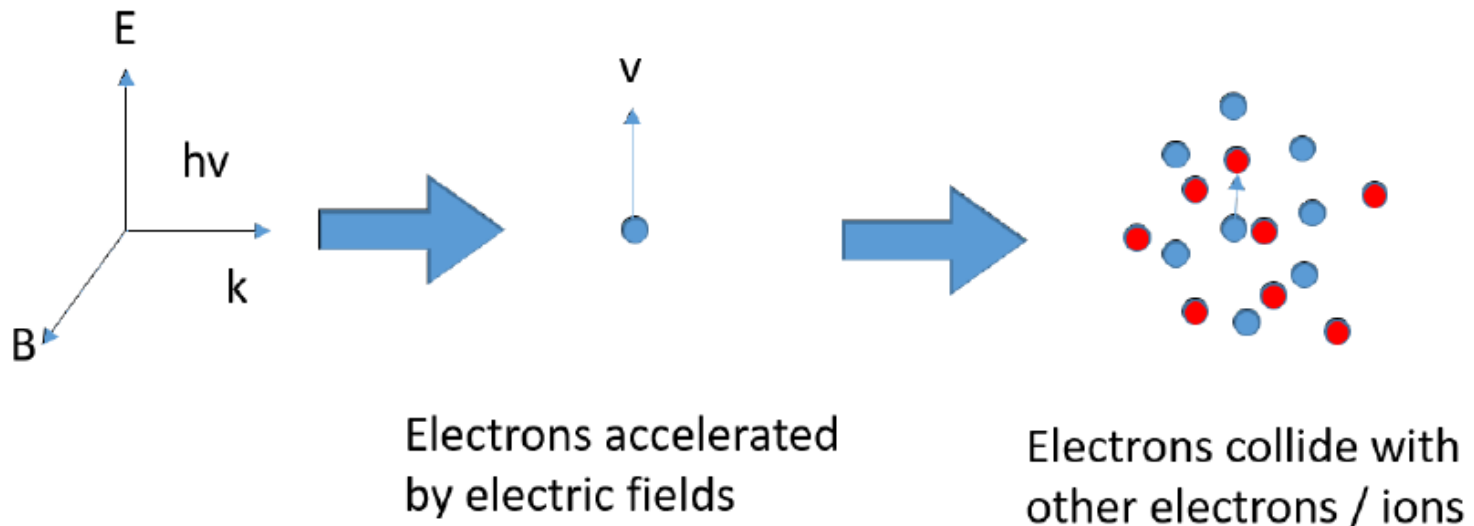
# Laser is absorbed in underdense plasma through collisional process called inverse bremsstrahlung



- Bremsstrahlung



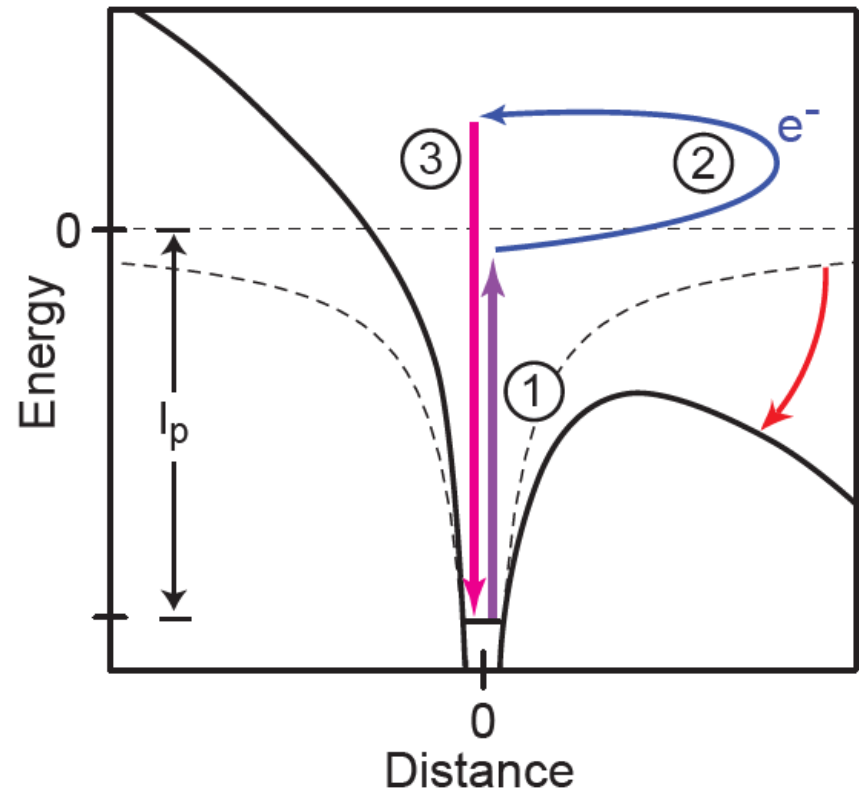
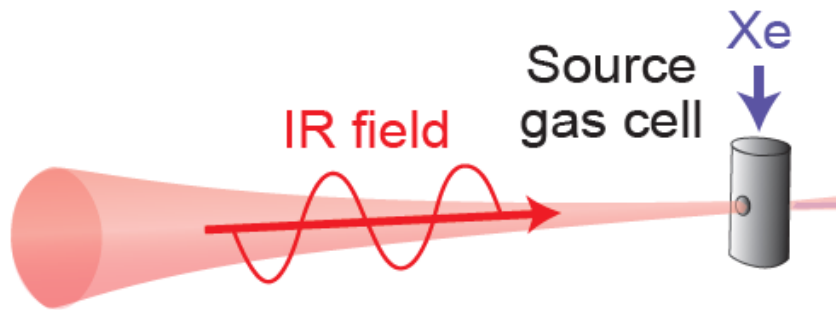
- Inverse bremsstrahlung (For  $I < 10^{18}$  w/cm<sup>2</sup>)



# Electric field of a high-power laser can perturb the potential of a nucleus and thus ionize the atom directly



- For  $I < 10^{18} \text{ w/cm}^2$



# AC electrical discharges deliver energy to the plasma without contact between electrodes and the plasma

---



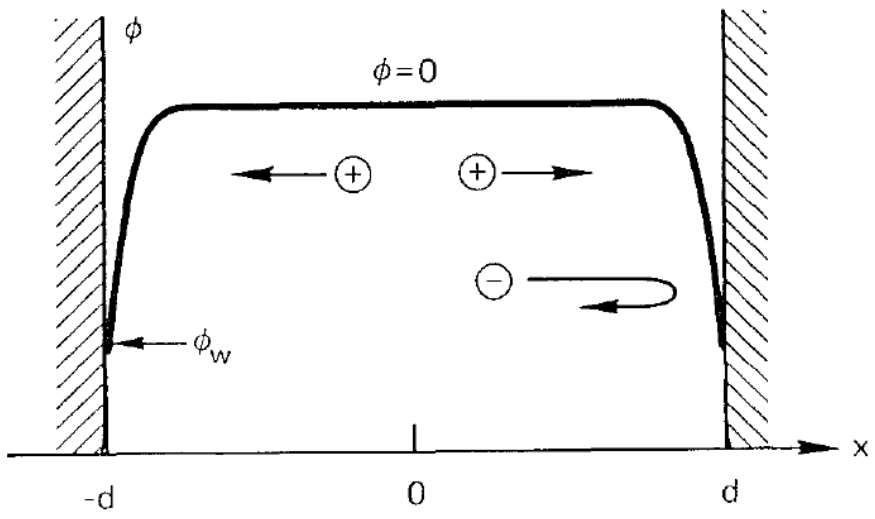
- DC electrical discharge – a true current in the form of a flow of ions or electrons to the electrodes.
- AC electrical discharge – the power supply interacts with the plasma by displacement current.
  - Inductive radio frequency (RF) electrical discharges
  - Capacitive RF electrical discharges
  - Microwave electrical discharges
  - Dielectric-barrier discharges (DBDs)
- Other mechanism
  - Laser produced plasma
  - Pulsed-power generated plasma – it will be introduced later.

# Diagnostics



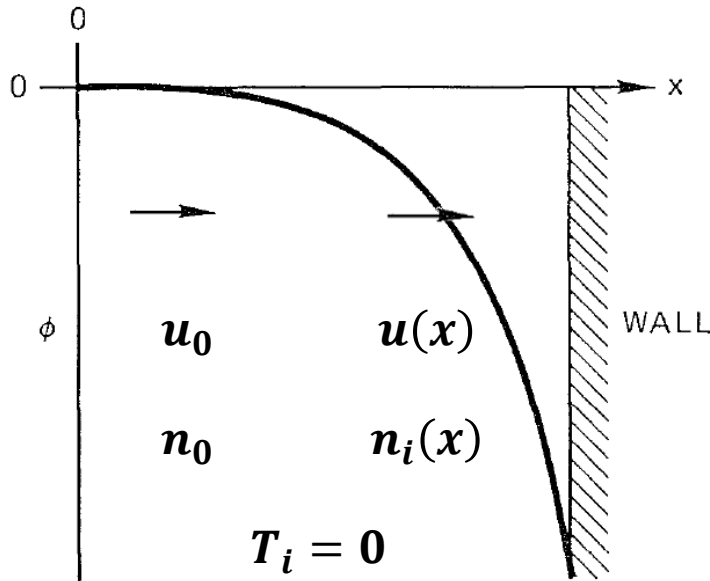
- Single/double Langmuir probe –  $n_e$ ,  $T_e$
- Interferometer –  $n_e$
- Schlieren –  $dn_e/dx$
- Faraday rotator – B
- Bdot probe – B
- Charged particle – B
- Spectroscopy –  $T_e$ ,  $n_e$
- Thomson scattering –  $T_e$ ,  $n_e$ ,  $T_i$ ,  $n_i$
- Faraday cup –  $dn_i/dt$
- Retarding Potential Analyzer -  $v_i$
- Intensified CCD – 2D image
- Framing camera – 2D image
- Streak camera – 1D image
- VISAR – shock velocity
- Neutron time of flight (NToF)
  - Neutron yield,  $T_i$
- Thomson parabola – e/m
- Stimulated Brillouin scattering
  - Laser pulse compression

# All plasmas are separated from the walls surrounding them by a sheath



- When ions and electrons hit the wall, they recombine and are lost.
- Since electrons have much higher thermal velocities than ions, they are lost faster and leave the plasma with a net positive charge.
- Debye shielding will confine the potential variation to a layer of the order of several Debye lengths in thickness.
- A potential barrier is formed to confine electrons electrostatically.
- The flux of electrons is just equal to the flux of ions reaching the wall.

# The planar sheath equation



- Boltzmann relation:

$$n_e(x) = n_0 \exp\left(\frac{e\phi}{KT_e}\right)$$

- Poisson's equation:

$$\epsilon_0 \frac{d^2\phi}{dx^2} = e(n_e - n_i)$$

$$= en_0 \left[ \exp\left(\frac{e\phi}{KT_e}\right) - \left(1 - \frac{2e\phi}{mu_0^2}\right)^{-1/2} \right]$$

$$\chi \equiv -\frac{e\phi}{KT_e}, \quad \xi \equiv \frac{x}{\lambda_D}, \quad M \equiv \frac{u_0}{(KT_e/m)^{1/2}}$$

$$\lambda_D = \left(\frac{KT_e}{4\pi ne^2}\right)^{1/2}$$

$$\chi'' = \left(1 + \frac{2\chi}{M^2}\right)^{-1/2} - e^{-\chi}$$

$$\frac{1}{2}mu^2 = \frac{1}{2}mu_0^2 - e\phi(x)$$

$$u = \left(u_0^2 - \frac{2e\phi}{m}\right)^{1/2}$$

$$n_0u_0 = n_i(x)u(x)$$

$$n_i(x) = n_0 \left(1 - \frac{2e\phi}{mu_0^2}\right)^{-1/2}$$

# The Bohm sheath criterion



$$\chi'' = \left(1 + \frac{2\chi}{M^2}\right)^{-1/2} - e^{-\chi} \qquad \chi' \chi'' = \chi' \left(1 + \frac{2\chi}{M^2}\right)^{-1/2} - \chi' e^{-\chi}$$

$$\frac{d}{d\xi} \left( \frac{\chi'^2}{2} \right) = \frac{d\chi}{d\xi} \left(1 + \frac{2\chi}{M^2}\right)^{-1/2} - \frac{d\chi}{d\xi} e^{-\chi} \qquad \chi_0 = 0, \chi'_0 = 0, @ \xi = 0$$

$$\int_{\chi_0'}^{\chi'} d \left( \frac{\chi'^2}{2} \right) = \int_0^{\chi} \left(1 + \frac{2\chi}{M^2}\right)^{-1/2} d\chi - \int_0^{\chi} e^{-\chi} d\chi$$

$$\frac{1}{2} (\chi'^2 - \chi_0'^2) = M^2 \left[ \left(1 + \frac{2\chi}{M^2}\right)^{1/2} - 1 \right] + e^{-\chi} - 1$$

- Needs to be solved numerically
- The right-hand side must be positive for all  $\chi$ .

# The Bohm sheath criterion - continued



$$\frac{1}{2}(\chi'^2 - \chi_0'^2) = M^2 \left[ \left( 1 + \frac{2\chi}{M^2} \right)^{1/2} - 1 \right] + e^{-\chi} - 1$$

• for  $\chi \ll 1$

$$\left( 1 + \frac{2\chi}{M^2} \right)^{1/2} - 1 = 1 + \frac{\chi}{M^2} - \frac{1}{2} \left( \frac{\chi}{M^2} \right)^2 + \dots - 1 \approx \frac{\chi}{M^2} - \frac{1}{2} \left( \frac{\chi}{M^2} \right)^2$$

$$e^{-\chi} - 1 = 1 - \chi + \frac{1}{2}\chi^2 + \dots - 1 \approx -\chi + \frac{1}{2}\chi^2$$

$$M^2 \left[ \left( 1 + \frac{2\chi}{M^2} \right)^{1/2} - 1 \right] + e^{-\chi} - 1 \approx M^2 \left[ \frac{\chi}{M^2} - \frac{1}{2} \left( \frac{\chi}{M^2} \right)^2 \right] - \chi + \frac{1}{2}\chi^2 = \frac{1}{2}\chi^2 \left( -\frac{1}{M^2} + 1 \right) > 0$$

$$M^2 > 1 \text{ or } \boxed{m u_0^2 > K T_e}$$

- Ions must enter the sheath region with a velocity greater than the acoustic velocity  $v_s$ .
- There must be a finite electric field in the plasma.
- The scale of the sheath region is usually much smaller than the scale of the main plasma region in which the ions are accelerated.



# The Child-Langmuir law



- The electron density can be neglected in the region of large  $\chi$  next to the wall.

$$\chi'' = \left(1 + \frac{2\chi}{M^2}\right)^{-1/2} - e^{-\chi} \approx \left(1 + \frac{2\chi}{M^2}\right)^{-1/2} \approx \frac{M}{(2\chi)^{1/2}}$$

$$\frac{1}{2}(\chi'^2 - \chi_s'^2) = \int_{\chi_s}^{\chi} \frac{M}{(2\chi)^{1/2}} d\chi = \sqrt{2}M(\chi^{1/2} - \chi_s^{1/2})$$

$$n_e \approx 0 @ \xi = \xi_s, \chi_s \ll \chi \text{ and } \chi_s' \ll \chi', \chi'^2 = 2^{3/2}M\chi^{1/2}$$

$$\frac{d\chi}{\chi^{1/4}} = 2^{3/4}M^{1/2}d\xi$$

- Integrating from  $\xi = \xi_s$  to  $\xi_s + \frac{d}{\lambda_D} = \xi_{\text{wall}}$

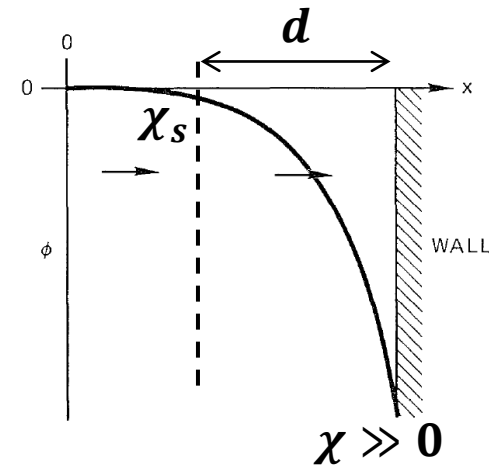
$$\frac{4}{3}\chi_w^{3/4} = 2^{3/4}M^{1/2}\frac{d}{\lambda_D}$$

$$M = \frac{4\sqrt{2}}{9}\frac{\chi_w^{3/2}}{d^2}\lambda_D$$

$$\chi \equiv -\frac{e\phi}{KT_e}, M \equiv \frac{u_0}{(KT_e/m)^{1/2}}$$

$$J = en_0u_0$$

$$J = \frac{4}{9}\left(\frac{2e}{m}\right)^{1/2}\frac{\epsilon_0|\phi_w|^{3/2}}{d^2}$$



# The potential variation in a plasma-wall system can be divided into three parts



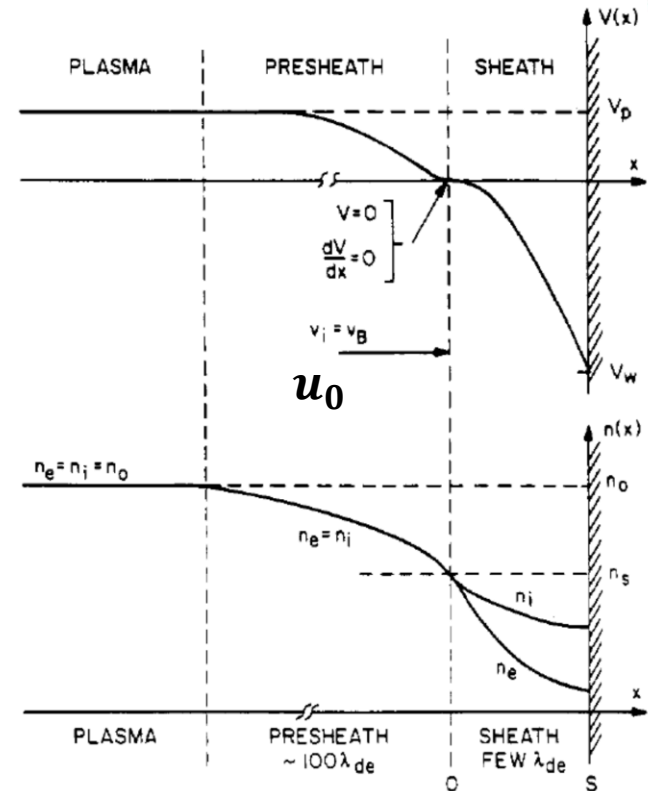
- **Electron-free region:**

$$J = \frac{4}{9} \left( \frac{2e}{M} \right)^{1/2} \frac{\epsilon_0 |\phi_w|^{3/2}}{d^2}$$

- J is determined by the ion production rate
- $\Phi_w$  is determined by the equality of electron and ion fluxes.

- **Sheath:**

- ~Debye length,  $n_e$  is appreciable.
- A dark layers where no electrons were present to excite atoms to emission.
- It has been measured by the electrostatic deflection of a thin electron beam shot parallel to a wall



- **Presheath: ions are accelerated to the required velocity  $u_0$  by a potential drop**

$$|\phi| \geq \frac{1}{2} \frac{KT_e}{e}$$

$$\frac{1}{2} m u_0^2 = |e\phi|, m u_0^2 > K T_e$$

# Electrostatic probes



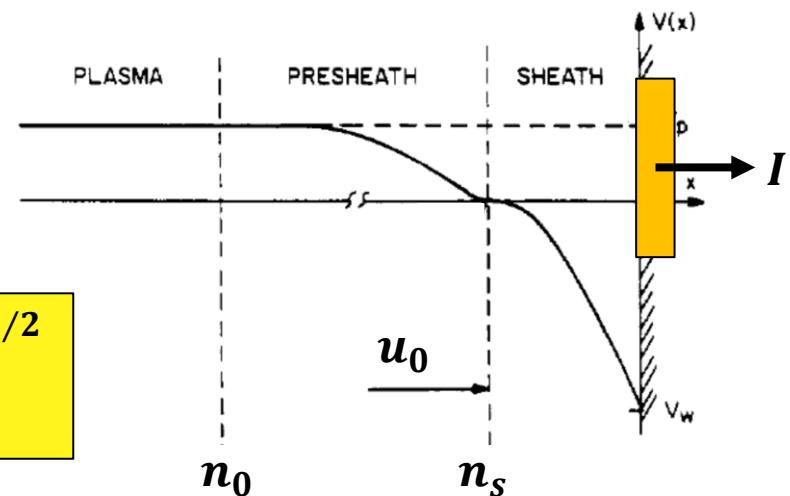
- The electron current can be neglected if the probe is sufficiently negative relative to the plasma to repel most electrons.

$$mu_0^2 > KT_e \quad J = enu \quad I = n_s e A \left( \frac{KT_e}{m} \right)^{1/2}$$

$$|\phi| \approx \frac{1}{2} \frac{KT_e}{e}$$

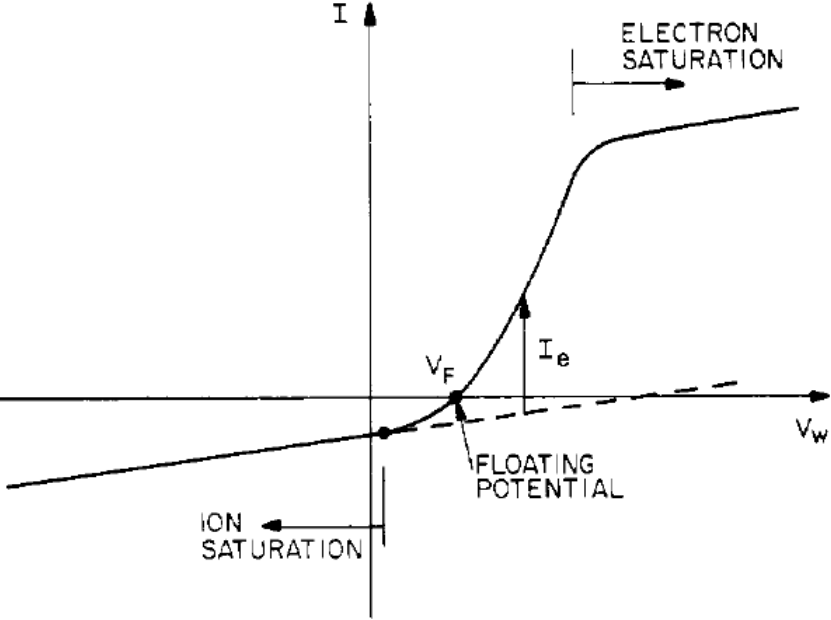
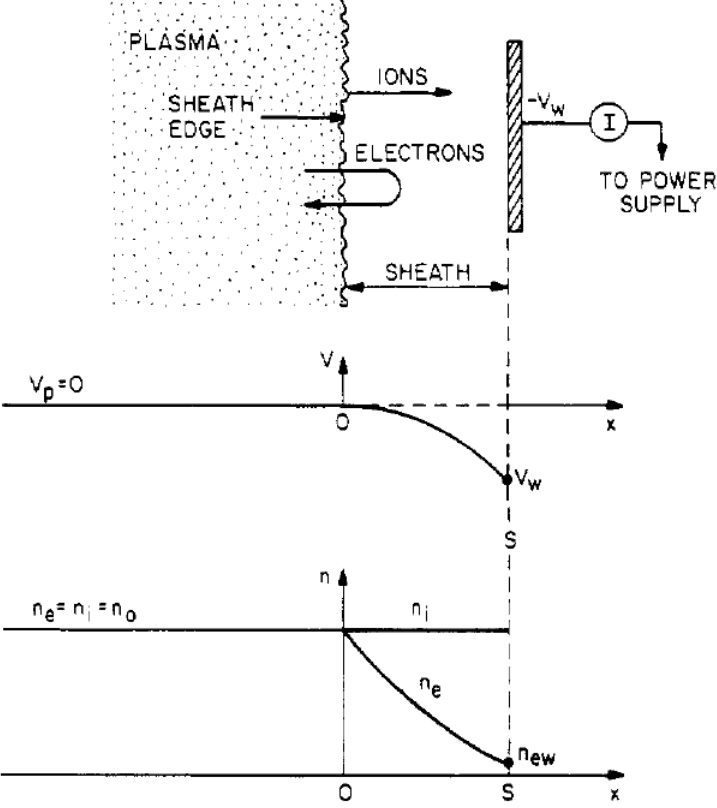
$$n_s = n_0 \exp\left(\frac{e\phi}{KT_e}\right) = n_0 e^{-1/2} = 0.61n_0$$

**Bohm current:  $I_B \approx 0.5n_0 e A \left( \frac{KT_e}{m} \right)^{1/2}$**



- The plasma density can be obtained once the temperature is known.

# A plasma sheath is formed when plasma is contact to a surface



# Floating voltage is determined when ion flux is balanced by electron flux



- Wall flux of ions:

$$\Gamma_i = \frac{1}{4} n_0 \bar{v}_i = n_0 \sqrt{\frac{8KT_i}{\pi m_i}}$$

- Wall flux of electrons due to random motion:

$$n_{ew} = n_0 \exp\left(\frac{e\Phi_w}{KT_e}\right) \quad (\text{Boltzman equation})$$

$$\Gamma_e = \frac{1}{4} n_{ew} \bar{v}_e = n_0 \exp\left(\frac{e\Phi_w}{KT_e}\right) \sqrt{\frac{8KT_e}{\pi m_e}}$$

- Balance between electron and ion flux (current)

$$I = eA(\Gamma_i - \Gamma_e) = 0$$

$$\Phi_w = -\frac{KT_e}{2e} \ln\left(\frac{m_i T_e}{m_e T_i}\right)$$

# Floating voltage can also be calculated using Bohm's velocity



- Wall flux of ions using Bohm's velocity:

$$u_0 = \sqrt{\frac{KT_e}{m_i}} \quad \Gamma_i = n_s u_0$$

- Wall flux of electrons due to random motion:

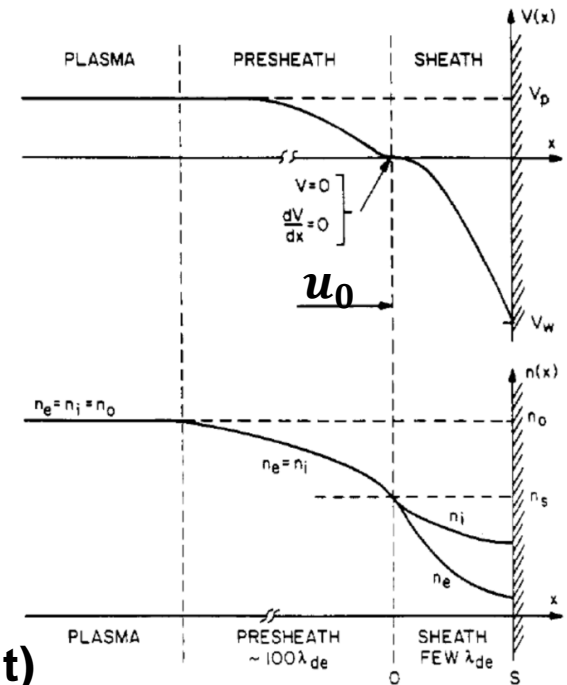
$$n_{ew} = n_s \exp\left(\frac{e\Phi_w}{KT_e}\right)$$

$$\Gamma_e = \frac{1}{4} n_w \bar{v}_e = \frac{1}{4} n_s \exp\left(\frac{e\Phi_w}{KT_e}\right) \sqrt{\frac{8KT_e}{\pi m_e}}$$

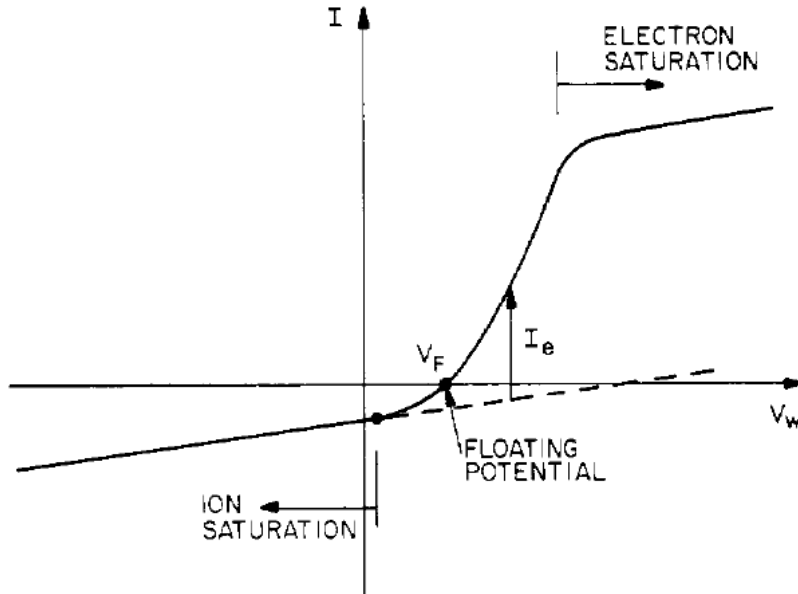
- Balance between electron and ion flux (current)

$$I = eA(\Gamma_i - \Gamma_e) = 0$$

$$\Phi_{wB} = -\frac{KT_e}{2e} \ln\left(\frac{m_i}{2\pi m_e}\right) \iff \Phi_w = -\frac{KT_e}{2e} \ln\left(\frac{m_i T_e}{m_e T_i}\right)$$



# Electron temperature can be determined by the slope of the I-V curve between ion and electron saturation



- Ion saturation current:

$$\begin{aligned}
 I_{is} &= A J_{is} = e A \Gamma_{is} \\
 &= e A \frac{1}{4} n_i \bar{v}_i \\
 &= \frac{e A n_i}{4} \sqrt{\frac{8 K T_i}{\pi m_i}}
 \end{aligned}$$

$$n_i = \frac{4 I_{is}}{e A} \sqrt{\frac{\pi m_i}{8 K T_i}}$$

- Total current:  $I = I_{is} + I_e = I_{is} + \frac{1}{4} n_s \exp\left(\frac{eV}{K T_e}\right) \bar{v}_e e A \quad V \equiv \Phi$

Assuming:  $\frac{dI_{is}}{dV} \ll \frac{dI}{dV}$

$$\frac{dI}{dV} = \frac{dI_{is}}{dV} + \frac{1}{4} \frac{e}{K T_e} n_s \exp\left(\frac{eV}{K T_e}\right) \bar{v}_e e A = \frac{dI_{is}}{dV} + \frac{e}{K T_e} I_e = \frac{dI_{is}}{dV} + \frac{e}{K T_e} (I - I_{is})$$

$$\approx \frac{e}{K T_e} (I - I_{is})$$

$$T_e = \frac{e(I - I_{is})}{dI/dV}$$

# Electron temperature can be obtained alternatively by finding the slope of I-V curve in Log-Linear plot

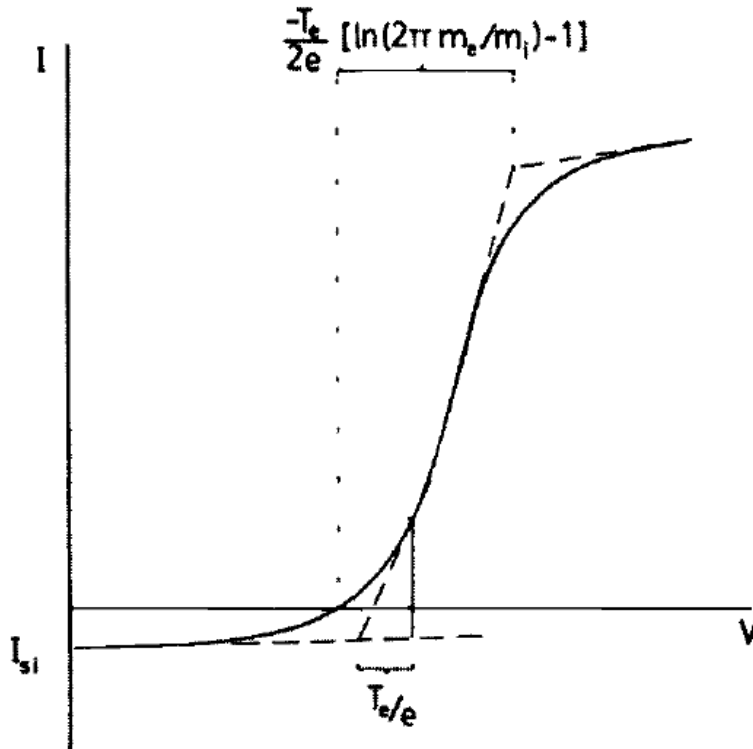


- Electron saturation

$$V = V_p \quad I_{es} = \frac{1}{4} n_s \exp\left(\frac{eV_p}{KT_e}\right) \bar{v}_e eA$$

$$\begin{aligned} I &= I_e + I_{is} \approx I_{es} = \frac{1}{4} n_s \exp\left(\frac{eV}{KT_e}\right) \bar{v}_e eA \\ &= \frac{1}{4} n_s \exp\left(\frac{eV - eV_p + eV_p}{KT_e}\right) \bar{v}_e eA \\ &= \frac{1}{4} n_s \exp\left(\frac{eV_p}{KT_e}\right) \exp\left(e \frac{V - V_p}{KT_e}\right) \bar{v}_e eA \\ &= I_{es} \exp\left(e \frac{V - V_p}{KT_e}\right) \end{aligned}$$

$$T_e = \frac{e(V - V_p)}{K(\ln I_{es} - \ln I)}$$





# Plasma density can be obtained by finding the electron saturation current

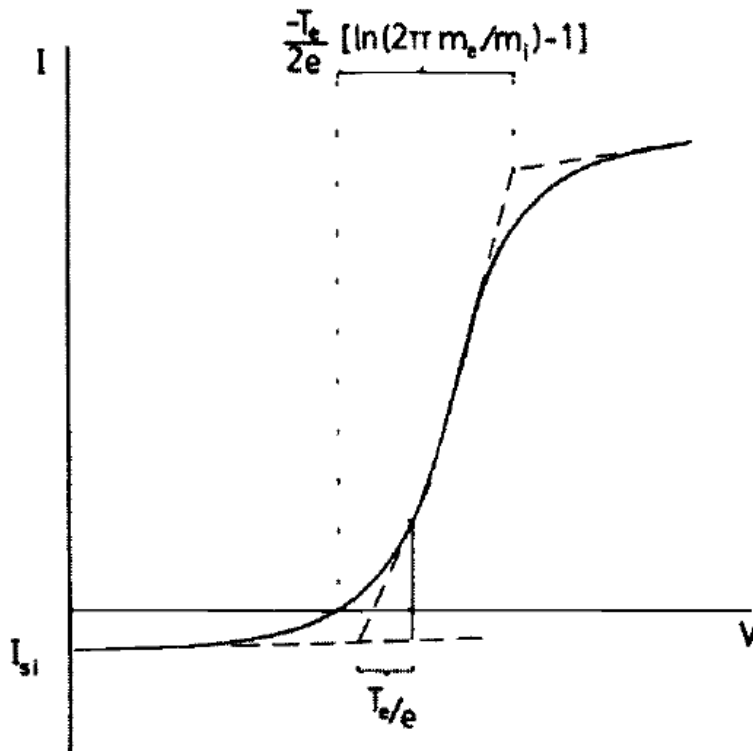


- Electron saturation current:

$$I_{es} = \frac{1}{4} n_s \exp\left(\frac{eV_p}{KT_e}\right) \bar{v}_e eA$$

$$= \frac{1}{4} n_0 eA \sqrt{\frac{8KT_e}{\pi m_e}}$$

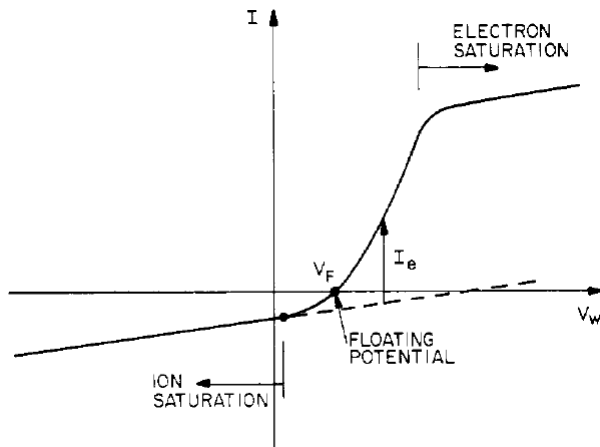
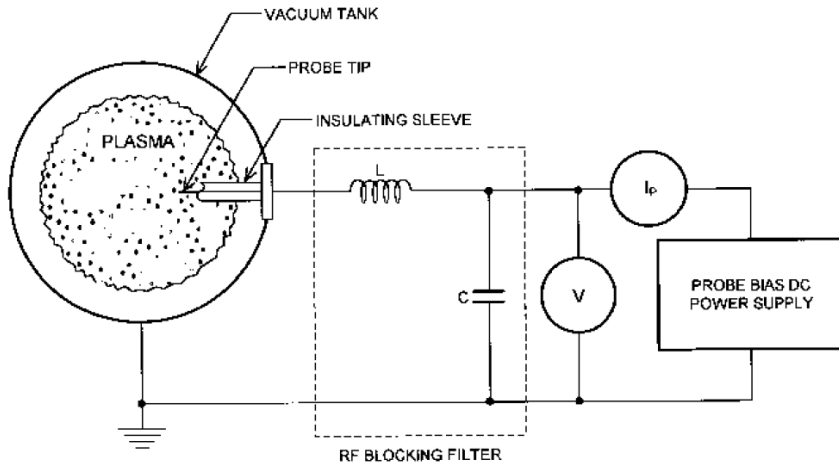
$$n_0 = \frac{4I_{es}}{eA} \sqrt{\frac{\pi m_e}{8T_e}}$$



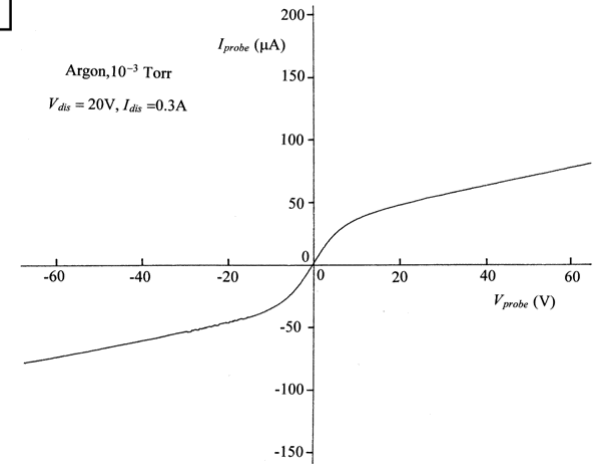
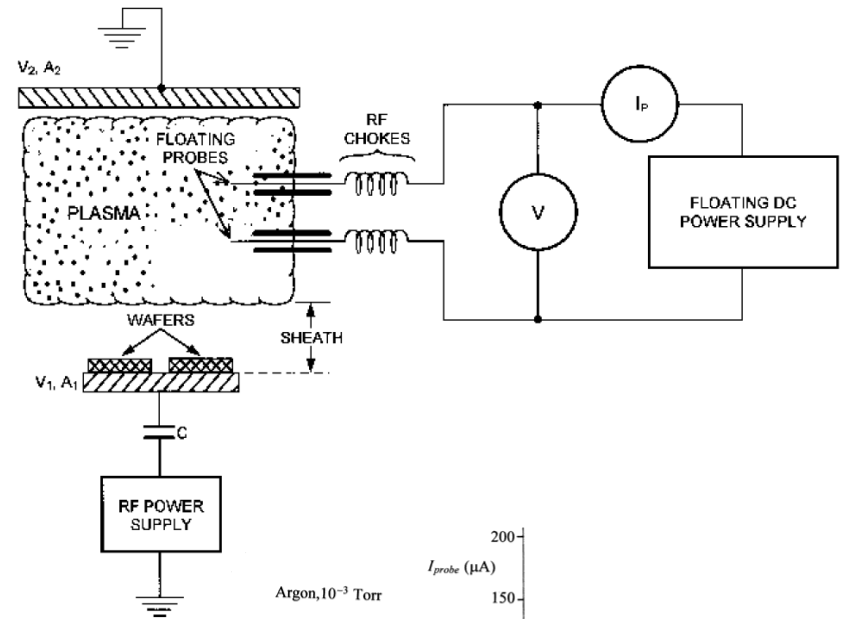
# Two Langmuir probes can be operated simultaneously



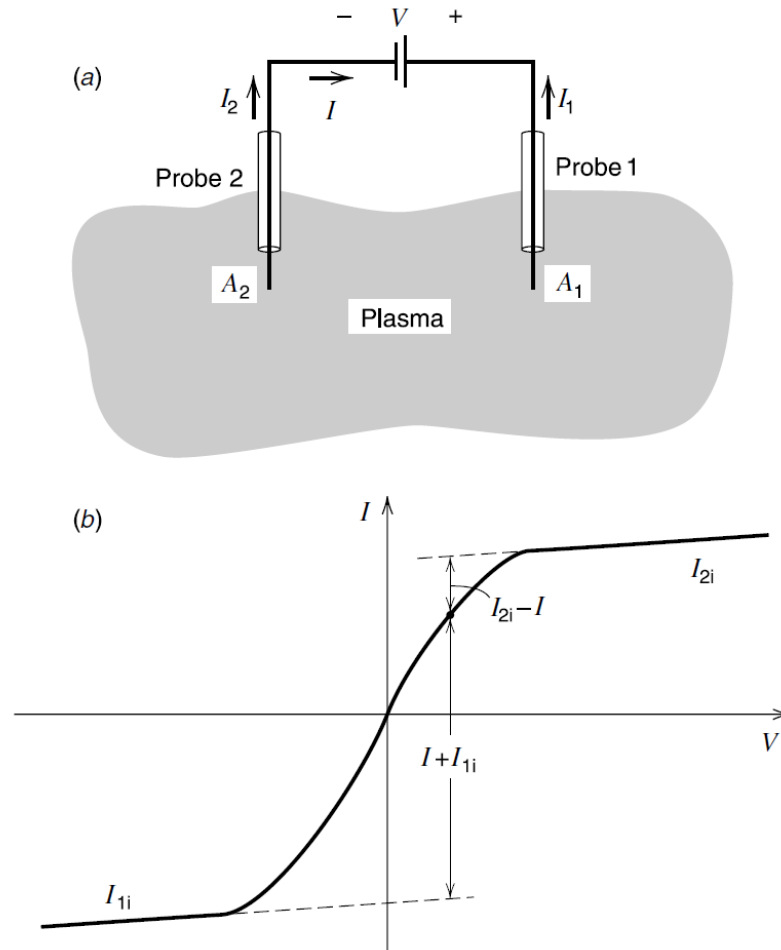
## Single Probe



## Double Probe



# Double Langmuir probe is not disturbed by the discharge



$$I = I_{1e} - I_{1i} = I_{2i} - I_{2e}$$

$$I_{1e} = A_1 \frac{\bar{v}_e e}{4} n_s \exp\left(\frac{eV_1}{KT_e}\right)$$

$$I_{2e} = A_2 \frac{\bar{v}_e e}{4} n_s \exp\left(\frac{eV_2}{KT_e}\right)$$

$$I_{1e} = I + I_{1i} \quad I_{2e} = I_{2i} - I$$

$$\frac{I + I_{1i}}{I_{2i} - I} = \frac{A_1}{A_2} \exp\left(\frac{V_1 - V_2}{T_e}\right)$$

$$= \frac{A_1}{A_2} \exp\left(\frac{V}{T_e}\right)$$

$$I = I_i \tanh\left(\frac{V}{2T_e}\right) \quad \left. \frac{dI}{dV} \right|_{v=0} = \frac{I_i}{2T_e}$$

- The net current never exceeds the ion saturation current, minimizing the disturbance to the discharge.

# An electromagnetic wave is described using Maxwell's equation



$$\begin{cases} \nabla \times \vec{E} &= -\frac{\partial \vec{B}}{\partial t} \\ \nabla \times \vec{B} &= \mu_0 \vec{j} + \epsilon_0 \mu_0 \frac{\partial \vec{E}}{\partial t} \end{cases}$$

$$\nabla \times (\nabla \times \vec{E}) = -\frac{\partial}{\partial t} (\nabla \times \vec{B}) = -\frac{\partial}{\partial t} \left( \mu_0 \vec{j} + \epsilon_0 \mu_0 \frac{\partial \vec{E}}{\partial t} \right)$$

**Conductivity:**  $\vec{j} = \overleftarrow{\sigma} \cdot \vec{E}$

$$\nabla \times (\nabla \times \vec{E}) = -\frac{\partial}{\partial t} (\nabla \times \vec{B}) = -\frac{\partial}{\partial t} \left( \mu_0 \overleftarrow{\sigma} \cdot \vec{E} + \epsilon_0 \mu_0 \frac{\partial \vec{E}}{\partial t} \right)$$

**Plane wave:**  $\vec{E} = \vec{E} \exp \left[ i \left( \vec{k} \cdot \vec{x} - \omega t \right) \right]$

$$i\vec{k} \times (i\vec{k} \times \vec{E}) = i\omega \left( \mu_0 \overleftarrow{\sigma} \cdot \vec{E} - i\omega \epsilon_0 \mu_0 \vec{E} \right)$$

# Dispersion relation is determined by the determinant of the matrix of coefficient



$$-\vec{k} \times (\vec{k} \times \vec{E}) = - \left[ (\vec{k} \cdot \vec{E}) \vec{k} - (\vec{k} \cdot \vec{k}) \vec{E} \right] = - (\vec{k} : \vec{k}) \vec{E} + k^2 \vec{E}$$

$$\begin{aligned} i\omega \left( \mu_0 \overleftrightarrow{\sigma} \cdot \vec{E} - i\omega\epsilon_0\mu_0\vec{E} \right) &= i\omega \left( \mu_0 \overleftrightarrow{\sigma} \cdot \vec{E} - \frac{i\omega}{c^2} \vec{E} \right) = \frac{\omega^2}{c^2} \left[ -\frac{c^2}{i\omega} \mu_0 \overleftrightarrow{\sigma} \cdot \vec{E} + \vec{E} \right] \\ &= \frac{\omega^2}{c^2} \left( \overleftrightarrow{1} + \frac{i}{\omega\epsilon_0} \overleftrightarrow{\sigma} \right) \vec{E} \equiv \frac{\omega^2}{c^2} \overleftrightarrow{\epsilon} \vec{E} \end{aligned}$$

**Dielectric tensor:**  $\overleftrightarrow{\epsilon} \equiv \overleftrightarrow{1} + \frac{i}{\omega\epsilon_0} \overleftrightarrow{\sigma}$

$$\left( \vec{k} : \vec{k} - k^2 \overleftrightarrow{1} + \frac{\omega^2}{c^2} \overleftrightarrow{\epsilon} \right) \vec{E} = 0$$

$$\det \left( \vec{k} : \vec{k} - k^2 \overleftrightarrow{1} + \frac{\omega^2}{c^2} \overleftrightarrow{\epsilon} \right) = 0$$

# Two mode can propagate in the plasma



$$\det \left( \vec{k} : \vec{k} - k^2 \overleftrightarrow{1} + \frac{\omega^2}{c^2} \overleftrightarrow{\epsilon} \right) = 0$$

Assuming the wave propagates along the z direction and isotropic medium:

$$\begin{aligned} \vec{k} &= k \hat{z} \\ \overleftrightarrow{\epsilon} &= \epsilon \overleftrightarrow{1} \end{aligned} \quad \left( \begin{array}{ccc} -k^2 + \frac{\omega^2}{c^2} \epsilon & 0 & 0 \\ 0 & -k^2 + \frac{\omega^2}{c^2} \epsilon & 0 \\ 0 & 0 & \frac{\omega^2}{c^2} \epsilon \end{array} \right) = 0$$

$$\left( -k^2 + \frac{\omega^2}{c^2} \epsilon \right)^2 \frac{\omega^2}{c^2} \epsilon = 0$$

$$\frac{\omega^2}{c^2} \epsilon = 0$$

**Longitudinal wave**

$$\left( -k^2 + \frac{\omega^2}{c^2} \epsilon \right)^2 = 0$$

**Transverse wave**

# The reflective index is determined by the dielectric



- **Longitudinal wave:**  $\frac{\omega^2}{c^2} \varepsilon = 0$

$$\begin{pmatrix} -k^2 + \frac{\omega^2}{c^2} \varepsilon & 0 & 0 \\ 0 & -k^2 + \frac{\omega^2}{c^2} \varepsilon & 0 \\ 0 & 0 & 0 \end{pmatrix} \begin{pmatrix} E_x \\ E_y \\ E_z \end{pmatrix} = 0 = \begin{pmatrix} \left( -k^2 + \frac{\omega^2}{c^2} \varepsilon \right) E_x \\ \left( -k^2 + \frac{\omega^2}{c^2} \varepsilon \right) E_y \\ 0 \end{pmatrix}$$

$$E_x = E_y = 0$$

- **Transverse wave:**  $\left( -k^2 + \frac{\omega^2}{c^2} \varepsilon \right)^2 = 0$

$$\begin{pmatrix} 0 & 0 & 0 \\ 0 & 0 & 0 \\ 0 & 0 & \frac{\omega^2}{c^2} \varepsilon \end{pmatrix} \begin{pmatrix} E_x \\ E_y \\ E_z \end{pmatrix} = 0$$

$$E_z = 0$$

**Reflective index:**  $n \equiv \frac{kc}{\omega} = \varepsilon^{1/2}$

# Conductivity tensor can be determined from equation of motion for electron

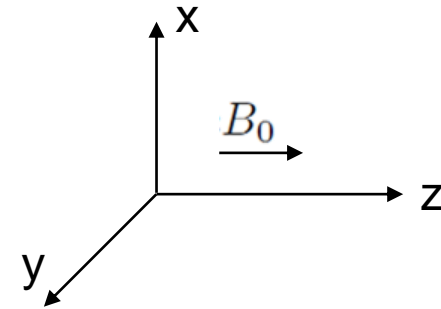


$$m_e \frac{\partial \vec{v}}{\partial t} = -e \left( \vec{E} + \vec{v} \times \vec{B} \right)$$

$$\vec{v} = \vec{v} \exp \left[ i \left( \vec{k} \cdot \vec{x} - \omega t \right) \right]$$

$$\begin{cases} -i\omega m_e v_x &= -eE_x - eB_0 v_y \\ -i\omega m_e v_y &= -eE_y + eB_0 v_x \\ -i\omega m_e v_z &= -eE_z \end{cases}$$

$$\Omega \equiv \frac{eB_0}{m_e}$$



$$\begin{cases} v_x &= -\frac{ie}{\omega m_e} \frac{1}{1 - \Omega^2/\omega^2} \left( E_x - i\frac{\Omega}{\omega} E_y \right) \\ v_y &= -\frac{ie}{\omega m_e} \frac{1}{1 - \Omega^2/\omega^2} \left( i\frac{\Omega}{\omega} E_x + E_y \right) \\ v_z &= -\frac{ie}{\omega m_e} E_z \end{cases}$$

$$\vec{j} = -en_e \vec{v}_e \equiv \overleftrightarrow{\sigma} \vec{E}$$

$$\overleftrightarrow{\sigma} = -en_e \left( \frac{-ie}{\omega m_e} \right) \frac{1}{1 - \Omega^2/\omega^2} \begin{pmatrix} 1 & -i\frac{\Omega}{\omega} & 0 \\ i\frac{\Omega}{\omega} & 1 & 0 \\ 0 & 0 & 1 - \frac{\Omega^2}{\omega^2} \end{pmatrix}$$

$$= i \frac{n_e e^2}{\omega m_e} \frac{1}{1 - \Omega^2/\omega^2} \begin{pmatrix} 1 & -i\frac{\Omega}{\omega} & 0 \\ i\frac{\Omega}{\omega} & 1 & 0 \\ 0 & 0 & 1 - \frac{\Omega^2}{\omega^2} \end{pmatrix}$$



# Dielectric tensor is obtained from conductivity tensor



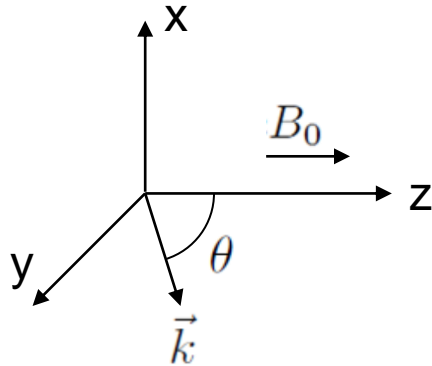
$$\begin{aligned}
 \frac{i}{\omega\epsilon_0} \overleftrightarrow{\sigma} &= -\frac{n_e e^2}{\epsilon_0 m_e} \frac{1}{\omega^2} \frac{1}{1 - \Omega^2/\omega^2} \begin{pmatrix} 1 & -i\frac{\Omega}{\omega} & 0 \\ i\frac{\Omega}{\omega} & 1 & 0 \\ 0 & 0 & 1 - \frac{\Omega^2}{\omega^2} \end{pmatrix} \\
 &= -\frac{\omega_p^2}{\omega^2 - \Omega^2} \begin{pmatrix} 1 & -i\frac{\Omega}{\omega} & 0 \\ i\frac{\Omega}{\omega} & 1 & 0 \\ 0 & 0 & 1 - \frac{\Omega^2}{\omega^2} \end{pmatrix} \quad \omega_p^2 = \frac{n_e e^2}{\epsilon_0 m_e} \\
 &= \begin{pmatrix} -\frac{\omega_p^2}{\omega^2 - \Omega^2} & i\frac{\Omega}{\omega} \frac{\omega_p^2}{\omega^2 - \Omega^2} & 0 \\ -i\frac{\Omega}{\omega} \frac{\omega_p^2}{\omega^2 - \Omega^2} & -\frac{\omega_p^2}{\omega^2 - \Omega^2} & 0 \\ 0 & 0 & -\frac{\omega_p^2}{\omega^2} \end{pmatrix}
 \end{aligned}$$

$$\overleftrightarrow{\epsilon} = \overleftrightarrow{1} + \frac{i}{\omega\epsilon_0} \overleftrightarrow{\sigma} = \begin{pmatrix} 1 - \frac{\omega_p^2}{\omega^2 - \Omega^2} & i\frac{\Omega}{\omega} \frac{\omega_p^2}{\omega^2 - \Omega^2} & 0 \\ -i\frac{\Omega}{\omega} \frac{\omega_p^2}{\omega^2 - \Omega^2} & 1 - \frac{\omega_p^2}{\omega^2 - \Omega^2} & 0 \\ 0 & 0 & 1 - \frac{\omega_p^2}{\omega^2} \end{pmatrix}$$

# Assuming the wave is on the yz plane



let  $X \equiv \frac{\omega_p^2}{\omega^2}$        $Y \equiv \frac{\Omega}{\omega}$        $\overleftrightarrow{\epsilon} = \begin{pmatrix} 1 - \frac{X}{1-Y^2} & i\frac{XY}{1-Y^2} & 0 \\ -i\frac{XY}{1-Y^2} & 1 - \frac{X}{1-Y^2} & 0 \\ 0 & 0 & 1-X \end{pmatrix}$



$$\vec{k} = k (0, \sin \theta, \cos \theta)$$

$$k_i = 0, \quad k_j = k \sin \theta, \quad k_k = k \cos \theta$$

$$\vec{k}: \vec{k} = \begin{pmatrix} 0 \\ k \sin \theta \\ k \cos \theta \end{pmatrix} \cdot (0 \quad k \sin \theta \quad k \cos \theta) = \begin{pmatrix} 0 & 0 & 0 \\ 0 & \sin^2 \theta & \sin \theta \cos \theta \\ 0 & \sin \theta \cos \theta & \cos^2 \theta \end{pmatrix}$$

$$n \equiv \frac{kc}{\omega} \quad \frac{\omega^2}{c^2} \overleftrightarrow{\epsilon} = \frac{k^2 \omega^2}{k^2 c^2} \overleftrightarrow{\epsilon} = \frac{k^2}{n^2} \overleftrightarrow{\epsilon}$$

$$\det \left( \vec{k}: \vec{k} - k^2 \overleftrightarrow{1} + \frac{\omega^2}{c^2} \overleftrightarrow{\epsilon} \right) = 0$$

# Reflective index



$$\begin{vmatrix} -k^2 + \frac{k^2}{n^2} \left(1 - \frac{X}{1-Y^2}\right) & i \frac{k^2}{n^2} \frac{XY}{1-Y^2} & 0 \\ -i \frac{k^2}{n^2} \frac{XY}{1-Y^2} & k^2 \sin^2 \theta - k^2 + \frac{k^2}{n^2} \left(1 - \frac{X}{1-Y^2}\right) & k^2 \sin \theta \cos \theta \\ 0 & k^2 \sin \theta \cos \theta & k^2 \cos^2 \theta - k^2 + \frac{k^2}{n^2} (1 - X) \end{vmatrix} = 0$$

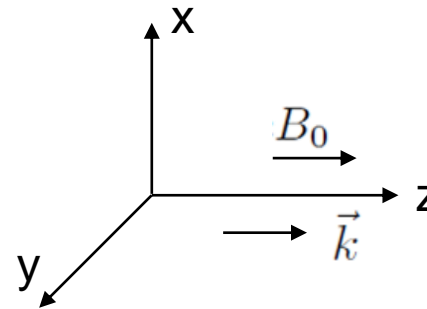
$$\begin{vmatrix} -n^2 + 1 - \frac{X}{1-Y^2} & i \frac{XY}{1-Y^2} & 0 \\ -i \frac{XY}{1-Y^2} & -n^2 \cos^2 \theta + 1 - \frac{X}{1-Y^2} & n^2 \sin \theta \cos \theta \\ 0 & n^2 \sin \theta \cos \theta & -n^2 \sin^2 \theta + 1 - X \end{vmatrix} = 0$$

$$n^2 = 1 - \frac{X(1-X)}{1 - X - \frac{1}{2}Y^2 \sin^2 \theta \pm \left[ \left(\frac{1}{2}Y^2 \sin^2 \theta\right)^2 + (1-X)^2 Y^2 \cos^2 \theta \right]^{1/2}}$$

# Wave is circular polarized propagating along the magnetic field



- Parallel to  $\mathbf{B}_0$  ( $\theta = 0$ )



$$n^2 = 1 - \frac{X(1-X)}{1-X \pm [(1-X)^2 Y^2]^{1/2}} = 1 - \frac{X}{1 \pm Y} = 1 - \frac{\omega_p^2/\omega^2}{1 \pm \Omega/\omega} = 1 - \frac{\omega_p^2}{\omega(\omega \pm \Omega)}$$

$$\begin{pmatrix} -n^2 + 1 - \frac{X}{1-Y^2} & i\frac{XY}{1-Y^2} & 0 \\ -i\frac{XY}{1-Y^2} & -n^2 \cos^2 \theta + 1 - \frac{X}{1-Y^2} & 0 \\ 0 & 0 & 1-X \end{pmatrix} \begin{pmatrix} E_x \\ E_y \\ E_z \end{pmatrix} = 0$$

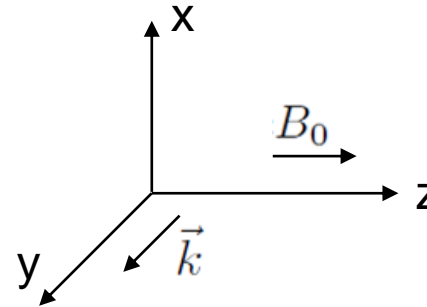
$$\left(-n^2 + 1 - \frac{X}{1-Y^2}\right) E_x + i\frac{XY}{1-Y^2} E_y = \mp \frac{XY}{1-Y^2} E_x + i\frac{XY}{1-Y^2} E_y = 0$$

$$\frac{E_x}{E_y} = \pm i \quad \text{Left hand circular (LHC) or right hand circular (RHC) polarized.}$$

# Electric field is not necessary parallel to the propagating direction which is perpendicular to $B_0$



- Perpendicular to  $B_0$  ( $\theta = \frac{\pi}{2}$ )



$$n^2 = 1 - \frac{X(1-X)}{1-X-\frac{1}{2}Y^2 \pm \frac{1}{2}Y^2} = 1-X \text{ or } 1 - \frac{X(1-X)}{1-X-Y^2}$$

$$\begin{pmatrix} -n^2 + 1 - \frac{X}{1-Y^2} & i\frac{XY}{1-Y^2} & 0 \\ -i\frac{XY}{1-Y^2} & 1 - \frac{X}{1-Y^2} & 0 \\ 0 & 0 & -n^2 + 1 - X \end{pmatrix} \begin{pmatrix} E_x \\ E_y \\ E_z \end{pmatrix} = 0$$

$$n^2 = 1 - \frac{\omega_p^2}{\omega^2} \quad E_x = E_y = 0 \quad \text{Ordinary wave (O-wave)}$$

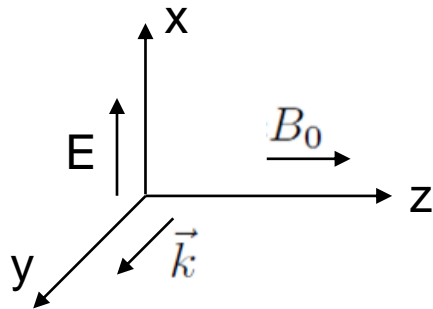
$$n^2 = 1 - \frac{\omega_p^2(1 - \omega_p^2/\omega^2)}{\omega^2 - \omega_p^2 - \Omega^2} \quad \frac{E_x}{E_y} = -i\omega \left( \frac{\omega^2 - \omega_p^2 - \Omega^2}{\omega_p^2\Omega} \right) \quad E_z = 0$$

**Extraordinary wave (E-wave)**

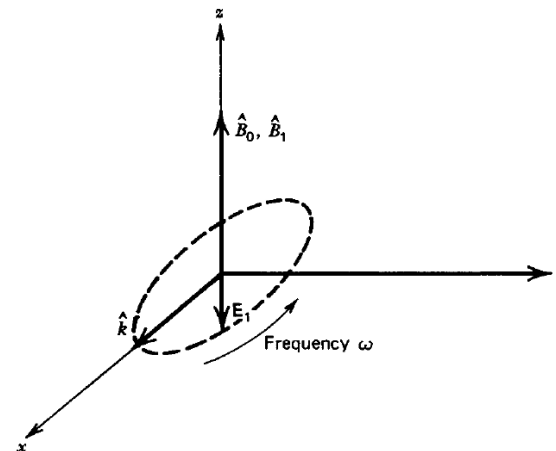
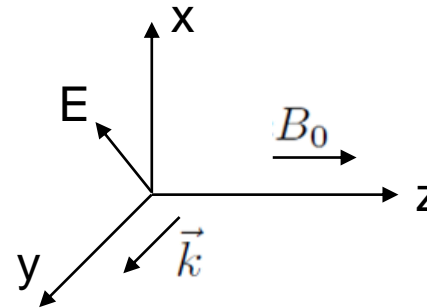
# The electric field of an extraordinary wave rotates elliptically



Ordinary wave (O-wave)



Extraordinary wave (E-wave)



# Electromagnetic wave can be used to measure the density or the magnetic field in the plasma



- **Nonmagnetized isotropic plasma (interferometer needed):**

$$n^2 = 1 - \frac{X(1-X)}{1 - X - \frac{1}{2}Y^2 \sin^2 \theta \pm \left[ \left( \frac{1}{2}Y^2 \sin^2 \theta \right)^2 + (1-X)^2 Y^2 \cos^2 \theta \right]^{1/2}}$$

$$= 1 - X = 1 - \frac{\omega_p^2}{\omega^2} = 1 - \frac{n_e}{n_{cr}} \quad \left( Y \equiv \frac{\Omega}{\omega} \equiv 0 \right)$$

**Note:**  $\omega_p^2 = \frac{n_e e^2}{\epsilon_0 m_e}$        $n_{cr} = \frac{\epsilon_0 m_e \omega^2}{e^2}$

- **Magnetized isotropic plasma (Polarization detected needed):**

Parallel to  $B_0$

$$n^2 = 1 - \frac{\omega_p^2}{\omega(\omega \pm \Omega)} \quad \frac{E_x}{E_y} = \pm i \quad \Omega \equiv \frac{eB_0}{m_e}$$

**Faraday rotation: linear polarization rotation caused by the difference between the speed of LHC and RHC polarized wave.**

# Electromagnetic wave can be used to measure the density or the magnetic field in the plasma



- **Nonmagnetized isotropic plasma (interferometer needed):**

$$n^2 = 1 - \frac{X(1-X)}{1 - X - \frac{1}{2}Y^2 \sin^2 \theta \pm \left[ \left( \frac{1}{2}Y^2 \sin^2 \theta \right)^2 + (1-X)^2 Y^2 \cos^2 \theta \right]^{1/2}}$$

$$= 1 - X = 1 - \frac{\omega_p^2}{\omega^2} = 1 - \frac{n_e}{n_{cr}} \quad \left( Y \equiv \frac{\Omega}{\omega} \equiv 0 \right)$$

**Note:**  $\omega_p^2 = \frac{n_e e^2}{\epsilon_0 m_e}$        $n_{cr} = \frac{\epsilon_0 m_e \omega^2}{e^2}$

- **Magnetized isotropic plasma (Polarization detected needed):**

Parallel to  $B_0$

$$n^2 = 1 - \frac{\omega_p^2}{\omega(\omega \pm \Omega)} \quad \frac{E_x}{E_y} = \pm i \quad \Omega \equiv \frac{eB_0}{m_e}$$

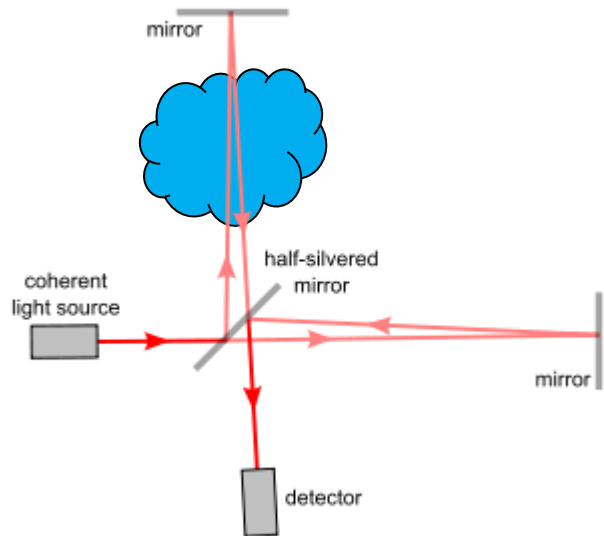
**Faraday rotation: linear polarization rotation caused by the difference between the speed of LHC and RHC polarized wave.**



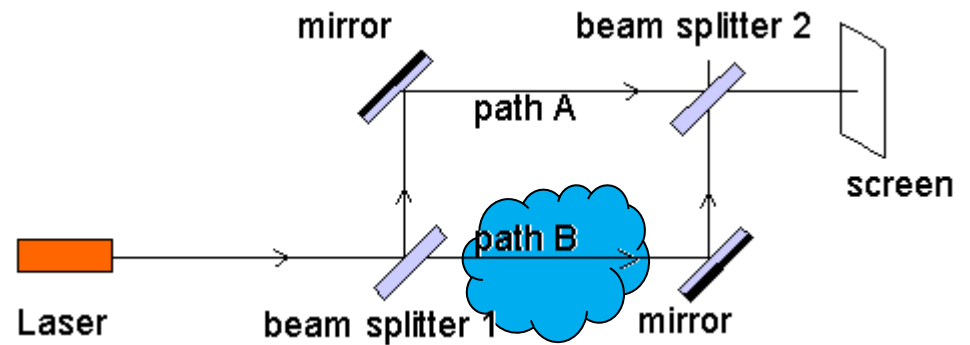
# There are two main style of interferometer



## Michelson interferometer



## Mach-zehnder interferometer

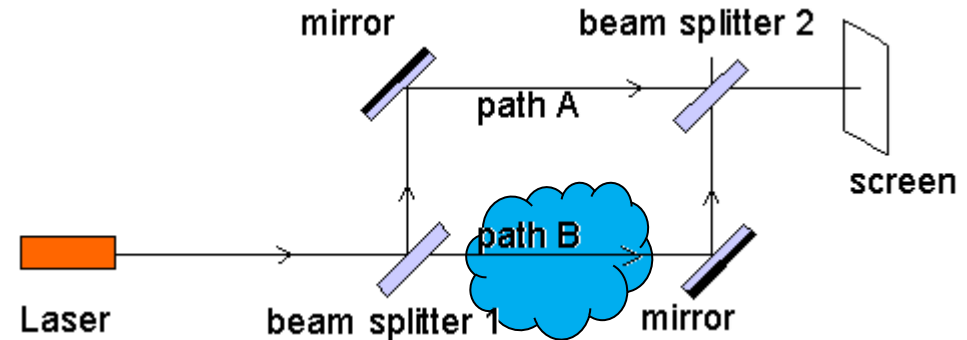


# Interference pattern are due to the phase difference between two different path



$$E_1 = E_1 \exp(-i\omega t)$$

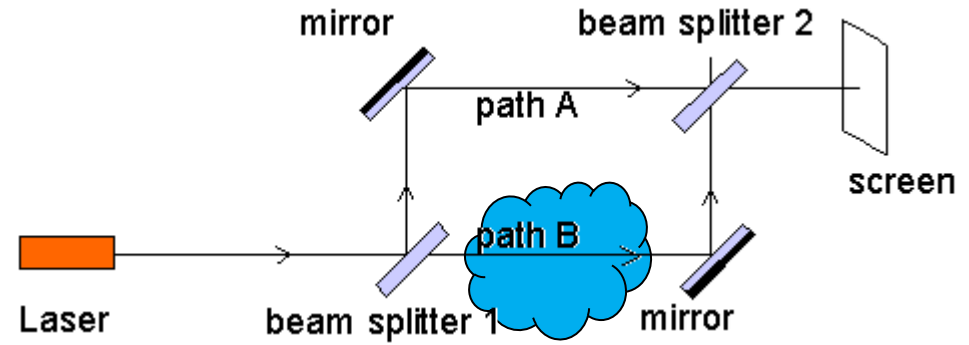
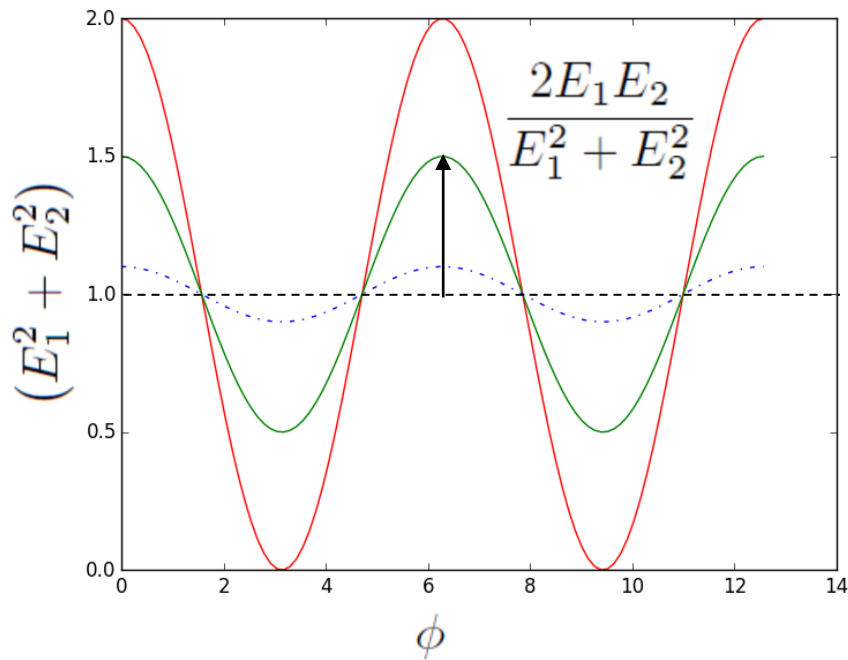
$$E_2 = E_2 \exp(-i\omega t + i\phi)$$



$$E = E_1 + E_2 = [E_1 + E_2 \exp(i\phi)] \exp(-i\omega t)$$

$$\begin{aligned} I &= |E|^2 = E^* E = [E_1 + E_2 \exp(-i\phi)] \exp(i\omega t) [E_1 + E_2 \exp(i\phi)] \exp(-i\omega t) \\ &= E_1^2 + E_2^2 + E_1 E_2 \exp(i\phi) + E_1 E_2 \exp(-i\phi) \\ &= E_1^2 + E_2^2 + 2E_1 E_2 \cos \phi \\ &= (E_1^2 + E_2^2) \left( 1 + \frac{2E_1 E_2}{E_1^2 + E_2^2} \cos \phi \right) \end{aligned}$$

# The intensity on screen depends on the phase different between two paths



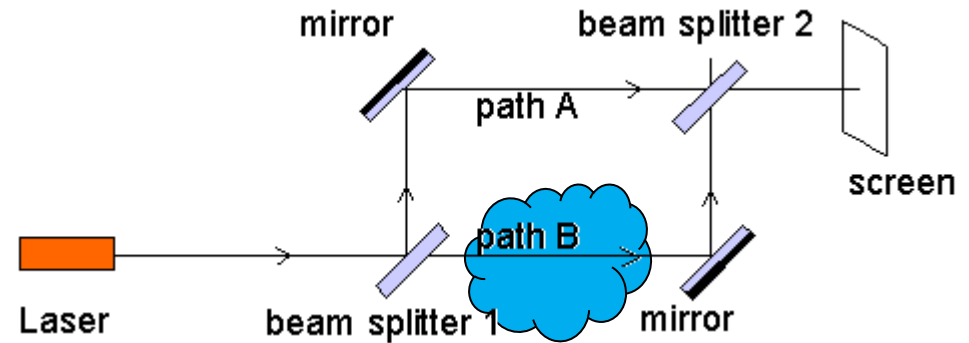
$$I = (E_1^2 + E_2^2) \left( 1 + \frac{2E_1E_2}{E_1^2 + E_2^2} \cos \phi \right)$$

# The phase different depends on the line integral of the electron density along the path



$$\phi = \int k dl = \int n \frac{\omega}{c} dl$$

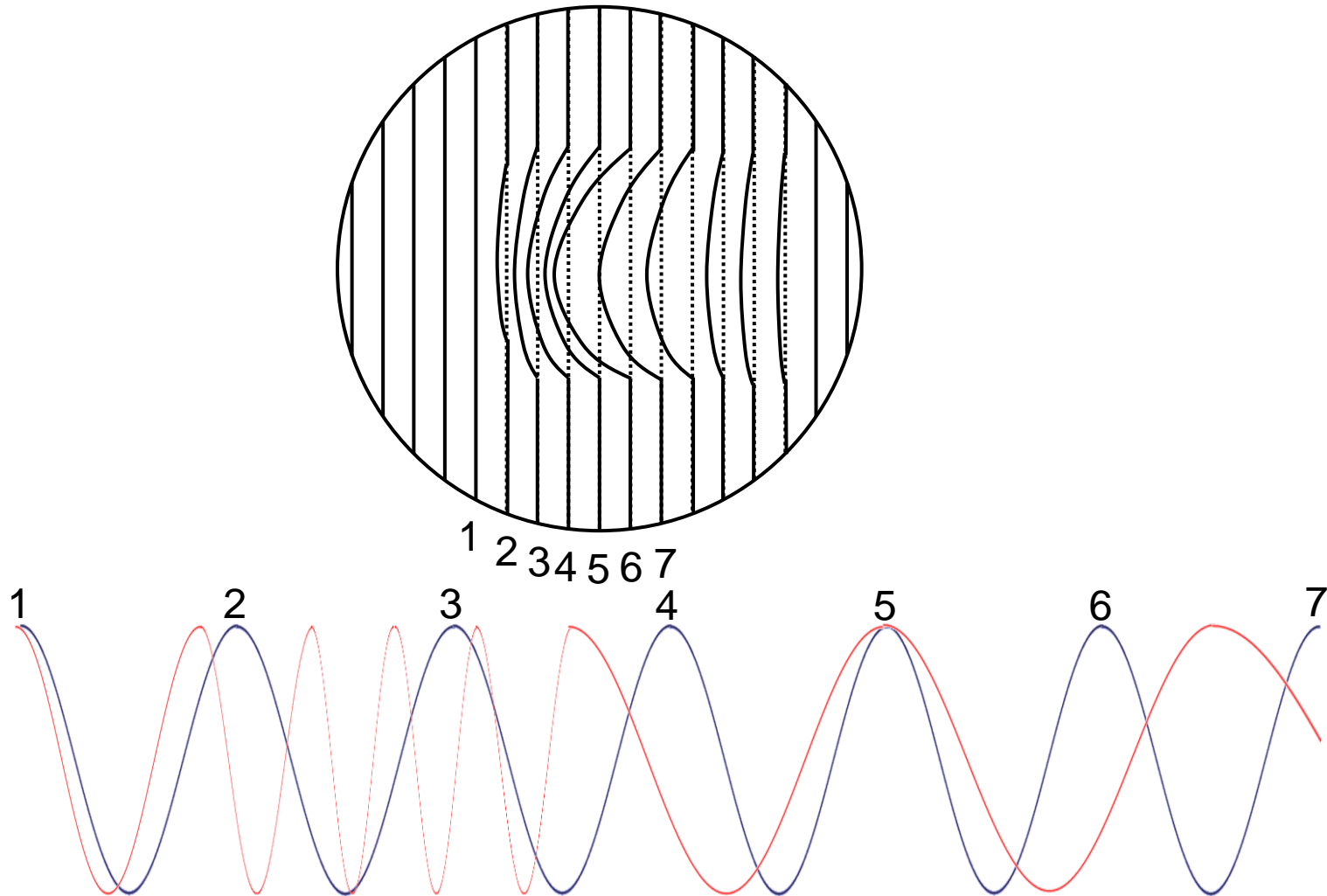
$$n^2 = 1 - \frac{n_e}{n_{cr}} \quad n_{cr} = \frac{\epsilon_0 m_e \omega^2}{e^2}$$



$$\begin{aligned} \Delta\phi &= \int (k_{\text{plasma}} - k_0) dl = \frac{\omega}{c} \int (n - 1) dl \\ &= \frac{\omega}{c} \int \left( \sqrt{1 - \frac{n_e}{n_{cr}}} - 1 \right) dl \approx \frac{\omega}{c} \int \left( 1 - \frac{1}{2} \frac{n_e}{n_{cr}} - 1 \right) dl \\ &= -\frac{\omega}{2cn_{cr}} \int n_e dl \end{aligned}$$

Note that  $n_e \ll n_{cr}$  is assumed,  $\sqrt{1 - \frac{n_e}{n_{cr}}} \approx 1 - \frac{1}{2} \frac{n_e}{n_{cr}}$

# The phase is determined by comparing to the pattern without the phase shift



# Fourier transform can be used to retrieve the data from the interferometer image



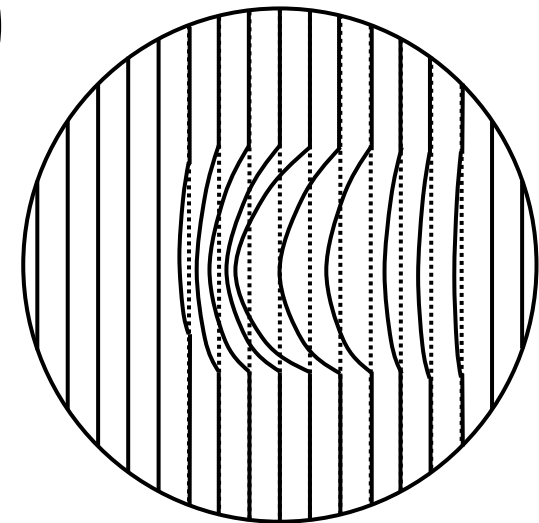
$$\begin{aligned}
 I(x, y) &= I_0(x, y) + m(x, y) \cos[2\pi\nu_0 x + \phi(x, y)] & \cos(x) &= \frac{e^{ix} + e^{-ix}}{2} \\
 &= I_0(x, y) + \frac{1}{2} m(x, y) (e^{i[2\pi\nu_0 x + \phi(x, y)]} + e^{-i[2\pi\nu_0 x + \phi(x, y)]}) \\
 &= I_0(x, y) + \frac{1}{2} m(x, y) e^{i\phi(x, y)} e^{i2\pi\nu_0 x} + \frac{1}{2} m(x, y) e^{-i\phi(x, y)} e^{-i2\pi\nu_0 x} \\
 &= I_0(x, y) + c(x, y) e^{i2\pi\nu_0 x} + c^*(x, y) e^{-i2\pi\nu_0 x}
 \end{aligned}$$

$$c(x, y) \equiv \frac{1}{2} m(x, y) e^{i\phi(x, y)} \quad \phi(x, y) = \tan^{-1} \left( \frac{\text{Im}[c(x, y)]}{\text{Re}[c(x, y)]} \right)$$

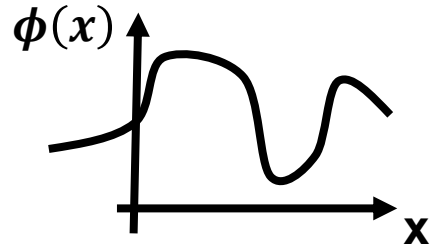
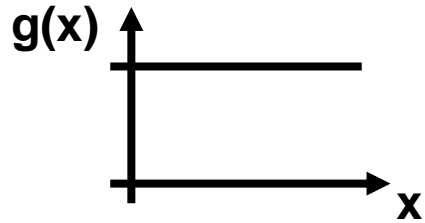
$$\hat{g}(f_x, y) \equiv \text{FT}[g(x, y)]$$

$$\hat{g}(f_x - \nu_0, y) = \text{FT}[g(x, y) e^{i2\pi\nu_0 x}]$$

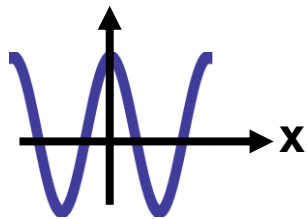
$$\hat{I}(f_x, y) = \hat{I}_0(f_x, y) + \hat{c}(f_x - \nu_0, y) + \hat{c}^*(f_x + \nu_0, y)$$



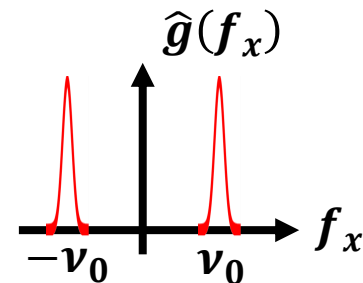
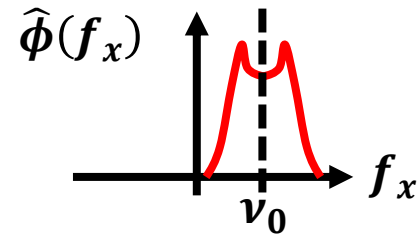
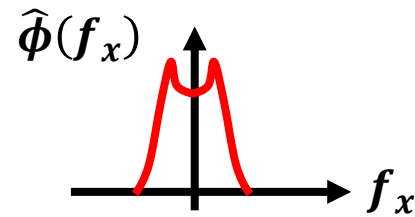
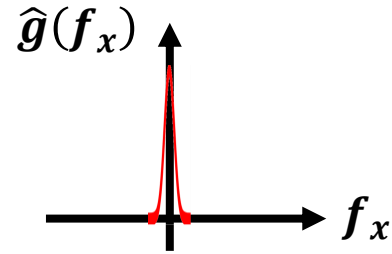
# Basic knowledge of Fourier transform



$$h(x) = \phi(x) \times e^{-i2\pi\nu_0 x}$$



$$g(x) = \cos(2\pi\nu_0 x) = \frac{e^{i2\pi\nu_0 x} + e^{-i2\pi\nu_0 x}}{2}$$

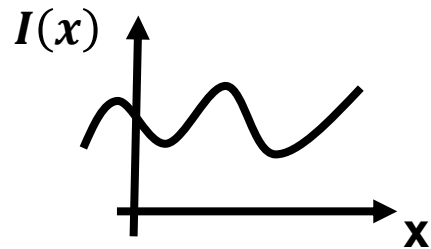
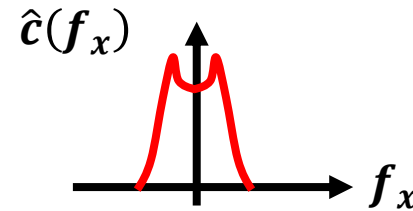
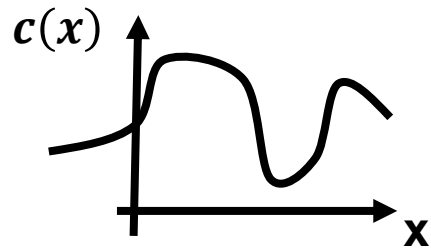


# Procedure of retrieving data

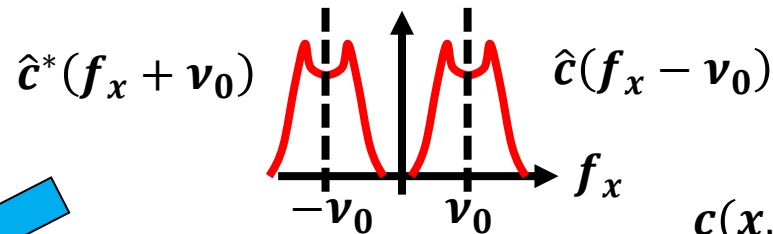


$$\begin{aligned}
 I(x) &= I_0(x) + m(x)\cos[2\pi\nu_0x + \phi(x)] \\
 &\equiv \cos[2\pi\nu_0x + \phi(x)] \\
 &= c^*(x, y)e^{i2\pi\nu_0x} + c(x, y)e^{-i2\pi\nu_0x}
 \end{aligned}$$

$$\hat{I}(f_x) = \hat{c}(f_x - \nu_0) + \hat{c}^*(f_x + \nu_0)$$

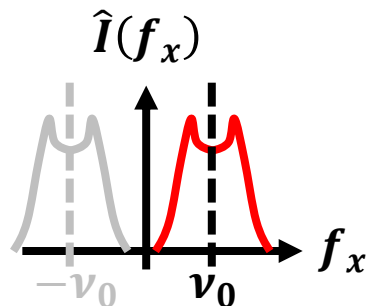


$\hat{I}(f_x)$

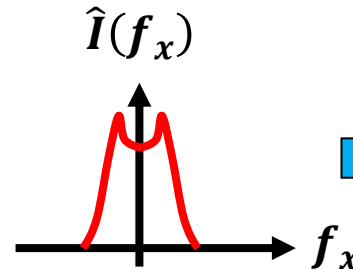


$$c(x, y) \equiv \frac{1}{2} e^{-i\phi(x, y)}$$

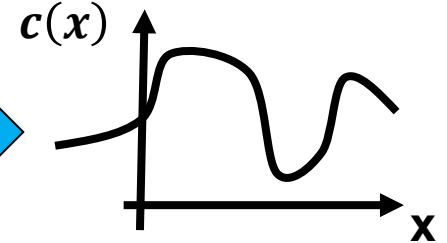
Filter



Shift

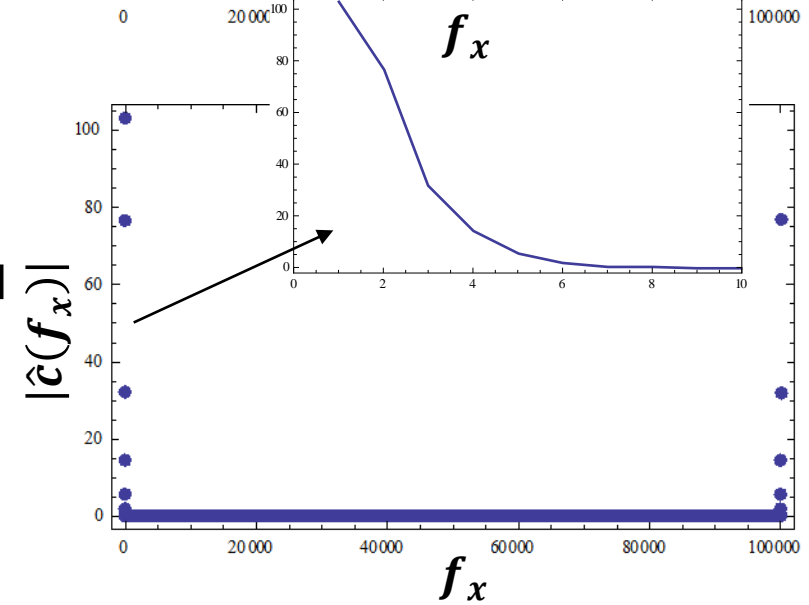
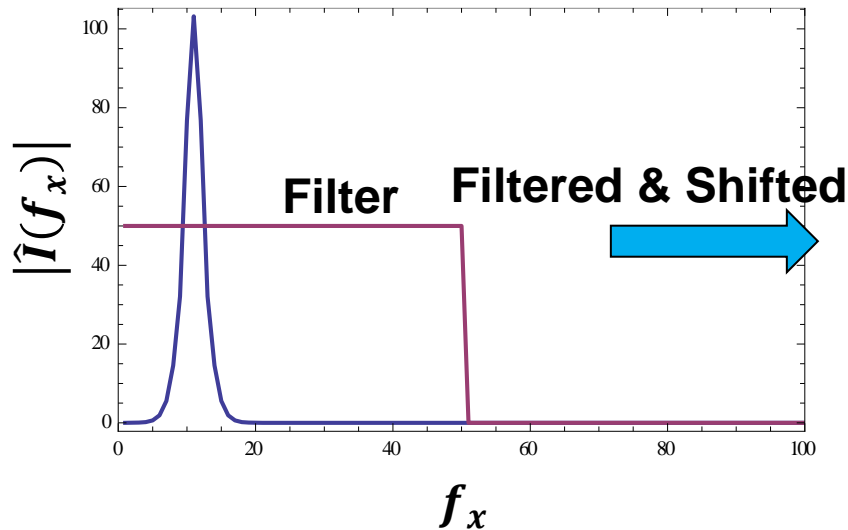
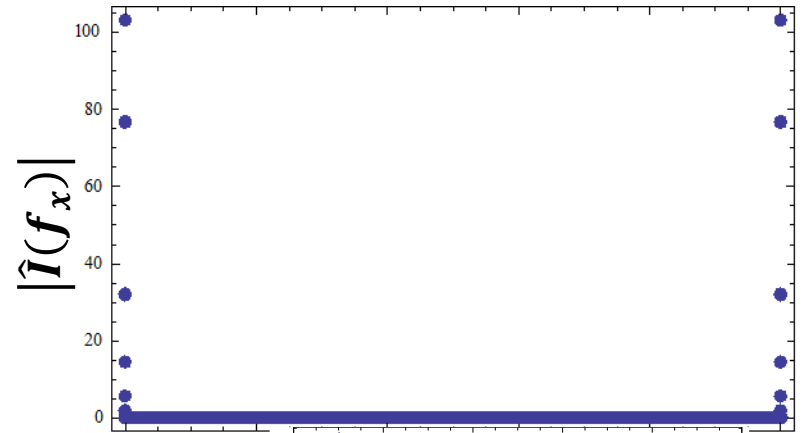
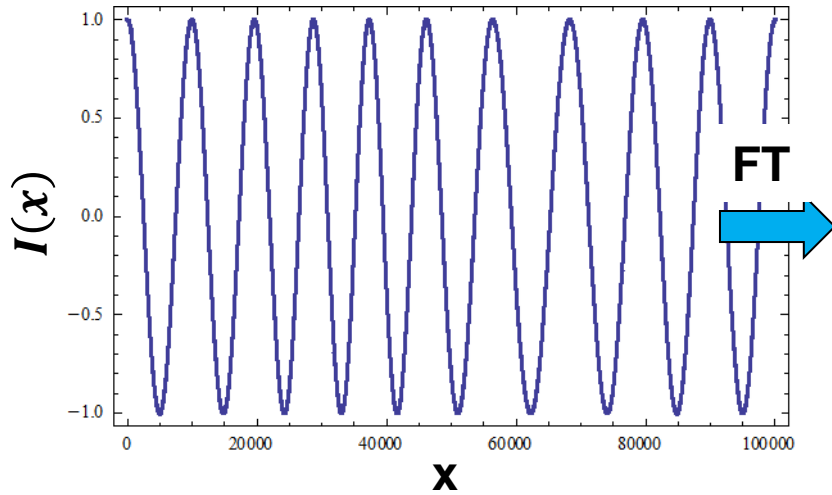


FT<sup>-1</sup>

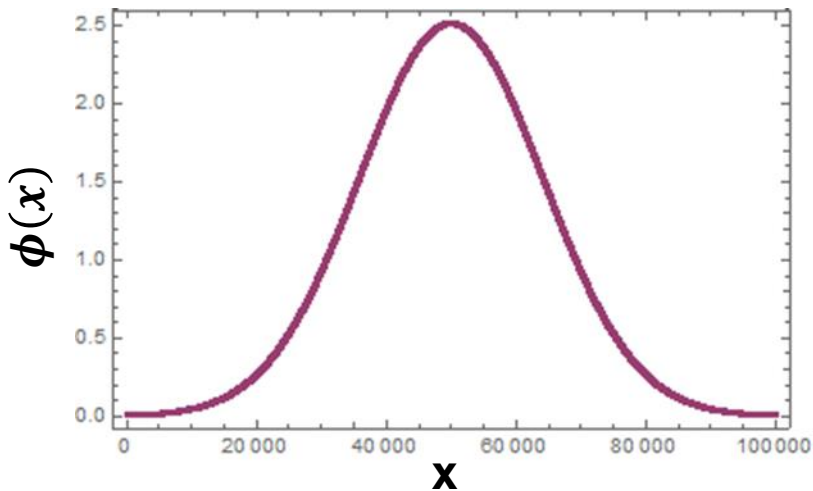
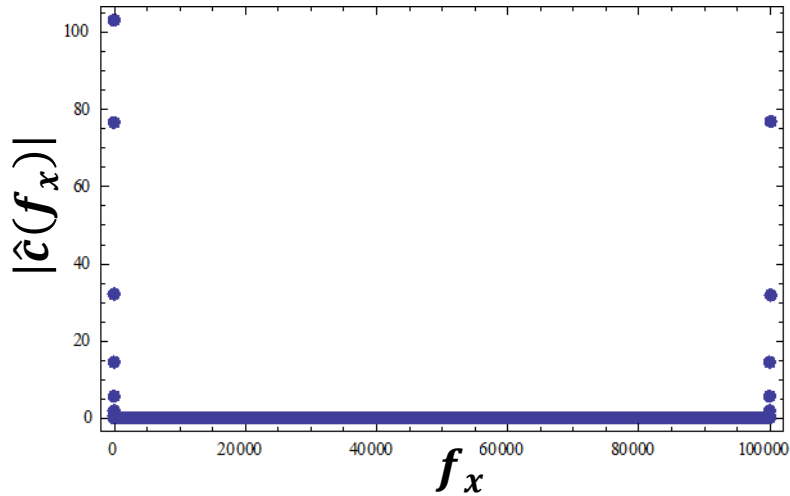




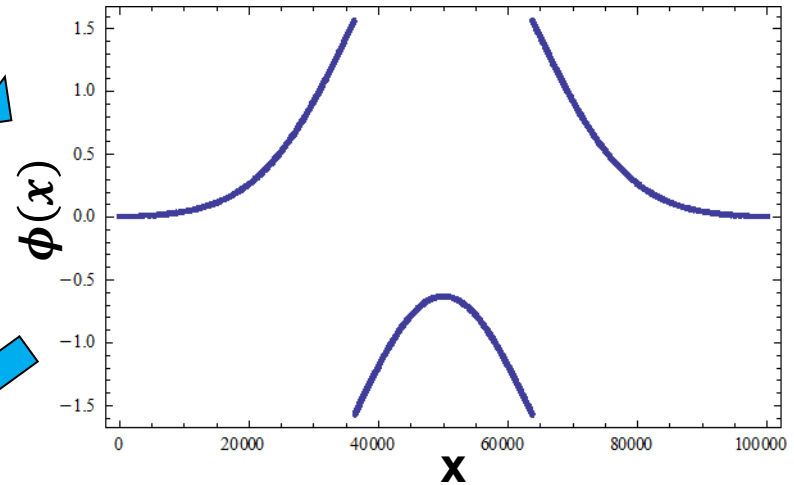
# Example of retrieving data from 1D interferometer



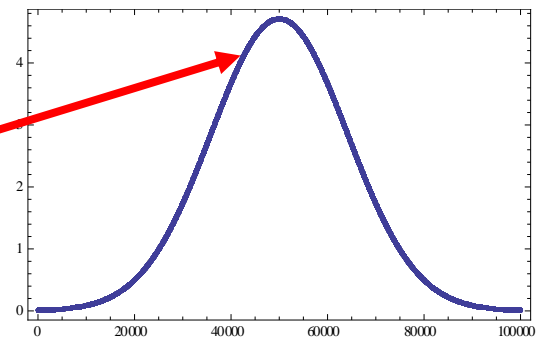
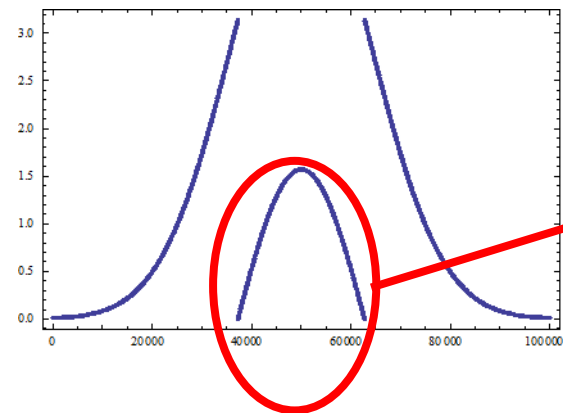
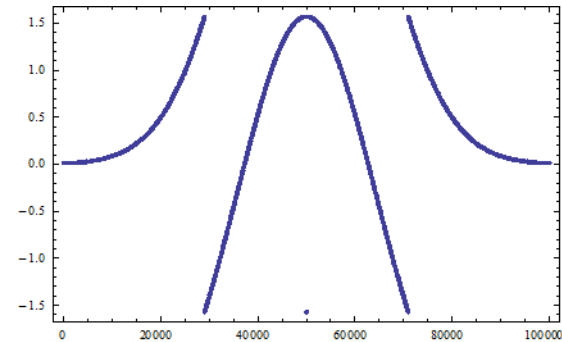
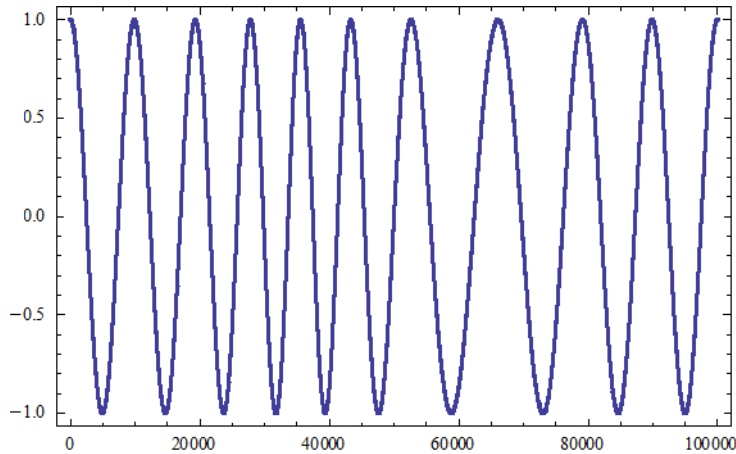
# The retrieved data need to be modified if the phase change is too much



$$\text{FT}^{-1} \& \phi(x) = \tan^{-1} \left( \frac{\text{Im}[c(x)]}{\text{Re}[c(x)]} \right)$$



# The final phase difference needs to be determined manually since it may exceeds $2\pi$

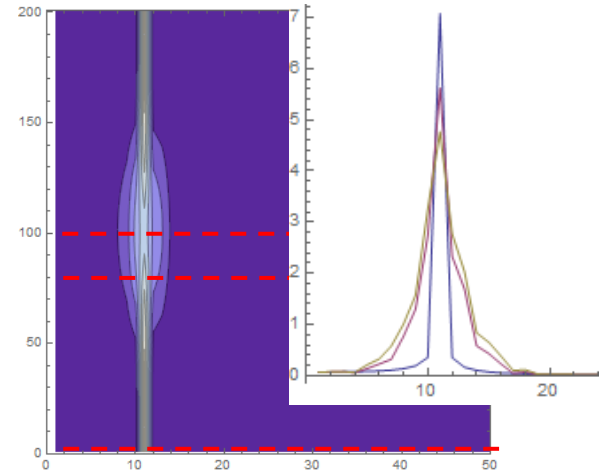
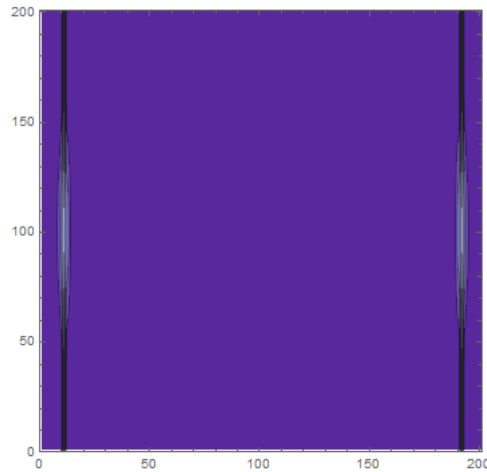
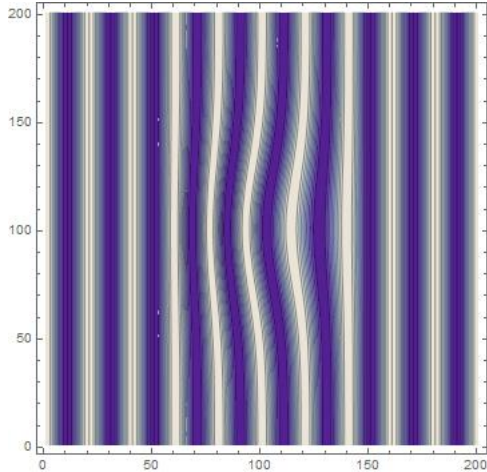


# Example of retrieving data from 2D interferometer

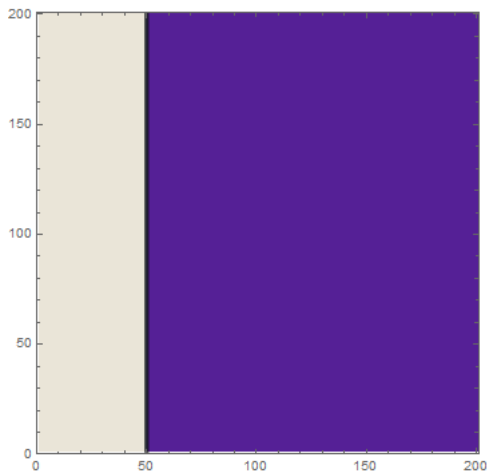


$$I(x, y) = \cos[2\pi\nu_0x + \phi(x, y)]$$

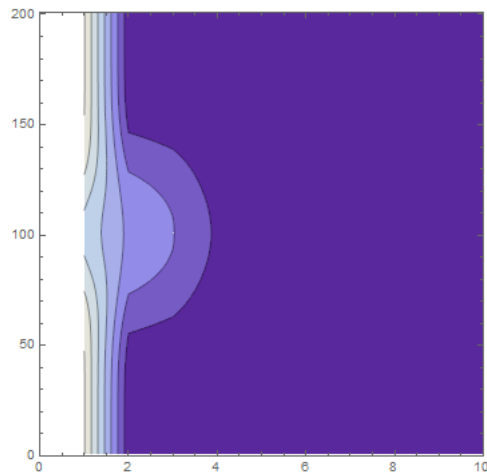
$$\hat{I}(f_x, y) = \hat{c}(f_x - \nu_0, y) + \hat{c}^*(f_x + \nu_0, y)$$



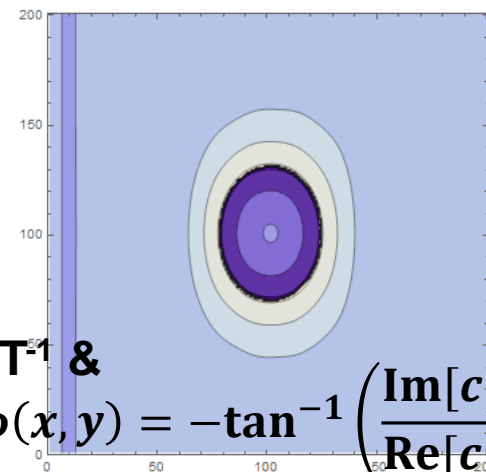
**Filter**



**Filtered & Shifted**



**Retrieved data**



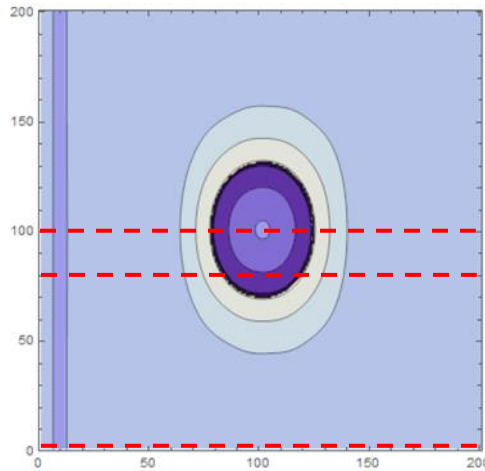
**FT<sup>-1</sup> &**  

$$\phi(x, y) = -\tan^{-1} \left( \frac{\text{Im}[c(x, y)]}{\text{Re}[c(x, y)]} \right)$$

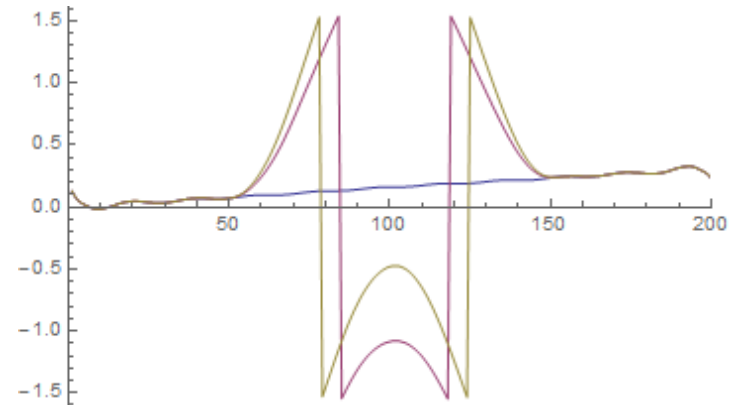
# The retrieved data may need to be modified if the phase change is too large



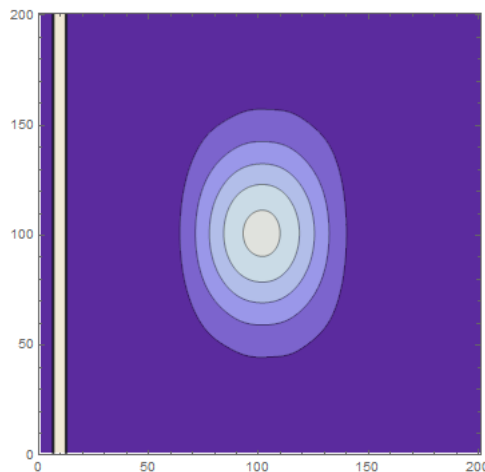
## Retrieved data



## 1D profile

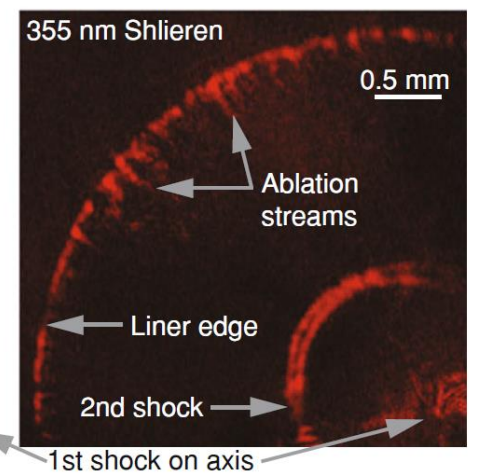
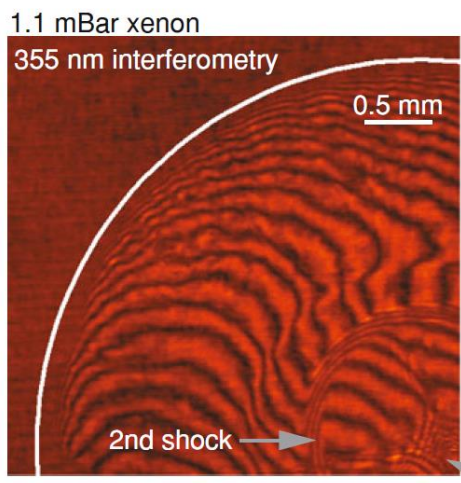
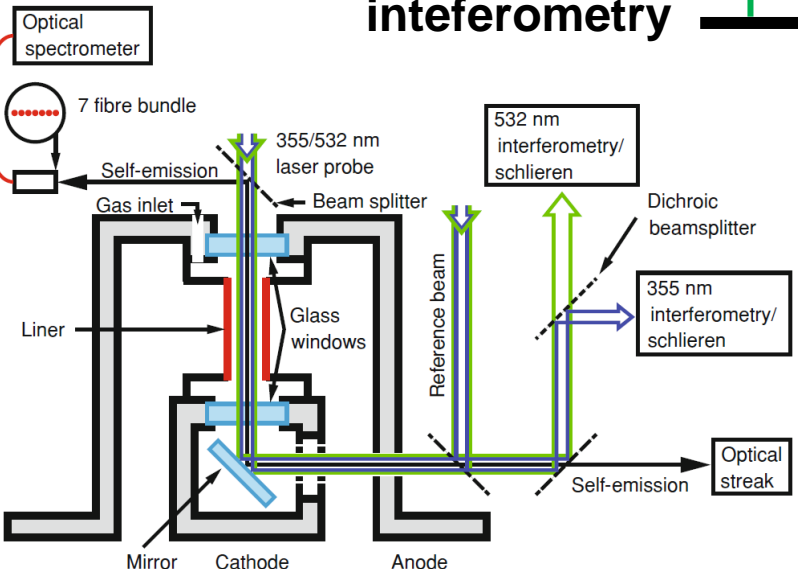
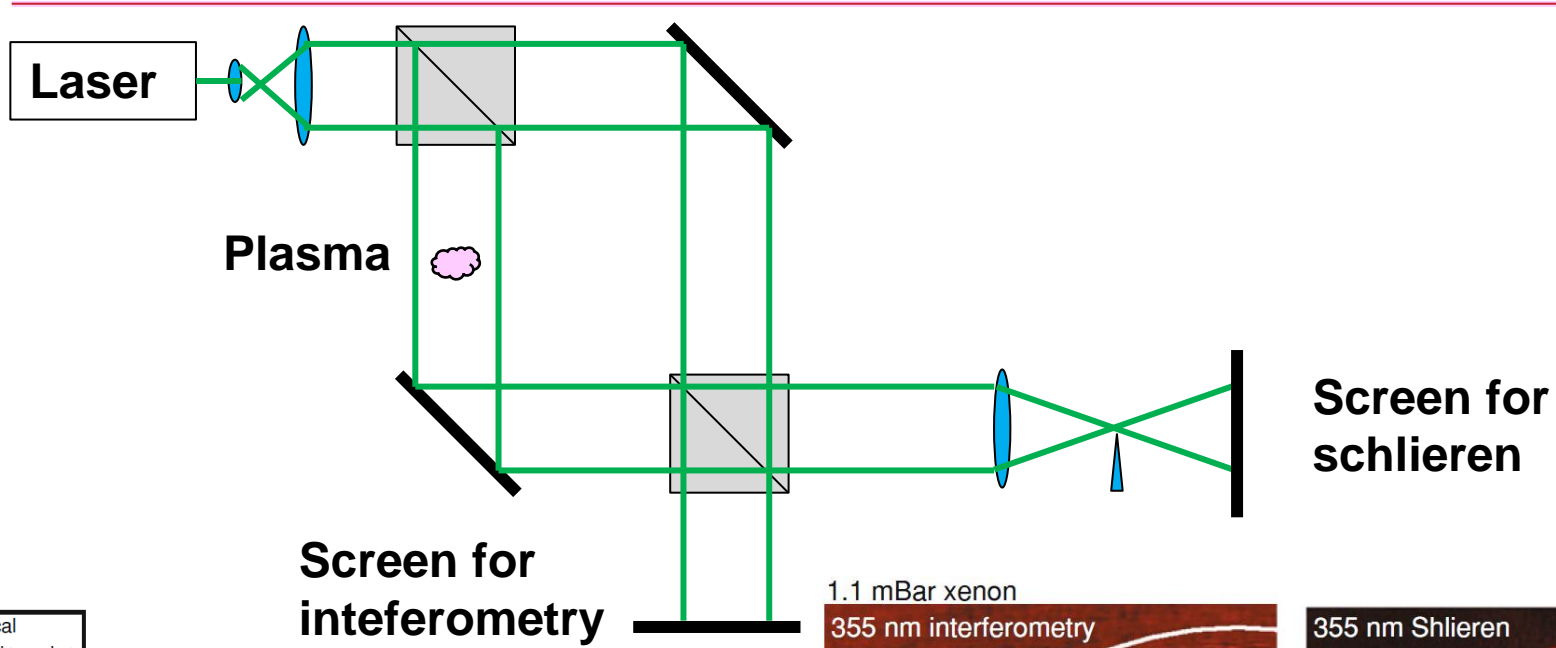


## Modified result



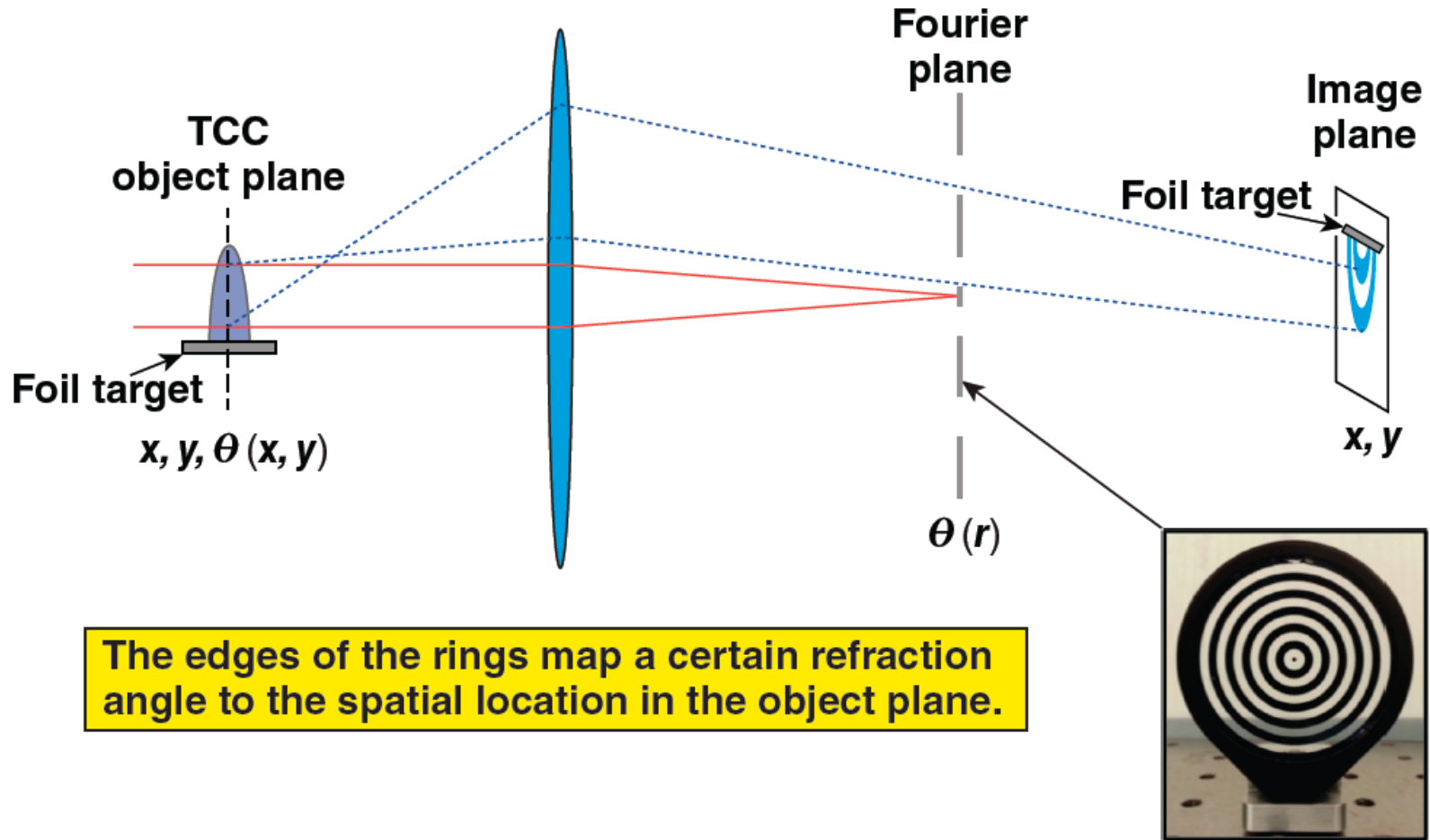
- Noise came from low spatial resolution.

# Schlieren imaging system can detect density gradient

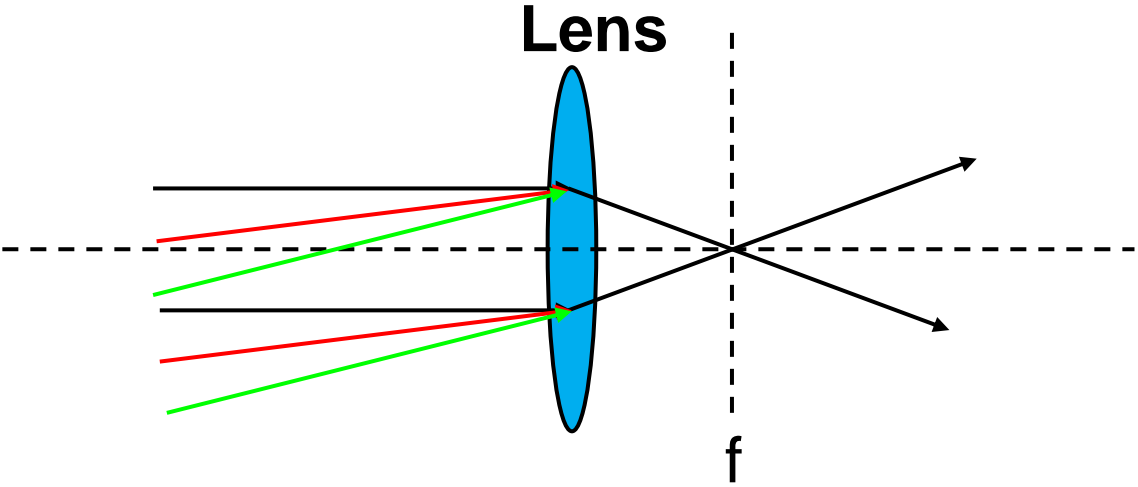


G. C. Burdiak, Cylindrical liner z-pinch as drivers for converging strong shock experiments

Angular filter refractometry (AFR) maps the refraction of the probe beam at TCC to contours in the image plane

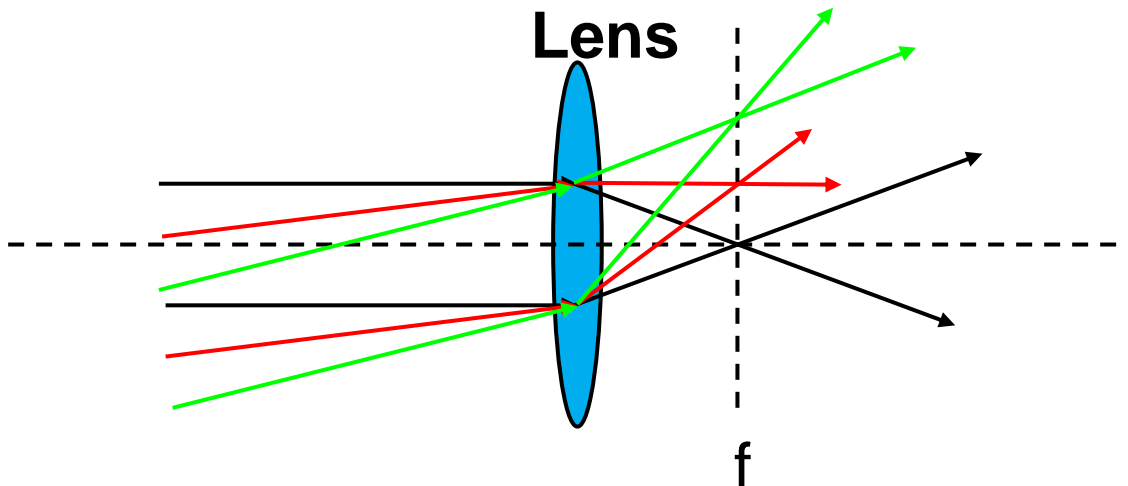
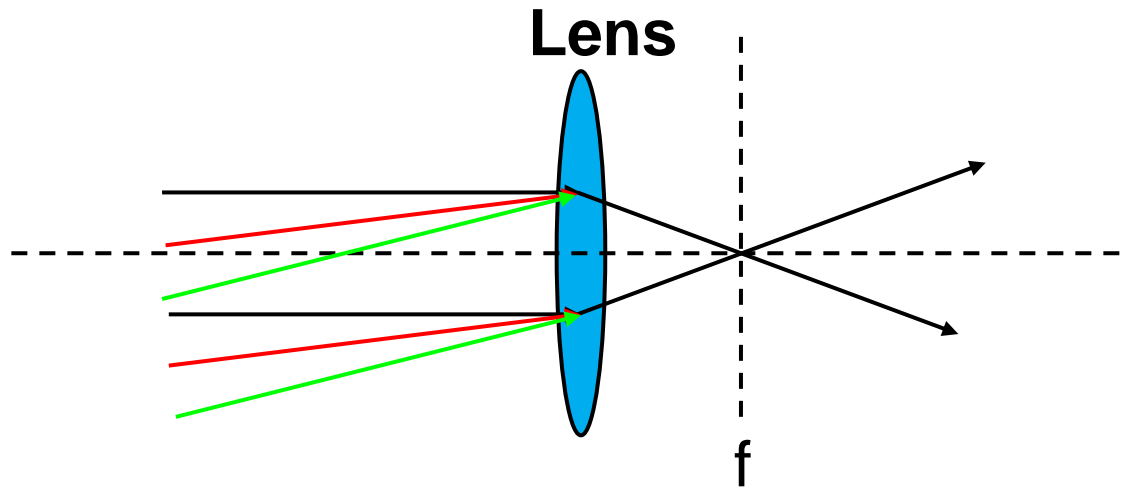


# Angular spectrum of plane waves can be used for diagnostic

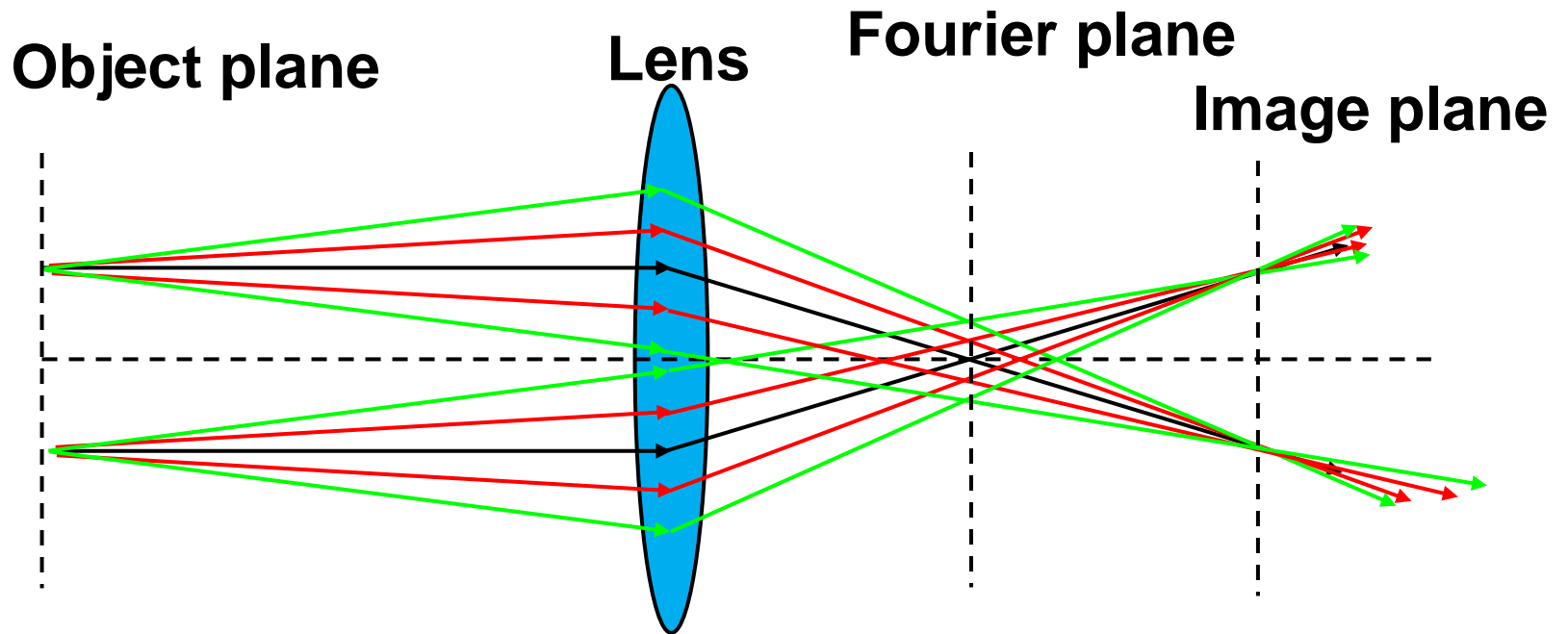




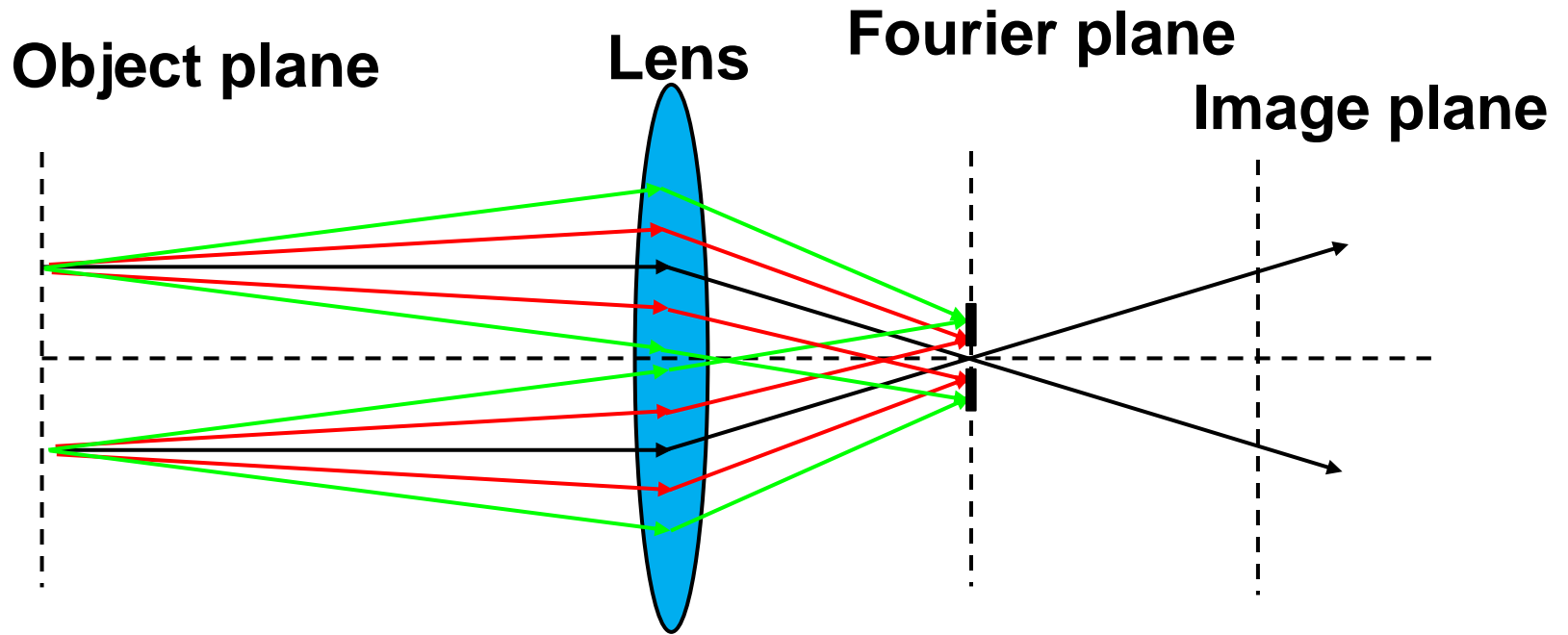
# Angular spectrum of plane waves can be used for diagnostic



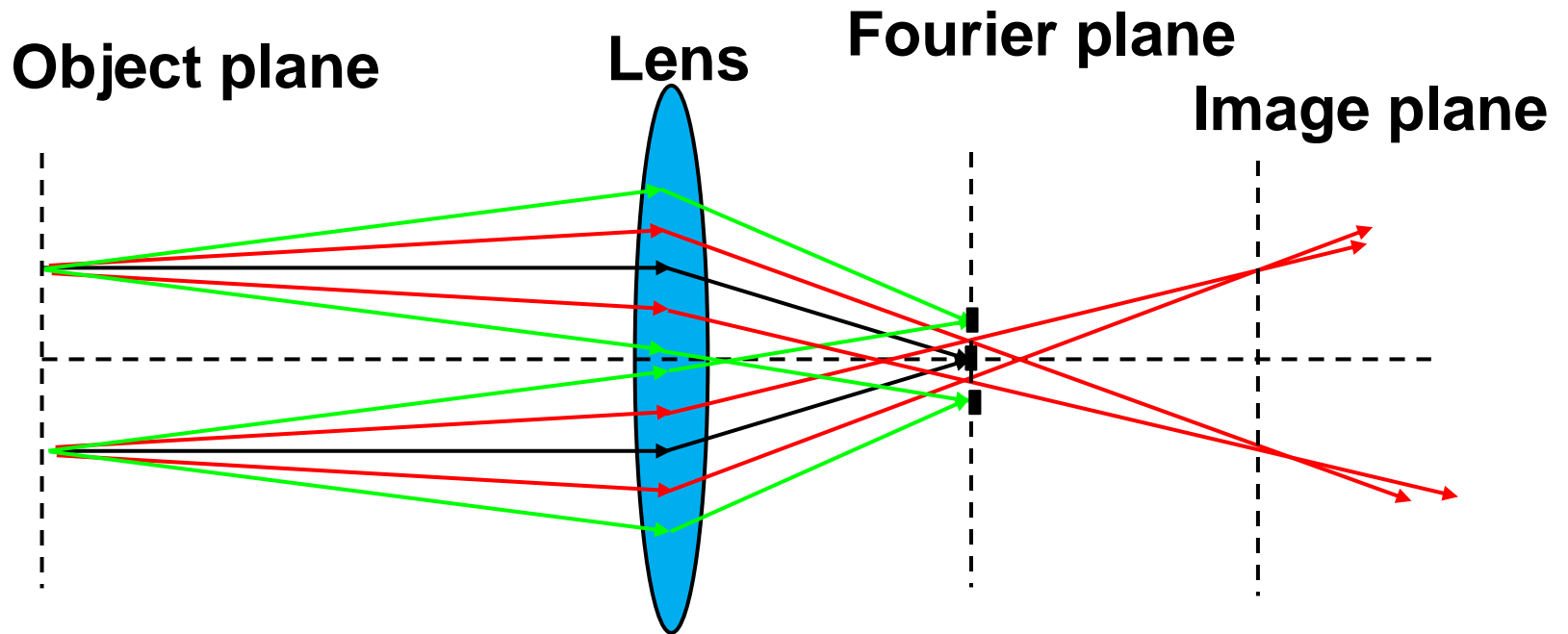
# Rays with different angles go through different focal points on the focal points



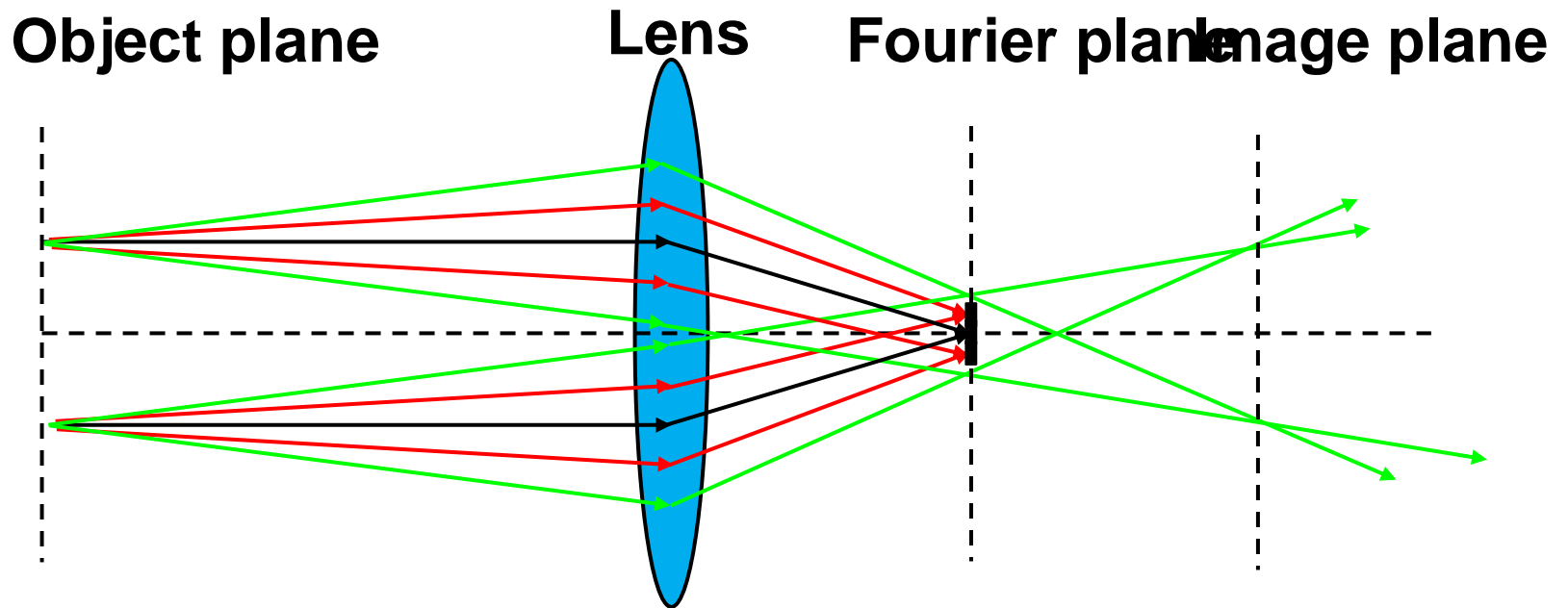
# Rays with different angles can be selected by blocking different focal points



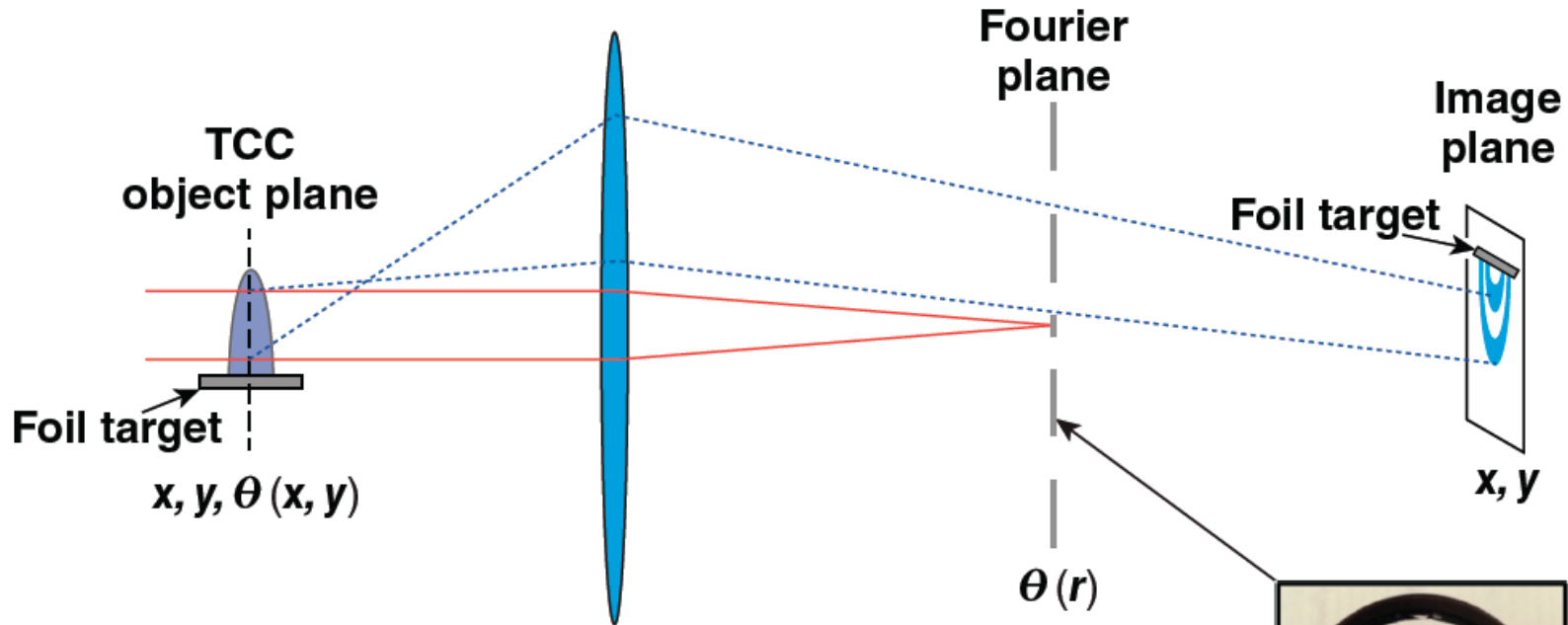
# Rays with different angles go through different focal points on the focal points



# Rays with different angles go through different focal points on the focal points



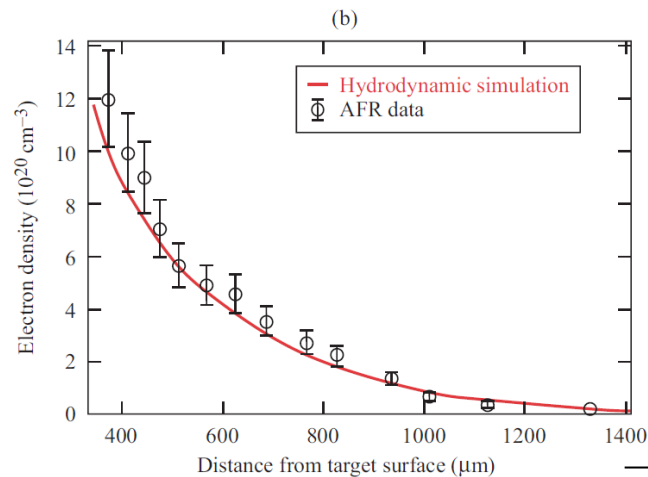
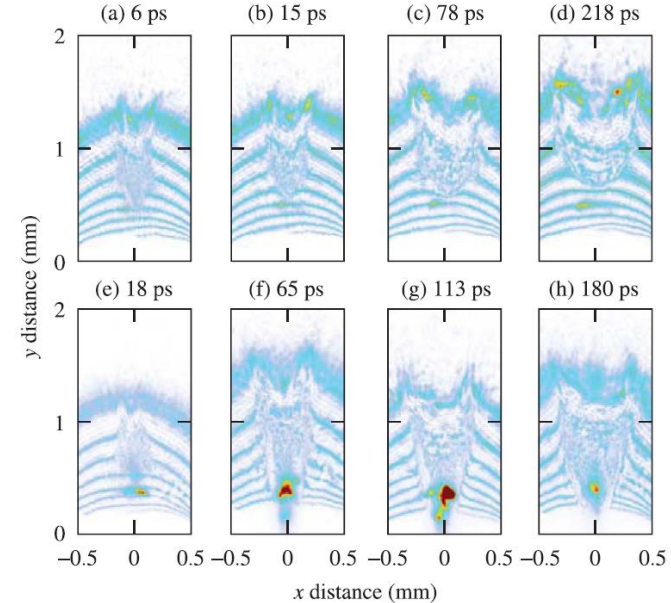
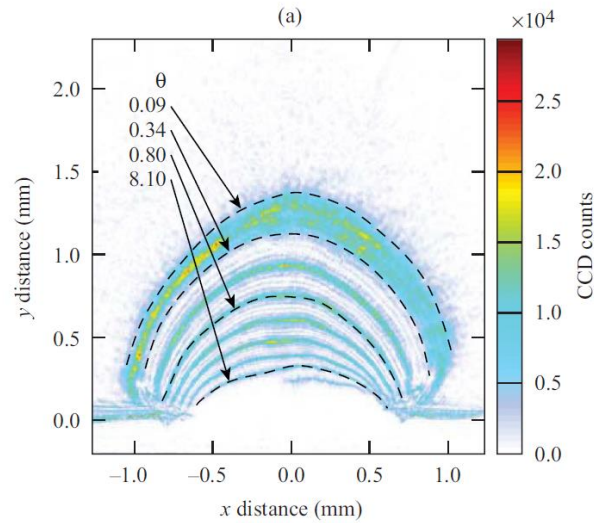
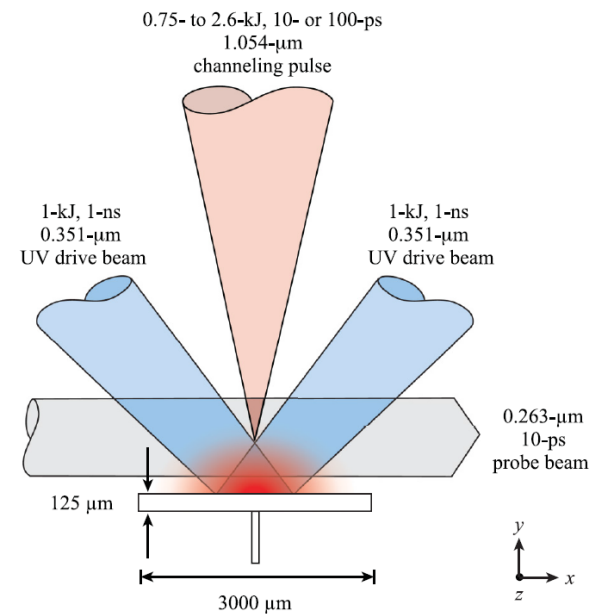
# Angular filter refractometry (AFR) maps the refraction of the probe beam at TCC to contours in the image plane



The edges of the rings map a certain refraction angle to the spatial location in the object plane.



# Channeling of multi-kilojoule high-intensity laser beams in an inhomogeneous plasma was observed using AFR



# Electromagnetic wave can be used to measure the density or the magnetic field in the plasma



- **Nonmagnetized isotropic plasma (interferometer needed):**

$$n^2 = 1 - \frac{X(1-X)}{1 - X - \frac{1}{2}Y^2 \sin^2 \theta \pm \left[ \left( \frac{1}{2}Y^2 \sin^2 \theta \right)^2 + (1-X)^2 Y^2 \cos^2 \theta \right]^{1/2}}$$

$$= 1 - X = 1 - \frac{\omega_p^2}{\omega^2} = 1 - \frac{n_e}{n_{cr}} \quad \left( Y \equiv \frac{\Omega}{\omega} \equiv 0 \right)$$

**Note:**  $\omega_p^2 = \frac{n_e e^2}{\epsilon_0 m_e}$        $n_{cr} = \frac{\epsilon_0 m_e \omega^2}{e^2}$

- **Magnetized isotropic plasma (Polarization detected needed):**

Parallel to  $B_0$

$$n^2 = 1 - \frac{\omega_p^2}{\omega(\omega \pm \Omega)} \quad \frac{E_x}{E_y} = \pm i \quad \Omega \equiv \frac{eB_0}{m_e}$$

**Faraday rotation: linear polarization rotation caused by the difference between the speed of LHC and RHC polarized wave.**

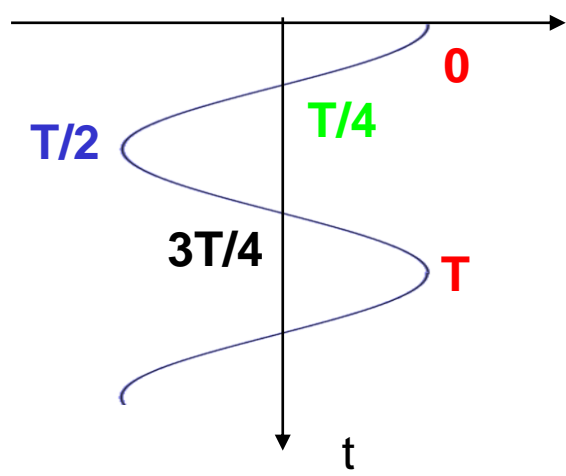
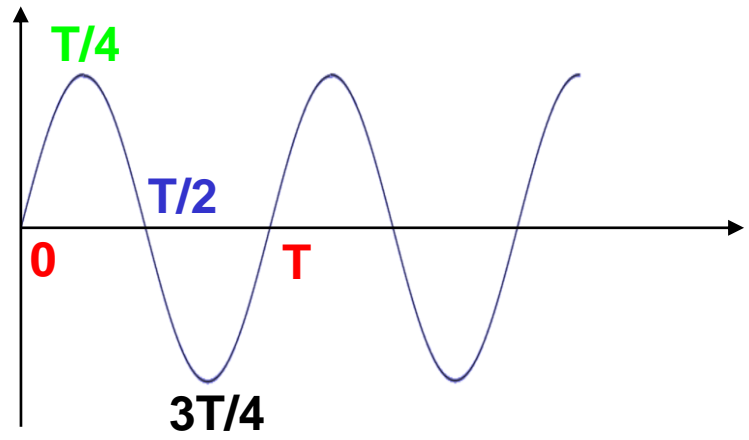
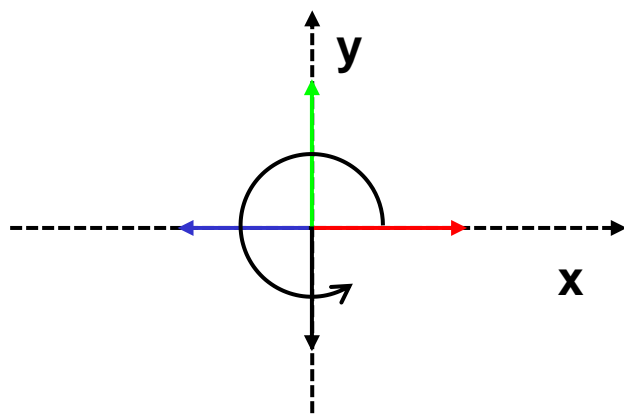


# Circular polarization



$$E_x = E_0 \exp(-i\omega t)$$

$$E_y = iE_x = iE_0 \exp(-i\omega t) = E_0 \exp\left(i\frac{\pi}{2}\right) \exp(-i\omega t) = E_0 \exp\left[-i\left(\omega t - \frac{\pi}{2}\right)\right]$$



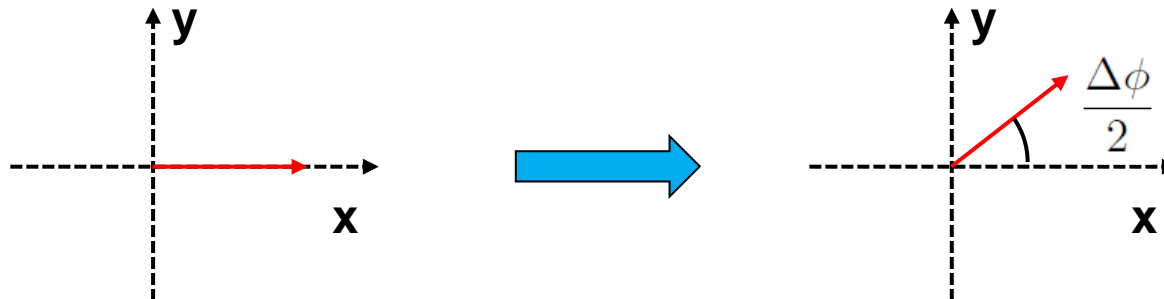
# Linear polarization rotates as the wave propagates with different speed in LHC and RHC polarization



$$\vec{E} = E_0 \hat{x} = \frac{E_0}{2} [(\hat{x} + i\hat{y}) + (\hat{x} - i\hat{y})]$$

$$\vec{E}(z) = \vec{E} \exp(i\phi) \quad \phi_R \neq \phi_L \quad \bar{\phi} \equiv \frac{\phi_R + \phi_L}{2}, \quad \Delta\phi = \frac{\phi_R - \phi_L}{2}$$

$$\begin{aligned} \vec{E}(z) &= \frac{E_0}{2} [(\hat{x} + i\hat{y}) e^{i\phi_R} + (\hat{x} - i\hat{y}) e^{i\phi_L}] \\ &= \frac{E_0}{2} [\hat{x} (e^{i\phi_R} + e^{i\phi_L}) + \hat{y}i (e^{i\phi_R} - e^{i\phi_L})] \\ &= \frac{E_0}{2} \left[ \hat{x} \left( e^{i(\bar{\phi} + \Delta\phi)} + e^{i(\bar{\phi} - \Delta\phi)} \right) + \hat{y}i \left( e^{i(\bar{\phi} + \Delta\phi)} - e^{i(\bar{\phi} - \Delta\phi)} \right) \right] \\ &= E_0 e^{i\bar{\phi}} \left[ \hat{x} \cos\left(\frac{\Delta\phi}{2}\right) + \hat{y} \sin\left(\frac{\Delta\phi}{2}\right) \right] \end{aligned}$$



# The rotation angle of the polarization depends on the linear integral of magnetic field and electron density



$$\phi = \int k dl = \int n \frac{\omega}{c} dl \quad \alpha = \frac{\Delta\phi}{2} = \frac{\omega}{2c} \int (n_R - n_L) dl$$

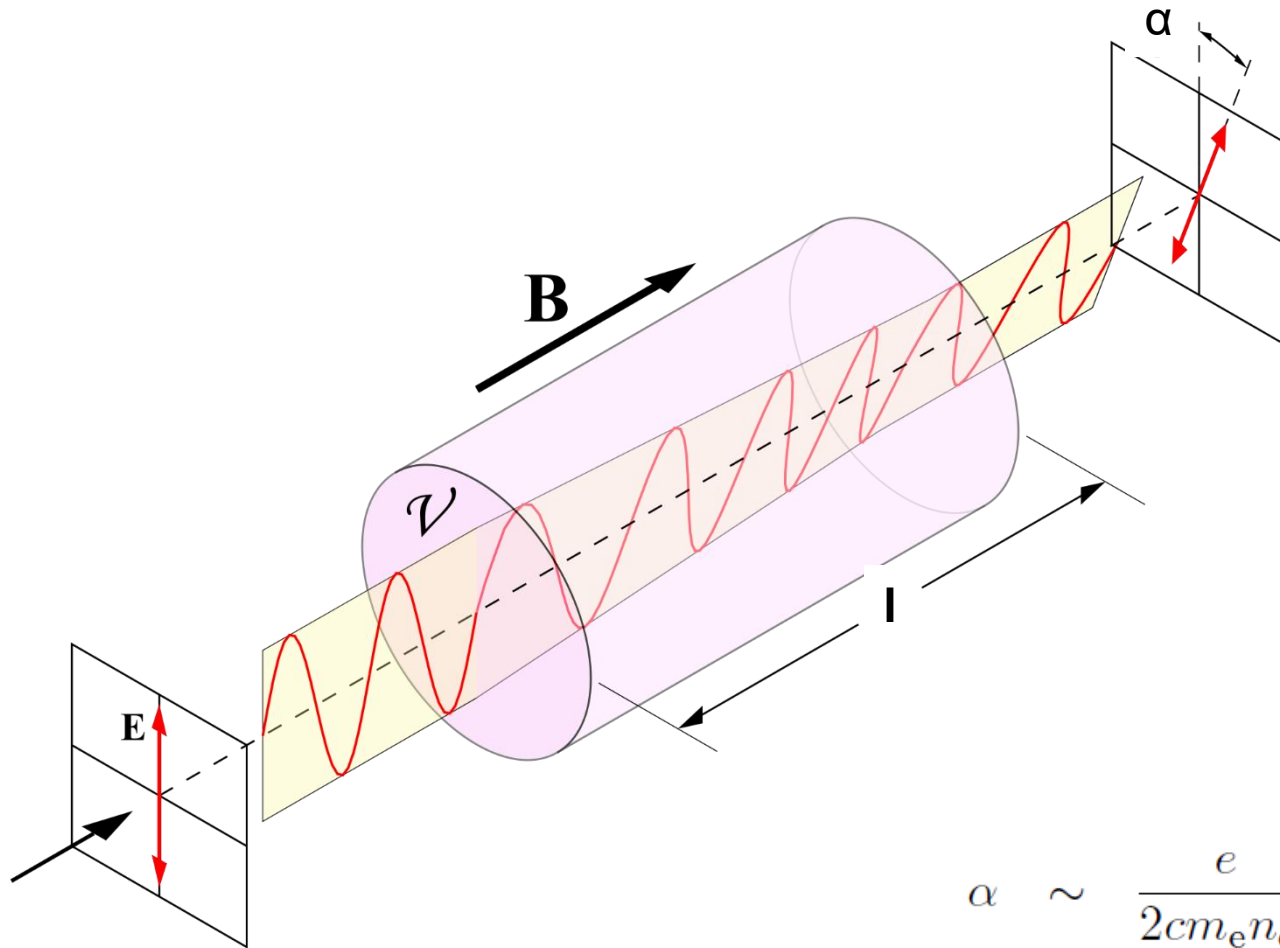
$$n_R = \sqrt{1 - \frac{X}{1+Y}} \sim 1 - \frac{1}{2} \frac{X}{1+Y} \quad X, Y \ll 1$$

$$n_L \sim 1 - \frac{1}{2} \frac{X}{1-Y} \quad \frac{X}{1 \pm Y} \ll 1$$

$$n_R - n_L \sim \frac{X}{2} \left( \frac{1}{1-Y} - \frac{1}{1+Y} \right) = \frac{XY}{1-Y^2} \sim XY$$

$$\begin{aligned} \alpha &\sim \frac{\omega}{2c} \int XY dl = \frac{\omega}{2c} \int \frac{\omega_p^2}{\omega^2} \frac{\Omega}{\omega} dl = \frac{1}{2c} \int \frac{n_e}{n_{cr}} \frac{eB}{m_e} dl \\ &= \frac{e}{2cm_e n_{cr}} \int n_e B dl \end{aligned}$$

# The rotation angle of the polarization depends on the linear integral of magnetic field and electron density



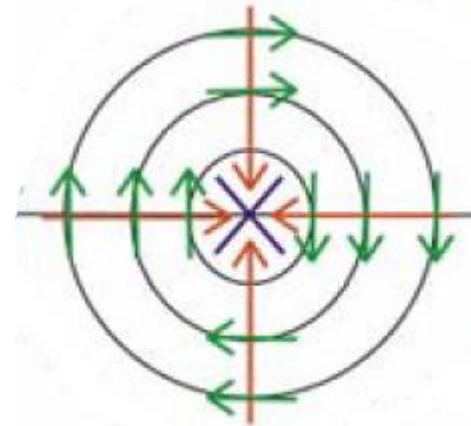
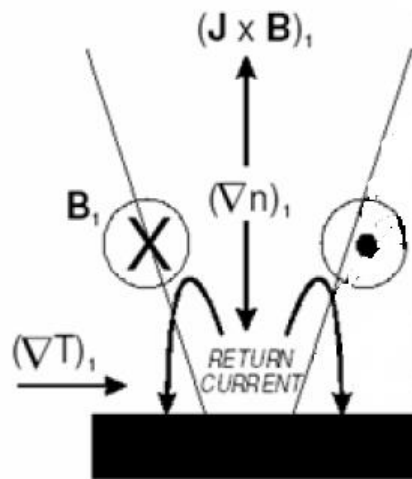
$$\alpha \sim \frac{e}{2cm_e n_{cr}} \int n_e B dl$$

# Magnetic field can be generated when the temperature and density gradients are not parallel to each other



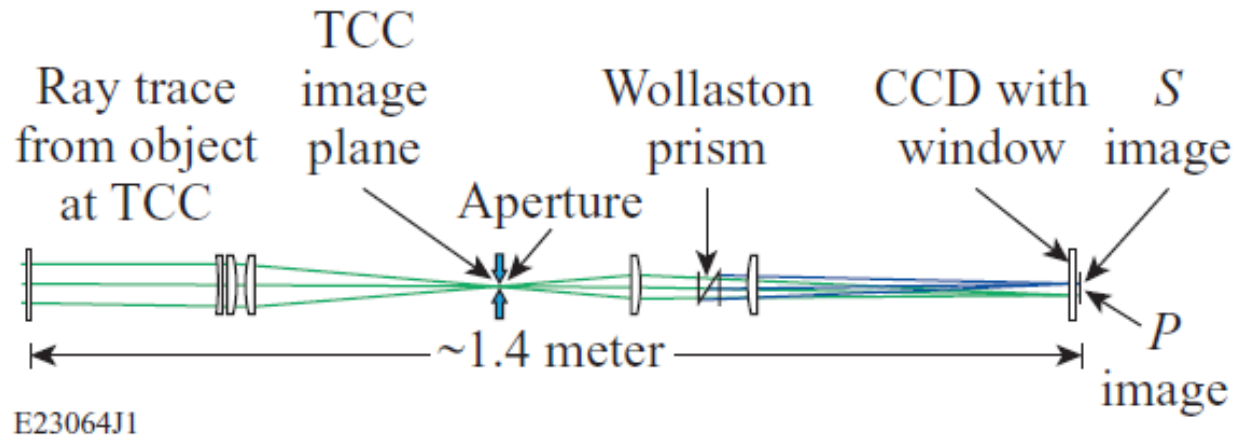
$$\frac{\partial \vec{B}}{\partial t} = \nabla \times \left[ \underbrace{\vec{u} \times \vec{B}}_{\text{Convection term}} + \underbrace{\frac{1}{\sigma \mu_0} \nabla \times \vec{B}}_{\text{Diffusion term}} + \underbrace{\frac{\nabla p_e}{n_e e}}_{\text{self generated field}} - \underbrace{\frac{1}{\mu_0} \left( \frac{\nabla \times \vec{B}}{n_e e} \times \vec{B} \right)}_{\text{Hall term}} \right]$$

$$\nabla \times \frac{\nabla p_e}{n_e e} = - \frac{k_B}{e} \frac{\nabla n_e \times \nabla T_e}{n_e}$$

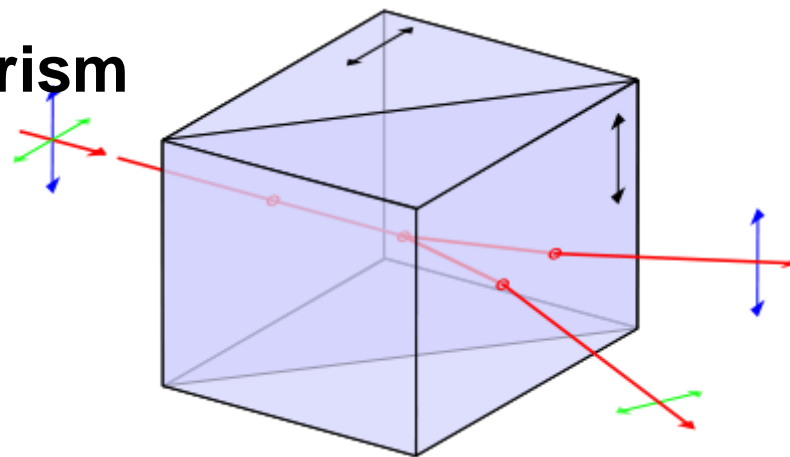


$$(\text{grad } n_e) \times (\text{grad } T_e) \longrightarrow \text{B field} \longrightarrow$$

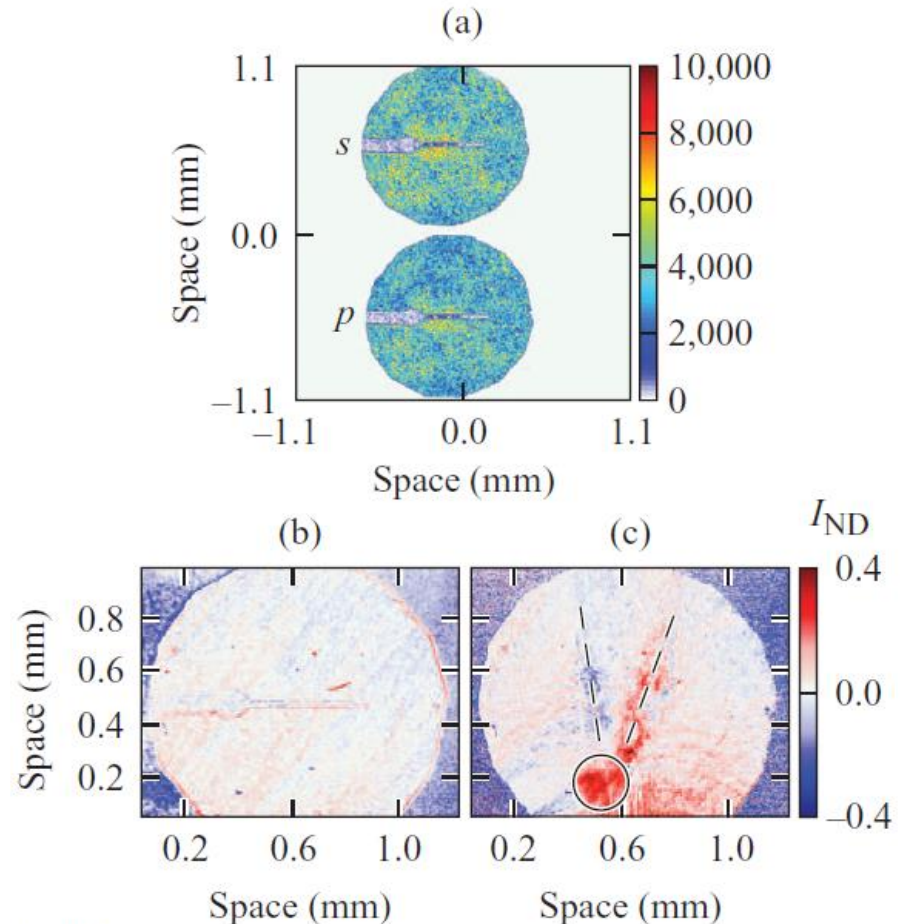
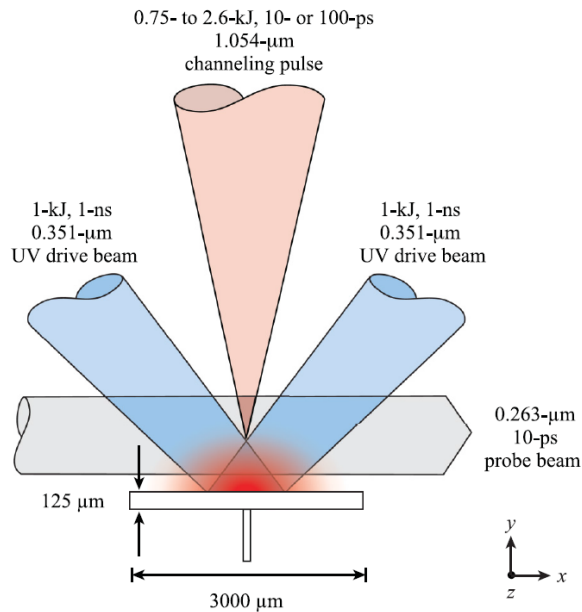
# Polarimetry diagnostic can be used to measure the magnetic field



## Wollaston prism

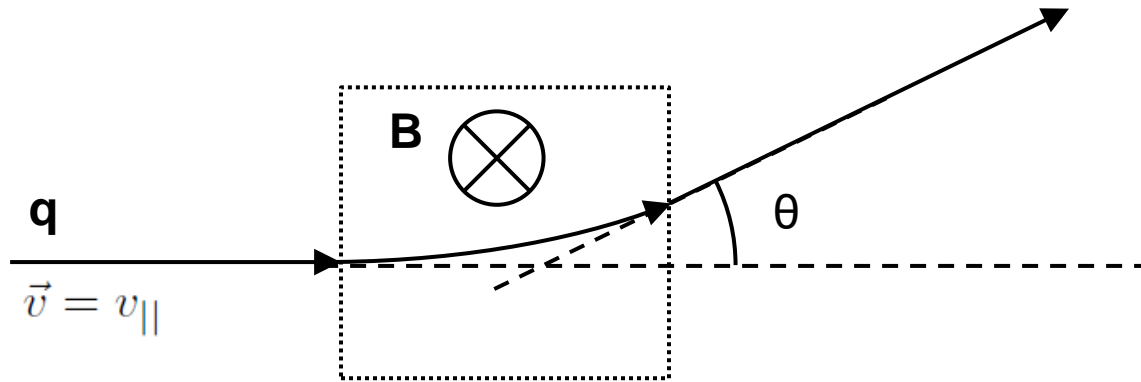


# Self-generated field was suggested when multi-kilojoule high-intensity laser beams illuminated on an inhomogeneous plasma



E23066J1

# The magnetic field can be measured by measuring the deflected angle of charged particles



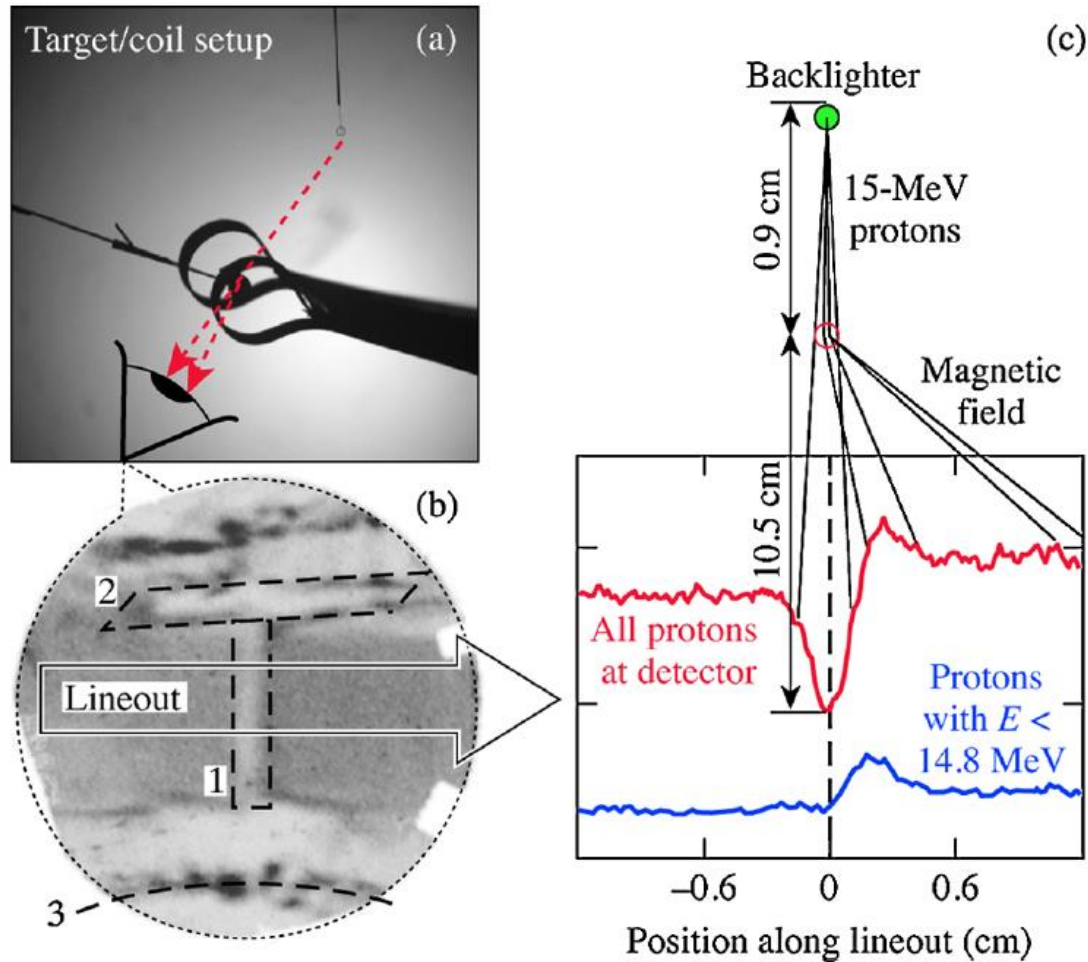
$$F_{\perp} = q\vec{v} \times \vec{B} = qv_{\parallel}B = m\frac{dv_{\perp}}{dt}$$

$$v_{\perp} = \int \frac{qv_{\parallel}B}{m} dt = \frac{qv_{\parallel}}{m} \int B dt \frac{dx}{dx} = \frac{qv_{\parallel}}{m} \int \frac{B}{v_{\parallel}} dx = \frac{q}{m} \int B dx$$

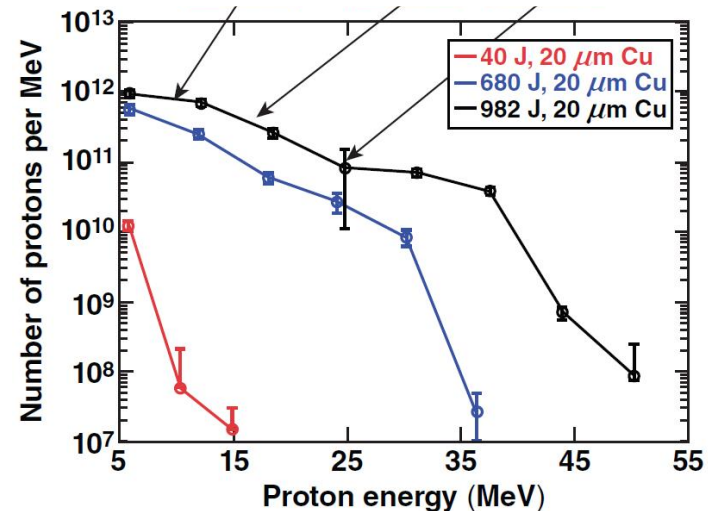
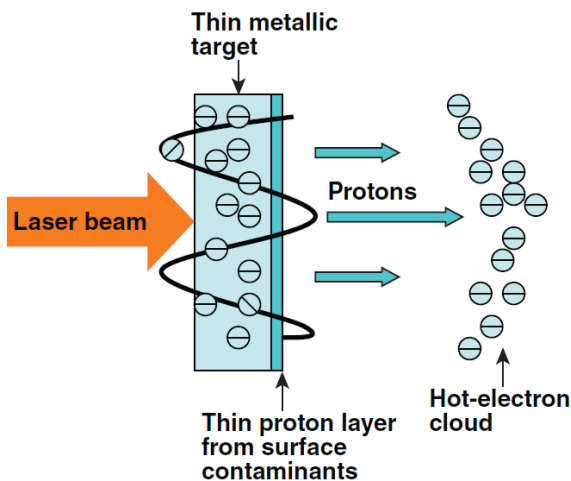
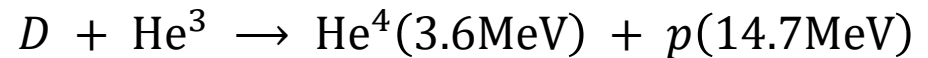
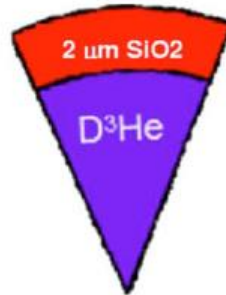
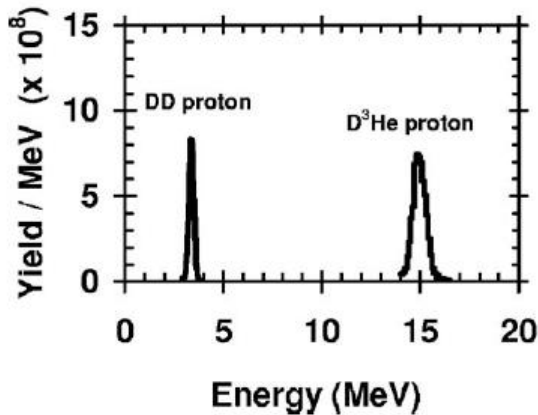
$$\tan \theta = \frac{v_{\perp}}{v_{\parallel}} = \frac{q}{mv_{\parallel}} \int B dx = \frac{q}{\sqrt{2mE}} \int B dx \quad \int B dx = \frac{\sqrt{2mE}}{q} \tan \theta$$



# Magnetic field was measured using protons



# Protons can be generated from fusion product or copper foil illuminated by short pulse laser



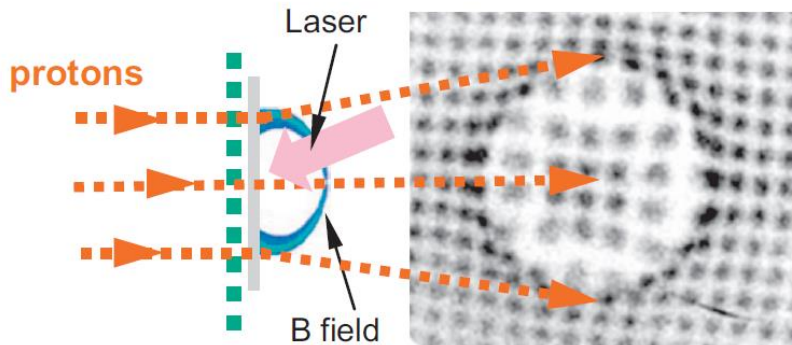
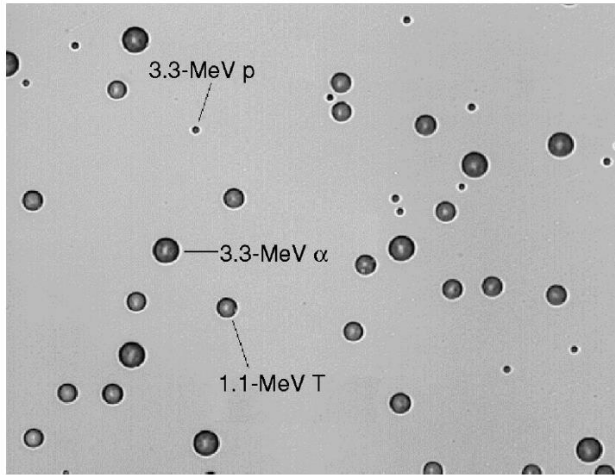
## Target normal sheath acceleration (TNSA)

C. K. Li *et al.*, Rev. Sci. Instrum. **77**, 10E725 (2006)  
L. Gao, PhD Thesis

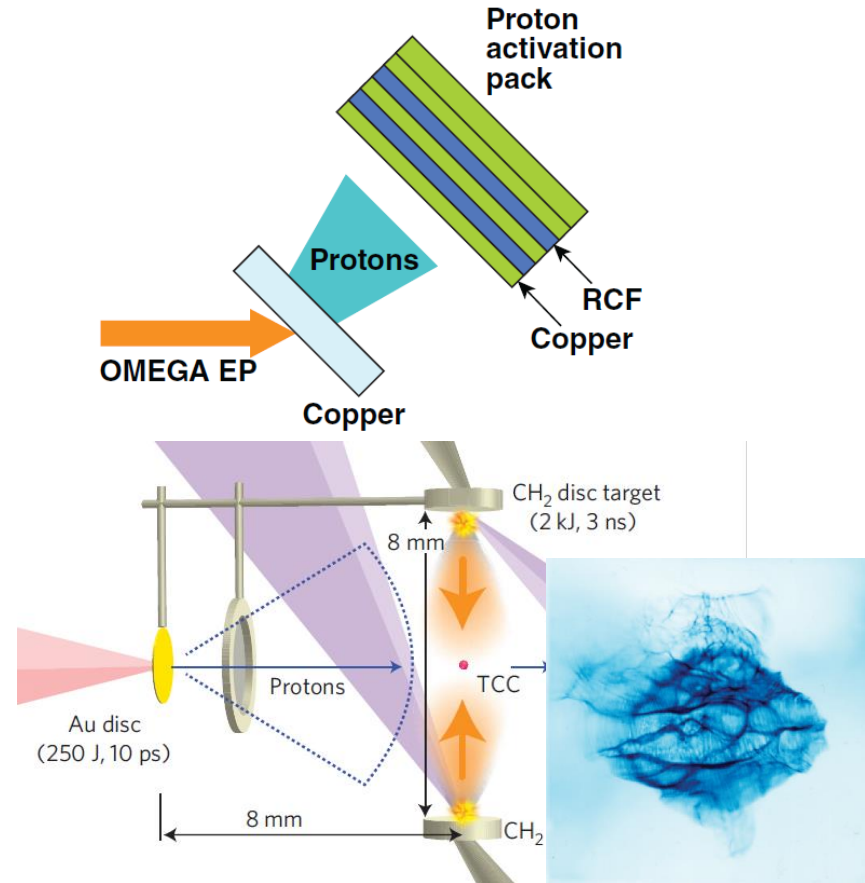
# Protons can leave tracks on CR39 or film



## CR 39



## Radiochromic film pack



F. H. Seguin *et al.*, *Rev. Sci. Instrum.* **74**, 975 (2003)

C. K. Li *et al.*, *Phys. Plasmas* **16**, 056304 (2009)

L. Gao, PhD Thesis

N. L. Kugland *et al.*, *Nature Phys.* **8**, 809 (2012)

# Time dependent magnetic field can be measured using B-dot probe



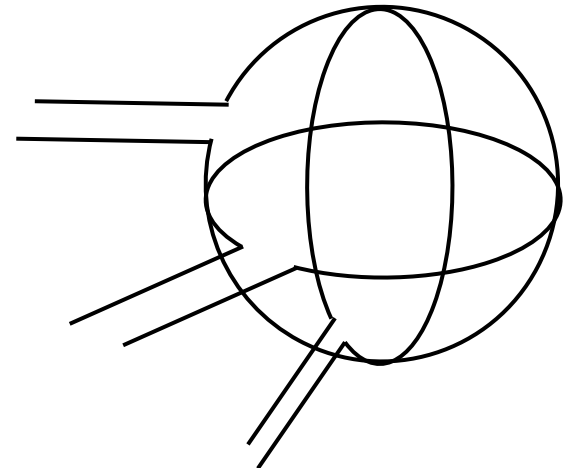
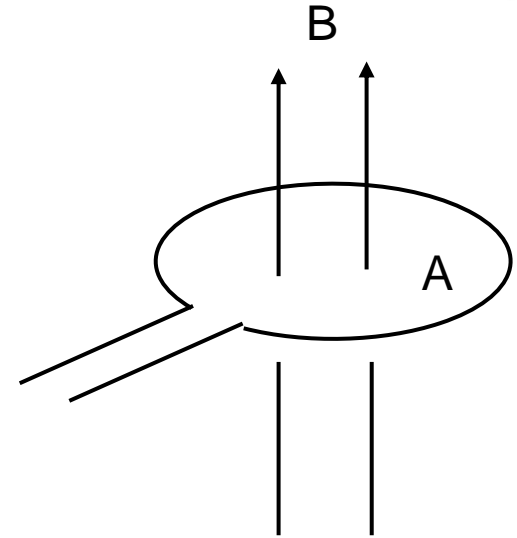
$$B = B(t)$$

$$\nabla \times \vec{E} = -\frac{\partial \vec{B}}{\partial t}$$

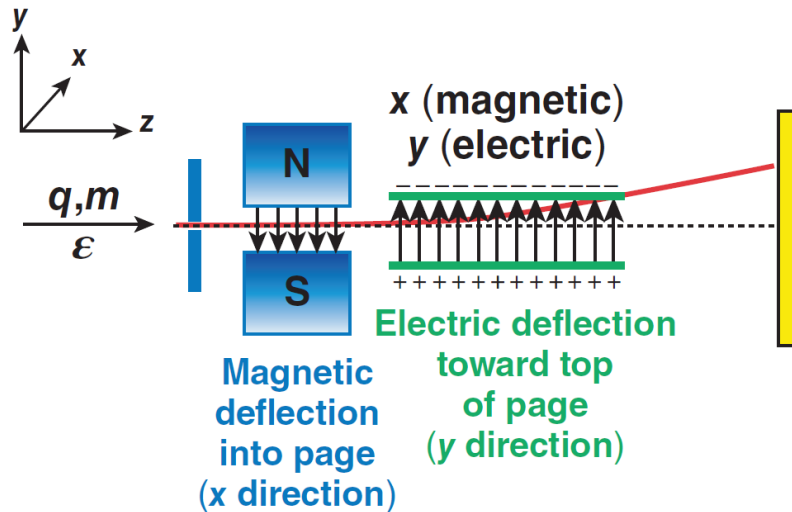
$$\int d\vec{A} \nabla \times \vec{E} = \oint \vec{E} d\vec{l} = V = -\int d\vec{A} \frac{\partial}{\partial t} \vec{B}$$

$$V \sim -A \frac{\partial B}{\partial t}$$

$$B = -\int \frac{V}{A} dt \sim -\frac{1}{A} \int V dt$$



# A Thomson parabola uses parallel electric and magnetic fields to deflect particles onto parabolic curves that resolve $q/m$



- Deflection caused by magnetic field  $\sim q/p$
- Deflection caused by electric field  $\sim q/KE$
- Ion traces form parabolic curves on detector plane

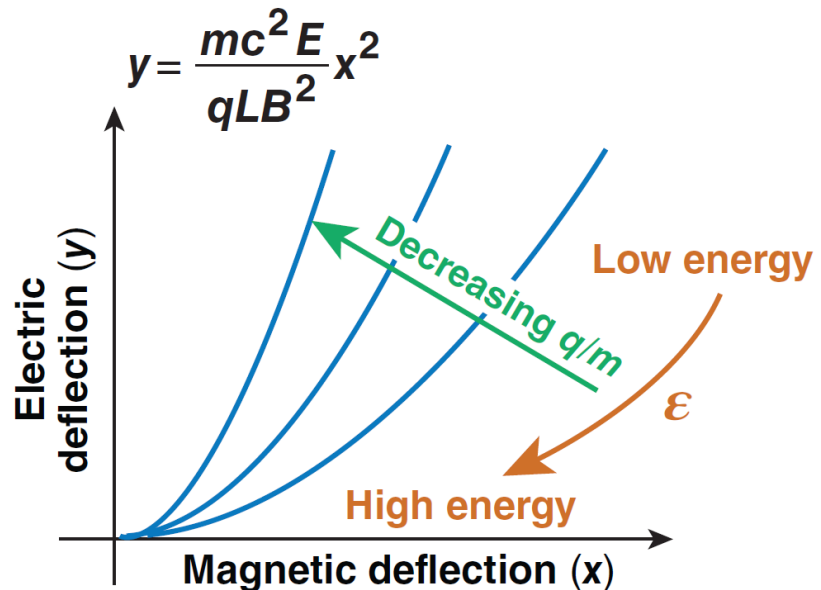
$$\tan \Delta\theta_x = \Delta\theta_x = \frac{qBL}{c\sqrt{2m\epsilon}}$$

$$y \text{ deflection} \quad \epsilon = \frac{q^2 B^2 L^2}{c^2 2m \Delta\theta_x^2}$$

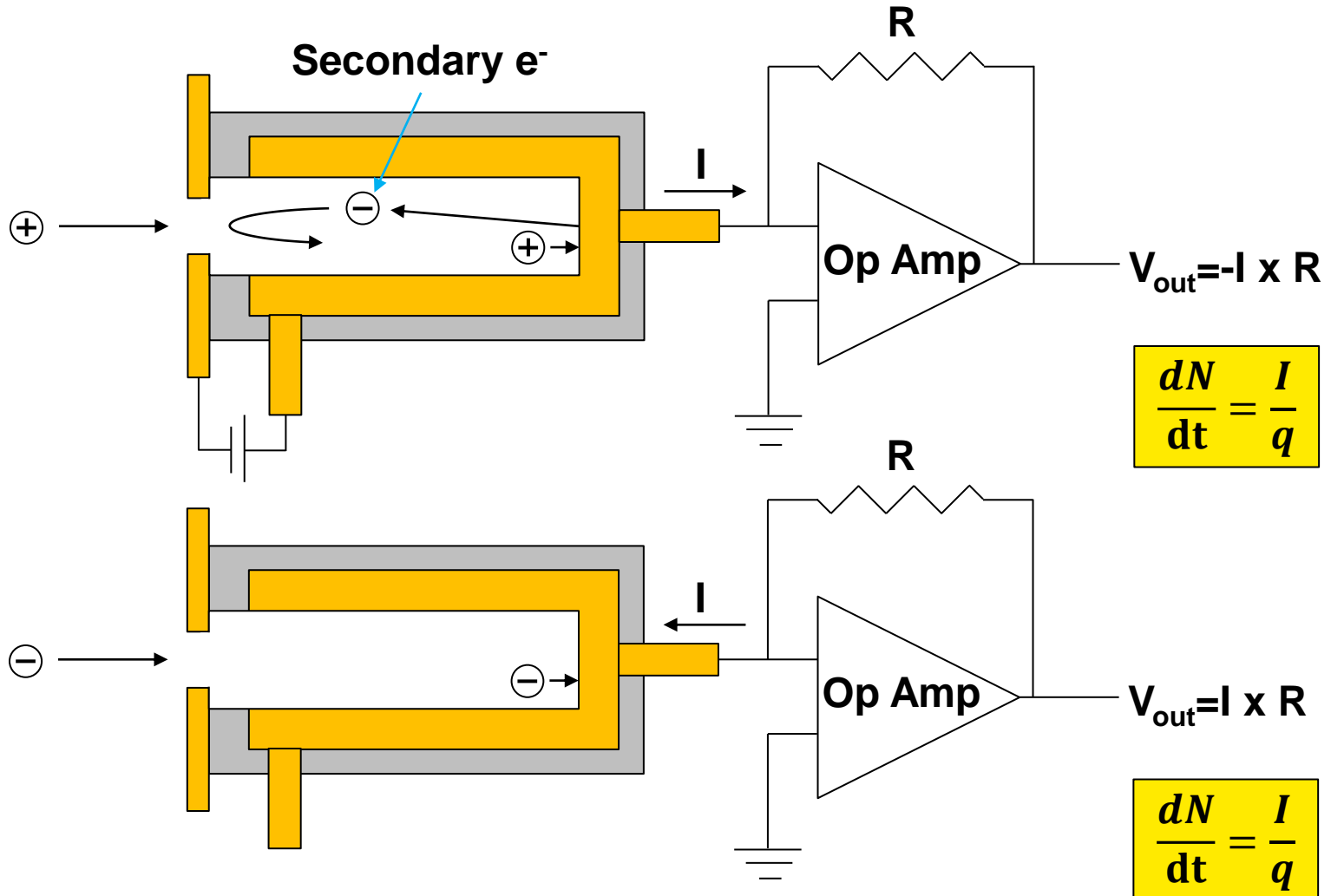
$$F_{\perp} = qE$$

$$\Delta m V_y = qE\tau = \frac{qEL}{v}$$

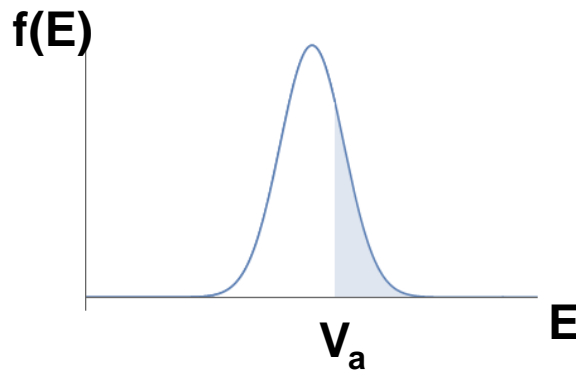
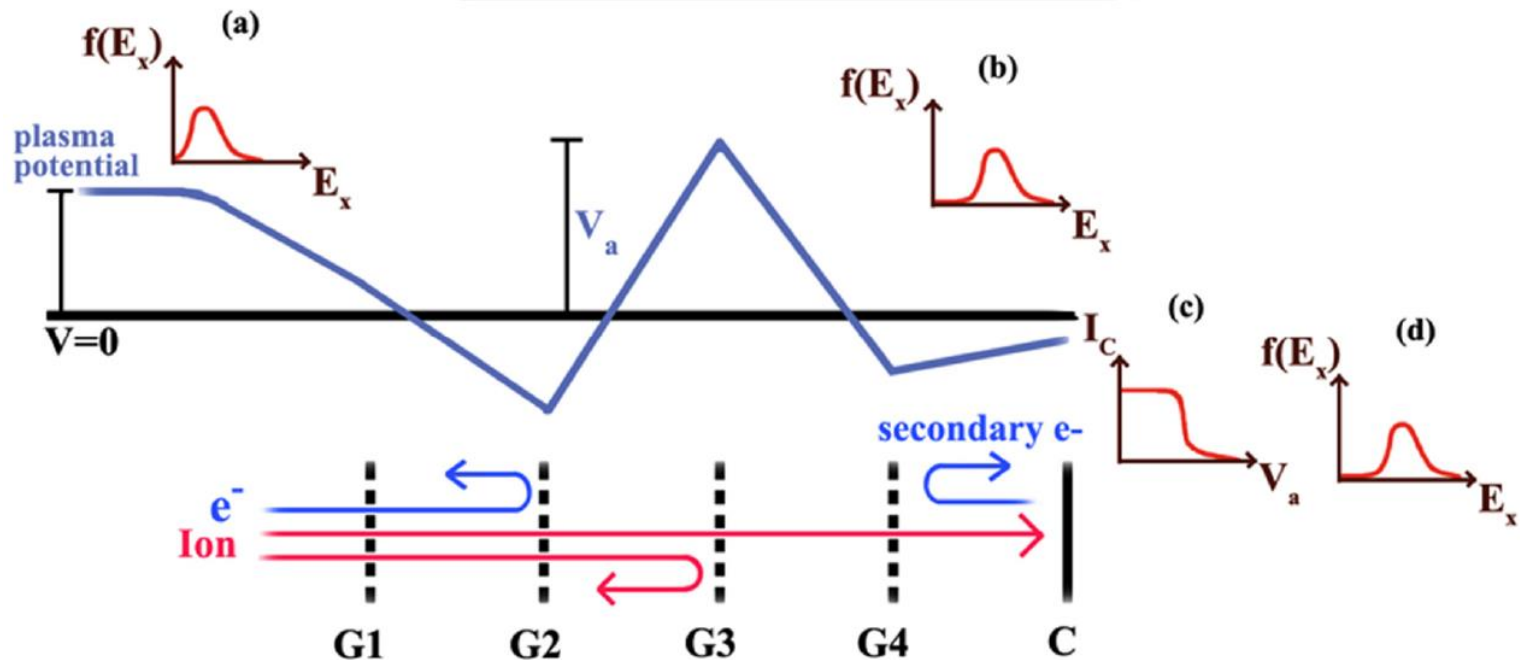
$$\tan \theta_y \sim \theta_y = \frac{\Delta m V_y}{mV} = \frac{qEL}{2\epsilon}$$



## A faraday cup measures the flux of charge particles



## Retarding potential analyzer measures the energy / velocity distribution function



# The photon energy spectrum provides valuable information

---



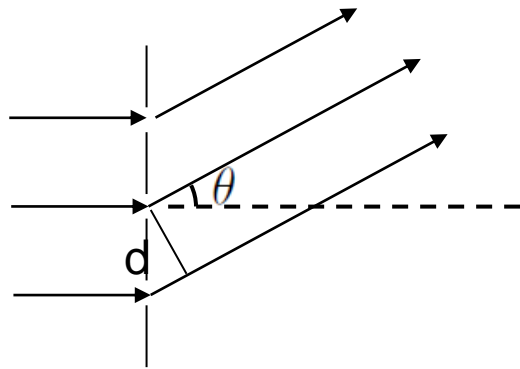
- **Plasma conditions can be determined from the photon spectrum**
  - **visible light: absorption and laser-plasma interactions**
  - **x rays: electron temperature, density, plasma flow, material mixing**
- **There are three basic tools for determining the spectrum detected**
  - **filtering**
  - **grating spectrometer**
  - **Bragg spectrometer**



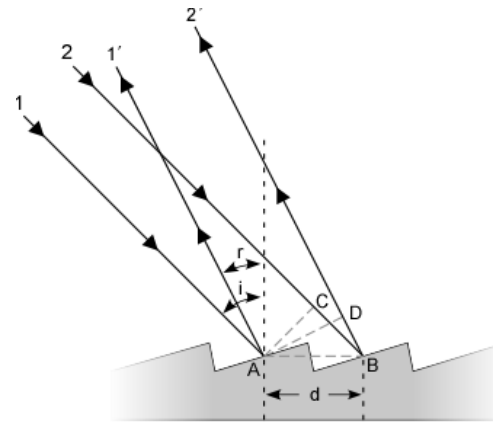
# Spectrum can be obtained using grating



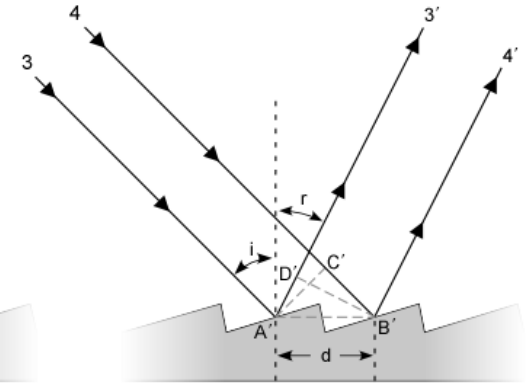
- Grating is used to disperse the light



$$d \sin \theta = m \lambda$$

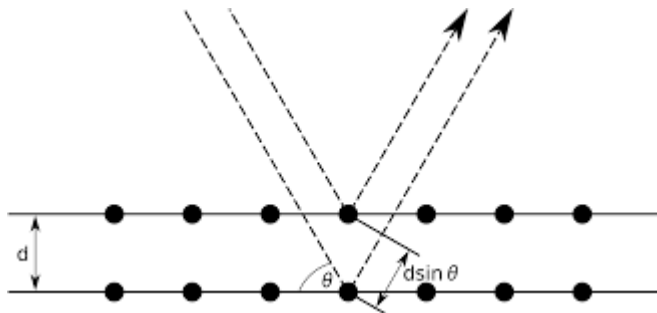


$$n \lambda = d(\sin(i) + \sin(r))$$



$$n \lambda = d(\sin(i) - \sin(r))$$

- Bragg condition in the crystal is used for X-ray.

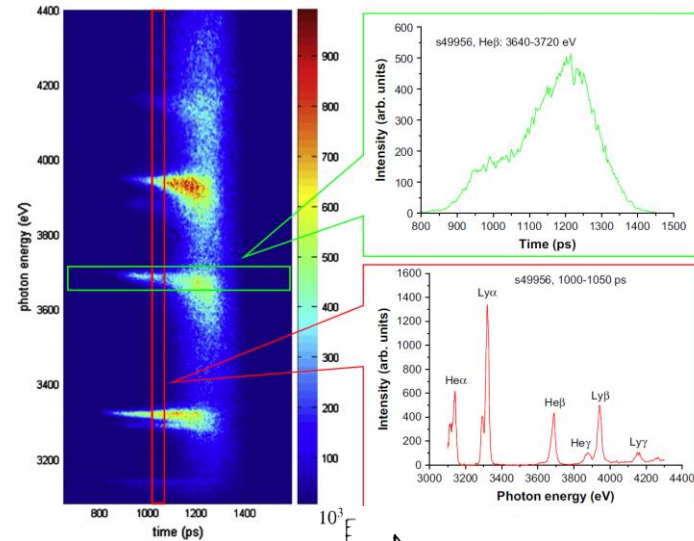
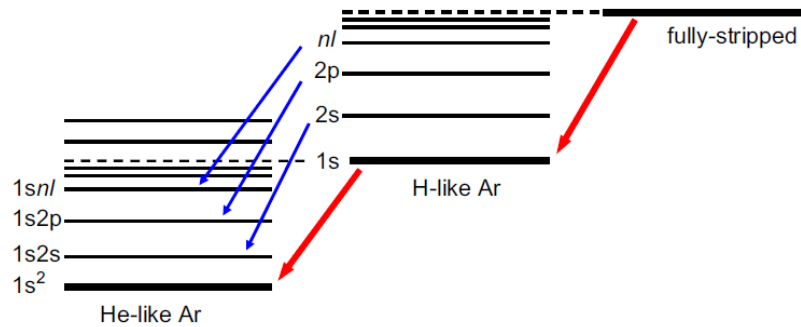


$$2d \sin \theta = m \lambda$$

# Temperature and density can be obtained from the emission

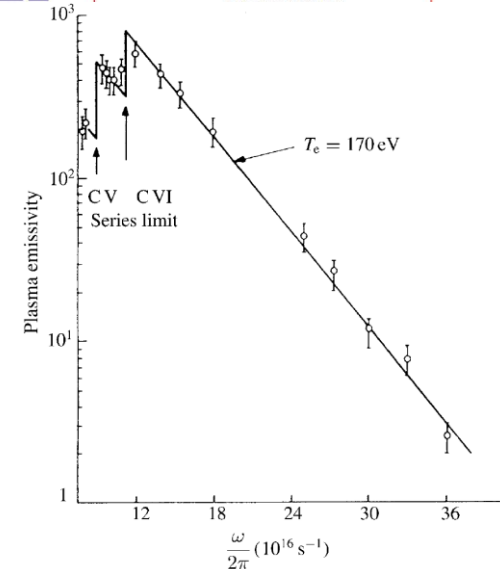


## Line emission



## Bremsstrahlung emission

$$\eta_\nu = \frac{16\pi}{3\sqrt{6\pi}} \frac{e^6}{m_e^2 c^3} \frac{Z_i^2 n_e}{\sqrt{k_B T_e / m_e A m_p}} \exp\left(-\frac{h\nu}{k_B T_e}\right)$$



# Information of x-ray transmission or reflectivity over a surface can be obtained from the Center for X-Ray Optics



- [http://henke.lbl.gov/optical\\_constants/](http://henke.lbl.gov/optical_constants/)



## X-Ray Database

- Nanomagnetism
- X-Ray Microscopy
- EUV Lithography
- EUV Mask Imaging
- Reflectometry
- Zoneplate Lenses
- Coherent Optics
- Nanofabrication
- Optical Coatings
- Engineering
- Education
- Publications
- Contact



The Center for X-Ray Optics is a multi-disciplined research group within Lawrence Berkeley National Laboratory's (LBNL)

## X-Ray Interactions With Matter

### Introduction

- Access the [atomic scattering factor](#) files.
- Look up [x-ray properties of the elements](#).
- The [index of refraction](#) for a compound material.
- The x-ray [attenuation length](#) of a solid.

### X-ray transmission

- Of a [solid](#).
- Of a [gas](#).

### X-ray reflectivity

- Of a [thick mirror](#).
- Of a [single layer](#).
- Of a [bilayer](#).
- Of a [multilayer](#).

The diffraction efficiency of a [transmission grating](#).

### Related calculations:

- [Synchrotron bend magnet radiation](#).

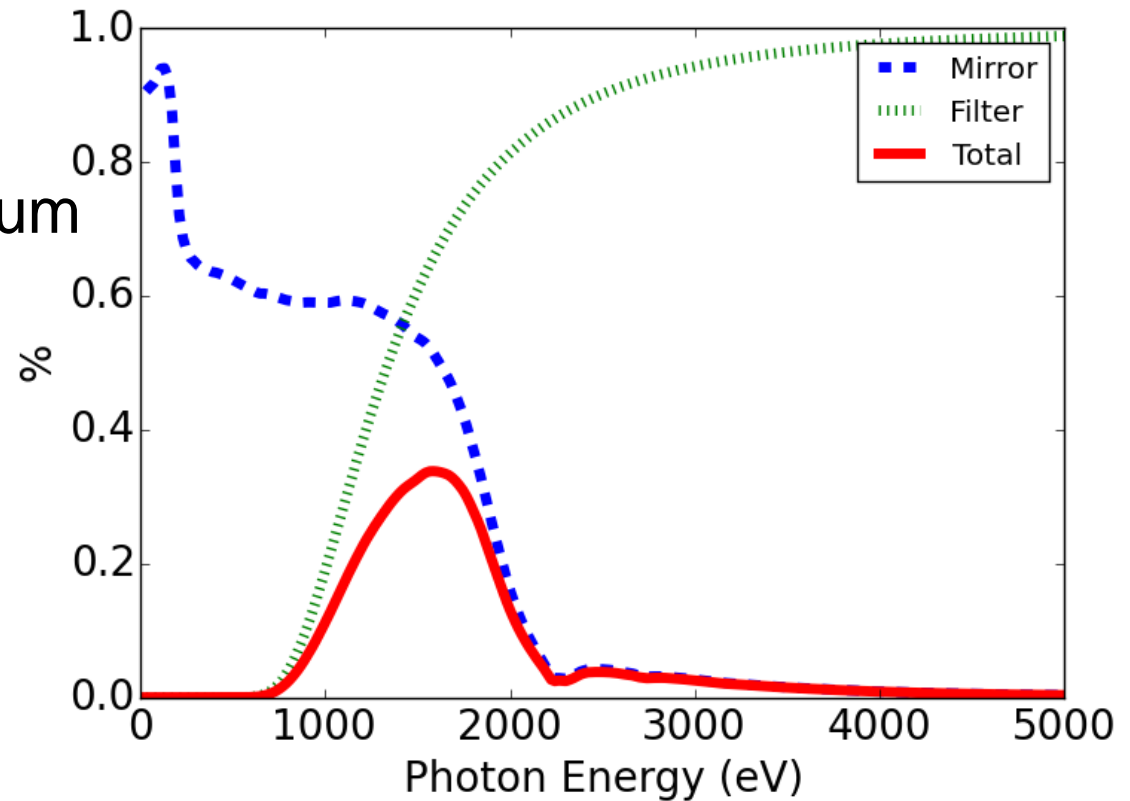
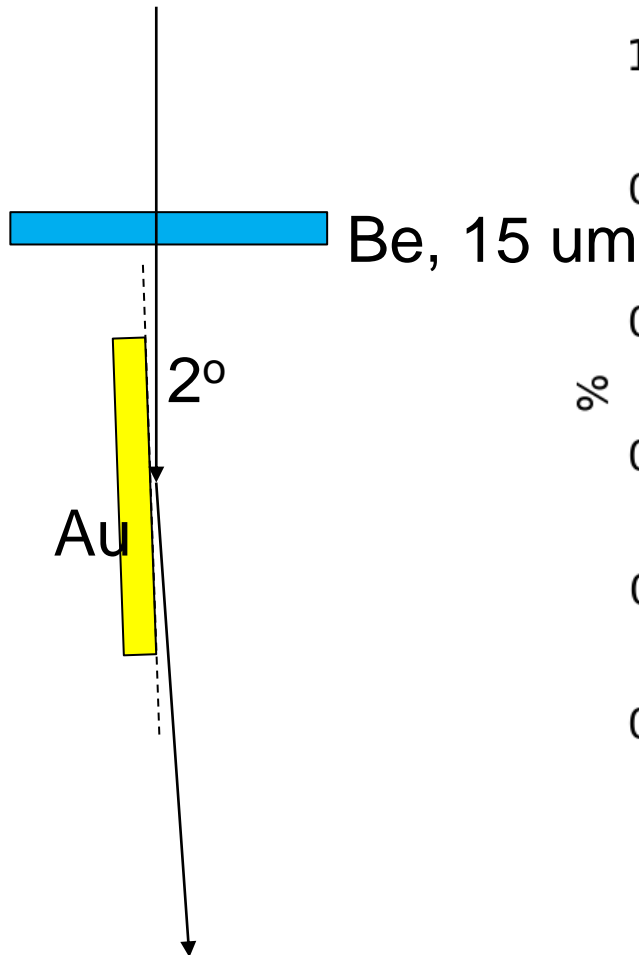
[Other x-ray web resources](#).

[X-ray Data Booklet](#)

## Reference

B.L. Henke, E.M. Gullikson, and J.C. Davis. *X-ray interactions: photoabsorption, scattering, transmission, and reflection at E=50-30000 eV, Z=1-92*, Atomic Data and Nuclear Data Tables Vol. **54** (no.2), 181-342 (July 1993).

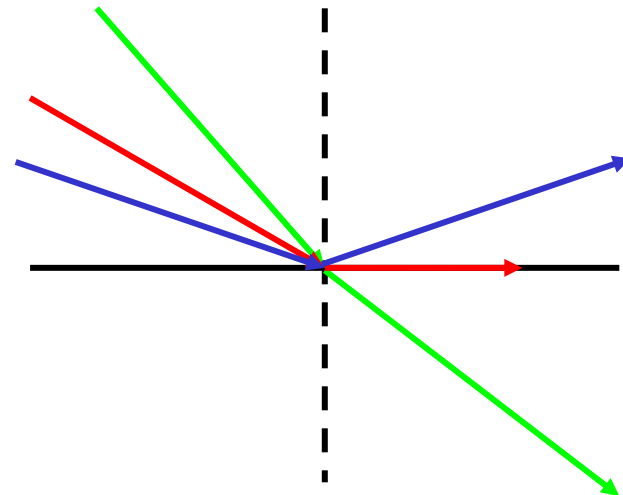
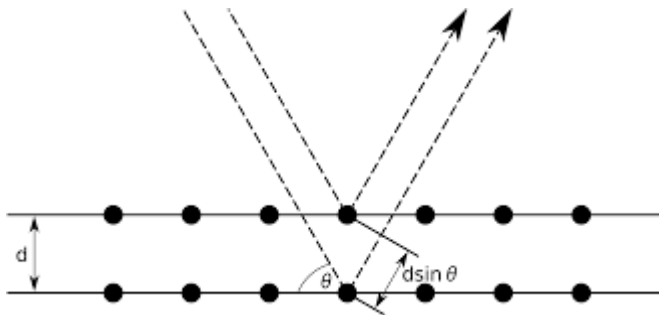
# A band pass filter is obtained by combining a filter and a mirror



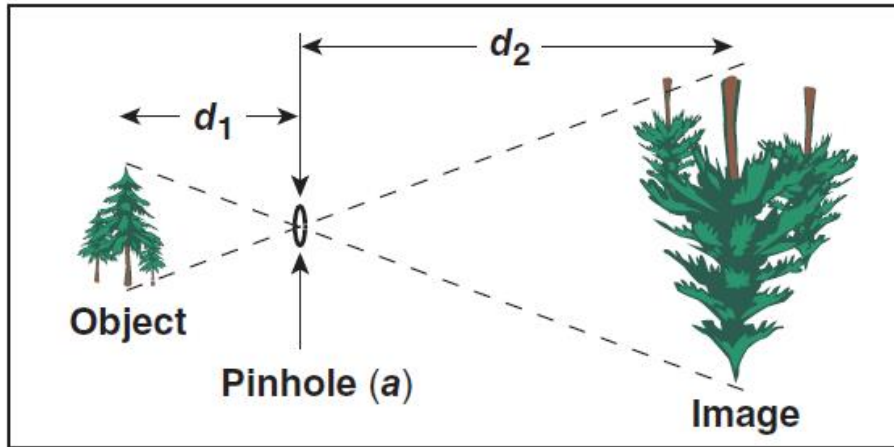
# X rays can not be concentrated by lenses



- X-ray refractive indices are less than unity,  $n \lesssim 1$
- For those with lower refractive indices, the absorption is also strong
- X-ray mirrors can be made through
  - Bragg reflection
  - External total reflection with a small grazing angle



# The simplest imaging device is a pinhole camera



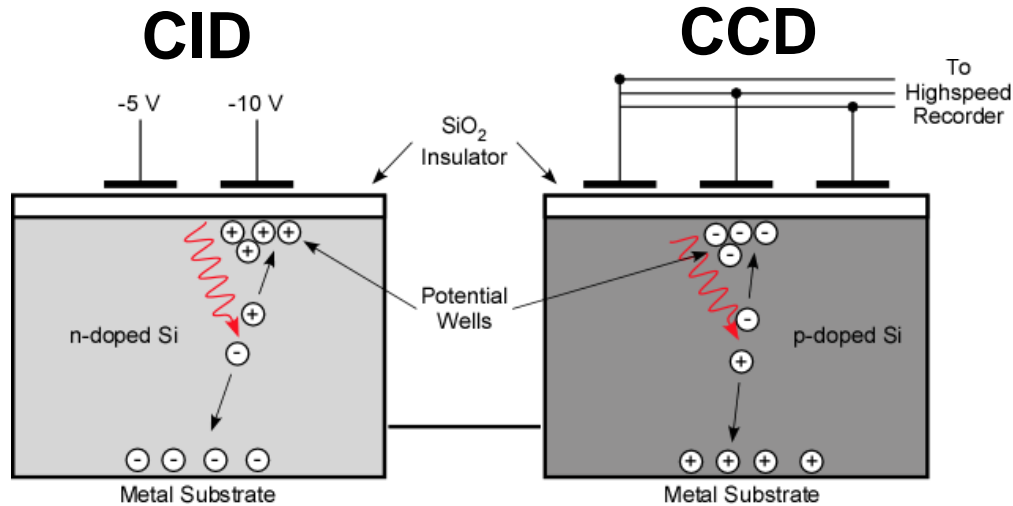
Kodak Brownie camera



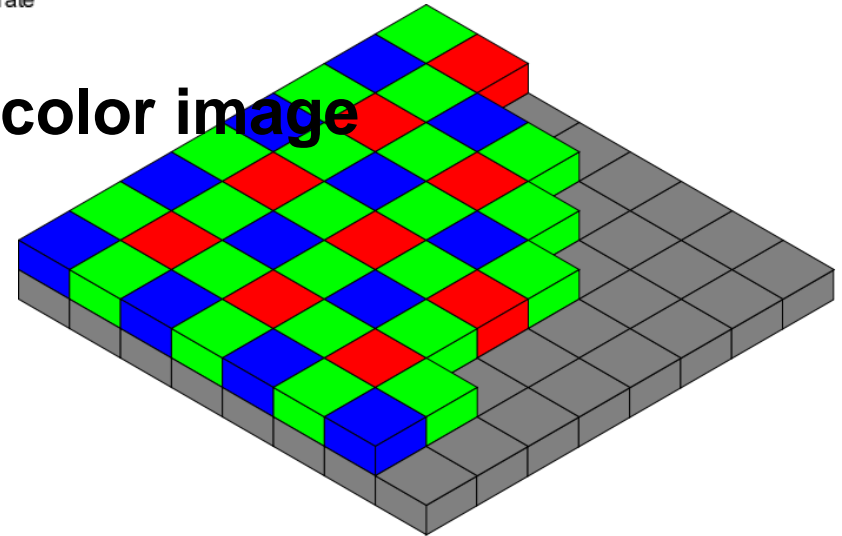
- Magnification =  $\frac{d_2}{d_1}$
- Infinite depth of field (variable magnification)
- Pinhole diameter determines
  - resolution  $\sim a$
  - light collection:  $\Delta\Omega = \frac{\pi}{4} \frac{a^2}{d_1^2}$

**Imaging optics (e.g., lenses) can be used for higher resolutions with larger solid angles.**

# 2D images can be taken using charge injection device (CID) or charge coupled device (CCD)



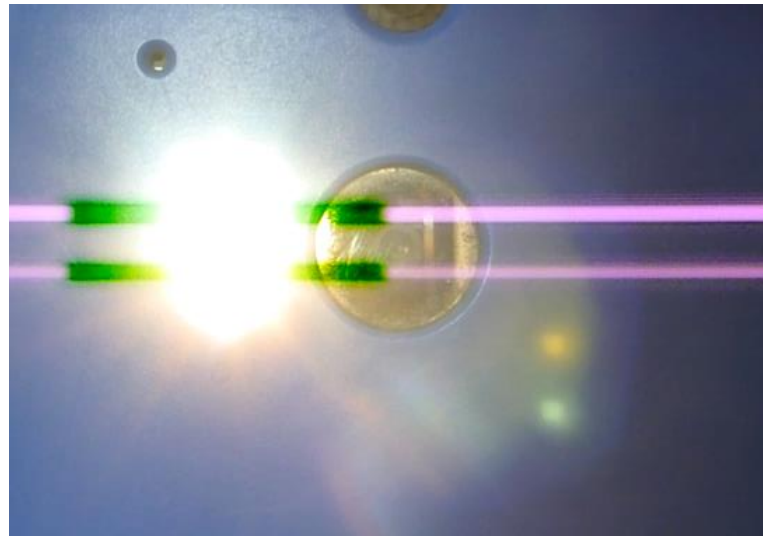
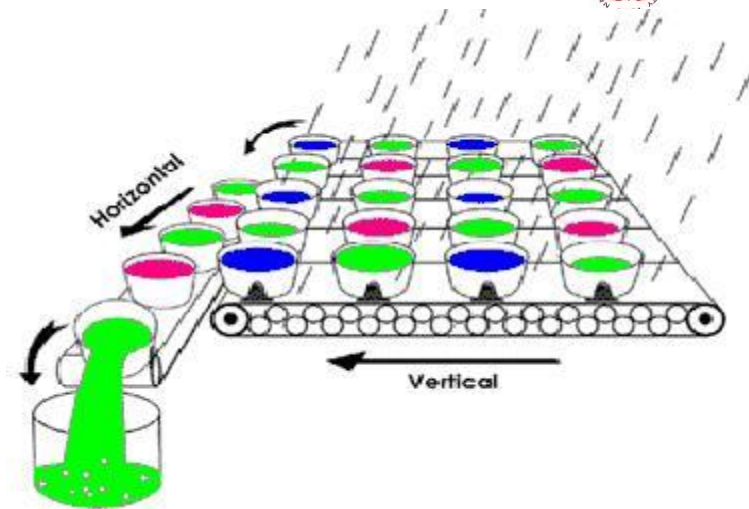
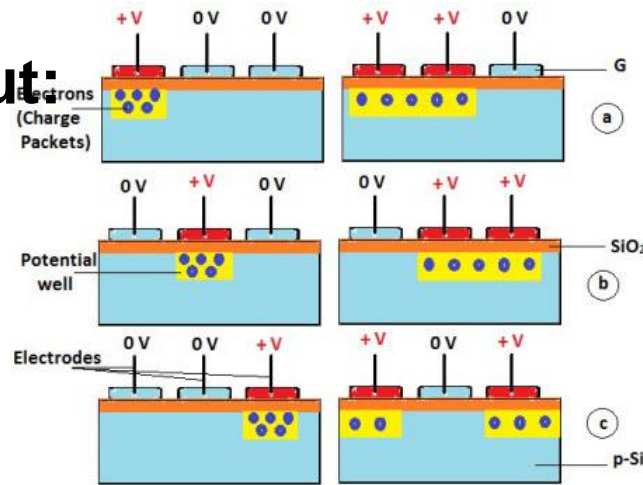
- Color mask is used for color image



# Charges are transferred along the array for readout in CCD

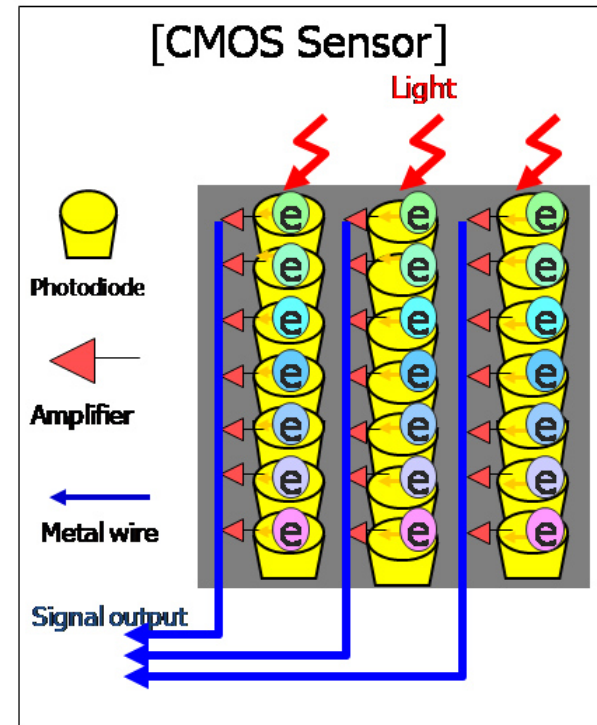
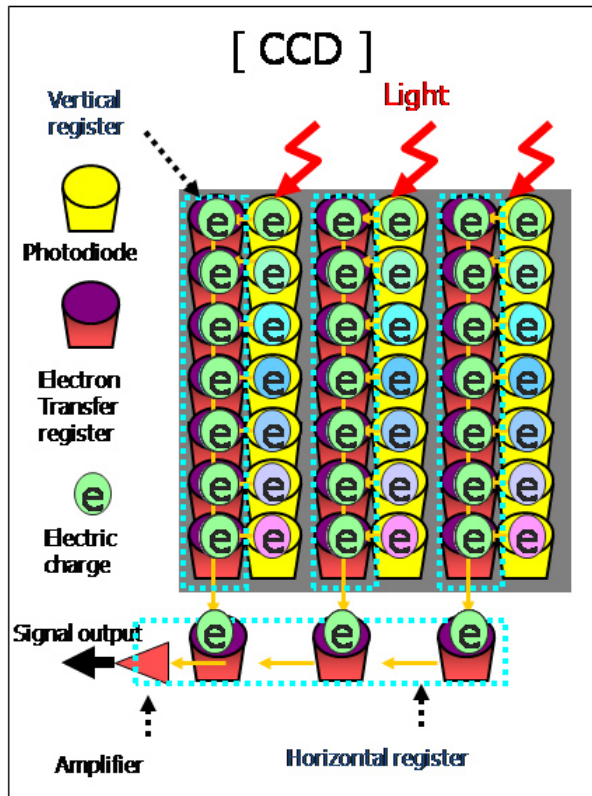


## CCD readout:

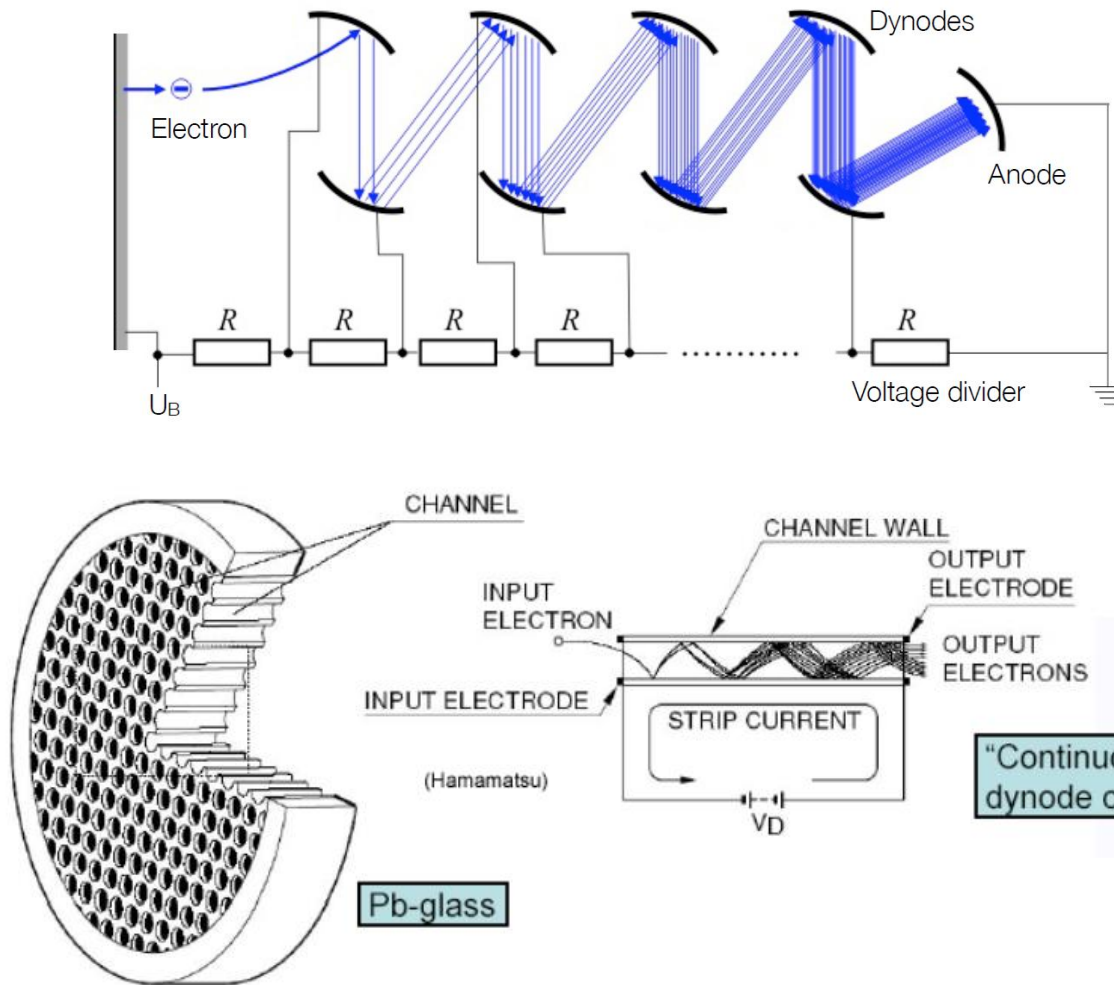




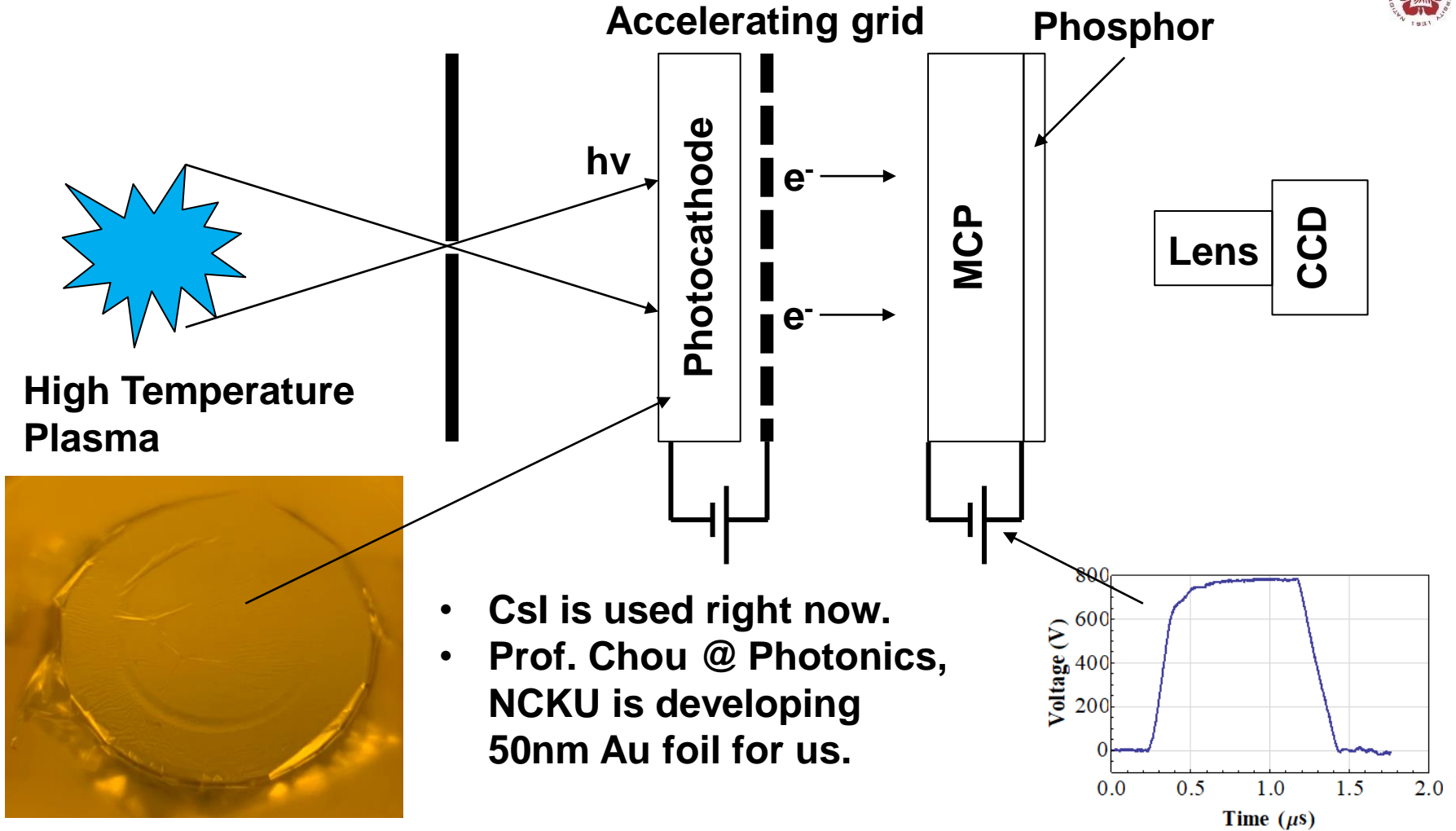
# Signal is readout individually in CMOS sensor



# The number of electrons can be increased through photomultipliers or microchannel plate (MCP)

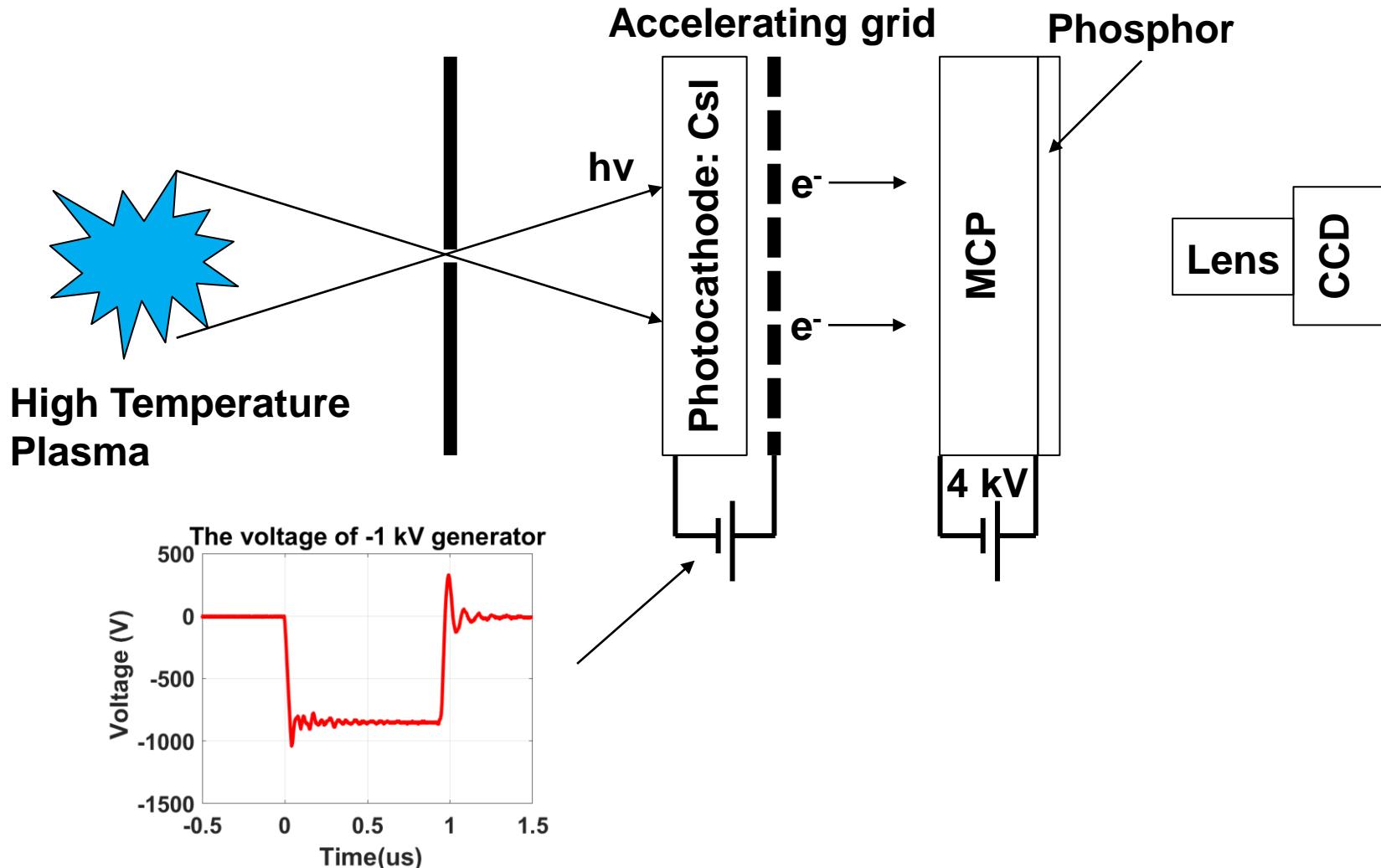


# X-rays are imaged using photocathode, MCP, phosphor, and CCD



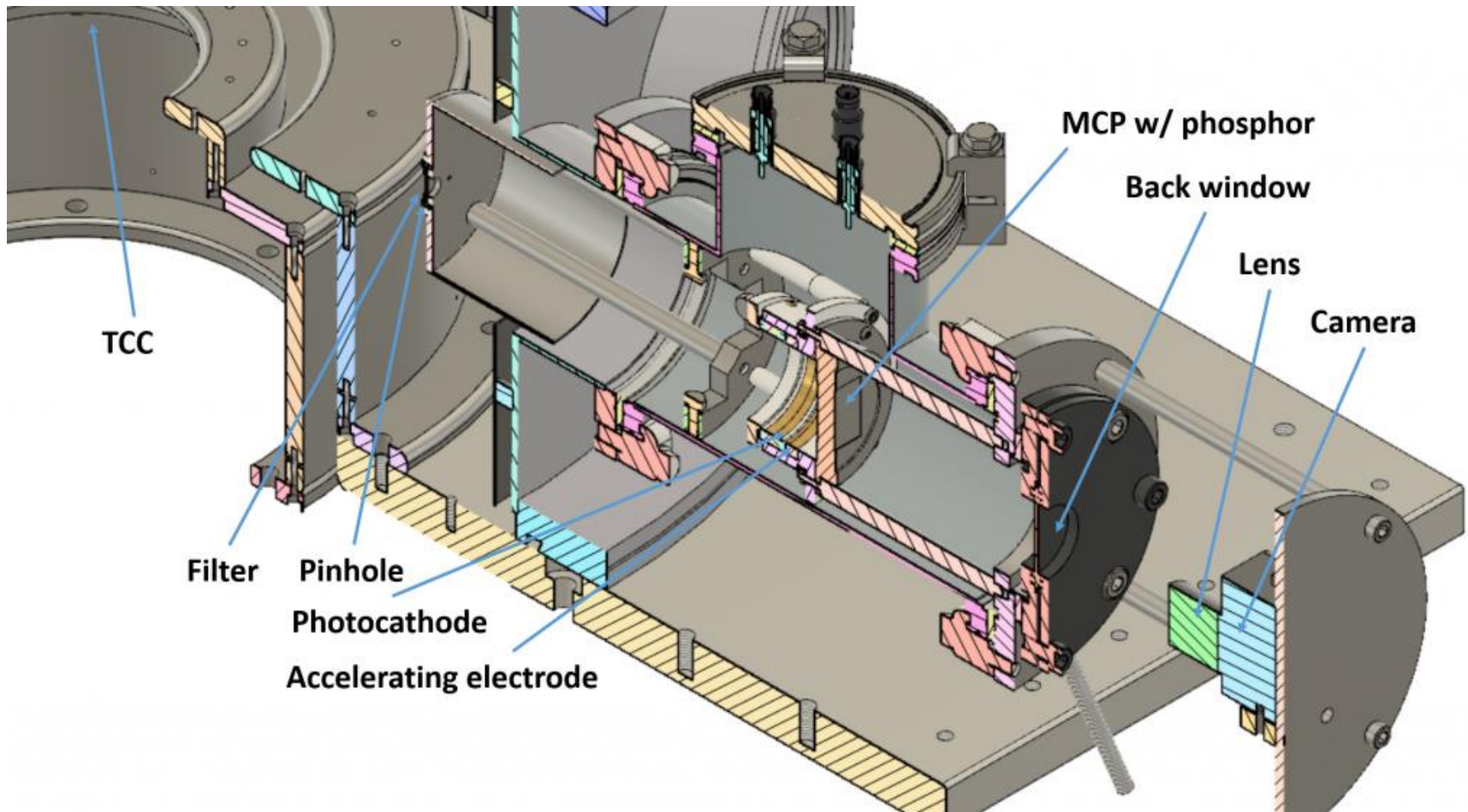
• Images can be gated using fast high voltage pulses.

# A negative high-voltage pulse is used in our x-ray pinhole camera



- The x-ray camera with a shutter opening time of  $\leq 10$  ns will be built.

# A pinhole camera was designed and was built

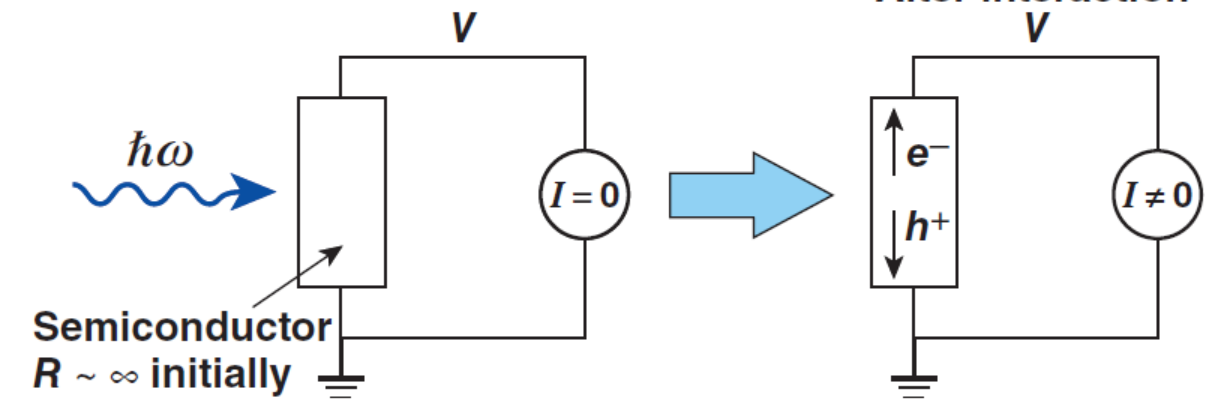


# Electronic detectors provide rapid readout

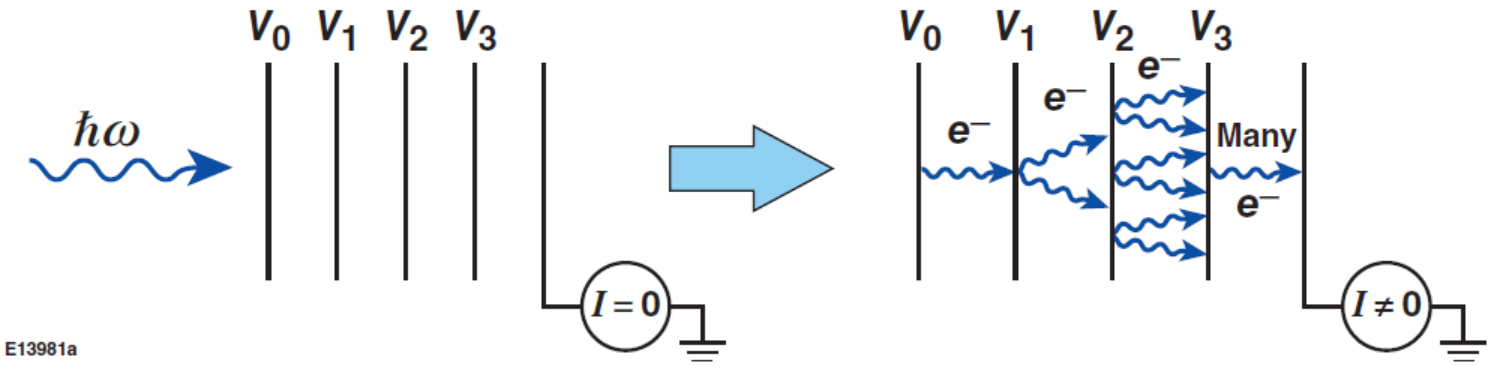


- Electronic detectors are typically semiconductors or ionization-based stacks (e.g., photomultipliers)

## Semiconductor detectors



## Ionization detectors

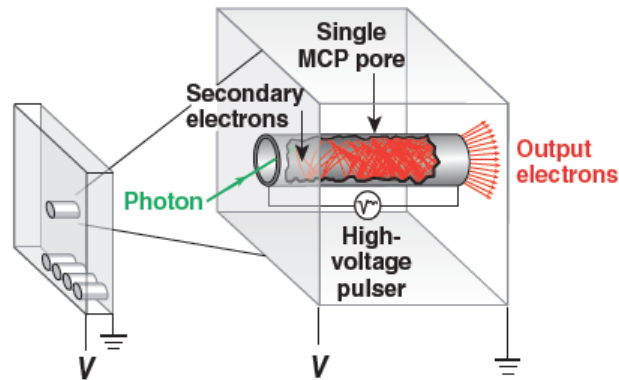


E13981a

# A framing camera provides a series of time-gated 2-D images, similar to a movie camera



- The building block of a framing camera is a gated microchannel-plate (MCP) detector
- An MCP is a plate covered with small holes, each acts as a photomultiplier



Multiple electrons are produced each time an electron or photon hits the wall

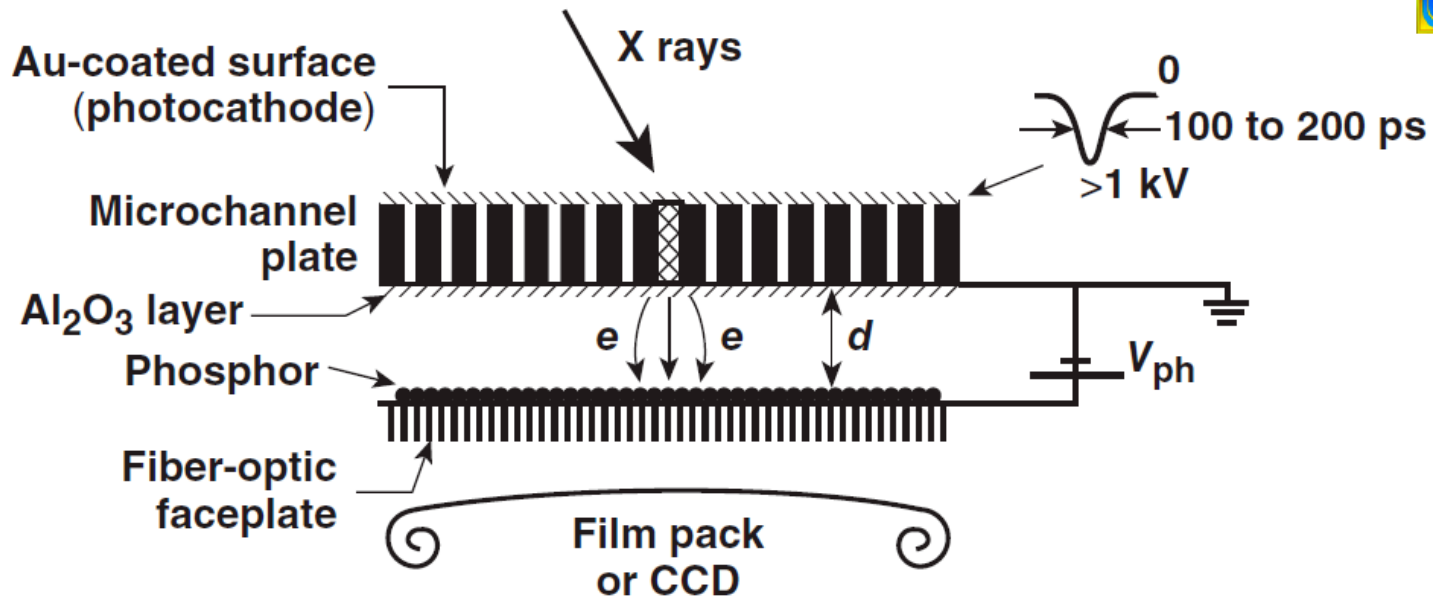
- A voltage pulse is sent down the plate, gating the detector



The detector is only on when the voltage pulse is present



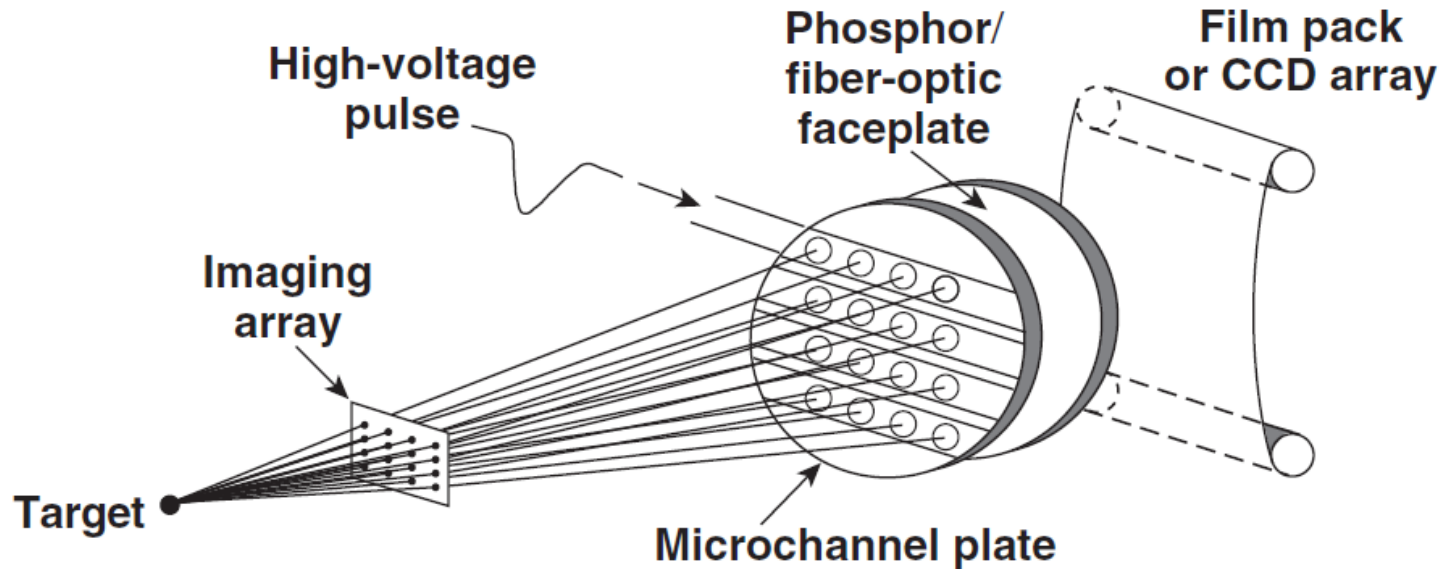
# A framing camera detector consists of a microchannel plate (MCP) in front of a phosphor screen



- Electrons are multiplied through MCP by voltage  $V_c$
- Images are recorded on film behind phosphor
- Insulating  $\text{Al}_2\text{O}_3$  layer allows for  $V_{ph}$  to be increased, thereby improving the spatial resolution of phosphor

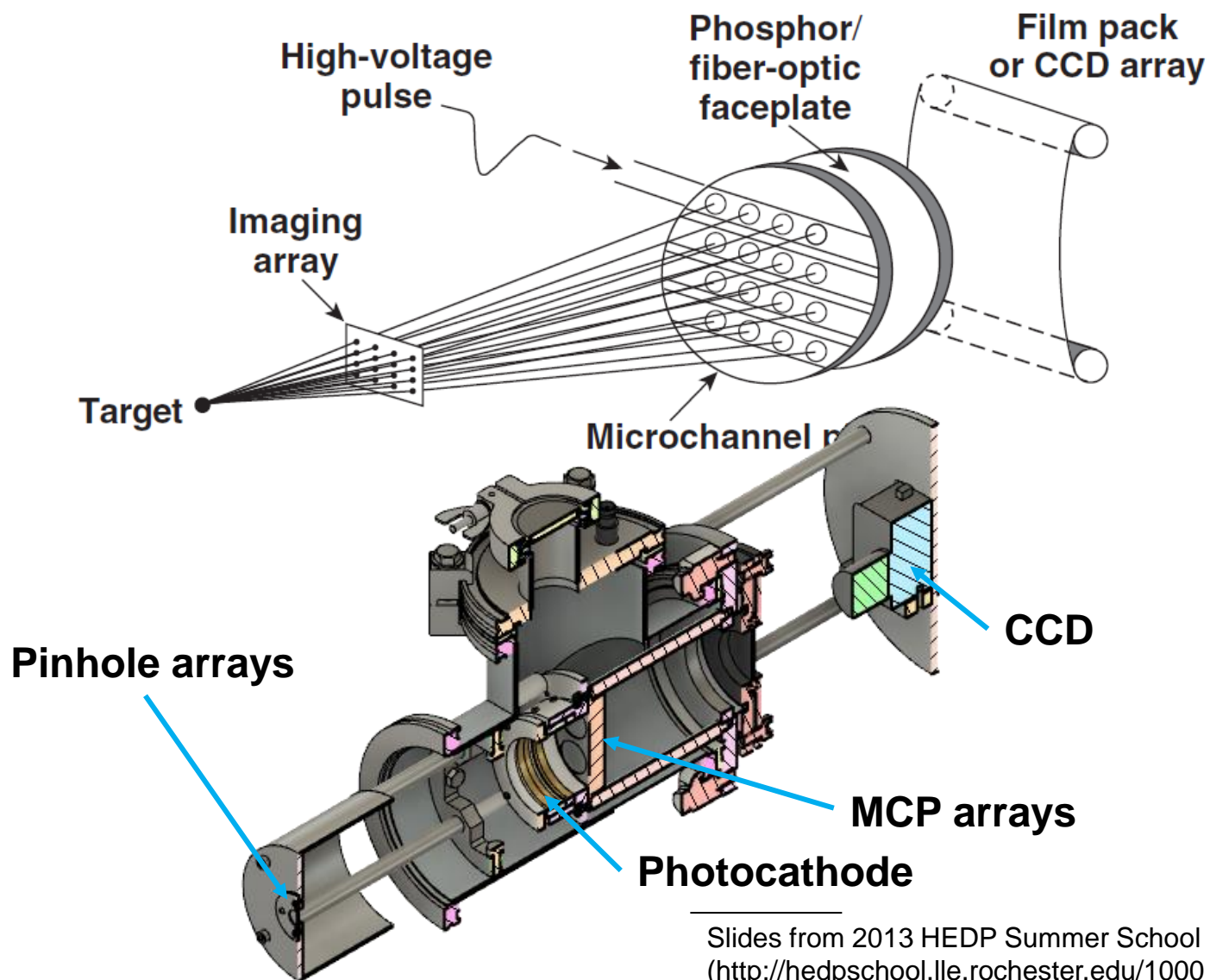


# Two-dimensional time-resolved images are recorded using x-ray framing cameras

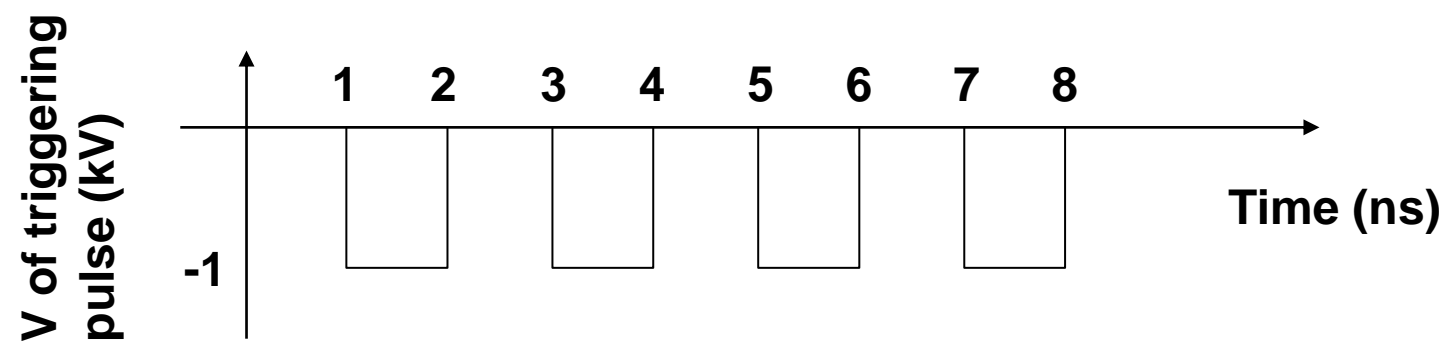
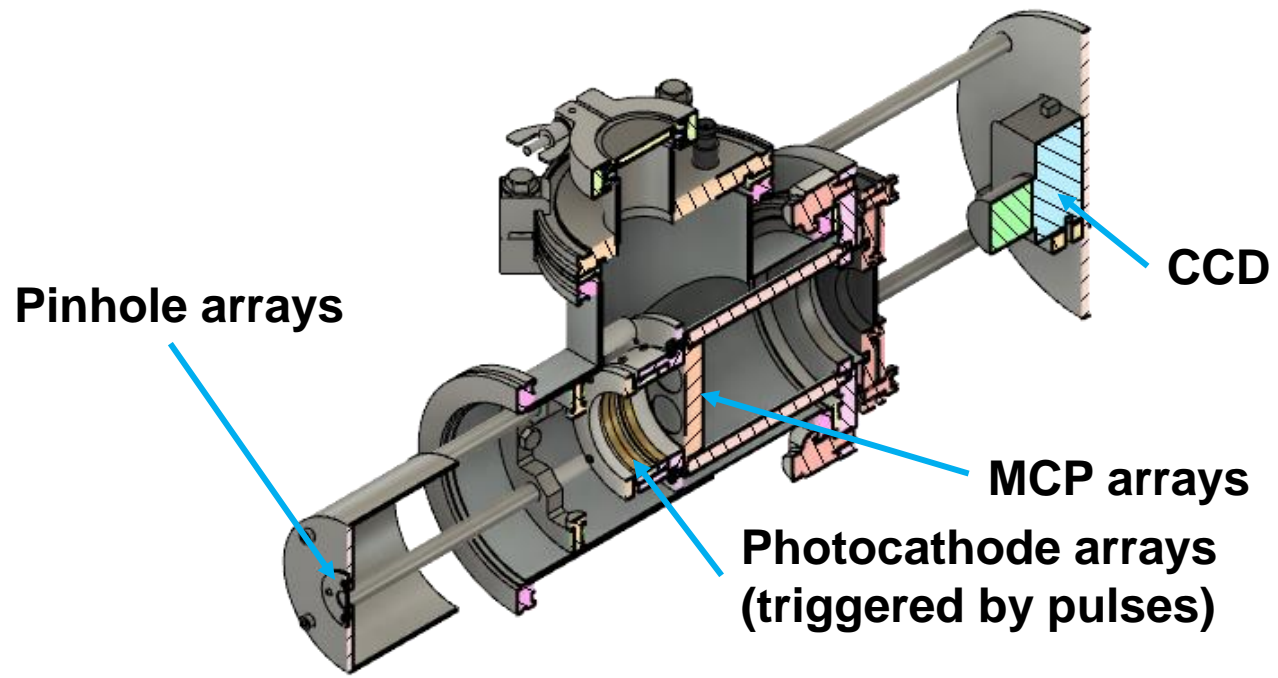


- Temporal resolution = 35 to 40 ps
- Imaging array: Pinholes: 10- to 12- $\mu\text{m}$  resolution, 1 to 4 keV
- Space-resolved x-ray spectra can be obtained by using Bragg crystals and imaging slits

# X-ray framing cameras for recording two-dimensional time-resolved images will be built by the end of 2021



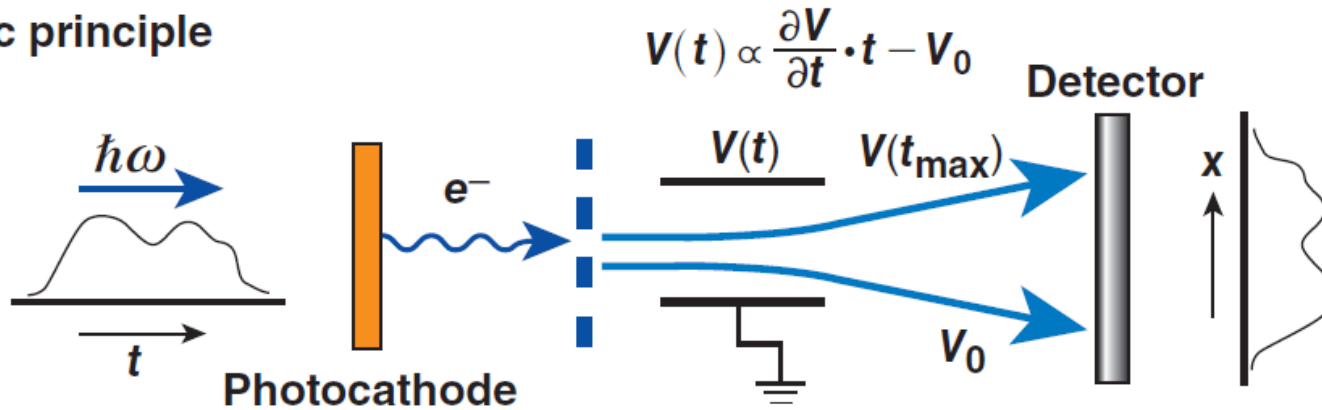
# Each pinhole camera will be triggered separately



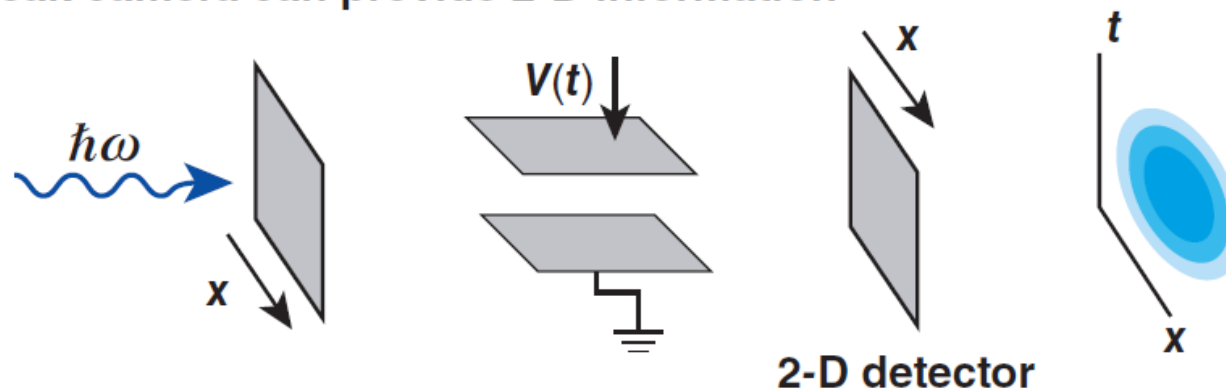
# A streak camera provides temporal resolution of 1-D data



Basic principle



A streak camera can provide 2-D information

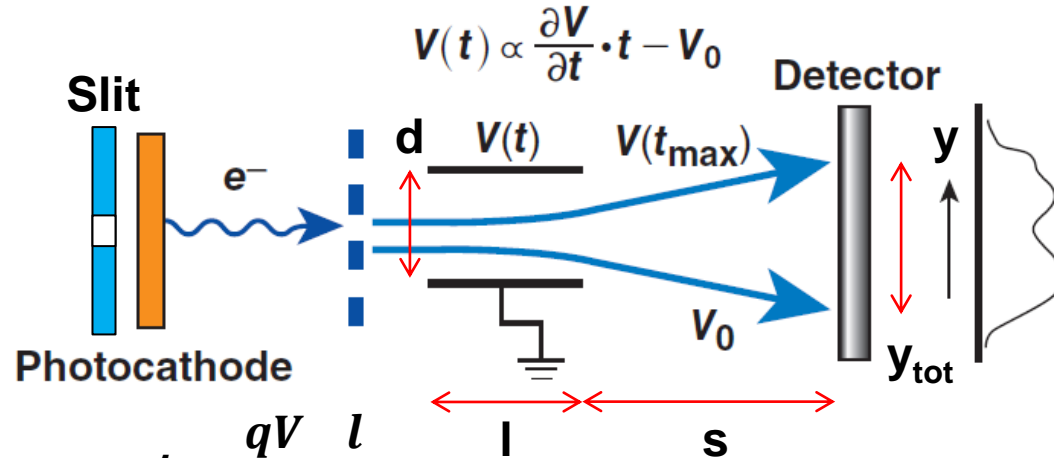


# A temporal resolution higher than 15 ps is expected



**Imaging system**

- Visible light: regular lens
- X rays: pinhole



$$a = \frac{F}{m} = \frac{qE}{m} = \frac{qV}{md}$$

$$v_{\perp} = at = \frac{qV}{md} \frac{l}{v_{\parallel}}$$

$$y = s \tan \theta = s \frac{v_{\perp}}{v_{\parallel}} = \frac{1}{2E_k} \frac{l}{d} sqV = \frac{1}{2E_k} \frac{l}{d} sq(V_0 + V't)$$

- Let  $d=10$  mm,  $l=20$  mm,  $s=50$  mm,  $E_k=1$  keV,  $V=-200 \sim 200$  V

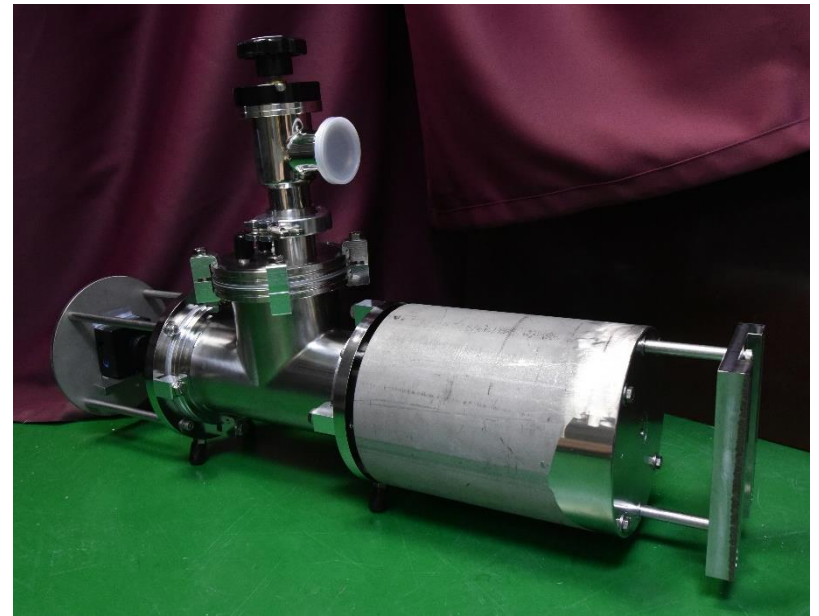
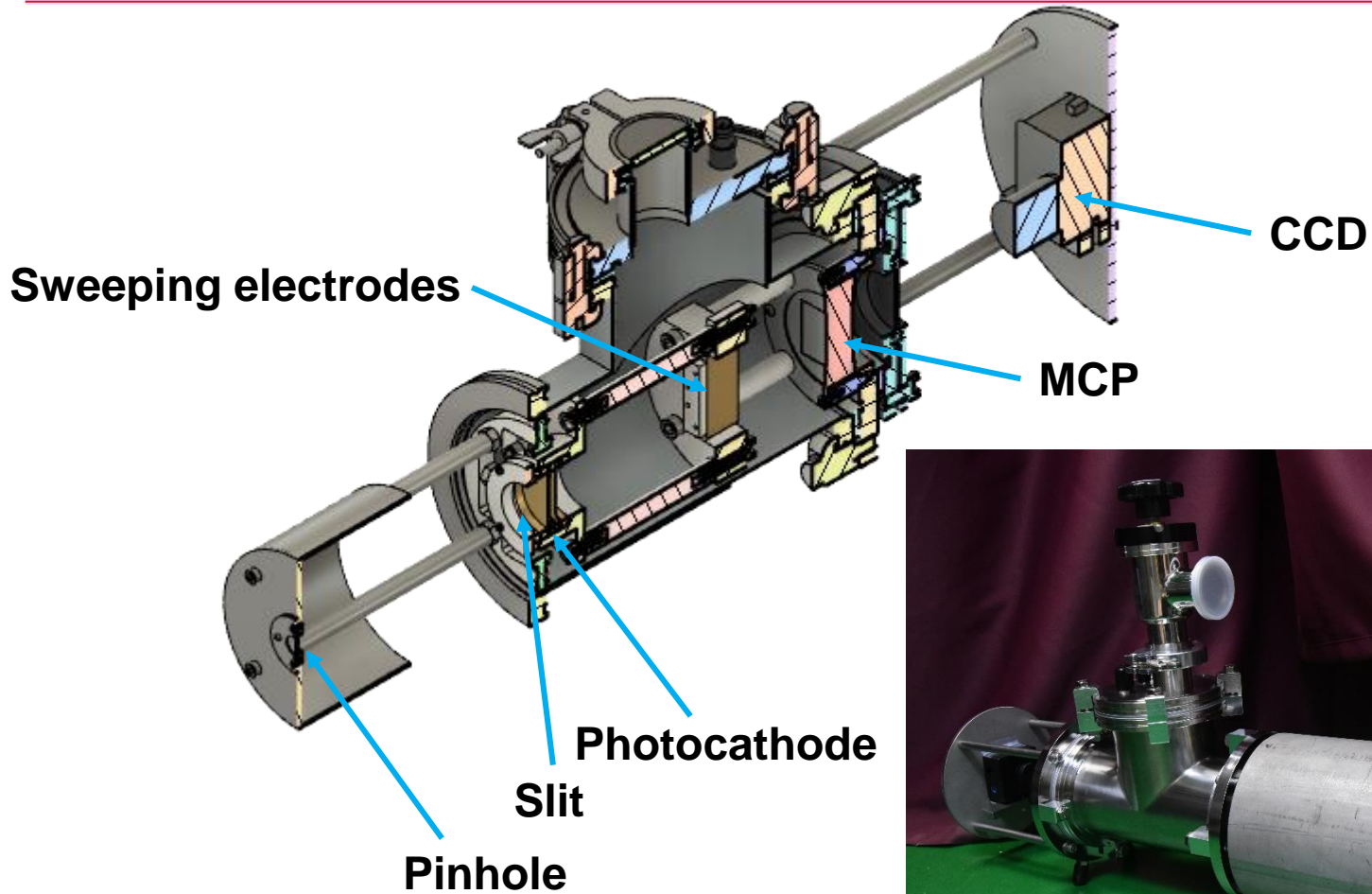
$$V' \equiv \frac{V_{\text{tot}}}{t_{\text{tot}}} = 0.06 \text{ kV/ns} \quad y_{\text{tot}} = 15\text{mm} \quad y_{\text{tot}} = 15\text{mm}$$

- Temporal resolution:

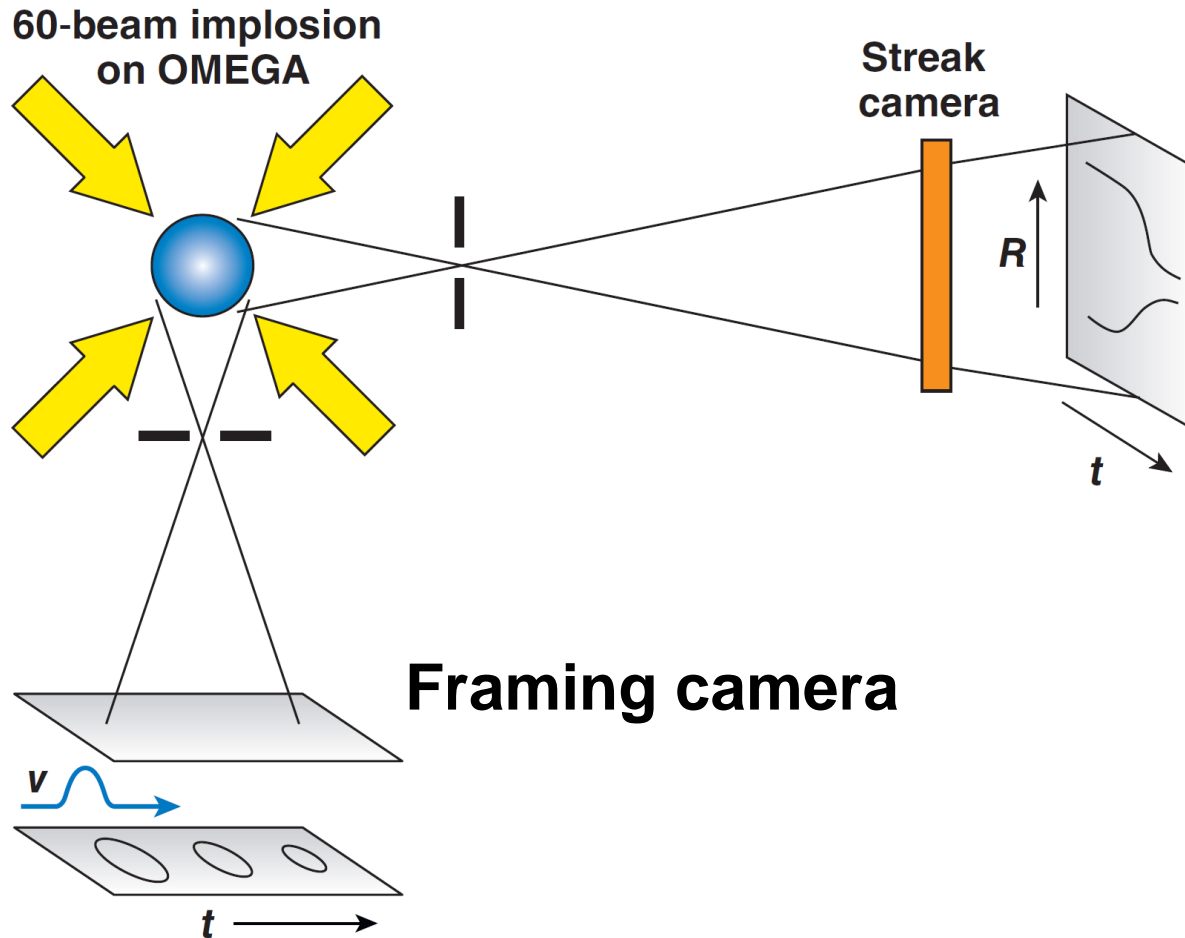
$$\delta t = \delta y \frac{2E_k d}{lsqV'} = 15 \text{ ps for } \delta y = 45\mu\text{m}$$

- $\delta t$  will be adjusted by changing  $E_k$ .

# A streak camera with temporal resolution of 15 ps has been developed



# Shell trajectories can be measured using framing camera or streak camera



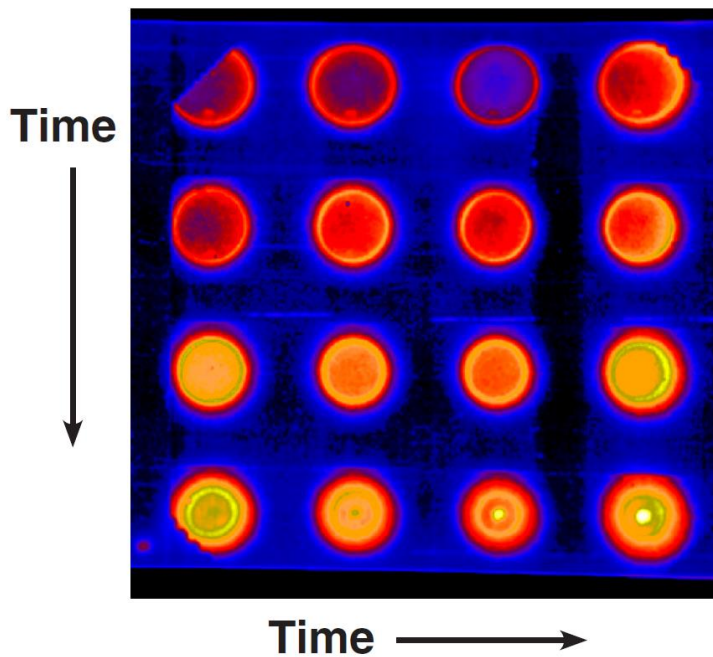


# Comparison of images from framing camera versus streak camera



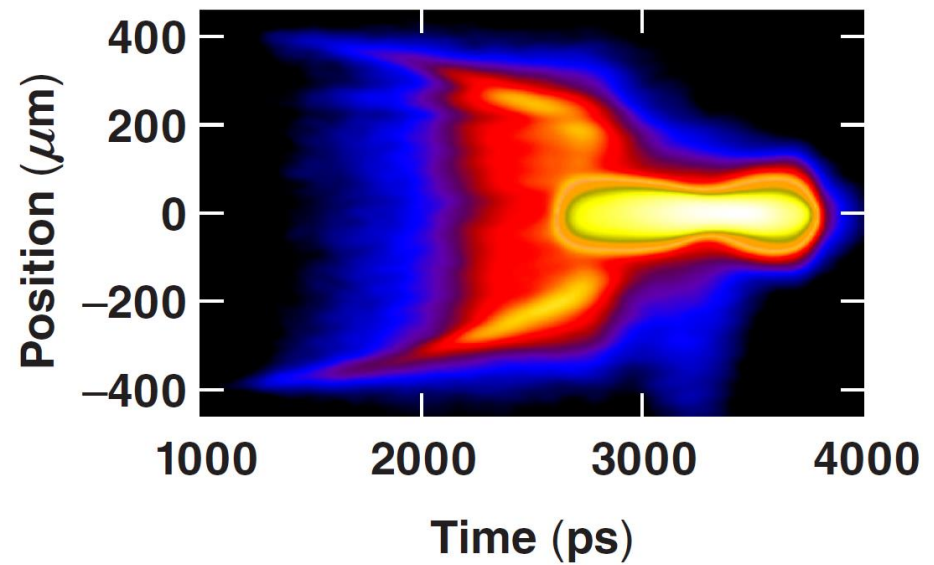
Framing-camera image  
6× magnification

Shot 13377



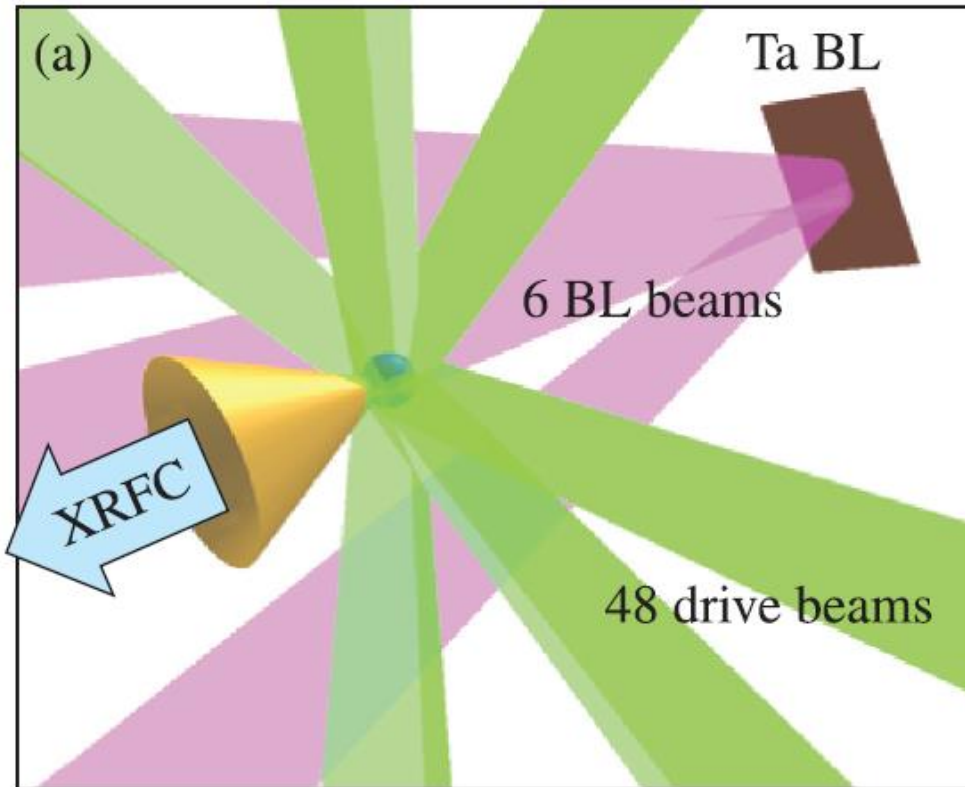
Streak-camera image

Shot 13377





# The optical density can be measured using the absorption of a backlighter

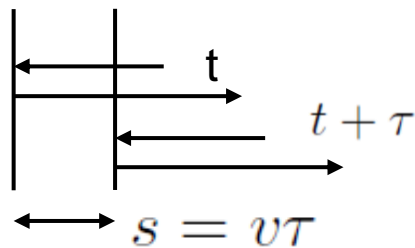
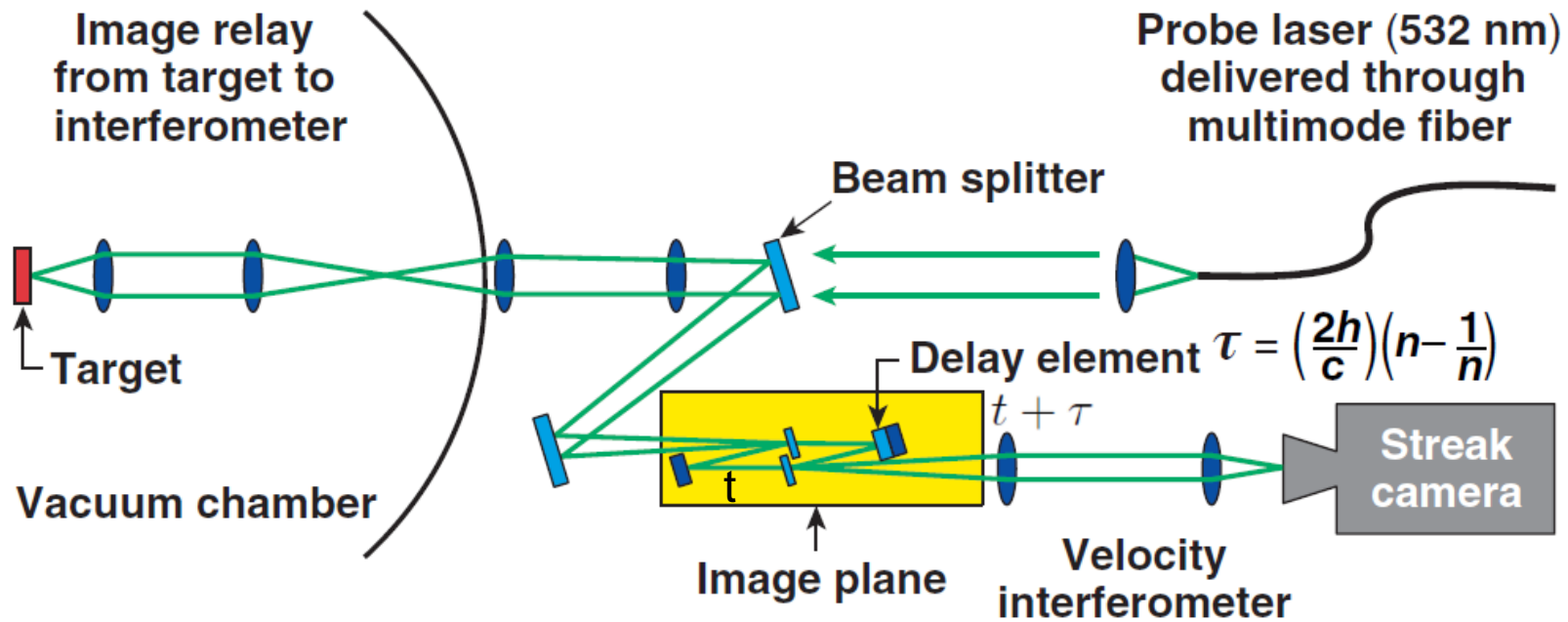


$$I = \int I(\varepsilon) \exp(-\mu(\varepsilon) \rho \delta) d\varepsilon$$

$$I = I_{BL} \exp(-\bar{\mu} \rho \delta)$$

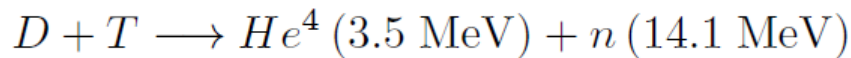
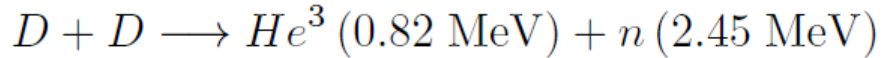
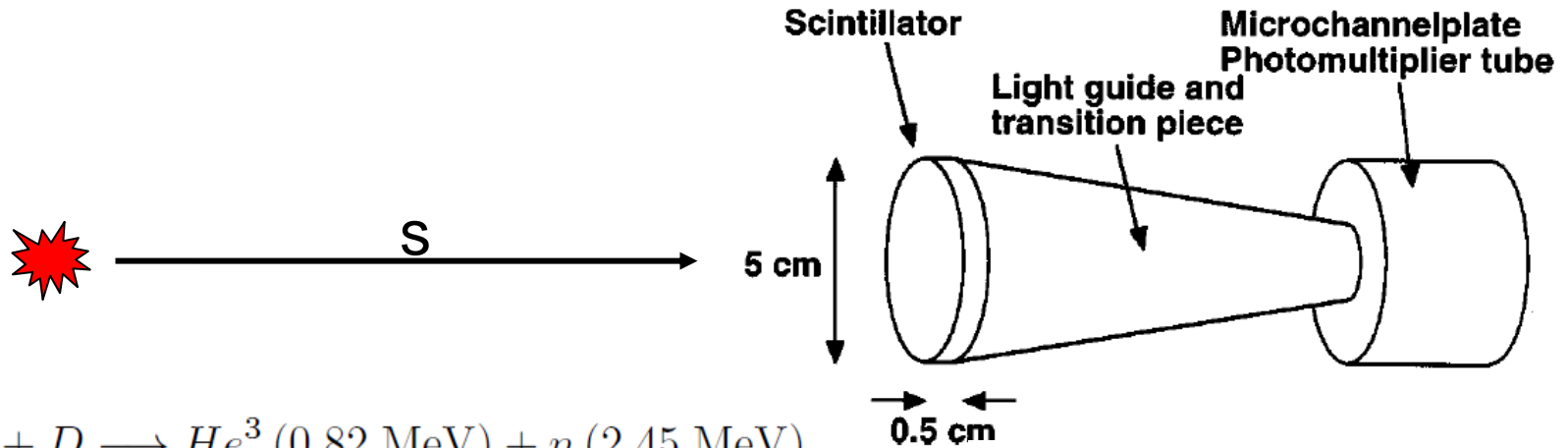
$$\ln I = \ln I_{BL} - \mu \rho r$$

# Shock velocities are measured using time-resolved Velocity Interferometer System for Any Reflector (VISAR)



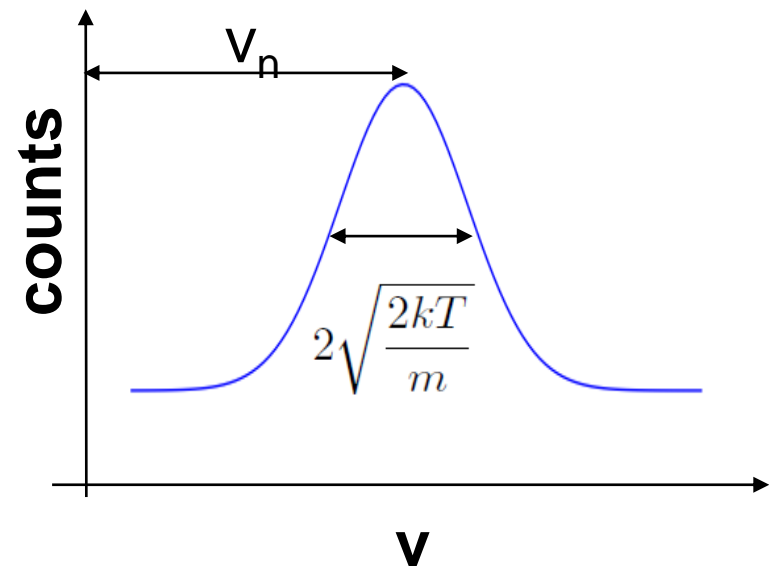
$$\Delta\phi = \frac{vT}{\lambda} \propto v$$

# Neutron average temperature is obtained using Neutron Time of Flight (NToF)



$$s = vt \quad v = \frac{s}{t}$$

$$f(v) = \sqrt{\left(\frac{m}{2\pi kT}\right)} \exp\left(-\frac{mv^2}{2kT}\right)$$



# The OMEGA Facility is carrying out ICF experiments using a full suite of target diagnostics

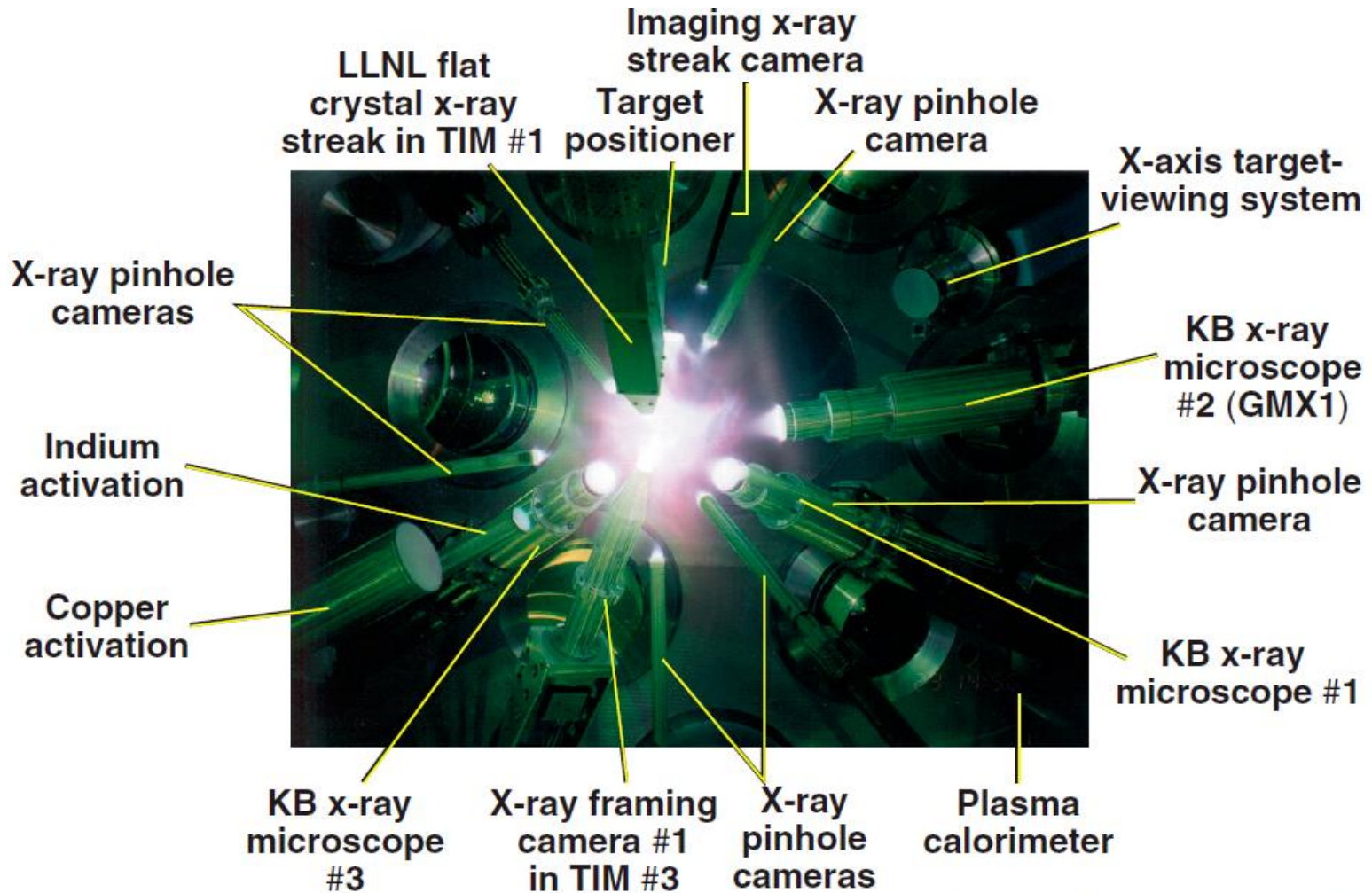
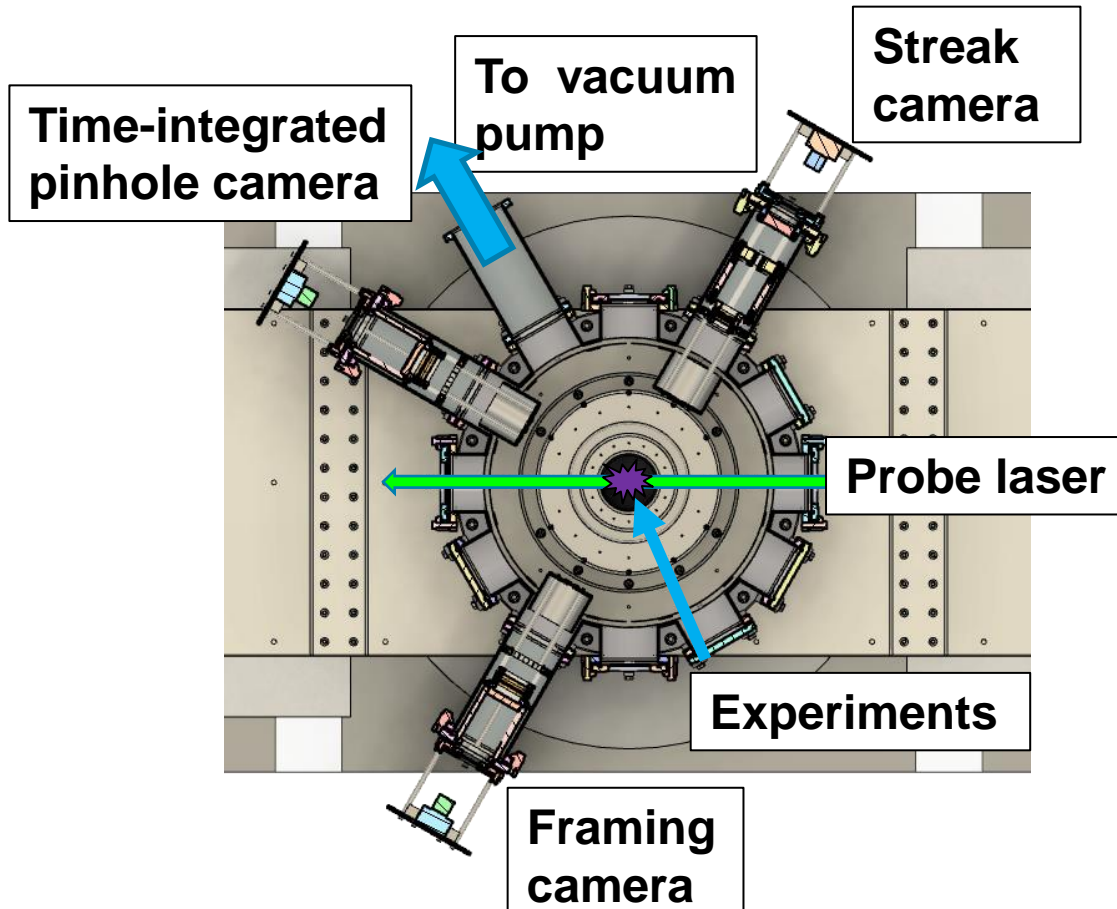


Photo taken from port H11B

# A suit of diagnostics in the range of (soft) x-ray are being built



- CsI are used as the photocathode for all x-ray imaging system.
- Au photocathode may be used in the future.

- Pinhole camera:
  - Magnification: 1x
  - Exposure time: 1  $\mu$ s
- Streak camera:
  - Magnification: 1x
  - Temporal resolution: 15 ps
- Framing camera:
  - Magnification: 0.3x
  - Temporal resolution:  $\sim$ ns using 4 individual MCPs
- Laser probing:
  - For interferometer, schlieren, shadowgraphy, Thomson scattering.
  - Temporal resolution:  $\sim$ 300 ps using stimulated brillouin scattering (SBS) pulse compression in water

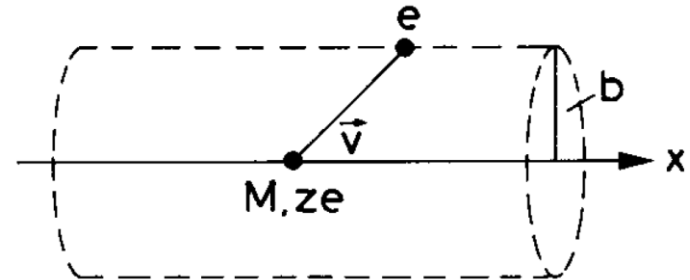


# Energetic charged particles losses most of its energy right before it stops



Momentum transfer:

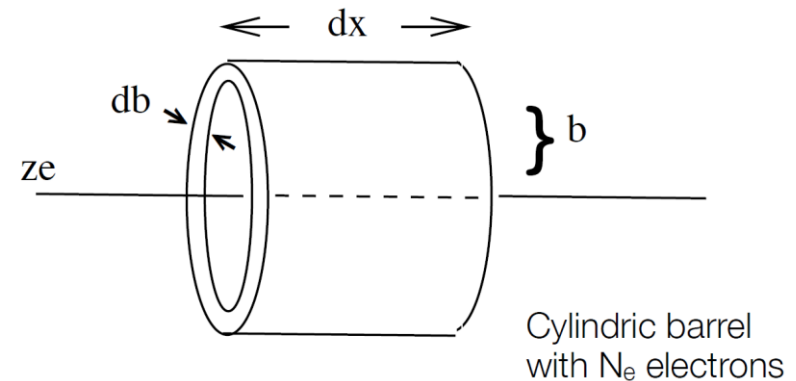
$$\Delta p_{\perp} = \int F_{\perp} dt = \int F_{\perp} \frac{dt}{dx} dx = \int F_{\perp} \frac{dx}{v}$$



$$= \int_{-\infty}^{\infty} \frac{ze^2}{(x^2 + b^2)} \cdot \frac{b}{\sqrt{x^2 + b^2}} \cdot \frac{1}{v} dx = \frac{ze^2 b}{v} \left[ \frac{x}{b^2 \sqrt{x^2 + b^2}} \right]_{-\infty}^{\infty} = \frac{2ze^2}{bv}$$

$\Delta p_{\parallel}$  : averages to zero

$$\Delta E(b) = \frac{\Delta p^2}{2m_e} \quad N_e = n \cdot (2\pi b) \cdot db dx$$

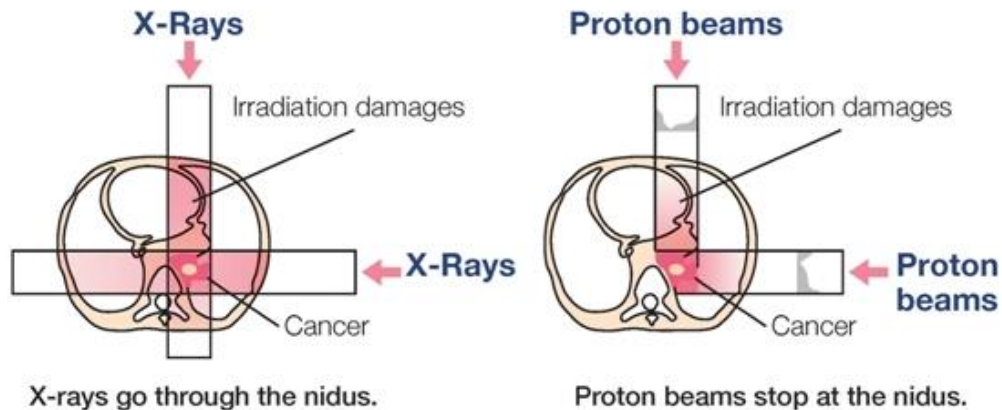
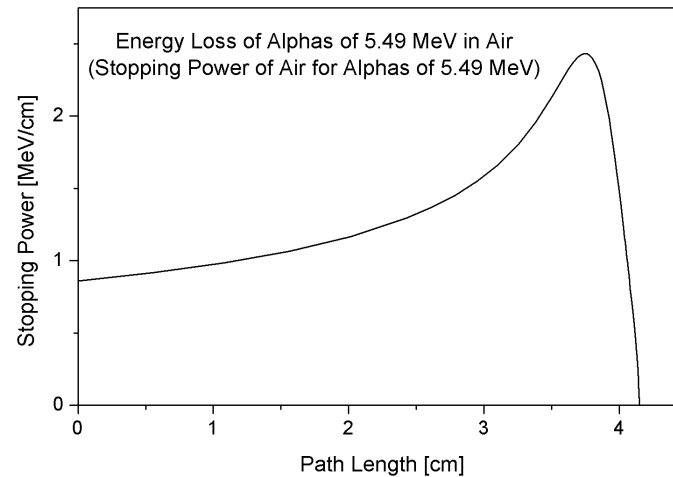


$$-dE(b) = \frac{\Delta p^2}{2m_e} \cdot 2\pi n b db dx$$

$$-\frac{dE}{dx} = \frac{4\pi n z^2 e^4}{m_e v^2} \cdot \int_{b_{\min}}^{b_{\max}} \frac{db}{b} = \frac{4\pi n z^2 e^4}{m_e v^2} \ln \frac{b_{\max}}{b_{\min}}$$



# Proton therapy takes the advantage of using Bragg peak



# There are two suggested website for getting the information of proton stopping power in different materials



<http://www.nist.gov/pml/data/star/>

<http://www.srim.org/>

NIST Physical Measurement Laboratory

NIST Home > PML > Physical Reference Data > Stopping-Power & Range Tables: e-, p+, Helium Ions

NISTIR 4999 | Version History | Disclaimer

## Stopping-Power and Range Tables for Electrons, Protons, and Helium Ions

M.J. Berger, J.S. Coursey, M.A. Zucker and J. Chang  
(NIST, Physical Measurement Laboratory)

**Abstract:**  
The databases ESTAR, PSTAR, and ASTAR calculate stopping-power and range tables for electrons, protons, or helium ions, according to methods described in ICRU Reports 37 and 49. Stopping-power and range tables can be calculated for electrons in any user-specified material and for protons and helium ions in 74 materials.

**Contents:**

1. Introduction
2. ESTAR: Stopping Powers and Ranges for Electrons
3. PSTAR and ASTAR: for Protons and Helium Ions (alpha particles)

References  
Appendix: Significance of Calculated Quantities

**Access the Data:**

1. Electrons
2. Protons

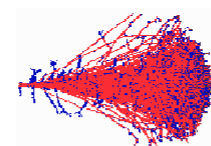
Language selection: 請選擇語言  
由「Google 翻譯」技術提供

© Creations/2010 Shutterstock.com

**Access the Data**  
Electrons | Protons | Helium Ions

NIST Standard Reference Database 124  
Rate our products and services.  
**Online:** October 1998 - **Last update:** August 2005

Contact  
Stephen Saltzer



**SRIM Textbook**

<b>Software</b>	<b>Science</b>
<a href="#">SRIM / TRIM Introduction</a>	<a href="#">Historical Review</a>
<a href="#">Download SRIM-2013</a>	<a href="#">Details of SRIM-2013</a>
<a href="#">SRIM Install Problems</a>	<a href="#">Experimental Data Plots</a>
<a href="#">SRIM Tutorials</a>	<a href="#">Stopping of Ions in Matter</a>
<a href="#">Download TRIM Manual Part-1, Part-2</a>	<a href="#">Stopping in Compounds</a>
<a href="#">Stopping Range and Dose</a>	<a href="#">Scientific Citations of Experimental Data</a>
<a href="#">High Energy Stopping</a>	



# The thickness of a filter can be decided from the range data from NIST website



## COPPER

To download data in spreadsheet (array) form, choose a delimiter and use the checkboxes in the table heading. After downloading, save the output by using your browser's Save As feature.

### Delimiter:

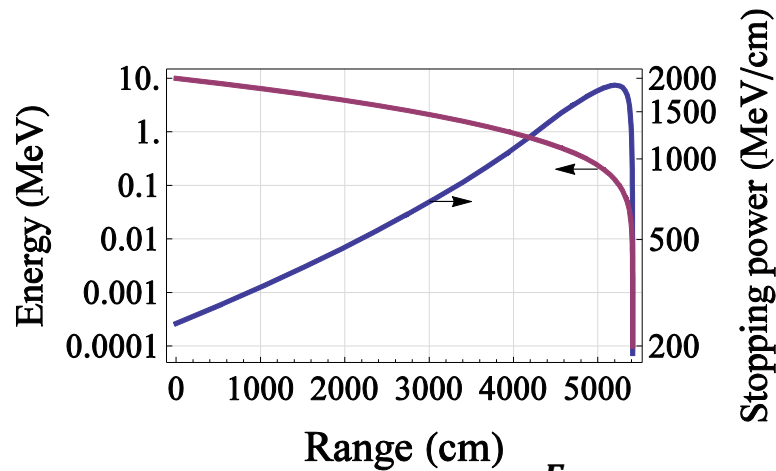
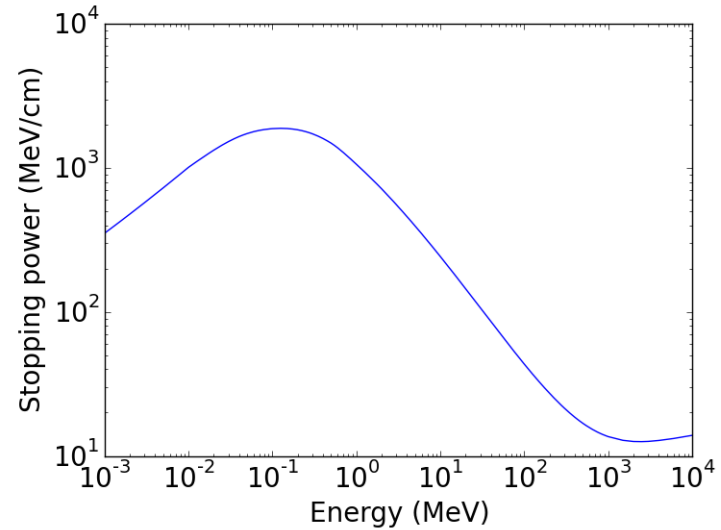
- space
- (vertical bar)
- tab (some browsers may use spaces instead)
- newline

Download data

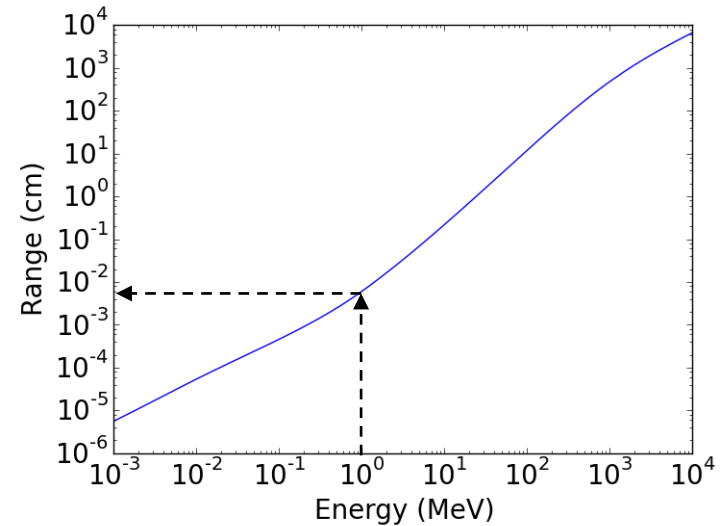
$$\frac{dE}{\rho dx}$$

$$\rho x$$

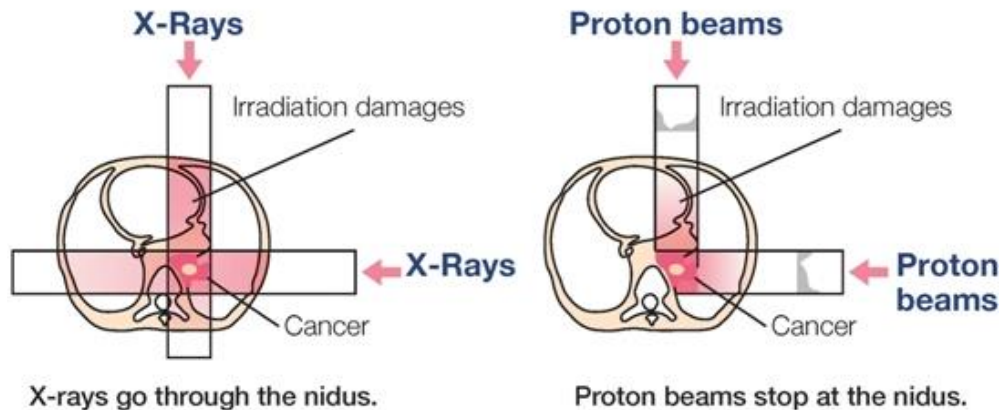
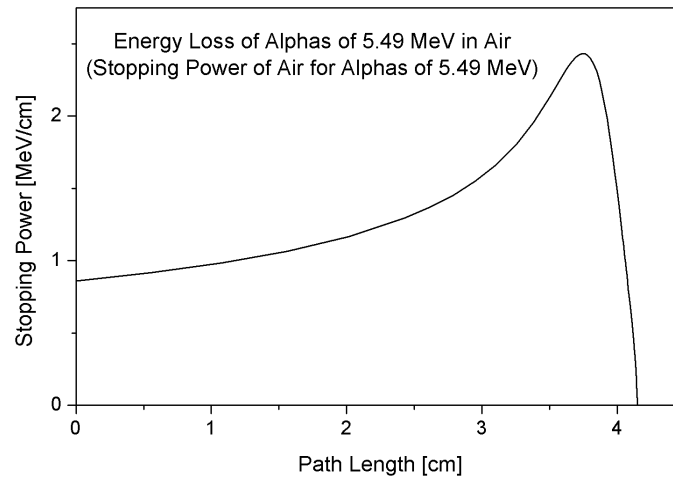
(required) Kinetic Energy (MeV)	Stopping Power (MeV cm <sup>2</sup> /g)			CSDA (g/cm <sup>2</sup> )	Projected	Detour Factor Projected / CSDA
	Electronic	Nuclear	Total		Range (g/cm <sup>2</sup> )	
1.000E-03	3.490E+01	4.408E+00	3.931E+01	4.116E-05	5.620E-06	0.1365
1.500E-03	4.274E+01	4.231E+00	4.697E+01	5.267E-05	8.301E-06	0.1576
2.000E-03	4.935E+01	4.049E+00	5.340E+01	6.263E-05	1.101E-05	0.1759
2.500E-03	5.518E+01	3.876E+00	5.906E+01	7.152E-05	1.374E-05	0.1921
3.000E-03	6.045E+01	3.718E+00	6.416E+01	7.964E-05	1.647E-05	0.2068
4.000E-03	6.980E+01	3.440E+00	7.324E+01	9.419E-05	2.194E-05	0.2329
5.000E-03	7.804E+01	3.207E+00	8.124E+01	1.071E-04	2.739E-05	0.2556
6.000E-03	8.548E+01	3.010E+00	8.849E+01	1.189E-04	3.280E-05	0.2758
7.000E-03	9.233E+01	2.840E+00	9.517E+01	1.298E-04	3.817E-05	0.2940
8.000E-03	9.871E+01	2.692E+00	1.014E+02	1.400E-04	4.347E-05	0.3106
9.000E-03	1.047E+02	2.561E+00	1.073E+02	1.496E-04	4.872E-05	0.3258
1.000E-02	1.104E+02	2.445E+00	1.128E+02	1.587E-04	5.391E-05	0.3398



$$\frac{dE}{dx} = f(E) \Rightarrow x = \int_{E_i}^{E_f} \frac{dE}{f(E)}$$



# Proton therapy takes the advantage of using Bragg peak



# Saha equation gives the relative proportions of atoms of a certain species that are in two different states of ionization in thermal equilibrium

---



$$\frac{n_{r+1}n_e}{n_r} = \frac{G_{r+1}g_e}{G_r} \frac{(2\pi m_e KT)^{3/2}}{h^3} \exp\left(-\frac{\chi_r}{KT}\right)$$

- $n_{r+1}$ ,  $n_r$ : Density of atoms in ionization state  $r+1$ ,  $r$  ( $\text{m}^{-3}$ )
- $n_e$ : Density of electrons ( $\text{m}^{-3}$ )
- $G_{r+1}$ ,  $G_r$ : Partition function of ionization state  $r+1$ ,  $r$
- $g_e=2$ : Statistical weight of the electron
- $m_e$ : Mass of the electron
- $\chi_r$ : Ionization potential of ground level of state  $r$  to reach to the ground level of state  $r+1$
- $T$ : Temperature
- $h$ : Planck's constant
- $K$ : Boltzmann constant

# Some backgrounds of quantum mechanics



- Planck blackbody function:

$$u(\nu, T) = \frac{8\pi h\nu^3}{c^3} \frac{1}{e^{h\nu/KT} - 1} \quad (W/m^3 \text{ Hz})$$

- Boltzmann formula:

- $g_i, g_j$ : statistical weight

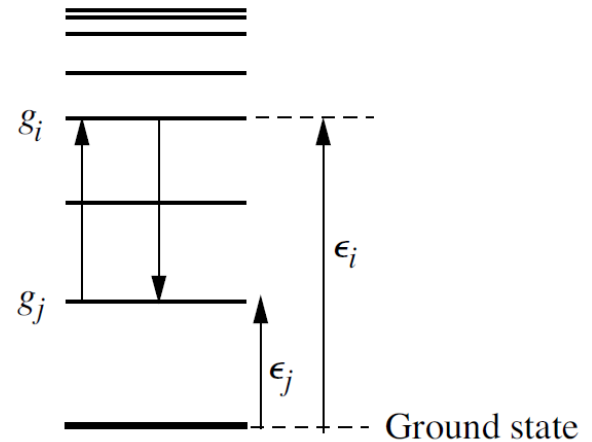
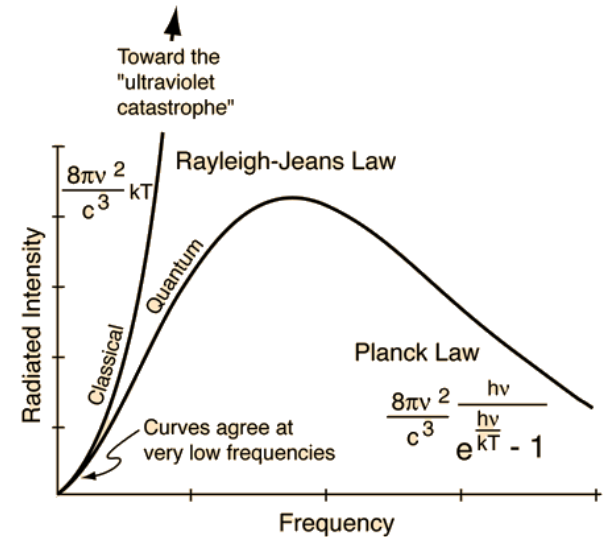
$$\frac{n_i}{n_j} = \frac{g_i e^{-\epsilon_i/KT}}{g_j e^{-\epsilon_j/KT}} = \frac{g_i}{g_j} e^{-h\nu_{ij}/KT} \quad \frac{g_i}{g_j} = \frac{2J_i + 1}{2J_j + 1}$$

( $J$ : angular momenta quantum number)

- Number in the  $i^{\text{th}}$  state to the total atom:

$$\frac{n_i}{n} = \frac{n_i}{\sum n_j} \equiv \frac{g_i e^{-\epsilon_i/KT}}{G} \quad G \equiv \sum g_j e^{-\epsilon_j/KT}$$

**G**: partition function of statistical weight for the atom, taking into account all its excited states.



# Einstein coefficient



- Probability of electron energy transition:

– Excitation ( $\uparrow$ ):  $P_{ji} = B_{ji}u(\nu, T)$

– De-excitation ( $\downarrow$ ):  $P_{ij} = A_{ij} + B_{ij}u(\nu, T)$

- In thermal equilibrium:

$$n_i(A_{ij} + B_{ij}u) = n_j B_{ji}u$$

$$\frac{g_i}{g_j} e^{-x}(A_{ij} + B_{ij}u) = B_{ji}u$$

$$u = a(e^x - 1)^{-1}$$

$$a \left( e^x B_{ji} - \frac{g_i}{g_j} B_{ij} \right) = (e^x - 1) \frac{g_i}{g_j} A_{ij}$$

$$x \equiv \frac{h\nu}{kT}$$

$$a \equiv \frac{8\pi h\nu^3}{c^3}$$

- The Einstein coefficients are independent of T or  $\nu$ .

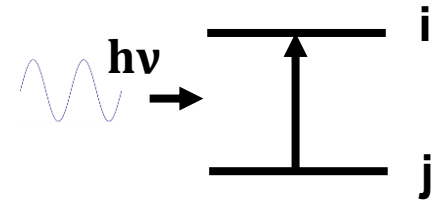
$$x \rightarrow 0, e^x \rightarrow 1$$

$$x \rightarrow \infty, e^x \rightarrow \infty$$

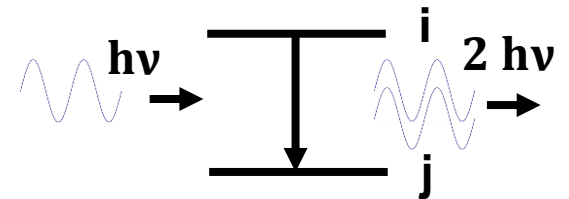
$$\frac{B_{ij}}{B_{ji}} = \frac{g_j}{g_i}$$

$$a B_{ji} = \frac{g_i}{g_j} A_{ij} \quad \frac{A_{ij}}{B_{ij}} = \frac{8\pi h\nu^3}{c^3}$$

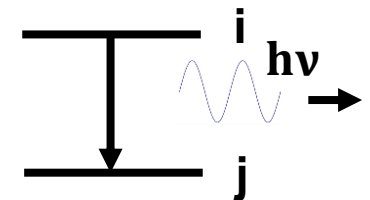
- Photoexcitation:



- Induced radiation:



- Spontaneous radiation:



# Saha equation is derived using the transition between different ionization states



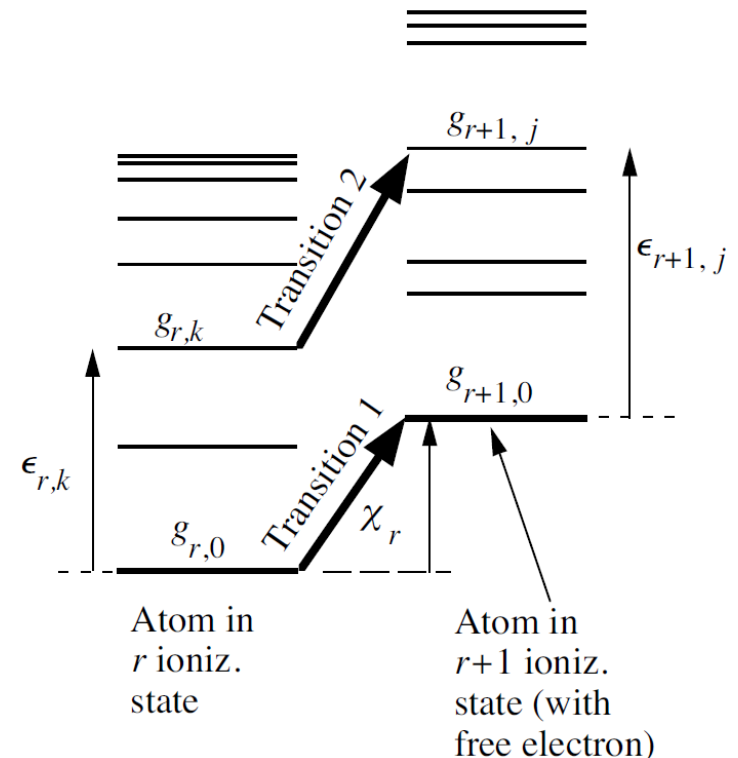
- Required photon energy for transition (1) from the ground state of  $r$  ionization state to the ground state of  $r+1$  ionization state:

$$h\nu = \chi_r + \frac{p^2}{2m}$$

← Energy of the free electron

- Required photon energy for transition (1) from the energy level  $k$  of  $r$  ionization state to the energy level  $j$  of  $r+1$  ionization state:

$$h\nu = \chi_r + \epsilon_{r+1,j} - \epsilon_{r,k} + \frac{p^2}{2m}$$



# Saha equation is derived using the transition between different ionization states



- Photoionization:

$$R_{pi} = n_{r,k} u(\nu) B_{r,k \rightarrow r+1,j}$$

- Induced radiation:

$$R_{ir} = n_{r+1,j} n_{e,p}(\rho) u(\nu) B_{r+1,j \rightarrow r,k}$$

- Spontaneous emission:

$$R_{sr} = n_{r+1,j} n_{e,p}(\rho) A_{r+1,j \rightarrow r,k}$$

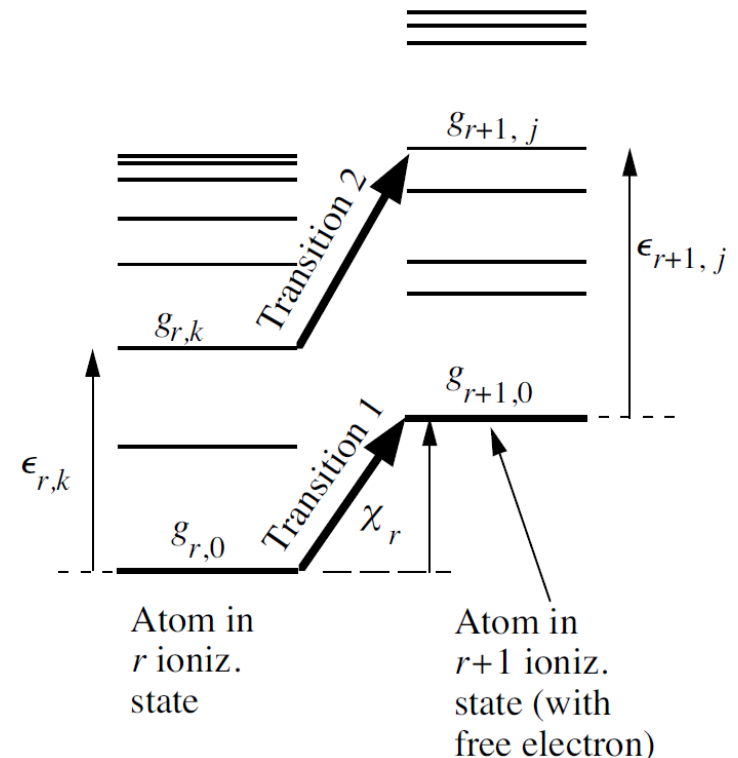
- In thermal equilibrium:

$$\begin{aligned} n_{r+1,j} n_{e,p} A_{r+1,j \rightarrow r,k} + n_{r+1,j} n_{e,p} u B_{r+1,j \rightarrow r,k} \\ = n_{r,k} u B_{r,k \rightarrow r+1,j} \end{aligned}$$

- Einstein coefficients:

$$\frac{B_{r,k \rightarrow r+1,j}}{B_{r+1,j \rightarrow r,k}} = \frac{g_{r+1,j}}{g_{r,k}} \frac{g_e 4\pi p^2}{h^3}$$

$$\frac{A_{r+1,j \rightarrow r,k}}{B_{r+1,j \rightarrow r,k}} = \frac{8\pi h\nu^3}{c^3}$$



# Saha equation - continued



$$n_{r+1,j}n_{e,p}A_{r+1,j \rightarrow r,k} + n_{r+1,j}n_{e,p}uB_{r+1,j \rightarrow r,k} = n_{r,k}uB_{r,k \rightarrow r+1,j}$$

$$n_{r+1,j}n_{e,p} \frac{A_{r+1,j \rightarrow r,k}}{B_{r+1,j \rightarrow r,k}} + n_{r+1,j}n_{e,p}u = n_{r,k}u \frac{B_{r,k \rightarrow r+1,j}}{B_{r+1,j \rightarrow r,k}}$$

$$\frac{n_{r+1,j}n_{e,p}}{n_{r,k}} = \left( \frac{A_{r+1,j \rightarrow r,k}}{uB_{r+1,j \rightarrow r,k}} + 1 \right)^{-1} \frac{B_{r,k \rightarrow r+1,j}}{B_{r+1,j \rightarrow r,k}}$$

$$\frac{B_{r,k \rightarrow r+1,j}}{B_{r+1,j \rightarrow r,k}} = \frac{g_{r+1,j}}{g_{r,k}} \frac{g_e 4\pi p^2}{h^3}$$

$$n_{e,p}(p) = \frac{n_e 4\pi p^2}{(2\pi mKT)^{3/2}} \exp\left(-\frac{p^2}{2mKT}\right)$$

$$\frac{A_{r+1,j \rightarrow r,k}}{B_{r+1,j \rightarrow r,k}} = \frac{8\pi h\nu^3}{c^3}$$

$$\frac{n_{r+1,j}n_e}{n_{r,k}} = \frac{(2\pi mKT)^{3/2}}{4\pi p^2} \exp\left(\frac{p^2}{2mKT}\right) \left[ \frac{c^3}{8\pi h\nu^3} (e^{h\nu/KT} - 1) \frac{8\pi h\nu^3}{c^3} + 1 \right]^{-1} \frac{g_{r+1,j}}{g_{r,k}} \frac{g_e 4\pi p^2}{h^3}$$

$$\frac{n_{r+1,j}n_e}{n_{r,k}} = \frac{(2\pi mKT)^{3/2}}{h^3} \frac{g_{r+1,j}g_e}{g_{r,k}} \exp\left[\frac{1}{KT} \left(\frac{p^2}{2m} - h\nu\right)\right]$$



# Saha equation - continued



$$\frac{n_{r+1,j}n_e}{n_{r,k}} = \frac{(2\pi mKT)^{3/2}}{h^3} \frac{g_{r+1,j}g_e}{g_{r,k}} \exp\left[\frac{1}{KT} \left(\frac{p^2}{2m} - hv\right)\right]$$

$$\frac{n_{r+1,j}n_e}{n_{r,k}} = \frac{(2\pi mKT)^{3/2}}{h^3} \frac{g_{r+1,j}g_e}{g_{r,k}} \exp\left[\frac{1}{KT} \left(\frac{p^2}{2m} - \chi_r - \epsilon_{r+1,j} + \epsilon_{r,k} - \frac{p^2}{2m}\right)\right]$$

$$\frac{n_{r+1,j}n_e}{n_{r,k}} = \frac{(2\pi mKT)^{3/2}}{h^3} \frac{g_{r+1,j} \exp\left(\frac{\epsilon_{r+1,j}}{KT}\right) g_e}{g_{r,k} \exp\left(\frac{\epsilon_{r,k}}{KT}\right)} \exp\left(-\frac{\chi_r}{KT}\right)$$

$$\frac{n_{r,k}}{n_r} = \frac{g_{r,k} e^{-\epsilon_{r,k}/KT}}{G_r}$$

$$G_r = \sum g_{r,k} e^{-\epsilon_{r,k}/KT}$$

$$\frac{n_{r+1,j}}{n_{r+1}} = \frac{g_{r+1,j} e^{-\epsilon_{r+1,j}/KT}}{G_{r+1}}$$

$$G_{r+1} = \sum g_{r+1,j} e^{-\epsilon_{r+1,j}/KT}$$

$$\frac{n_{r+1}n_e}{n_r} = \frac{G_{r+1}g_e}{G_r} \frac{(2\pi m_eKT)^{3/2}}{h^3} \exp\left(-\frac{\chi_r}{KT}\right)$$

# Saha equation – example: hydrogen plasma of the sun



- Photosphere of the sun – hydrogen atoms in an optically thick gas in thermal equilibrium at temperature  $T=6400$  K.

- Neutral hydrogen (r state / ground state)

$$G_r = \sum g_{r,k} = g_{r,0} + g_{r,1} \exp\left(-\frac{\epsilon_{r,1}}{KT}\right) + \dots = 2 + 8 \exp\left(-\frac{10.2\text{eV}}{0.56\text{eV}}\right) + \dots \\ = 2 + 9.8 \times 10^{-8} + \dots \approx 2$$

- Ionized state (r+1 state)

$$G_{r+1} = \sum g_{r+1,j} = g_{r+1,0} + g_{r+1,1} \exp\left(-\frac{\epsilon_{r+1,1}}{KT}\right) + \dots \approx 1$$

- Other information:  $g_e = 2$        $\chi_r = 13.6\text{eV}; KT = 0.56\text{eV}$        $n_{r+1} = n_e$

$$\frac{n_{r+1}^2}{n_r} = 2.41 \times 10^{21} \frac{1 \times 2}{2} (6400)^{3/2} \exp\left(-\frac{13.6}{0.56}\right) = 3.5 \times 10^{16} m^{-3}$$

# It is mostly neutral in the photosphere of the sun



- Assuming 50 % ionization:

$$n_{r+1} = n_r = 3.5 \times 10^{16} m^{-3} \quad n = n_{r+1} + n_r = 7 \times 10^{16} m^{-3}$$

- At lower densities  $n$  at the same temperature, there should be fewer collisions leading to recombination and thus the plasma to be more than 50 % ionization.
- In the photosphere of the sun:

$$\rho \sim 3 \times 10^{-4} \text{ kg}/m^3 \rightarrow n = 2 \times 10^{23} m^{-3} \gg 7 \times 10^{16} m^{-3}$$

⇒ Less than 50 % ionization

- Use the total number density to estimate the ionization percentage:

$$n_{r+1} + n_r = 2 \times 10^{23}$$

$$\frac{n_{r+1}}{n_r} = 4 \times 10^{-4} @ 6400K$$